GE Energy

Final Report

Analysis of Wind Generation Impact on ERCOT Ancillary Services Requirements

Prepared for:

Electric Reliability Council of Texas

March 28, 2008

FOREWORD

This document was prepared by General Electric International, Inc. under contract to Electric Reliability Council of Texas, Inc.

Project Manager:

Reigh A. Walling

GE Energy
One River Road
Building 2, Room 618
Schenectady, New York 12345

GE Project Team:

Venkat Banunarayanan
Amanvir Chahal
Lavelle Freeman
Jerry Martinez
Nicholas Miller
Devin Van Zandt
Mark Walling
Reigh Walling

LEGAL NOTICE

TABLE OF CONTENTS

1. INTRODUCTION

GE Energy has performed an extensive study of the ancillary service requirements for the Electric Reliability Council of Texas (ERCOT) system to accommodate large-scale expansion of wind generation capacity. This report documents the approach used to perform this study, the results obtained, and the final study recommendations.

1.1. Background

Texas is the leader among the United States in adding wind power to the state's power generation portfolio. Texas leads the country with the most installed wind capacity, and the greatest annual capacity additions. In contrast to many parts of the United States where transmission inadequacy presently constrains wind energy development, Texas has overcome the transmission barrier by the bold and progressive step of establishing Competitive Renewable Energy Zones (CREZs). The Public Utility Commission of Texas (PUCT), in consultation with ERCOT, has designated CREZs in areas suitable for renewable energy development, and is developing a plan to construct the necessary transmission capacity to deliver the energy from the renewable resources to the customers in the state.

Wind generation has technical characteristics which inherently differ from those of conventional generation facilities. Conventional generation can be controlled, or "dispatched", to a precise output level. The primary energy source for wind generation, however, is inherently variable and incompletely predictable. Thus, electrical output of wind generation plants cannot be dispatched[1].

Because electric energy cannot be easily or economically stored on a large-scale basis, the amount of power generation must be exactly matched, on a near-instantaneous basis, to the amount of customer load demand. There is considerable art and science applied to the operations of a power system to maintain the balance of load and generation. Because the ERCOT system is not synchronously interconnected with any other power system, a mismatch between instantaneous load and generation inherently results in variation of the system frequency. Load demand varies on a daily cyclic basis, and has a considerable degree of random variation around the daily trend. Load levels also cannot be precisely predicted in advance. Addition of wind generation resources increases the amount of variability and unpredictability that must be addressed in system operations.

[1] Wind generation can be "turned down", or curtailed, from its potential output, but cannot be increased beyond the power level provided by the existing wind velocity. Curtailment "spills" non-recoverable energy., thus curtailment on a continuous basis to render a wind plant equally dispatchable as a conventional plant is not practical. Where appropriate wind plant controls are installed, wind plant turndown can potentially be used to provide regulation service in certain circumstances.

A category of services, called "ancillary services", are procured by the ERCOT power market to facilitate the operation and balancing of the system. ERCOT currently uses several ancillary services to control system frequency and protect system reliability from imbalances between generation and load. In the past, this imbalance might occur due to the variability of load, inaccuracies in the prediction of load levels or resource utilization, or the unplanned loss of resources.

The ERCOT market structure will be transitioned in 2009 from the current zonal structure to a nodal structure. The ancillary services in the ERCOT nodal market design are:

- *Regulation Service* – is used to maintain the instantaneous balance between load and generation resources.
- *Responsive Reserve Service* – is generation resources held in reserve to address loss of generation resources and unexpected large changes in generation requirements.
- *Non-Spinning Reserve Service* – are generation resources that can come on line with short (presently thirty minute) notice to compensate for load forecast errors.
- *Replacement Reserves* – are used to commit additional capacity based on forecasted load, either for load balance or congestion.

The integration of increasing amounts of wind generation capacity into the ERCOT system inevitably leads to changing requirements for ancillary services procurement.

ERCOT has commissioned this study of ancillary services requirements to provide the information needed to guide ERCOT and the PUCT in evaluating the reliability implications of wind generation penetration, and to develop the procedures and protocols for ancillary services procurement needed to strike the proper balance between system reliability and economic operation of the system.

1.2. Project Scope and Objectives

The specific objectives of this study are to:

1. Quantitatively assess the impact of various wind development scenarios on the levels of ancillary services required.
2. Evaluate the methodology used by ERCOT to determine the amount of ancillary services required, and recommend improvements to that methodology where appropriate.
3. Estimate the impact of wind generation on the costs to procure ancillary services.
4. Identify changes to current procedures or new procedures required for operations with impending severe weather conditions.

This study is based on sequential time-series modeling of the wind and load behaviors, as well as the processes used to forecast both wind and load. Extensive statistical analyses are used to characterize the wind and load variability. Detailed modeling is performed of ancillary service deployments to determine both the amount of ancillary service required to be procured as a function of wind penetration, and to assess the suitability of procurement procedures.

The study focuses on five wind penetration scenarios that have been defined by ERCOT, ranging from zero to 15,000 MW of wind capacity. Although this 15,000 MW level of wind generation will take several years to evolve, and the present wind capacity is on the order of 5,000 MW, these wind scenarios are applied to a system model representing 2008 load levels and generation composition for consistency. The 15,000 MW of wind generation applied to the 2008 loading results in a 23% penetration on a nameplate wind generation capacity to peak load basis. This is equivalent in terms of wind penetration to 18,456 MW of wind generation applied to the forecast 2017 system load. The penetration is approximately 17% on an energy basis.

Applying the different wind scenarios to one system model implicitly assumes that the conventional (dispatchable) generation portfolio mix remains constant as wind penetration increases. This is not necessarily what will happen. However, forecasting how the conventional generation mix evolves in response to increasing wind generation, changing environmental requirements, shifts in capital markets, and generation technology improvements is extremely complex and highly speculative. Therefore, such prognostication is not included in the scope of this study.

This study, by design, also intentionally ignores present-day transmission constraints. Public policy in Texas is to develop the transmission system to support renewable generation additions. Thus, it would be inconsistent to incorporate constraints in the study which should not be present when the wind generation is developed, if this policy is carried out.

1.3. Study Participants

The prime contractor for this study is the Energy Applications and Systems Engineering group of GE Energy. This group is the power system consulting arm of GE, and has been involved in the cutting edge of power engineering technology for nearly a century. Recent activities of this group have included a number of important and pioneering studies of wind integration, including studies of the New York, California, and Ontario systems.

This study combines both power systems and meteorological aspects. AWS Truewind was retained by GE Energy as a subcontractor for this study, providing wind generation data, wind forecast data, and important insights on severe weather conditions. AWS

Truewind has performed previous studies of wind generation resources for ERCOT, and has been retained by ERCOT to provide wind forecasting services on an operational basis. The GE–AWS Truewind team has worked together on prior highly successful projects, and the benefits of that prior experience have been applied to this study.

1.4. Organization of Report

Section 2 describes the approach used in this study, with specific information on the generation of the contemporaneous load and wind generation data used as the basis for this study.

Section 3 provides an extensive analysis of the variability of the net load[2], with correlations of this variability with time of day, season, and load level.

Section 4 analyzes the impact of wind generation forecast errors on the resulting net load forecast error. Forecast errors are correlated with time of day, season.

Section 5 describes how the presence of wind generation affects the commitment and dispatch of the conventional generation fleet, showing impacts on energy production by various generation types, emissions, spot prices, and output ramping capabilities.

Section 6 provides the results of an extensive analysis of regulation service requirements, including the impacts on regulation procurements as wind penetration increases, evaluation of regulation procurement methodology, ability of the conventional generation to provide the needed regulation, and the impacts on costs of regulation service.

Section 7 discusses extreme weather conditions. Extensive meteorological analysis is provided of the critical issues associated with extreme weather, as it pertains to rapid wind generation output changes.

Section 8 discusses responsive and non-spin reserve services

Section 9 completes the main body of the report with conclusions and recommendations.

Appendix A provides the Table of Figures for this report.

Additional appendices provide supplemental and detailed information supporting the report. Of particular note is *Appendix H* which is AWS Truewind's report on the wind generation output characteristics during extreme weather conditions.

[2] Net load is defined as the load demand minus the wind generation output at that time. An extensive discussion of net load, and why this perspective of analysis is critical, is provided in Section 2. See Appendix A for definitions of other terms used in this report.

2. STUDY APPROACH

The overall study approach is outlined in this section. The types of analysis, study scenarios, data, and model development are all described below.

2.1. The Critical Importance of Net Load

Wind generation output and system electrical demand (load) have a number of common elements, as both are:

- Cyclic on an annual (seasonal) basis, and a diurnal (daily) basis
- Subject to random short-term variations around the multi-hour trends.
- Not directly controllable (i.e., non-dispatchable)
- Subject to deviations from predicted day-ahead behavior
- Mutually dependent on prevailing weather conditions.

From this, it can be seen that wind generation has more in common with load, on an operational basis, than it does with conventional, dispatchable generation resources. The major difference is one of sign; wind generation effectively acts like a negative load.

The impacts of wind generation on ancillary service requirements cannot be evaluated by examining wind generation output characteristics, such as variability and predictability, independently from the simultaneous behavior of the load. Factors causing inaccuracy in wind forecasting may also affect load forecasting (e.g., arrival time of a cold front).

Thus, analysis of wind variation independent of load variation is inadequate and inappropriate to determine impacts of wind on ancillary services requirements and procurement methodologies. The inherent variability and imperfect predictability of wind generation adds to the variability and prediction errors of system load. The variabilities cannot simply be combined as if they are independently random, as they are both affected by the common factor of the weather. Nor can they be added algebraically because the correlation is only partial and the coefficient can be either positive or negative, or vary in sign with time or location of the wind resource.

Operationally, the dispatchable generation output must conform to the characteristics of the *net load*, defined as the aggregate customer load demand minus the aggregate wind generation output. The fundamental approach of this study is to analyze the **net load** variability and the resulting impacts on ancillary services requirements brought on by increasing penetrations of wind generation.

2.2. Wind Generation Scenarios

ERCOT defined five different wind generation scenarios to be used as the basis for this study, with four levels of wind capacity ranging from zero to 15,000 MW. There are two 10,000 MW scenarios, with the second substituting capacity in South Texas near the Gulf of Mexico (CREZ 24) in lieu of similar capacity in the Panhandle in CREZ 4. In addition to the total wind generation capacity for each scenario, ERCOT also defined the capacity assignments for each CREZ shown in Table 2-1. Figure 2-1 provides the geographic location of the various CREZs.

Table 2-1 - Wind Capacity Allocation by CREZ

	Wind Development Scenario			
CREZ Zone	**5000 MW**	**10,000 MW (1)**	**10,000 MW (2)**	**15,000 MW**
none	120	120	120	120
2	60	1,560	1,560	2,340
4	0	1,500	0	0
5	355	1,355	1,355	1,355
6	400.5	400.5	400.5	1,278.3
7	65	65	65	97.5
9	814	1,314	1,314	1,971
10	2,464.5	2,964.5	2,964.5	4,446.8
12	400	400	400	600
14	160	160	160	240
15	60	60	60	90
19	101	101	101	211.5
24	0	0	1,500	2,250

Minute-by-minute ERCOT load data from 2005 and 2006, combined with synchronized wind generation expectations for the same time period, were used to build time series models for the scenarios. The load data were scaled such that the 2006 loads are at the forecast 2008 level, and the same scale factor is also applied to the 2005 data. The scaling and preparation of load data is described later in Section 2.2.2. Most of the wind generation resources in the scenarios have not yet been installed. Therefore, it was necessary to construct minute-by-minute wind generation output data from available meteorological data for 2005 and 2006. The derivation of wind generation data is described in Section 2.2.1.

Similarly, historical day-ahead load forecasts were obtained from ERCOT for each day of the 2005 – 2006 period. Day-ahead wind forecasts were synthesized by AWS Truewind using techniques that have been applied to previous wind integration studies.

This process developed a detailed minute-by-minute, synchronized model of ERCOT system load and wind generation. To the extent possible, this approach takes into account the mutual factors affecting both wind output and load demand, and factors affecting forecast errors.

The primary purpose for analyzing two years of data is because ERCOT's present methodology to determine regulation requirements is based on historical deployments of regulation for the same period in the prior year. Also, comparison of the statistical differences between the two years provides indication of year-to-year differences.

Although the 2006 data are scaled to the 2008 level, this report does not use "2008" for this year, and "2007" for the scaled 2005 data. Such a designation could be misleading as readers may note specific dates for events in the data which do not correlate to actual events in the 2007 and 2008 years. Therefore, the 2006 data scaled to 2008 are referred to as "Study Year", and the scaled 2005 data are called "Prior Year" in this report.

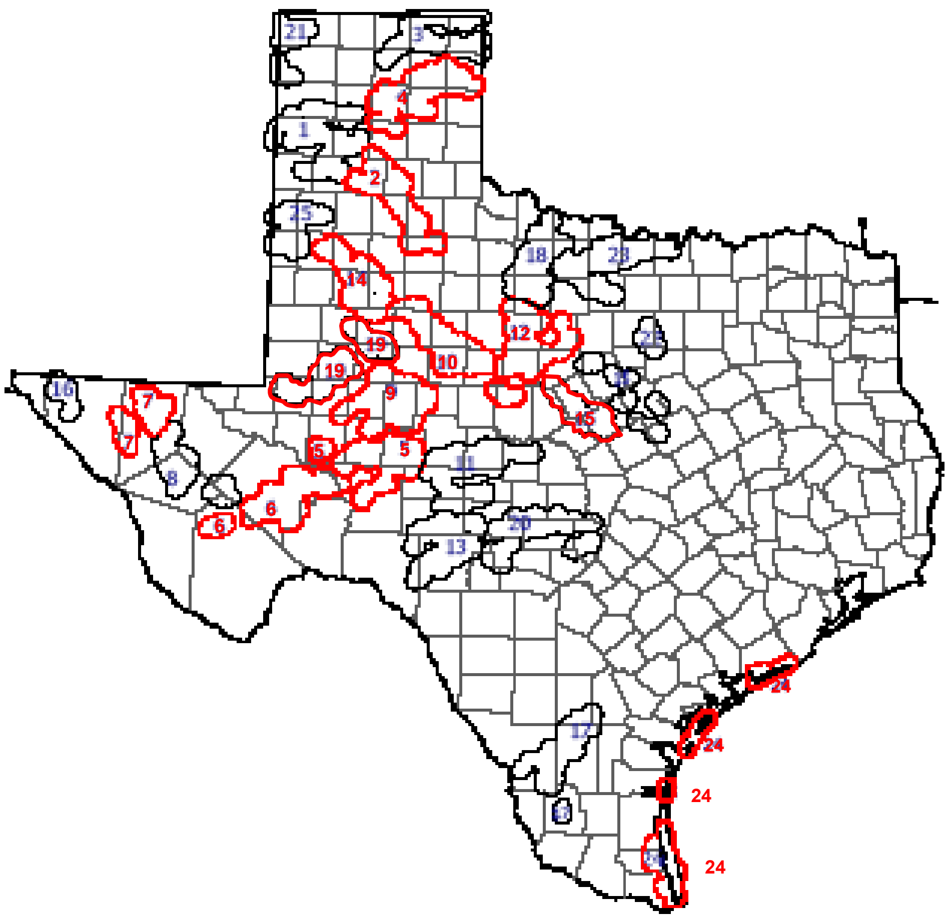

Figure 2-1 - CREZ map, zones included in the study are shown in red.

2.2.1. Wind Generation Power Output Data

The generation of wind data for this study was performed by AWS Truewind, LLC, (AWST) as a subcontractor to GE Energy. AWST's deliverables were:

- Wind generation, by individual plant, on a minute-by-minute basis.
- Day-ahead hourly wind generation output forecasts, by individual plant.

AWST also performed an evaluation of severe weather conditions, and the resulting potential for rapid changes in wind power output. This task is described separately in Section 7.1.

The generation of the wind generation data is summarized in this report section. A full report of AWST's work to develop wind generation data is attached as Appendix B.

Meso-Scale Weather Model

AWST had previously been engaged directly by ERCOT to develop wind generation data for 716 identified potential wind plant sites in 25 CREZs. For the present study, AWST used the same modeling approach to determine wind generation and forecast data for 2005 (Prior Year) and 2006 (Study Year) so that the wind data is for a contiguous time period synchronized with system load data provided by ERCOT.

AWST's starting point for developing the wind generation data was a highly-detailed meso-scale numerical weather model representing weather behavior on an hourly basis. This model was initialized and adjusted to conform to historic weather recordings, including tall-tower wind recordings, for the two-year period. The model was used to generate hourly wind velocities and directions for each of the identified sites.

Plant Generation Data

The wind velocity and direction were then converted to hourly electrical power levels for each plant using typical wind turbine-generator performance curves. Adjustments were made for a number of factors, including directionally-dependent wake interference, and various other non-directional losses and unit unavailability.

One-Minute Generation Data

The weather model yielded hourly wind plant output. Minute-by-minute variations in power output were synthesized using a process based on recordings of actual Texas wind plant output data with one-minute resolution. This synthesis process has been widely used for many wind integration studies.

Wind Forecasts

Wind forecasts for one day ahead and four hours ahead were synthesized by AWST using a Markov chain approach, using typical wind forecasting error patterns reflecting the current state of the wind forecasting art. An unbiased, or 50% confidence level, forecast was generated. The reasons for using a statistical, rather than a meteorological approach to developing the forecast data is explained in AWST's report. This process, too, has been widely used on other major wind integration studies in which AWST has participated.

Because a short-term load forecast is not applied to ERCOT's planned nodal operations, when the anticipatory "tuning factor"[1] is zero, the four hour forecast data developed by AWST were not used in this study.

CREZ Wind Output Data

Wind generation and forecast data were provided by AWST on a per-plant basis. Some of these are existing plants. In developing the wind generation output for each CREZ, existing plants were considered first. Then, potential plants, identified by AWST in the prior work for ERCOT, were added in the order of decreasing annual capacity value, until the total wind plant capacity in a CREZ equaled the capacity values defined in Table 2-1.

2.2.2. System Load Data

System load data for 2005 and 2006 were provided by ERCOT. The load for each minute in both years was scaled by a factor of 1.037 to reflect load growth from 2005-2006 to 2007-2008. The same factor was also applied to scale day-ahead load forecasts.

2.3. Types of Analysis

Three primary analytical methods were used to meet the objectives of this study; statistical analysis, production simulation analysis, and historical meteorological analysis.

Statistical analysis was applied to variability of load and net load, forecast errors, and regulation deployments. Correlations with time of day, season or month of year, and system load level were identified. The adequacy of present ancillary services procurement methodologies was statistically characterized.

[1] This tuning factor is discussed later in this section and in Section 6.

Production simulation analysis with GE-MAPS™ was used to evaluate hour-by-hour system operation for each scenario for 3 years with different assumptions regarding the use of wind generation forecasting in the day-ahead unit commitment. The results quantified numerous impacts on grid operation including:

- Amount of maneuverable generation on-line during a given hour, including its available ramp-up and ramp-down capability to deal with grid.
- Changes in dispatch of conventional generation resources due to the addition of wind generation
- Changes in emissions for oxides of sulfur (SO_X), oxides of nitrogen (NO_X) and carbon dioxide (CO_2) due to wind generation
- Changes in costs and revenues associated with grid operation, and changes in net cost of energy

The impacts of severe weather on system reliability, through potential large-scale loss of wind generation output, were assessed using multiple approaches. These approaches included statistical analysis of the modeled data, as well as historical analysis of critical wind generation output change events observed in the ERCOT system during recent years. For the identified events, AWS Truewind has examined the available data on wind output generation, and has researched the weather behavior of the same period to identify root causes for the generation output changes. With this meteorological analysis of historic wind-change events, predictions have been made regarding the severity and mean recurrence of severe wind-change events in the future.

2.4. Study Assumptions and Limitations

The following are major assumptions made in the performance of this study:

- Because actual historical wind measurements are not available for all the sites included in the scenarios, wind generation output is calculated using meso-scale weather modeling and typical wind turbine performance characteristics. Wind forecasts (50% confidence level) were also synthesized by a statistical process. Wind generation output and forecast data derivation are as described in Section 2.2.1 and Appendix B.
- The scope of this study was to analyze two years of data. Data gathered over a longer term may yield different results, particularly with regard to extreme conditions; i.e., statistical outliers.
- Transmission constraints are not considered in this study. The intent of the CREZ development is to make the transmission system additions needed to facilitate wind and other renewable forms of generation. The limitations of today's ERCOT transmission system is not a valid consideration for future scenarios of high wind penetration. Although building a completely constraint-free transmission system is not economically efficient, future transmission

constraints on a yet-to-be designed system cannot be determined at this time, and thus were excluded from the scope of this study.

- The composition of the non-wind generation portfolio in ERCOT is assumed to remain constant. This means that the percentages of generation, by type (i.e., nuclear, single-cycle GT, coal, etc.) is invariant. During the time required for up to 15,000 MW of wind to be developed in ERCOT, other generation additions will be also required to meet load growth. Some generation unit retirements may occur as well. The generation portfolio may very well shift in response to fuel costs, changing technologies, changed environmental and regulatory policies, and to the presence of wind generation as well. As shown later in this report, the presence of wind capacity tends to displace energy production from mid-merit units such as combined cycle gas turbines. The market may respond with a different mix of units than are presently on the ERCOT system. Forecasting this long-cycle impact of wind generation on generation unit development is beyond this study's scope.
- Wind conditions for the analyzed years (2005 and 2006 data) are assumed to be indicative of the long-term characteristics. Meteorologists indicate that the year-to-year variations in typical wind patterns are not large. However, there is uncertainty regarding the extrapolation of extreme wind events from the limited observation period.
- There will be "tuning factors" used in the ERCOT nodal market to predictively adjust economic dispatch for expected load change within a five-minute dispatch period, based on the short-term load forecast. The tuning factors have not yet been determined by ERCOT. This study proceeded with modeling regulation assuming that the tuning factor is always zero. Thus, predictive adjustment of dispatch was not represented.
- In the present ERCOT zonal market, units providing regulation service are required to have sufficient ramping capability to achieve the offered regulation range in ten minutes

3. NET LOAD VARIABILITY CHARACTERIZATION

For the purposes of this study, net load is defined as the instantaneous system load, minus the generation output of non-dispatchable wind generation (Load-Wind). Net load is the amount of generation required from dispatchable units. This section focuses on the variability of net-load rather than wind generation in isolation because experience has shown that some of the variation in load and wind output cancel each other in a combined series. In other words, given synchronized load and wind generation time series, the net variability of load-wind over a time period is less than the sum of the variability of the individual series over the same time period.

For illustration, Figure 3-1 charts the profile of load, wind generation, and net load for one hour on April 23rd of the study year, (from one-minute data). Load and net load are plotted on the left axis and wind generation output on the right axis. Table 3-1 quantifies the variation of the raw data over the entire hour, and the variation of minute-to-minute changes using the standard deviation (σ) statistic.

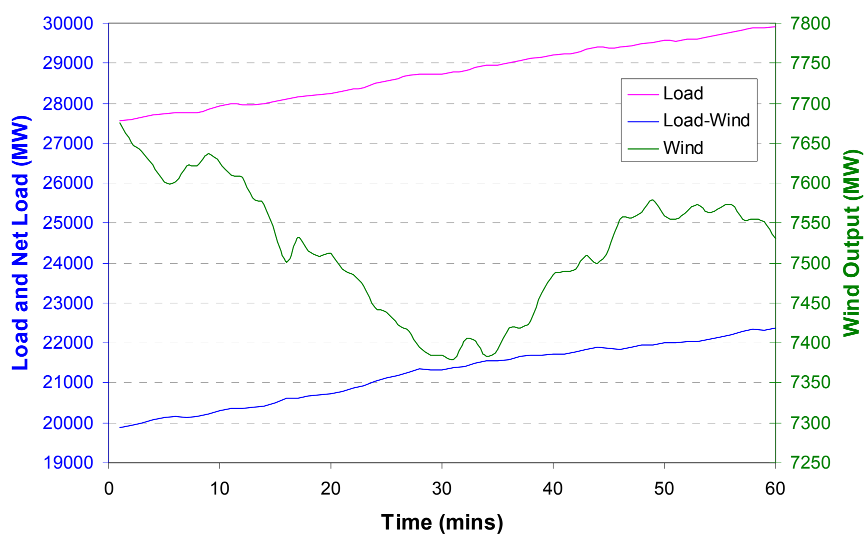

Figure 3-1 - Load, Wind and Net Load time series plots for April 23, 7-8 AM

Table 3-1 - Standard Deviation (σ) of Load, Wind and Net Load Series

	Load	Wind	Load-Wind
Raw Data σ (MW)	723.9	80.5	**750.4**
Min-to-Min Changes σ (MW)	28.8	16.9	**35.6**

In both cases, the net load standard deviation is *less than the sum* of the individual load and wind sigmas. Therefore, the best way to understand the incremental variability due to wind, is to measure the difference in variability between net load and load.

3.1. Wind and Load Relationships

The temporal relationship between wind output and load is the key driver for resulting net load variability. Depending on how the wind is behaving when load is rising or falling, the net variability could be better or worse than load alone. In some cases, wind may exaggerate or curtail net load peaks and valleys, increase or decrease ramp rates (period-period-changes), shift time-of-peak, and generally aggravate or mitigate operationally challenging periods. All these are important factors when considering the impact of wind on ancillary services, especially regulation, (discussed further in Section 6).

Figure 3-2 plots individual time series for load and 15,000 MW of wind generation during April of the study year. Note that wind output is plotted against the right scale with its dynamic range amplified by two for illustration. The plots illustrate that over the course of the month, load and wind output vary considerably from day to day and throughout the day, but a distinct diurnal cycle in the load can be observed. The wind output does not exhibit similarly strong periodic behavior, but *there is an observable tendency for wind output to be anti-correlated with the load*, i.e. load peaks tend to coincide with wind generation valleys. This is even more clearly illustrated in Figure 3-3 below which plots the average daily profiles[1] of load and 15,000 MW of wind generation for four seasonally representative months: January, April, July and October (see Appendix C.1 for other plots). Note that load is plotted against the left scale and wind generation against the right, amplified by five.

The average daily profiles reveal four general trends with regard to the relationship between load and wind output:

- Wind generation is generally out-of-phase with load during an average day across all seasons. The inverse-phase relationship appears to be stronger in the summer than other seasons, probably due to the heavy use of electric cooling during mid-day periods when wind tends to be less prevalent.
- Wind generation tends to drop sharply in the morning when load is rising quickly, generally between 6 and 9 AM. This tends to be heightened in the spring and summer where the load rise is steeper and more sustained, and the wind down-ramp is greater.
- Wind generation generally increases sharply in the evening when load is dropping. Across all seasons, load tends to rapidly decline between 9 PM and Midnight, during which time, wind output tends to be ramping up quickly.

[1] The average daily profile is created by taking the mean of observations occurring at the same time-of-day across all days of the month, to create a day-long series which reveals broad daily trends in the data over the month -- day-to-day variations and extreme observations are naturally subsumed by averaging

- During winter months, the late afternoon 5-7 PM load rise tends to coincide (roughly) with a general increase in wind production, but it is more variable.

These observations have implications for net-load variability (and operational requirements) at different times of the day and during the various seasons of the year, as discussed later in this section.

Figure 3-4 shows the April load and wind generation series (previously plotted in Figure 3-2) on the same scale, along with the net load resulting from the load-wind combination. To further illustrate the net load variability, a typical day from the same month, April 23rd, is plotted in Figure 3-5. The plots show that the net load shape is similar to the load shape but with some added nuances due to the influence of wind. Wind output produces an offset in the net load that varies in terms of its magnitude and phase. Naturally, the greatest offset is in the early morning when wind output is highest, and the smallest occurs at peak time. A slight shift in the time of peak for net load also occurs, as the minimum wind output does not coincide with the peak load for this day. Across the month, the overall superposition of load and wind output results in periods where the daily range (peak-to-trough measurement) of net load exceeds that of load alone. The result is that the net load ramp rates increase due to wind generation.

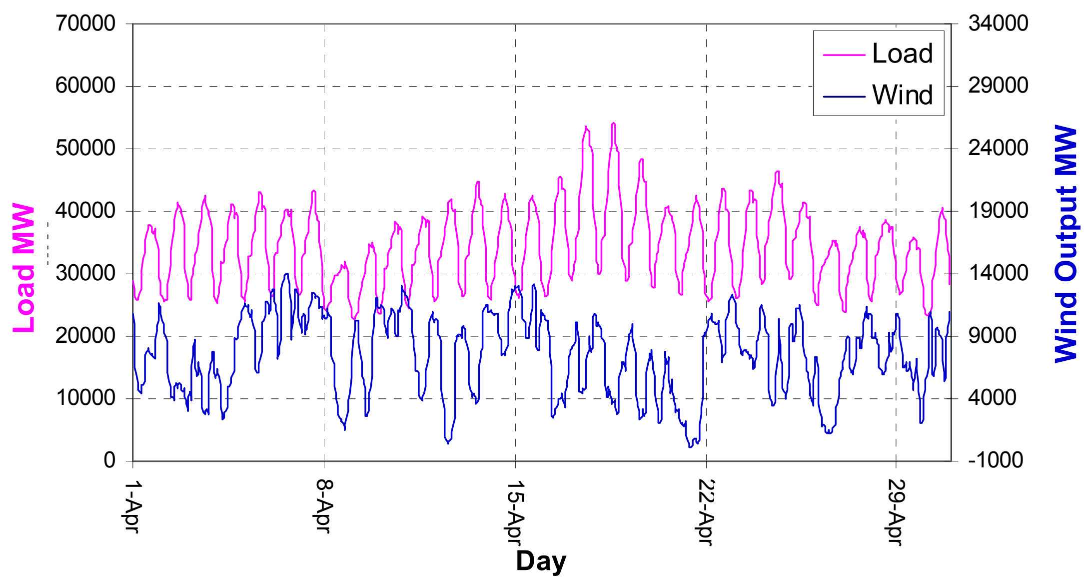

Figure 3-2 - Time series for load and 15 GW of wind generation for April of study year.

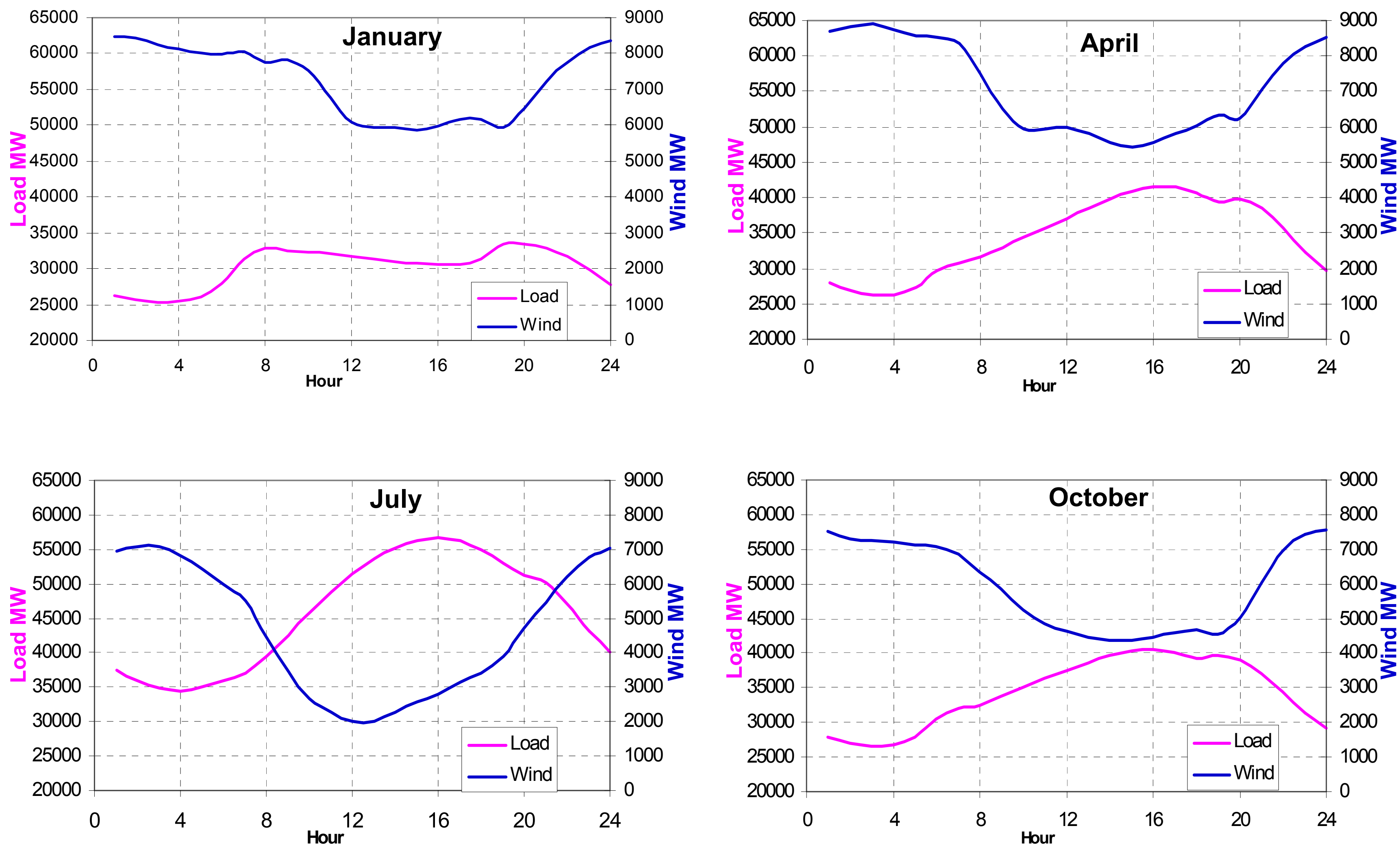

Figure 3-3 - Average daily profiles for load and 15 GW of wind generation for four seasonally representative months

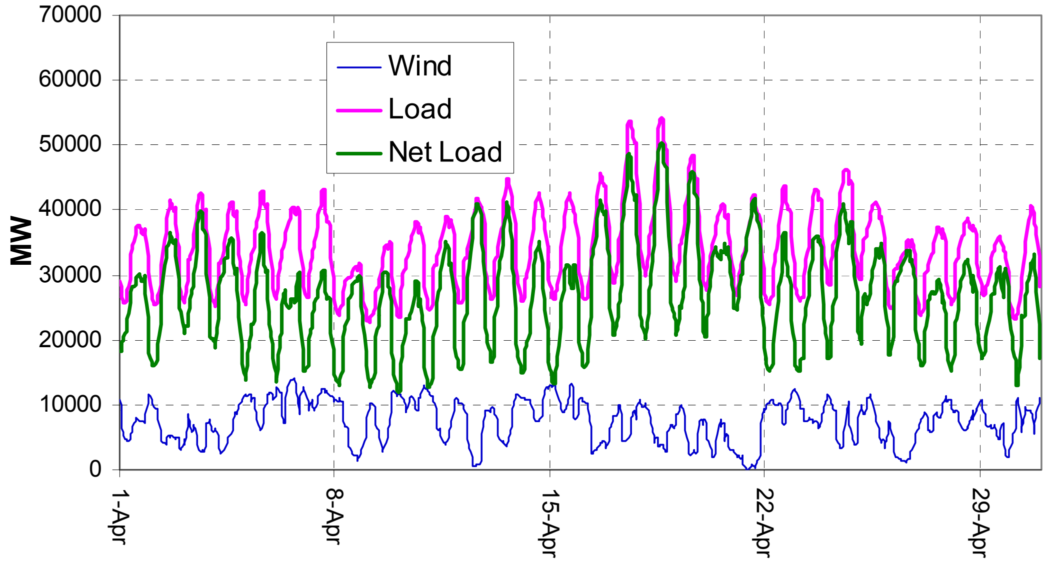

Figure 3-4 - Load, 15 GW of wind generation, and net load for April of study year

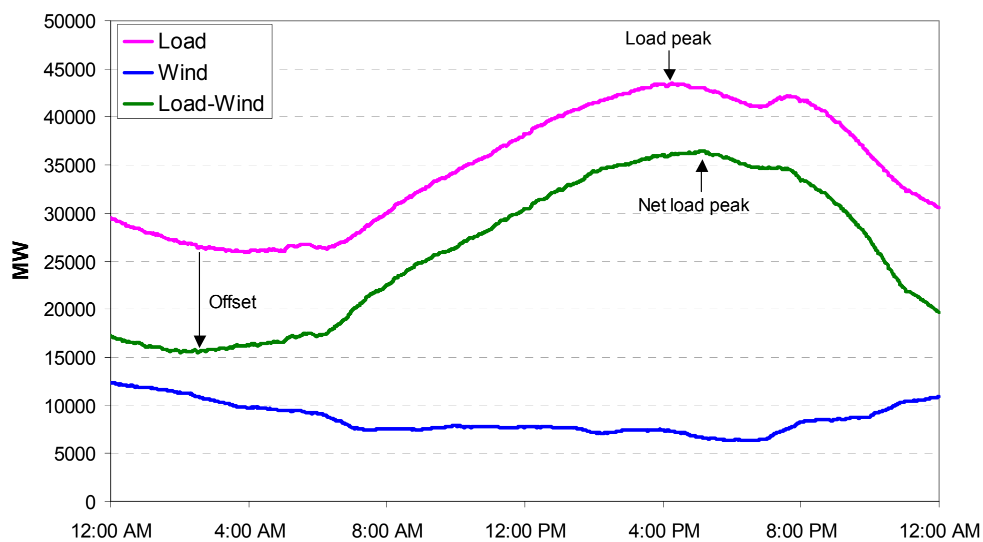

Figure 3-5 - Load, 15 GW of wind generation, and net load for April 23rd of study year

Similarly, higher wind generation penetration would produce larger net load ramp rates. Figure 3-6 plots the net load for the various wind output scenarios for one January week.

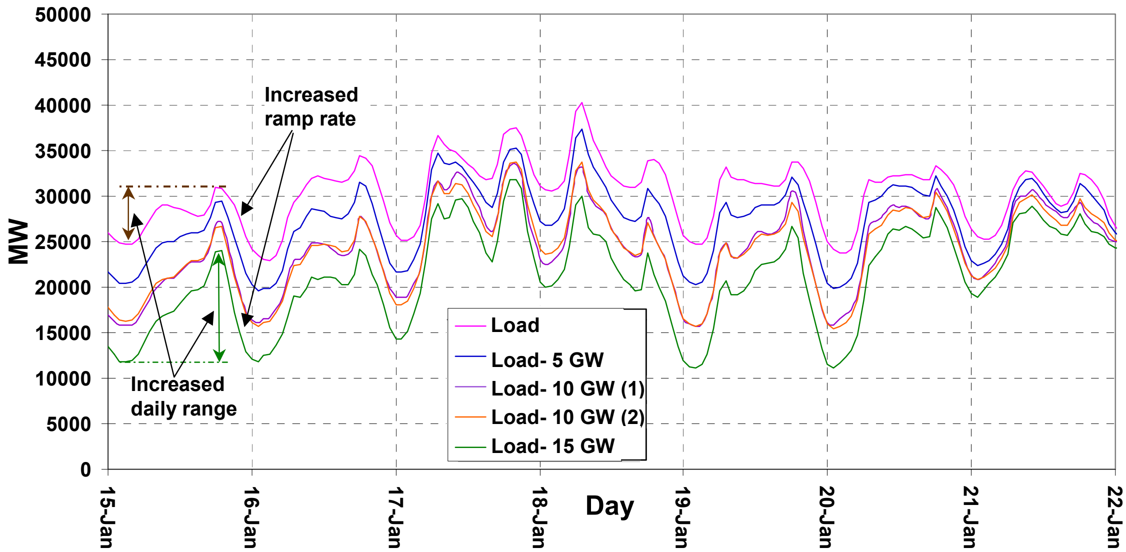

Figure 3-6 - Net load plots for various wind scenarios for a January week of the study year

As expected, the curve shape is relatively similar for all wind generation scenarios, but the daily peak-to-valley changes (range) increases with wind generation, and the period-to-period changes or ramp rates become increasingly larger. This is illustrated by the arrows on Figure 3-6, which highlight the differences in daily range and hourly ramp rate between load alone (no wind generation) and net load with 15,000 MW of wind generation.

Figure 3-7 shows the net load times series for one week in April. During this week, wind generation has less impact on the ramp rates than during the January week in Figure 3-6. However, this plot highlights a very important concept – the importance of load and wind time synchronization when studying net load.

On April 15th, there is a noticeable perturbation in the load which is even more pronounced in net load. Profiles for load, 15 GW of wind, and the net load on April 15th are shown on the bottom-left inset chart. At the time when the load dips, the wind generation increases. This perturbation in both wind and load *at the same time*, likely from common source such as a cold front, causes an even larger drop in net load. These types of phenomena are precisely why load and wind data should be time-synchronized.

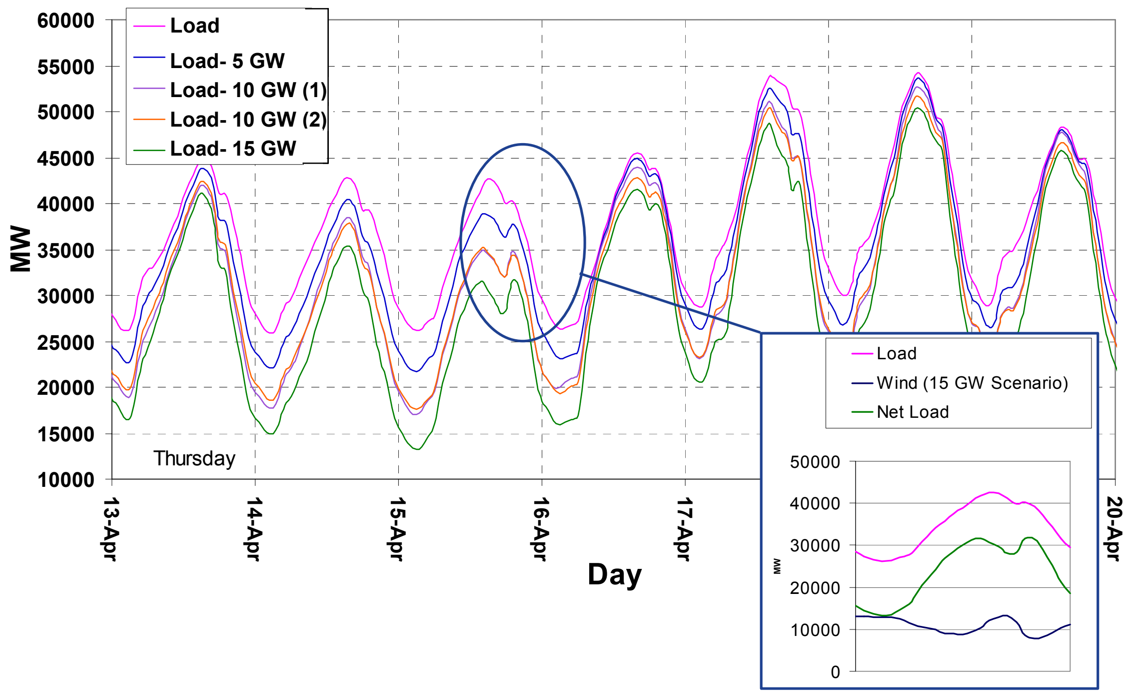

Figure 3-7 - Net load comparisons for an April week of the study year

The following subsections examine net load variability in different timeframes and discusses seasonal and daily trends. In all cases, the key driver is the load and wind coincidence. But seasonal and daily variation in load and wind generation due to lifestyle and meteorological influences, are manifest differently in the net load when it is examined at various levels of resolution, and in different timeframes.

3.2. Variability Over Different Timeframes

The variability of net load in different timeframes impacts various aspects of bulk power system operation. Implications for regulation requirements, ramp and range considerations, operating reserves and unit commitment issues can be drawn from an analysis of net load variability in the 1-, 5-, 15-, 30-, and 60-minute timeframes, depending on the ancillary service definitions and market rules. This section will focus on the statistical analysis of load and net load variability in the various timeframes and reserve a fuller discussion of operation requirements and ancillary services for later Sections.

In this section several terms are used to characterize the load and net load variability. They include:

- Delta (Δ) – The difference between successive data points in a series, or period-to-period ramp rate
- Sigma (σ) – The standard deviation of a dataset or a measure of how dispersed observations are, relative to the mean

Since deltas can be positive or negative depending on the slope of the series at a point in time, the average of the deltas is somewhat meaningless. In fact, for a series of a day or longer, the mean of the deltas is zero or near zero. The standard deviation of the deltas, however, is a good indication of how much the series changes from period-to-period, therefore *sigma of the deltas is used as a measure of variability in this study*. If the deltas are normally distributed (a rational assumption based on experience) then sigma relates to the proportion of deltas within a certain distance of the mean μ, (as illustrated to the right).

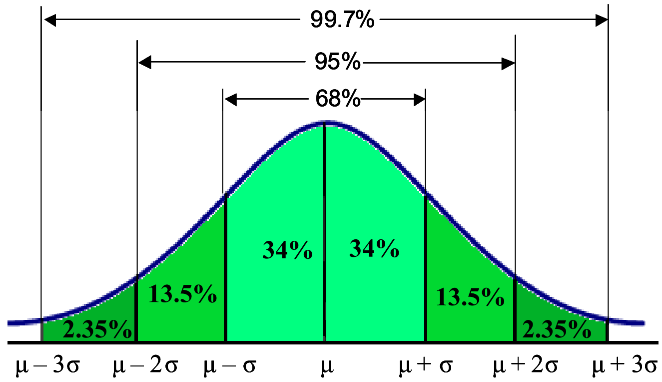

3.2.1. One-Minute Variability

Computing one-minute deltas is the statistical technique known as differencing, or first-differencing to be exact. Differencing, ($x_t - x_{t-1}$), essentially removes the long term trend in the mean, effectively converting a non-stationary time series into a stationary one. A "differenced" series (of deltas) is the first derivative of the original series.

This process is illustrated in Figure 3-8, which shows a three-hour segment of the load on April 23rd of the study year, and the series produced by computing and plotting one-minute deltas. Note that the original series is plotted against the left axis and the deltas are plotted against the right axis, magnified for display.

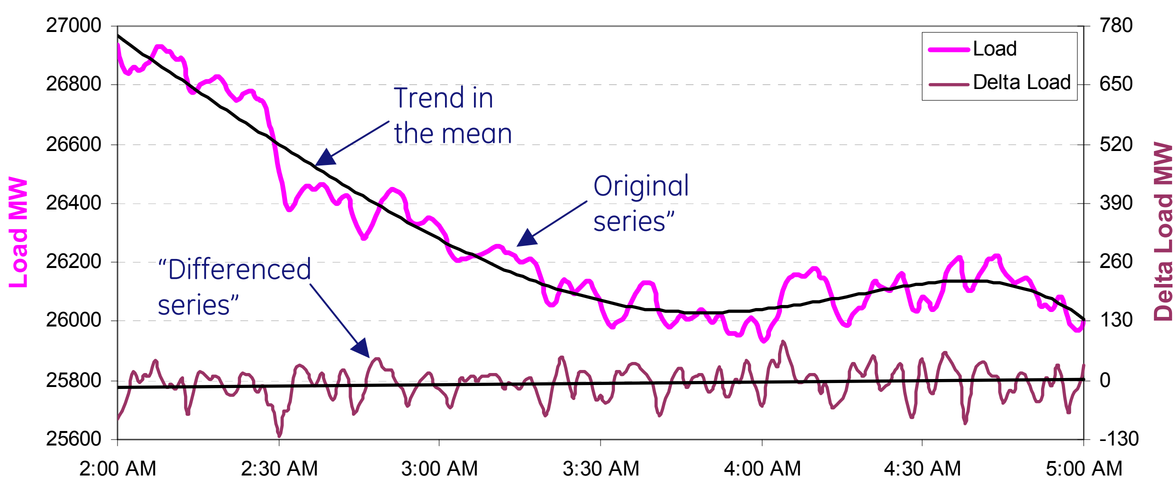

Figure 3-8 - Segment of a load series and the deltas produced by first "differencing"

Experience has shown that in this timeframe, variability of load and net load is driven mostly by "random" jitter in load and wind generation. In between dispatch cycles, these changes must be accommodated by a market-driven ancillary service. The degree to which wind generation increases the variability of net load in the one-minute timeframe (and by proxy ancillary service requirements) is quantified by computing the standard deviation of the deltas. Table 3-2 below summarizes the variability of load and net load in the one-minute timeframe for the entire study year.

Table 3-2 - Summary of One-Minute Net Load Variability for the Study Year

Case	Sigma (σ) of Net Load Deltas (MW/min)	Max. Negative Net Load Delta (MW/min)	Max. Positive Net Load Delta (MW/min)	No. Deltas > 2.5 (load) σ (–/+) (%)	σ % Increase with Wind
Base Case: Load w/ no Wind Generation	43.2	-513.7	491.6	4696 / 3805 (0.89 / 0.72)	**--**
Load w/ 5000 MW Wind Generation	45.6	-526.6	507.2	6181 / 4807 (1.17 / 0.91)	**5.4%**
Load w/ 10,000 MW Wind Generation (1)	47.7	-534.0	529.3	7635 / 6041 (1.45 / 1.15)	**10.5%**
Load w/ 10,000 MW Wind Generation (2)	47.3	-536.7	520.4	7350 / 5757 (1.40 / 1.10)	**9.4%**
Load w/ 15,000 MW Wind Generation	49.7	-552.6	538.3	9277 / 7408 (1.77 / 1.41)	**14.9%**

The results confirm that, overall, the one-minute net load variability *increases linearly* with wind penetration, going from just over 5% with 5 GW of wind generation to about 15% with 15 GW. In this short timespan, the random component of the wind is an incremental component superimposed upon the random load variations.

In addition, the results reveal that the number of "large" one-minute perturbations increases with additional wind generation. This is clearly seen in Figure 3-9 which shows the distribution of one-minute deltas for load-alone, and load with 5000 and 15,000 MW of wind generation for the study year. This was produced by sorting the 525,599 deltas into 15-MW-wide bins and plotting them on a histogram.

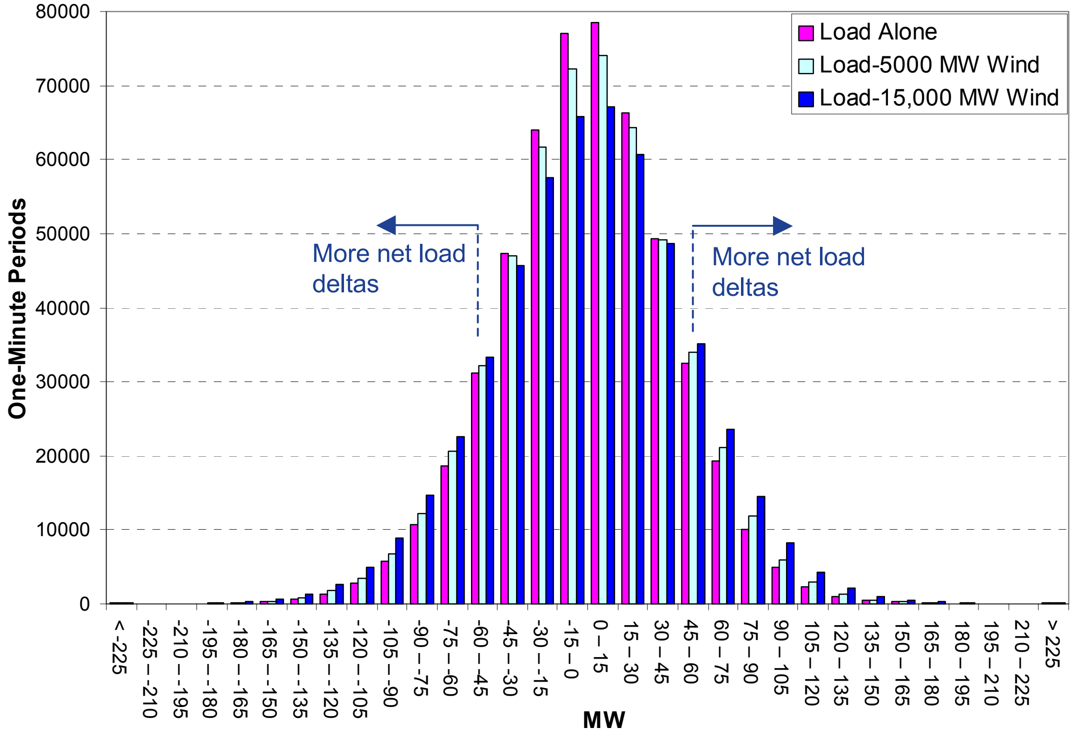

Figure 3-9 - Distribution of 1-minute deltas for load and net load with 5 and 15 GW of wind

On the frequency plot, the arrows indicate that there are more periods when net load deltas (blue bars) are larger than 45 MW/min, than periods when load deltas (magenta bars) are greater than this value. In fact, if 2.5 times sigma-of-the-load-deltas is a threshold for a large change[1], then the number of "large" one-minute down-ramps in Table 3-2 increases by 98% over load-alone, with the addition of 15 GW of wind generation. Similarly, the number of "large" one-minute up-ramps increases by 95%.

Not only does the number of large deltas increase, but the magnitude of extreme deltas also increase with wind generation. This would show up in Figure 3-9 as blue bars on extreme tails of the histogram, if the resolution were sufficiently increased. From Table 3-2, there is an approximately 40 MW/min increase in the largest down-ramp going from the no-wind case to the 15-GW wind generation case; and similarly, a 47 MW/min increase in the largest up-ramp. The same observations generally apply to the previous year's data. See Appendix C.2 for additional data and plots.

To summarize, in the one-minute timeframe, incremental wind output increases not only the overall net load variability but also the amount and size of large and extreme deltas.

[1] In a normal distribution of deltas, 98.8% of the area under the normal curve is within 2.5σ of the mean.

3.2.2. Five-Minute Variability

Five-minute time series for load and net load are produced by integrating the one minute data series. For every five minute block (or every five one-minute observations) a five-minute data point is produced by averaging the five one-minute samples. This produces one-year load and net load series with 105,120 observations each. Five-minute deltas for load and net load can then be computed in the same manner as with one-minute deltas.

Understanding variability in five-minute timeframe is important because in the nodal market units will be dispatched every five minutes. The additional operational burden imposed by wind in this timeframe will certainly translate into more ramp and range requirements for units on dispatch.

As the resolution decreases (i.e. in larger timeframes), the impact of the long term ramps in load and wind generation becomes more evident, and the impact of "random" jitter becomes less important.

Table 3-3 summarizes the variability of load and net load in the five-minute timeframe. Figure 3-10 plots the distribution of five-minute deltas for the entire study year.

Table 3-3 - Summary of Five-Minute Net Load Variability for the Study Year

Case	Sigma (σ) of Net Load Deltas (MW/5-min)	Max. Negative Net Load Delta (MW/5-min)	Max. Positive Net Load Delta (MW/5-min)	No. Deltas > 2.5 (load) σ (–/+) (%)	σ % Increase with Wind
Base Case: Load w/ no Wind Generation	167.4	-881.2	958.8	621 / 787 (0.59 / 0.75)	**--**
Load w/ 5000 MW Wind Generation	177.3	-916.6	988.9	1007 / 977 (0.96 / 0.93)	**5.9%**
Load w/ 10,000 MW Wind Generation (1)	188.0	-951.1	992.1	1482 / 1368 (1.41 / 1.30)	**12.3%**
Load w/ 10,000 MW Wind Generation (2)	185.2	-938.3	1002.4	1353 / 1273 (1.29 / 1.21)	**10.6%**
Load w/ 15,000 MW Wind Generation	197.1	-948.2	1022.2	1970 / 1856 (1.87 / 1.77)	**17.8%**

In this timeframe, the same general trends observed in the one-minute data with regard to sigma and large deltas can be observed. Incremental wind generation increases the overall net load variability (as measured by sigma of the deltas), as well as the number and magnitude of large period-to-period changes. However, a closer comparison of the one-minute and five-minute timeframes lead to several observations:

1. The standard deviations, sigma (σ), of the deltas are (as expected) larger in the five-minute timeframe, but *not* five times as large as the one-minute sigma.

2. For each wind generation scenario, the increase in net load variability over the load-alone case, in the five-minute timeframe, is larger than the corresponding scenario in the one-minute timeframe, i.e. *there is an additional component to five-minute variability.*

3. The *relative* (%) increase in the number of net load outliers over load-alone is greater in the five-minute timeframe, even though the *relative* increase in the size of the largest delta is comparable.

4. The distribution of the five-minute net load deltas is decidedly less bell-shaped (more triangular) than the distribution of one-minute net load deltas. This implies the presence or influence of a non-random source of variation.

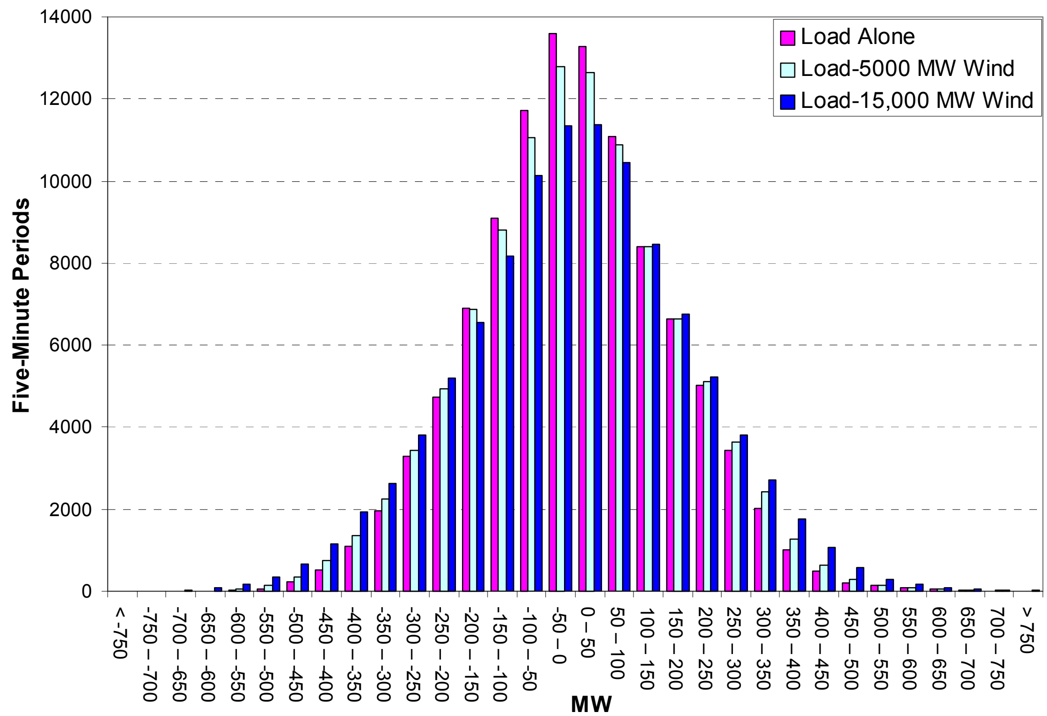

Figure 3-10 - Distribution of 5-minute deltas for load and net load with 5 and 15 GW of wind generation capacity.

These observations become even more pronounced in longer timeframes as the influence of short-term random variations begin to be dominated by the long-term ramp. This can be seen in the results for the fifteen minute and half-hour timeframes which are included in Appendix C.2.

3.2.3. Effect of Short Term Variations and Long Term of Ramping

Based on observations of net load variability over various timeframes from one minute to one hour (and longer) two general observations are:

- Variations over timespans greater than five minutes are primarily due to load cycle or long-term ramping, which dominate random noise variations
- Random "noise" variation is more influential during shorter timespans

Consider the Figure 3-11 below which shows a portion of the summer load pickup period, July 10, 6-7 AM on of the study year. The solid magenta and blue traces are load and net load series, plotted against the left scale, and the dotted magenta and blue traces and load and net load one-minute deltas, plotted against the right scale. Figure 3-12 shows the load and net load deviations from a straight line, i.e. load and net load with ramp component removed.

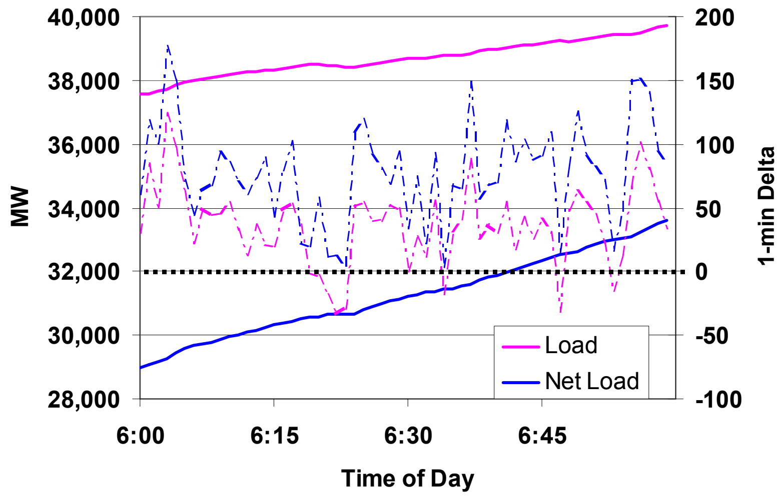

Figure 3-11 - Load and net load traces with 1-min deltas for July 10, 6-7 AM

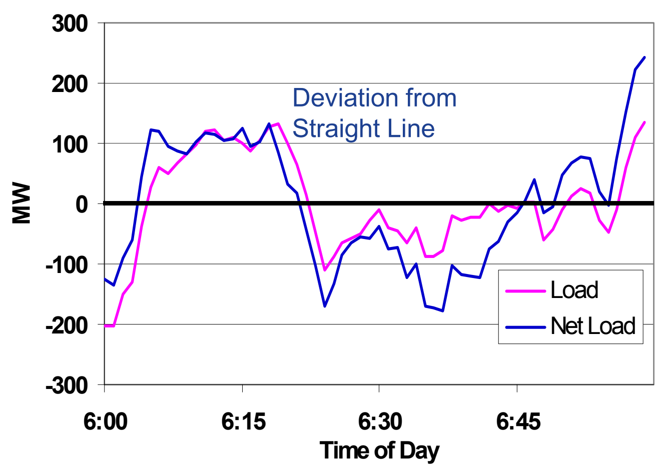

Figure 3-12 - Load and net load deviations from a straight line for summer morning period

Over the hour, load and net load vary randomly from minute to minute even while ramping steadily. The one-minute deltas in Figure 3-11 represent the minute-to-minute variation, which is essentially random noise variation with a small adder due to the portion of the long-term (hour) ramp that occurs in the minute. The effect of the ramp component is to bias the net load deltas and create incremental differences from the load deltas. Figure 3-12 illustrates without the long-term ramp component, load and net load variation exhibit similar characteristics, driven by stochastic load and wind variation.

During a light load period such as the early spring morning shown in Figure 3-13, load and net load may be fairly flat (little or no ramp). Consequently, the load and net load one-minute deltas (dotted magenta and blue traces) are more similar because the impact of the ramp component is reduced. Figure 3-14 shows the deltas without the ramp.

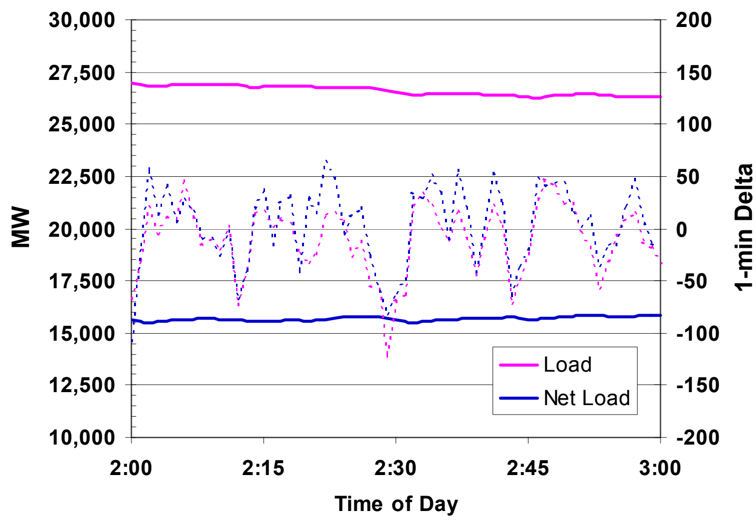

Figure 3-13 - Load and net load traces with 1-min deltas for April 23, 2-3 AM

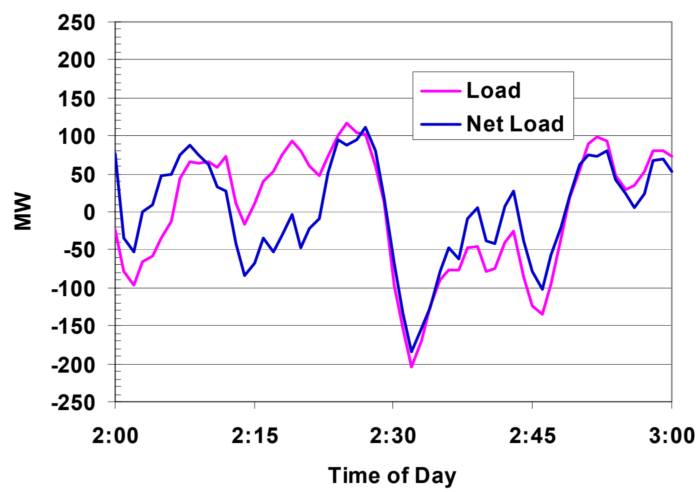

Figure 3-14 - Load and net load deviations from a straight line for light load period

As the timeframe becomes longer, the ramp component has a greater effect on the deltas because the portion of the ramp that occurs in a longer timeframe is greater. For the five-minute timeframe, the long-term ramp adder is five times as large as in the one-minute timeframe, but there is still a significant contribution from stochastic noise variation. However, by for fifteen minute timespans and greater, the deltas are dominated by the long-term ramp component (as summarized in Appendix C.2). The next section discusses variability in the one-hour timeframe, which is almost completely driven by the load and wind generation ramp rate.

3.2.4. Hourly Variability

The one-hour timeframe gives a good indication of the long term ramping requirements due to additional wind generation. At this resolution, the random perturbations of load and net load are less significant and long-term ramping dominates the net load variability. Table 3-4 summarizes one-hour load and net load variability for the study year. The results in Table 3-4 are consistent with observations in other timeframes; namely as wind penetration increases, the net load variability (as measured by sigma of the one-hour deltas) increases linearly. However, in this case, wind generation adds to variability primarily because it creates larger daily net load swings.

Table 3-4 - Summary of One-Hour Net Load Variability for the Study Year

Case	Sigma (σ) of Net Load Deltas (MW/hr)	Max. Negative Net Load Delta (MW/hr)	Max. Positive Net Load Delta (MW/hr)	No. Deltas > 2.5 (load) σ (–/+) (%)	σ % Increase with Wind
Base Case: Load w/ no Wind Generation	1758	-4838	5203	43 / 26 (0.49 / 0.30)	--
Load w/ 5000 MW Wind Generation	1867	-5813	5461	94 / 42 (1.07 / 0.48)	6.2%
Load w/ 10,000 MW Wind Generation (1)	1989	-6124	5797	127 / 85 (1.45 / 0.97)	13.1%
Load w/ 10,000 MW Wind Generation (2)	1954	-6175	5681	119 / 69 (1.36 / 0.79)	11.2%
Load w/ 15,000 MW Wind Generation	2086	-6726	6240	170 / 134 (0.94 / 1.53)	18.7%

Figure 3-15 shows the distribution of one-hour deltas for load-alone, and load with 5 GW and 15 GW of wind generation. This was produced by sorting the 8759 deltas into 400-MW-wide bins and plotting them on a histogram. The impact of the non-random ramp component can be seen in the frequency plot. As the timeframe becomes longer, the frequency plot of deltas becomes increasingly more triangular, than bell-shaped.

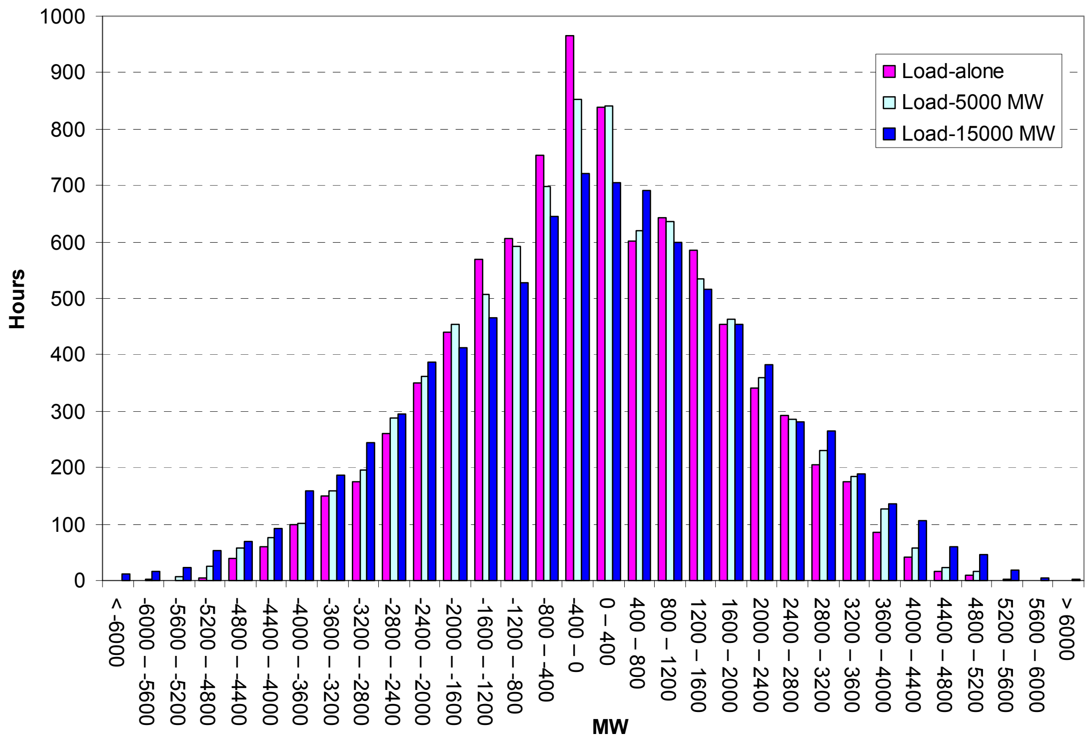

Figure 3-15 - Distribution of 1-hour load and net load deltas with 5 GW and15 GW of wind

The number and size of the extreme deltas also increases with additional wind generation. In accordance with the trend over timespans, the increase in the number of "large" deltas as wind penetration increases is greater in this time frame than previous timeframes. The next section examines this and other trends in variability over timeframes.

3.2.5. Trends in Variability over Timeframes

We have seen that in the one-minute timeframe, load and net load variability are driven primarily by random perturbations. As the timeframe becomes longer, the influence of the long-term ramp in load and wind generation has greater influence on period-to-period variability. Figure 3-16 plots the standard deviation of deltas for the wind generation scenarios over the one-minute, five-minute, fifteen-minute and one-hour timeframes. Figure 3-17 plots the normalized sigma for each timeframe in MW/min [2]. In both plots, the data points for each timeframe are fitted with a linear trend line to show the variation as wind penetration increases.

Both plots show that in each timeframe, the variability (sigma) increases linearly with wind penetration (as detailed in earlier data tables). The slope (from no wind generation to 15 GW) is relatively shallow, and *appears* to be more or less constant over all

[2] Sigma is normalized by dividing by the timespan to give sigma in MW/min (e.g. $\sigma_5/5$)

timespans in Figure 3-16. The normalized plot more clearly illustrates the increase and its linearity.

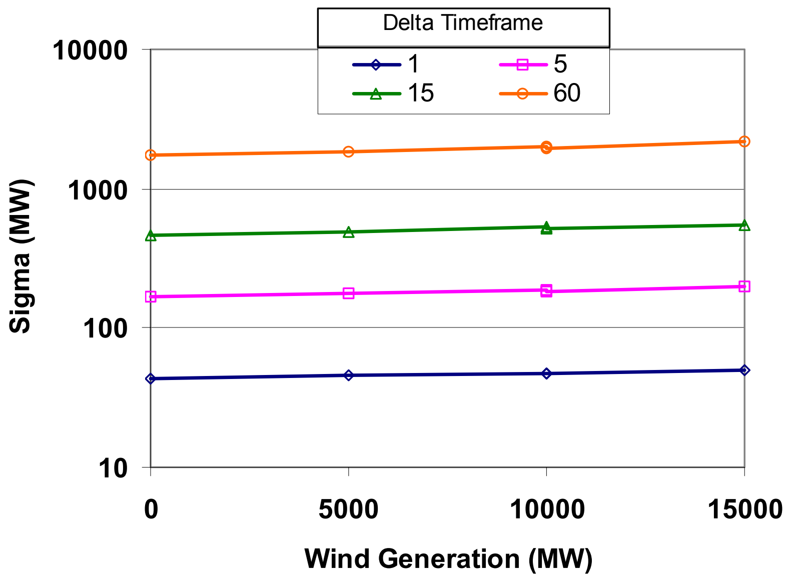

Figure 3-16 - Variability as a function of wind penetration

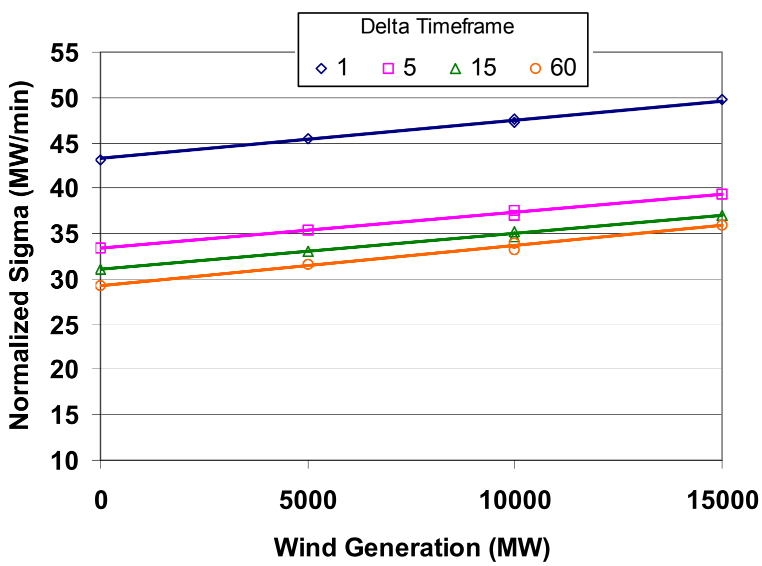

Figure 3-17 - Normalized variability as a function of wind penetration

Figure 3-18 shows a plot of normalized sigma *versus timespan* on a log scale. In this plot there is a distinct change in the slope of the normalized sigma trace as the timespan increases. The change occurs somewhere between the 5 and 15 minute timeframes. This is consistent with the observation that there is a baseline of variability that is a function of the longer-term load cycle, and an incremental amount of variation due to random noise appears at the shortest timeframes (1 and 5 minute).

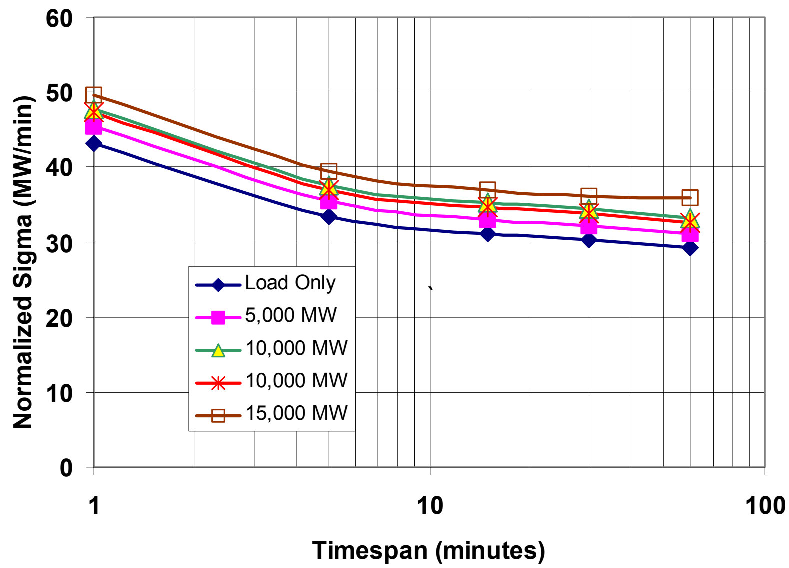

Figure 3-18 - Normalized variability as a function of timespan

Figure 3-19 shows the incremental variability (relative to load alone) due to wind generation in each timeframe. As the timespan becomes longer, the incremental variability increases, but begins to taper off, and appears saturate at longer timeframes.

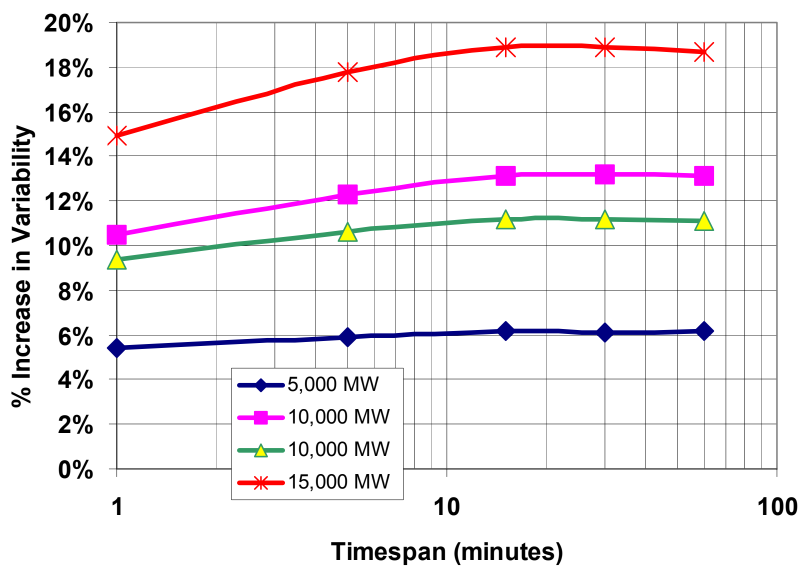

Figure 3-19 - Increase in variability due to wind as a function of time span

The key take-aways from the analysis of variability over the various timeframes are: (1) incremental wind generation causes a linear increase in period-to-period variability over all timespans, (2) in longer timespans variability is primarily driven by load cycling, but in shorter timespans there is an incremental component due to stochastic variation, and (3) the impact of wind generation on variability is more significant in longer timespans because wind generation creates larger swings in daily net load.

3.3. Seasonal Trends in Variability

Over the course of a typical year, load and net load vary with the seasons, as they are both largely driven by common weather-related factors. Therefore, some seasonal trends in period-to-period variability are expected. Figure 3-20 shows the daily average load and net load with 15 GW of wind generation over the study year, and the maximum positive and negative net load one-hour deltas for each day of the year. The upper solid magenta and blue traces are load and net load respectively. The two lower solid green traces are maximum positive and maximum negative one-hour net load deltas. The two lower dotted orange traces are maximum positive and maximum negative one-hour load deltas.

As expected, load and net load are greatest in the summer months and lowest in the spring and fall. The peak load day is August 17th and the minimum load day is March 27th. Across the year, incremental wind generation generally biases the net load, and increases the variability. The negative net load deltas or hourly down-ramps (lower green trace) generally tend to be larger in the late spring, summer, and early fall, while the up-ramps (upper green trace) are generally larger in late fall and winter. However, when the load deltas (dotted orange traces) are compared with net load deltas, it is clear that the *incremental* net load hour-to-hour change is greatest in the late spring and summer.

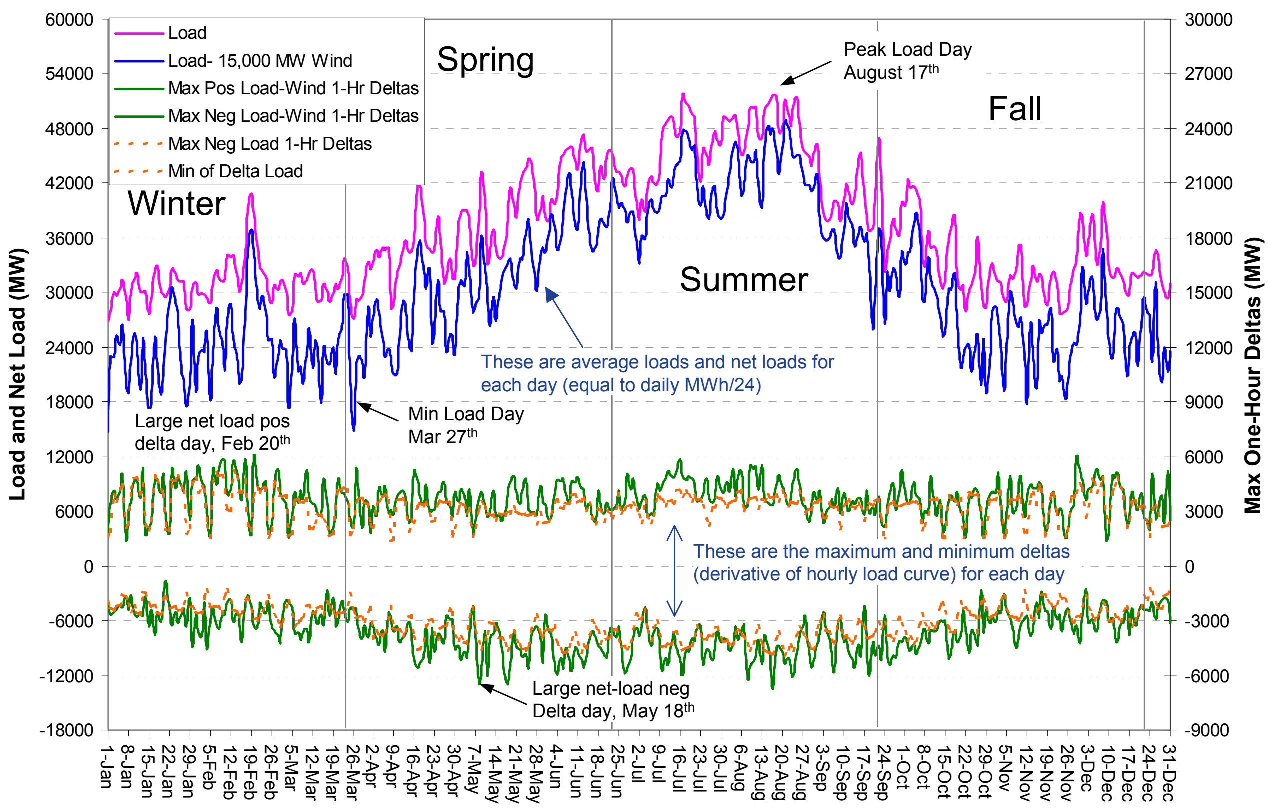

Figure 3-20 - Profiles of daily average load and net load, and maximum daily 1-hour deltas

The impact of wind generation throughout the year can be more clearly seen from an examination of a few “interesting” days from Figure 3-20. For example, load and net load variability on the peak load day (August 17th) and minimum load day (March 27th) are plotted in Figure 3-21 and Figure 3-22 for the 15-GW wind generation scenario.

Wind output has relatively little impact on the peak day, reducing the peak by about 3000 MW and shifting it by approximately 1 hour. On the minimum load day, wind generation pushes the minimum load point to a “very low” value and the ramp rate during load rise is increased. Key questions are what units are committed during this period, and do they have the required ramping capability? This issue is further explored in Section 6.

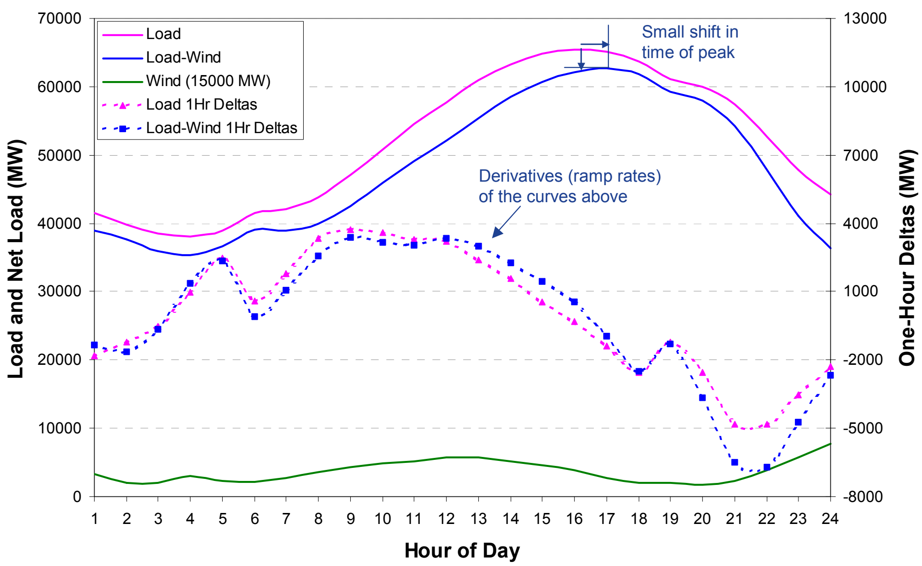

Figure 3-21 - Variability on peak load day

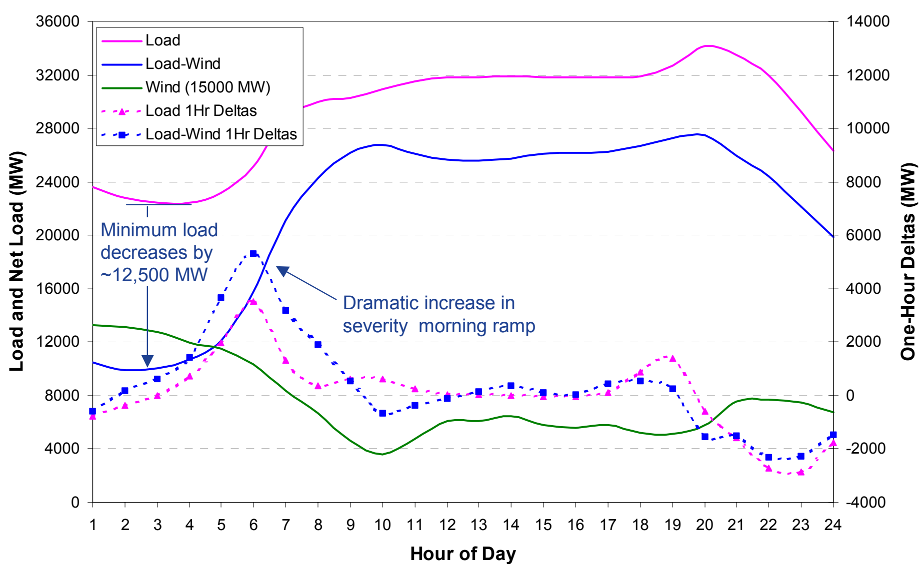

Figure 3-22 - Variability on minimum load day

Another interesting day is May 8th during which the largest net load one-hour down-ramp occurs. Figure 3-23 shows that wind generation drops precipitously in evening just before the evening load roll-off, causing a later than expected peak in net load, with resulting increases in hourly ramp rates.

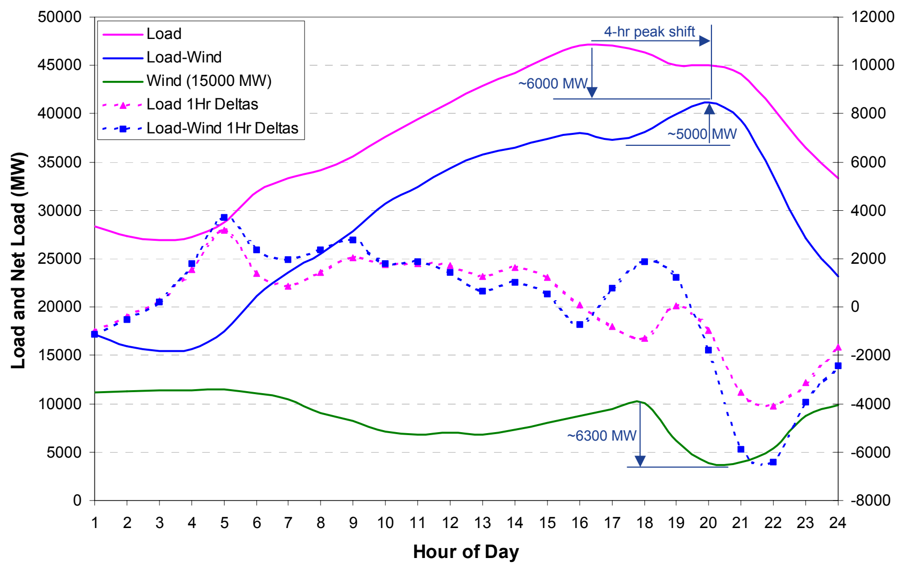

Figure 3-23 - Variability on the day with the largest net load 1-hour negative net load delta

July 12th is the day during which net load undergoes the largest hourly up-ramp and down ramp event in the same day. Figure 3-24 shows that severe anti-correlation of diurnal load and wind output curves causes large, sustained morning and evening ramps.

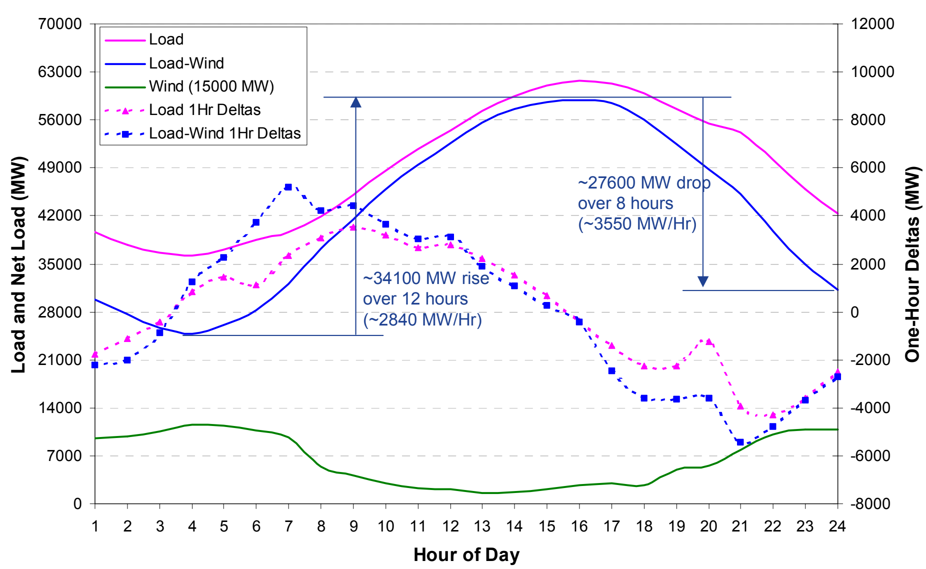

Figure 3-24 - Variability on the day with the largest net load 1-hour up-ramp and down-ramp

Another way to examine seasonal differences in load and net load variability is to look at typical winter, spring, summer, and fall days for broad trends. The plots in Figure 3-25 (next page) show load and net load variability during "typical" seasonal days for the 15-GW wind generation scenario. The representative seasonal days, January 27th, April 23rd, July 10th and October 25th were selected based on the fact that they did not significantly deviate from seasonal or expected averages.

On the plots, the solid magenta, green and blue traces are load, wind generation and net load respectively plotted against the right scale. The dotted magenta and blue traces are load deltas and net load deltas plotted against the left. Note that the scales for the typical summer day plot are different from the other three plots for display purposes.

Since these typical plots are merely snapshots of the seasonal variability, one should be careful when drawing broad inferences. However, from a macro perspective, the plots conform with previous observations: hour-to-hour changes (deltas) are generally larger in the summer, and there tends to be larger differences between load deltas and net load deltas for the non-winter days.

The bottom line from an analysis of the seasonal trends in variability is that wind generation tends to have a greater overall impact on variability in the summer, late spring and early fall, but variations in winter and early spring may be more operationally significant due to low net load levels.

Additional operational challenges may be created during periods where wind generation aggravates balance of generation ramp and range requirements. Some of these periods that may impact ancillary service requirements are discussed in the next two sections.

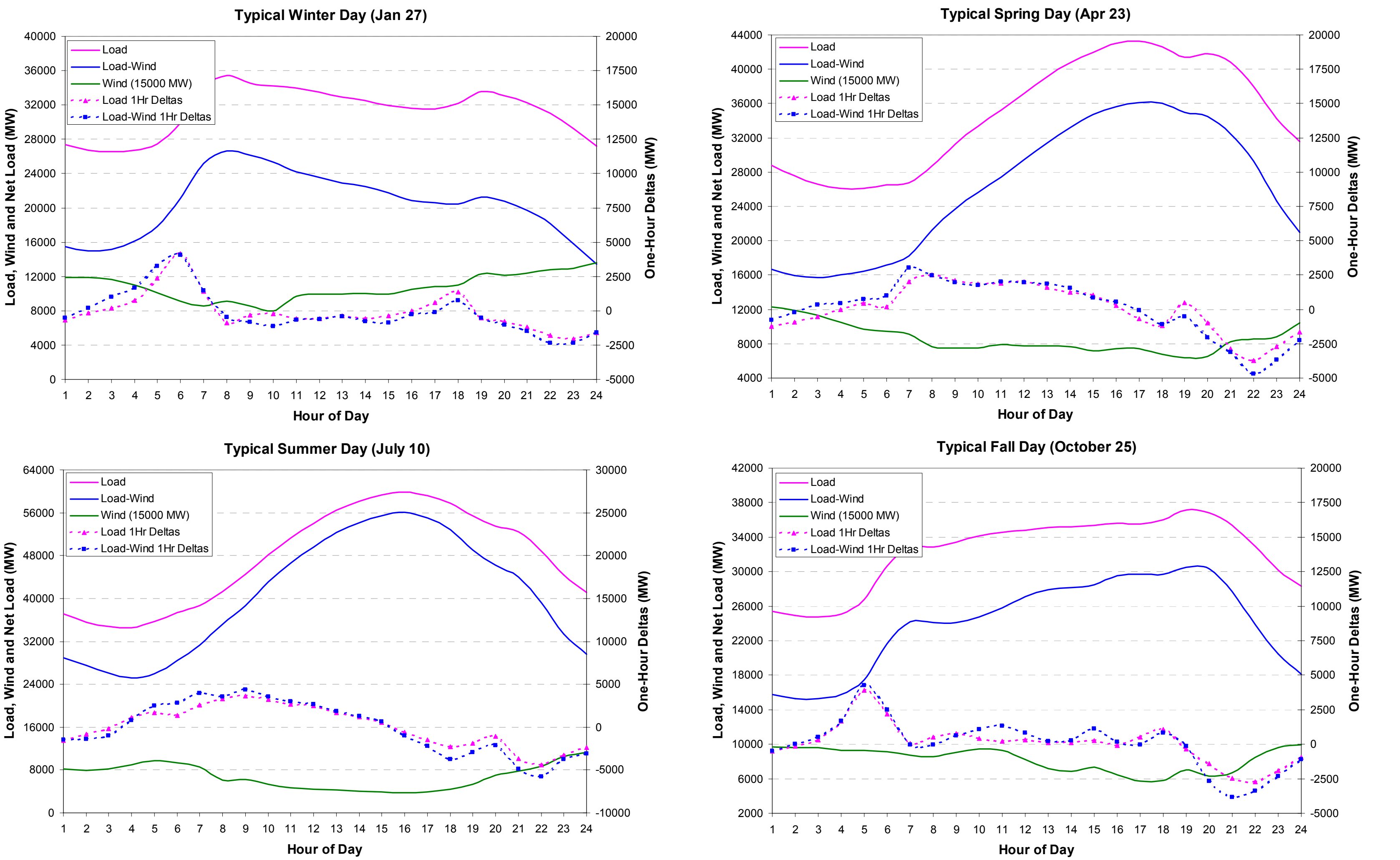

Figure 3-25 - Variability of load and net load with 15,000 MW of wind generation for typical seasonal days

3.4. Variability by Load Level

The ability of the system to accommodate net load variations is largely a function of the absolute net load level. System maneuverability tends to increase with the generation level because variations of a given magnitude are larger in proportion to the committed generators and units lower on the dispatch stack tend to be base load units that are less maneuverable. This section will examine the correlation of net load variability with load levels throughout the year. For clarity and brevity, most of the charts and discussion will focus on the largest wind generation scenario, 15,000 MW, but information on the other wind generation scenarios is included in Appendix C.3.

Figure 3-26 shows the cumulative distribution of wind generation and instantaneous wind penetration over the entire study year. The magenta trace is the total wind output for the 15 GW scenario, plotted against the left scale. The blue trace is the instantaneous wind penetration[1] plotted against the right scale. Both series of 8760 observations are sorted independently and plotted. Each point on the curves gives the number of hours of the year when wind output or wind penetration is at or above a certain value.

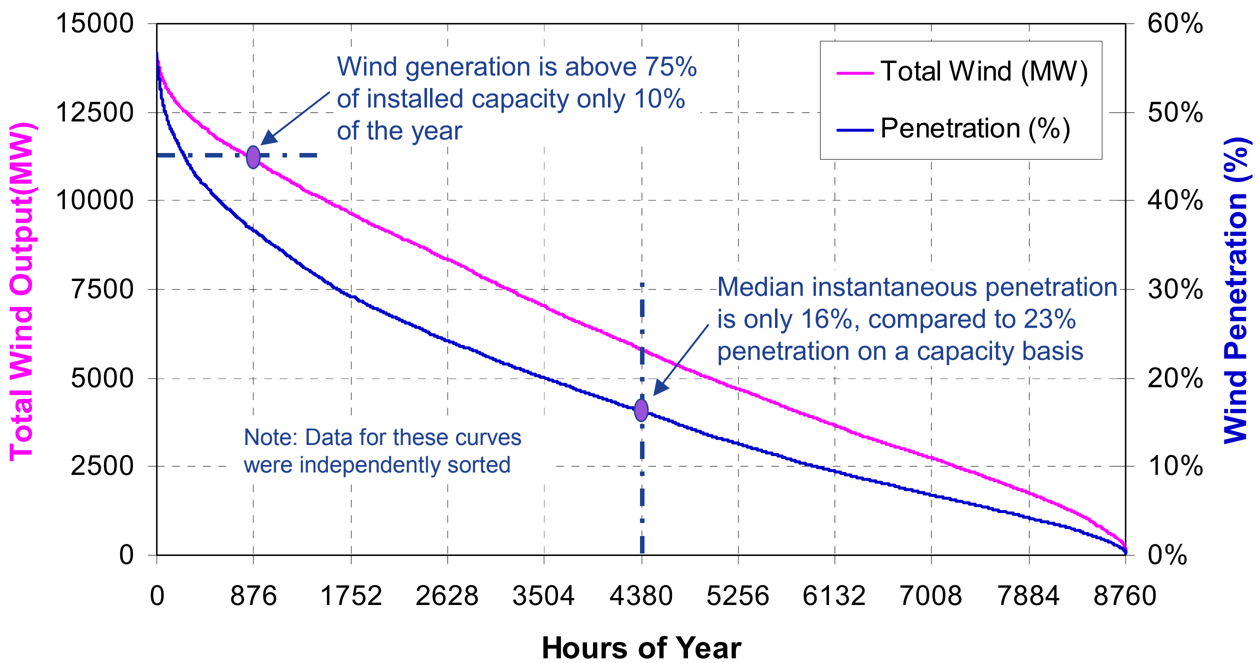

Figure 3-26 - Wind output duration and instantaneous penetration (15,000 MW)

For this wind generation scenario, there are a few hours of the year when the instantaneous wind penetration is over 50%. No doubt, this corresponds to minimum load periods, which tend to be operationally challenging (discussed later in this section).

[1] The instantaneous wind penetration is the wind generation at a particular hour divided by the load at that hour, expressed in percent.

Table 3-5 summarizes the maximum instantaneous wind penetration for all wind generation scenarios.

Table 3-5 - Maximum Instantaneous Wind Penetration for each Scenario

Wind Scenario (MW)	5000 MW	10,000 MW (1)	10,000 MW (2)	15,000 MW
Instantaneous Wind Penetration (%)	20%	39%	38%	57%

On a seasonal or monthly basis, there are considerable differences in wind duration and instantaneous penetration. Figure 3-27 and Figure 3-28 show duration plots for the peak load month, August, and the minimum load month, March for the 15-GW wind generation scenario. Additional duration plots are included in Appendix C.3.

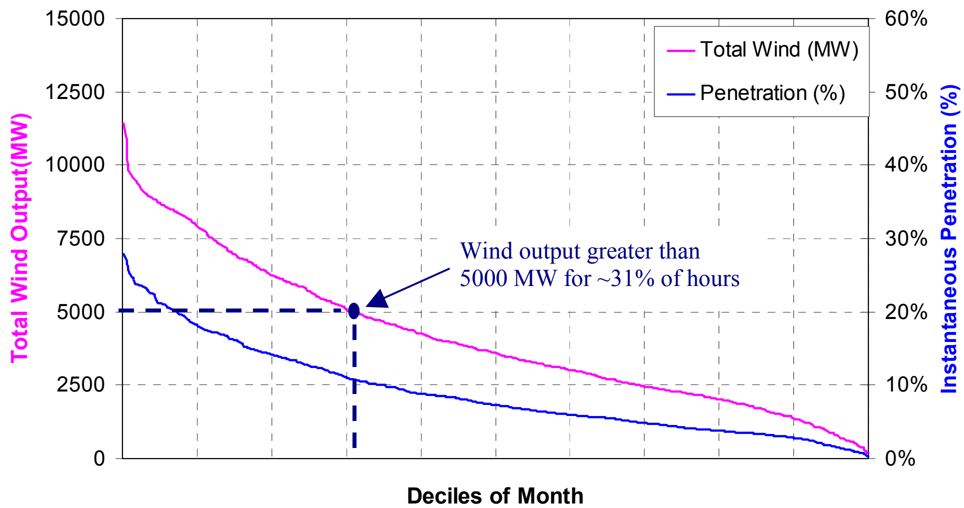

Figure 3-27 - 15 GW wind output duration and penetration for peak load month (August)

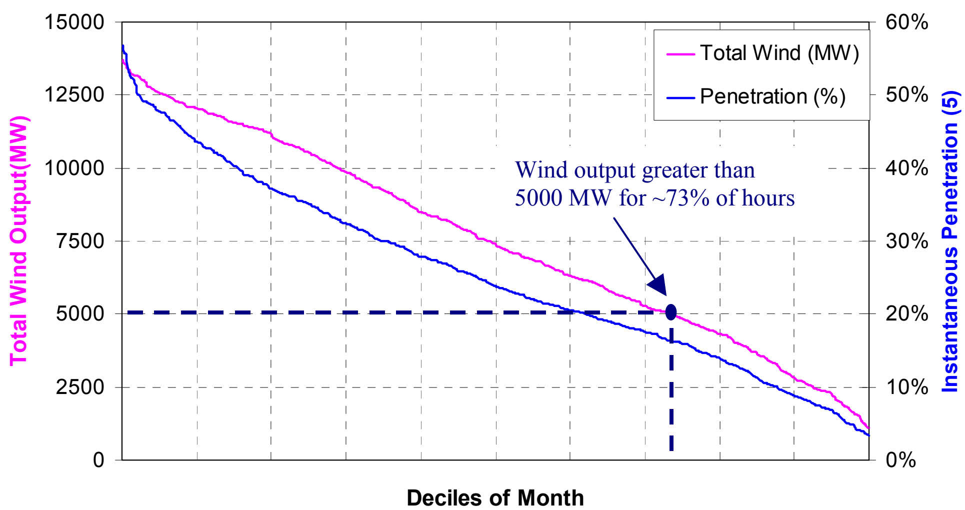

Figure 3-28 - 15 GW wind output duration and penetration for minimum load month (March)

The plots show that the instantaneous wind penetration is smallest at peak load (28%) and greatest at minimum load (57%), as expected. The load is greatest during the summer months and wind generation tends to be less during the mid-day peak load hours. In fact, total wind output is *less* than one-third rated capacity for about 70% of the hours in August. Conversely, at minimum load, the highest level of instantaneous wind penetration is seen, because wind output tends to be high in the very early morning hours when load is the lowest. For the month of March, total wind output is *greater* than one-third rated capacity for approximately 70% of the hours.

Considering the fact that wind penetration is higher at low load hours and lower at peak load hours, the question is, how does net load variability change with load level? The box and whisker plot in Figure 3-29 attempts to answer this question by charting load and net load variability at various load levels.

The chart is based on one-hour load and net load deltas (hour-to-hour changes) during the hours when the load level is in a particular decile. The top 10% of load hours (peak load) are in decile 1 and the bottom 10% (low load) are in decile 10, i.e. load level decreases from left to right. The length of the solid rectangular boxes represents a spread of one standard deviation (σ) around the mean of the deltas, and the dashed rectangular boxes represent a spread of 2.5σ. Hence, the longer the box, the greater the variability at that load level. The whiskers show the maximum up-ramps and down-ramps for the deciles.

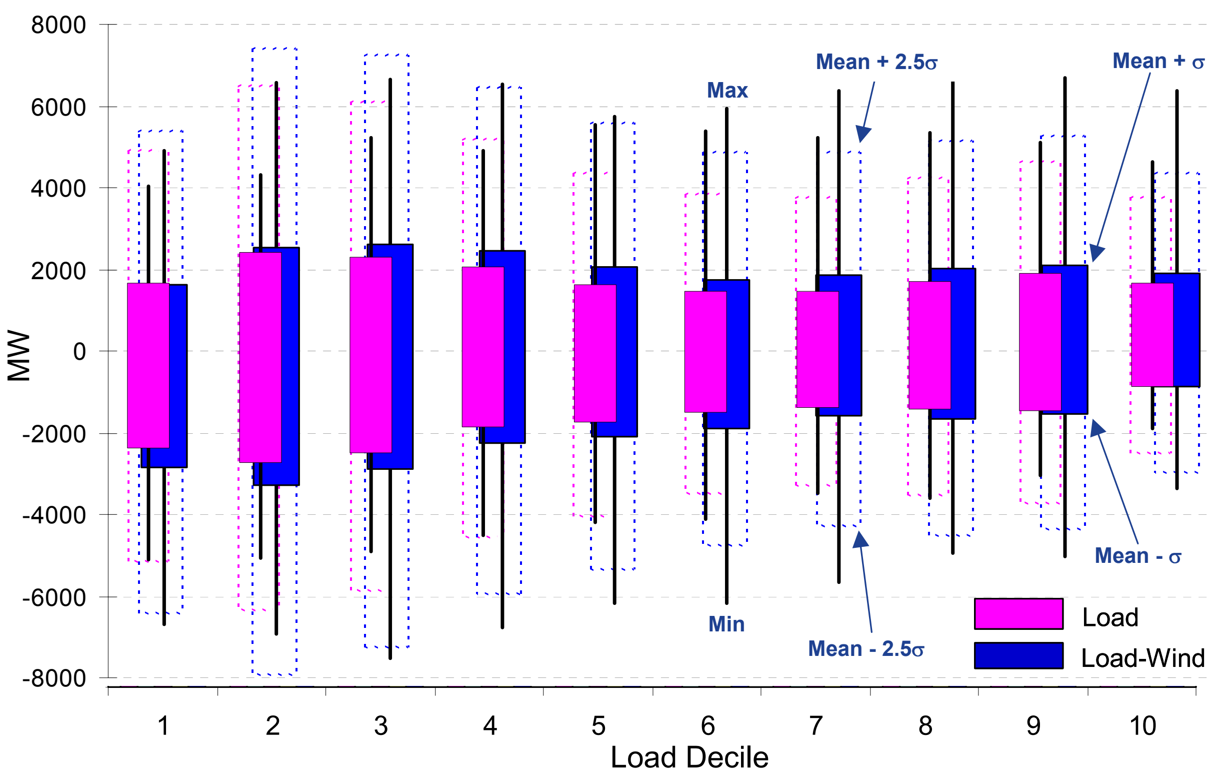

Figure 3-29 - Load and net load variability by load level for the 15 GW scenario

Considering the "whiskers" or max/min bars, it appears that wind generation increases the maximum up-ramps and (particularly) down-ramps at high and low load levels more than at mid-range load levels. The opposite seems to hold for variability. Comparing the magenta boxes (load-alone) to the blue boxes (net load with 15 GW of wind generation), there appears to be relatively little *incremental* variability due to wind output at the highest load levels and lowest load levels. Wind generation tends to have marginally more impact on variability at mid-range load levels. However, at low load hours, there are likely fewer dispatchable generators to accommodate the variability.

Figure 3-30 gives another view of the variability at different load levels by plotting the standard deviation of the one-hour deltas for load and net load.

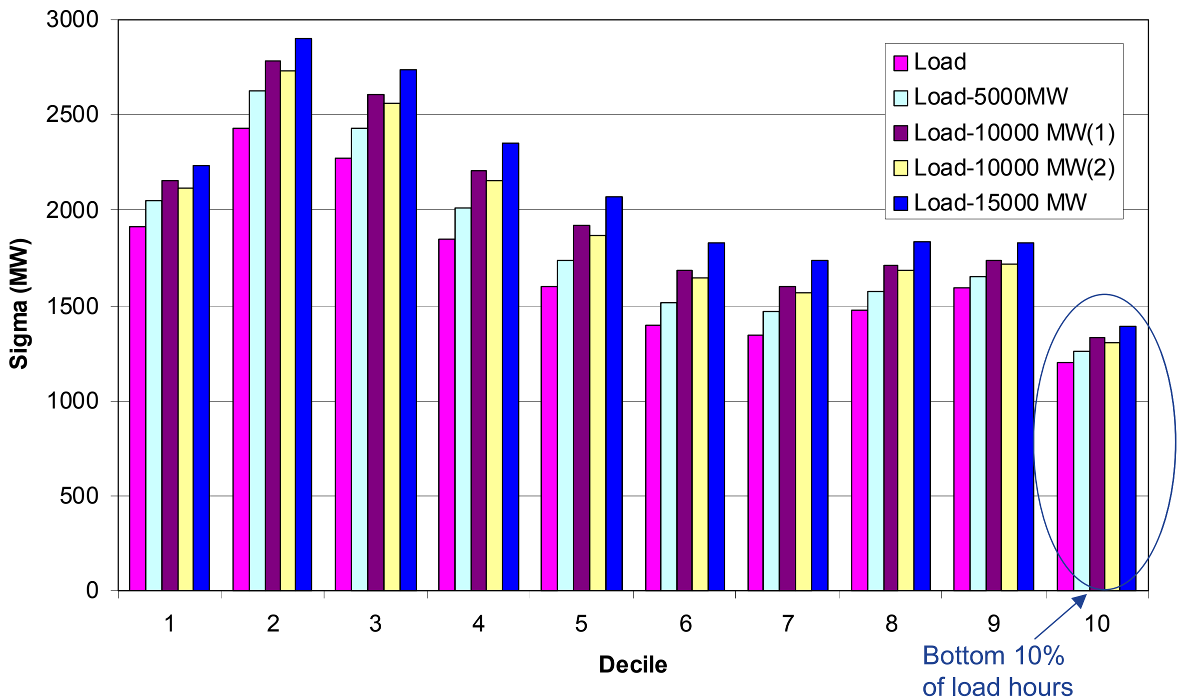

Figure 3-30 - Standard deviation of hourly deltas by load level

As wind penetration increases, the variability at the lowest 10% of load levels increases only slightly. As observed earlier, there are larger increases in variability at the mid-range load levels, but the low load period is operationally significant because flexible units might normally be de-committed during these hours.

Large amounts of wind generation online during low load hours would tend to push the "normal" minimum load point even lower, making the (economic) balance of generation mix even less flexible. Regardless of the capability of the system to maneuver at low load levels, there is potentially a point when the minimum net load is so low that non-conventional means may be needed to accommodate variability during these hours.

Figure 3-31 and Figure 3-32 illustrate the impact of increasing amounts of wind generation on net load, especially during low load hours.

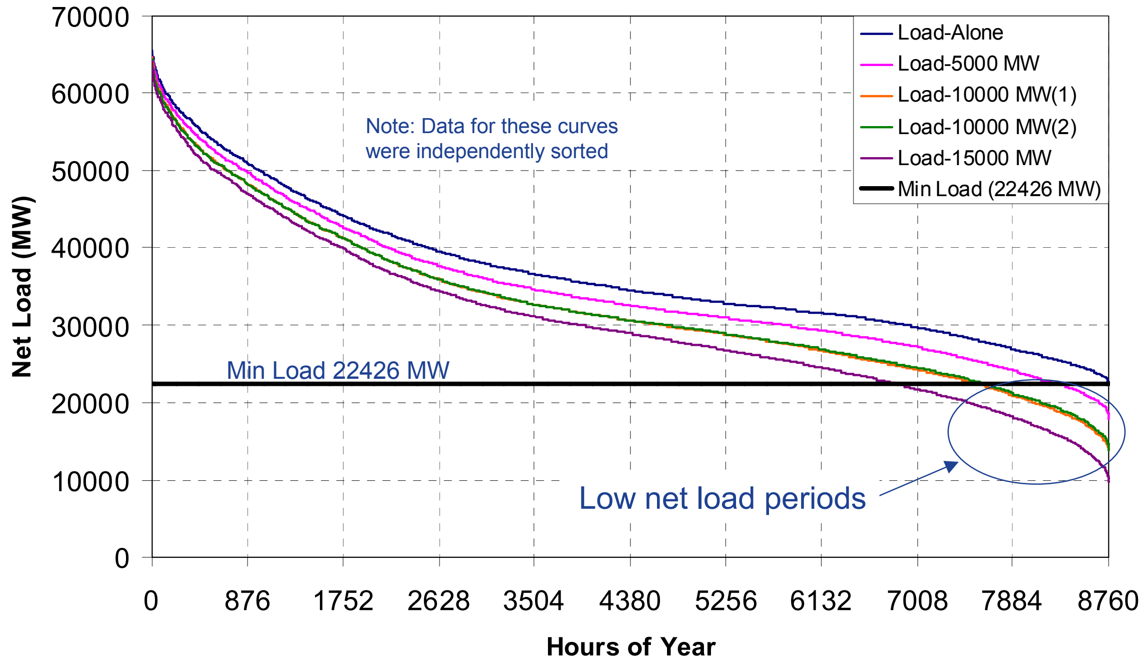

Figure 3-31 - Net load duration curves for various wind scenarios

Over the year, regardless of wind penetration, there are several hours when net load dips below the minimum load point (22,426 MW) for load alone. Admittedly, there is nothing inherently critical about this threshold. ERCOT may be able to operate their system well below this load level. However, it simply serves as a reference point for illustration. Figure 3-32 focuses on hours below the minimum load threshold.

For the 5 GW scenario, the minimum net load is 17933 MW. There are 470 hours when net load is lower than the minimum load point. Since the average wind output is double during low net-load hours, this represents about 10% of the wind energy. For the 15 GW scenario, the minimum net load is 9873 MW, a 56% reduction! Net load dips below the minimum load point for 1945 hours, representing 36% of the wind energy. Needless to say, curtailment of wind to hold the minimum load point would result in excessive energy loss. However, if the supply mix during these low load periods does not have adequate ramping capability to adjust for the wind variability, the reliable operation of the power system could be compromised. Mitigation measures to enable reliable operation with large wind penetration during low load hours are further discussed in Section 9.

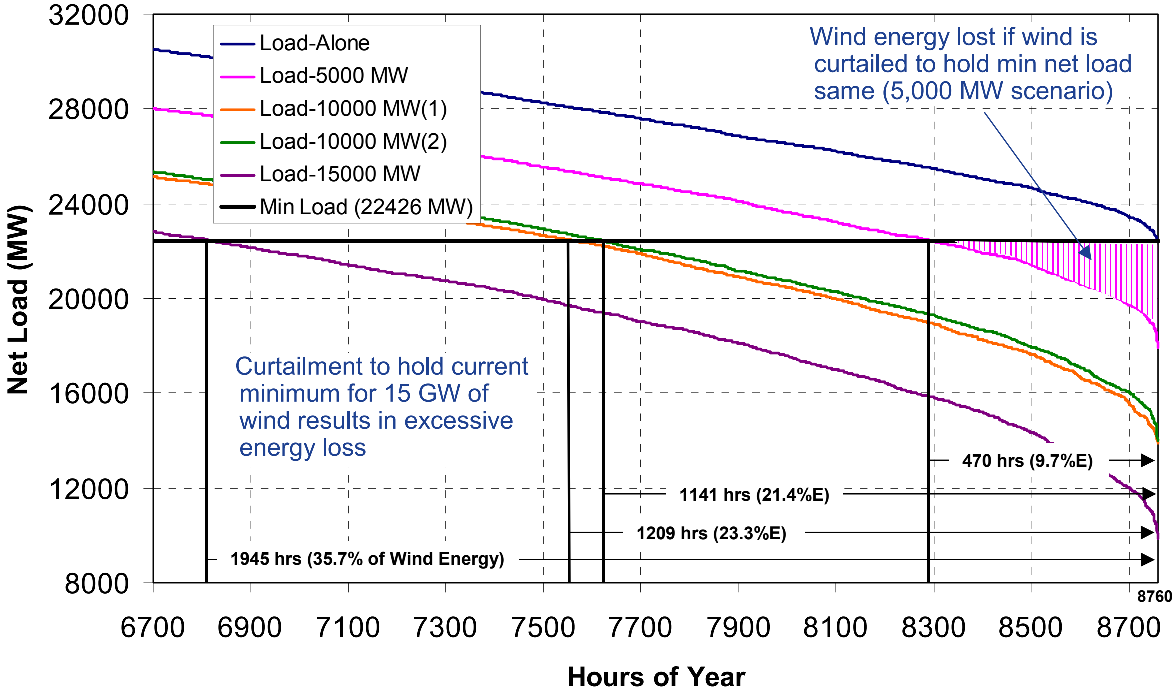

Figure 3-32 - Net load duration curves for various wind scenarios during low load hours

In summary, variability is relatively constant over the range of load levels, but tends to be greater during mid-range load levels than high and low load levels. Variability does increase with wind penetration but the increment tends to be less at high and low load levels. However, the low load periods are significant because net loads can be driven to extremely low levels with large wind penetration. The instantaneous wind penetration reaches 57% with 15 GW of wind and the minimum load point is reduced by 56%. Under these conditions additional measures may be needed to accommodate the net load variability.

3.5. Variability by Time-of-Day

Earlier sections have discussed broad trends in variability over various timeframes, across the year, and at different load levels. From a system operation point of view, broad trends in variability are not nearly as important as variability during particularly challenging periods. One such period, the minimum load, was discussed in the previous section. This section will discuss other challenging operating periods during the day created by large swings in net load.

In order to determine which are the "interesting" daily periods, average daily profiles for four seasonally representative months are created and overlaid with the hourly variability. Figure 3-33 shows these plots for load and net load with 15,000 MW of wind generation during January, April, July and October. Other plots are available in Appendix C.4.

The dashed magenta and blue curves are average daily load and net load, plotted against the left scale. Average daily profiles are created by averaging all similar hours during a month to create a 24-hour profile. The variability at each hour of the day, across the month, is captured by the box and whisker plot. The length of the rectangular boxes represents a spread of one standard deviation (σ) around the mean of the hourly change at a particular hour of the day. The whiskers show the maximum one-hour up-ramp and down-ramp over the month for a particular hour of the day.

Considering the relative length of the boxes in Figure 3-33, wind generation is a large contributor to variability over most of the day in the winter, particularly in the late afternoon and evening to early morning. Net load variability during the morning load rise period, is dominated by load changes. The largest one-hour net load rise is in late afternoon and the largest one-hour drop in the evening, both driven by large changes in wind production.

During the spring, wind output is a large contributor to ramping requirements during the morning load rise period and evening load drop-off. This can be more critical than an equivalent MW/hr rise in the summer, due to less generation committed. There are more extreme late evening load drops during the spring than winter, but wind generation tends to aggravate the one-hour drops even more.

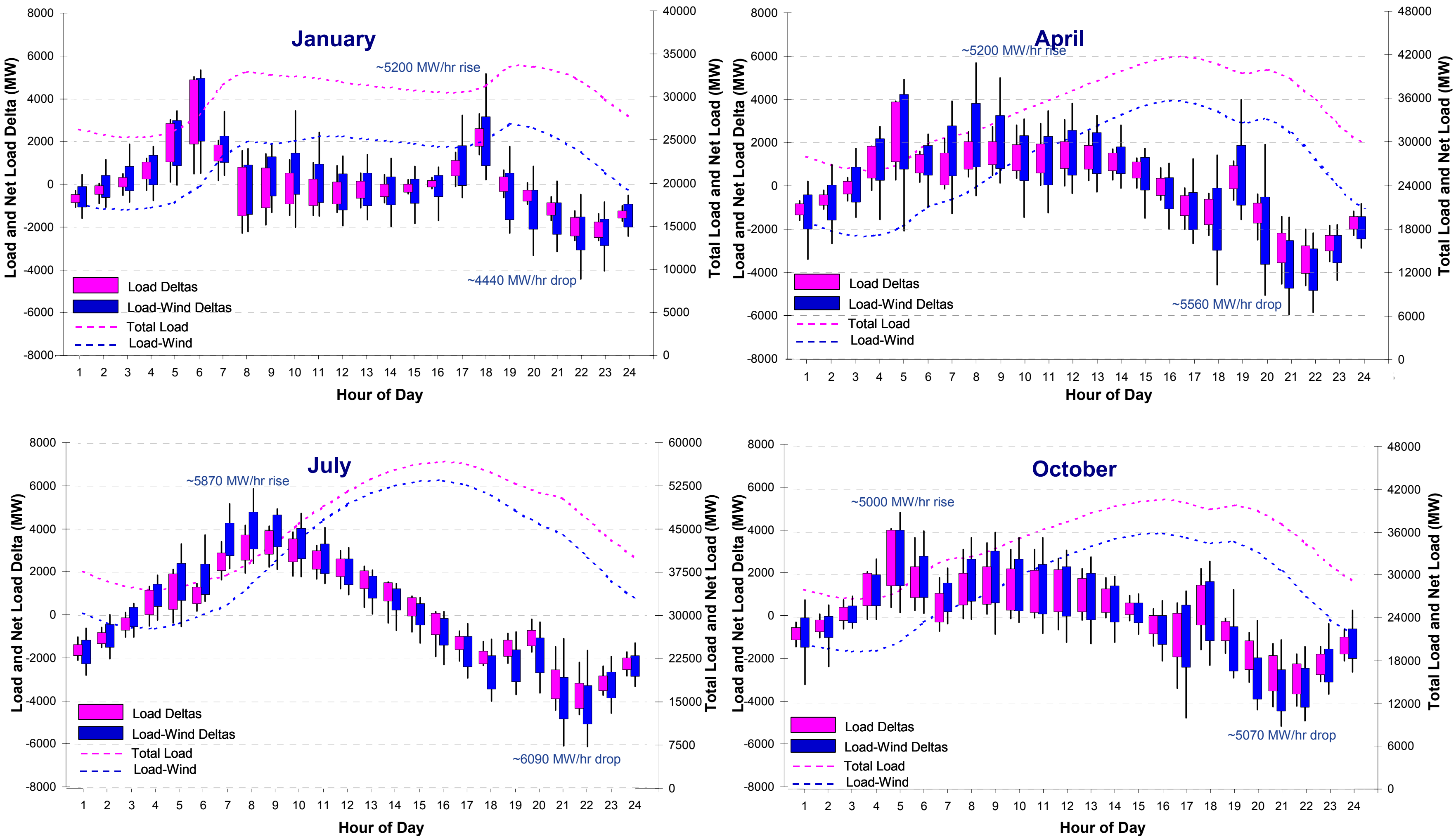

Figure 3-33 - Average daily profiles and hourly variability for load and load-15,000 MW of wind generation

In general, summer months experience less wind than other months, but output tends to drop faster in summer mornings and rise faster in the evenings than in other seasons (see Figure 3-3). With this in mind, it is not surprising that Figure 3-33 demonstrates that wind generation has the largest impact on net load variability during the early morning load rise period and evening load drop-off hours. The summer months also have the most extreme net load changes, which occur during the hours of greatest variability.

The profile of the typical fall month is similar to the typical spring month. Wind generation contributes to ramping requirements during morning load rise periods and evening load drop-off -- but to a lesser extent than the spring.

The charts in Figure 3-33 and discussion above, identify several daily periods of increased net load variability that merit closer examination. These include:

- Summer morning load rise: June – September, 7 – 11 AM
- Winter afternoon load rise: November – February, 4 – 6 PM
- Summer evening load drop: June – September, 8 PM – 12 Midnight

In addition, variability for spring morning load rise is plotted in Appendix C.4.

The following sections examine the net load variability during these periods, with particular emphasis on extreme ramps and trends for various scenarios.

3.5.1. Summer Morning Load Rise Period

The summer morning load rise period is designated as June to September, 7 – 11 AM. These daily hours are especially challenging because the load ramps are inherently steep and wind generation tends to be ramping down in the period (as shown in Figure 3-3). This anti-correlation only serves to aggravate the load-wind ramp, increasing variability and extreme ramps in the period. Figure 3-34 shows the distribution of hourly changes during the summer morning load rise period for load, and net load with 15 GW of wind generation capacity. The deltas for each five-hour morning load rise period from June to September were separated into 200-MW bins and plotted. Similar plots for the other wind generation scenarios are included in Appendix C.4.

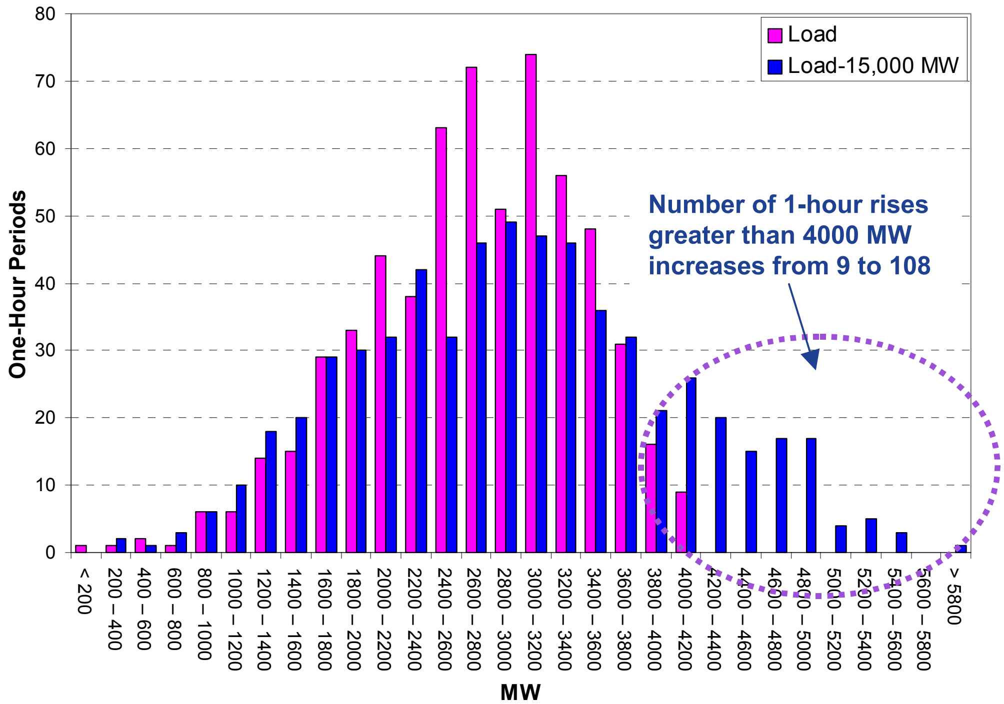

Figure 3-34 - Summer morning load rise hourly variability for load and net load (15 GW)

As expected, the distribution of hourly load changes is positive, because load is rising during the period. The median value is 2755 MW, which means that for half these periods the load is rising by over 2700 MW/hr. An additional 15,000 MW of wind generation increases variability in the period, creating more, and larger hourly up-ramps in net load. Where there were only nine hours when load rose by over 4000 MW/hr, there are 108 such instances with 15 GW of wind generation, and the maximum observed up-ramp increases by 41%.

Table 3-6 summarizes summer morning load rise variability statistics for the wind generation scenarios. By all measures, the observed variability increases linearly with wind, as shown in Figure 3-35, but the extrema tend to increase faster.

Table 3-6 - Summary of Summer Morning Load Rise Hourly Variability for Wind Scenarios

	Load	Load-5000 MW	Load-10,000 MW (1)	Load-10,000 MW (2)	Load-15,000 MW
Mean of Deltas (MW)	2694	2811	2919	2873	2963
σ of Deltas (MW)	729	808	923	894	1042
Max 1-Hour Drop (MW)	9	265	588	523	255
Max 1-Hour Rise (MW)	4160	4730	5479	5286	5871
Points ≥ ±2.5 * Load σ	0	2	27	14	53

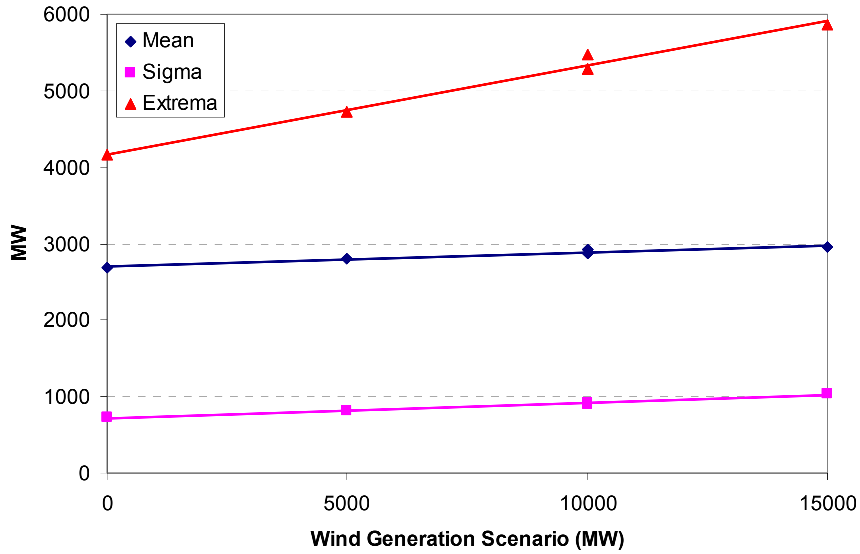

Figure 3-35 - Trend in summer morning load rise variability for wind scenarios

3.5.2. Winter Afternoon Load Rise Period

In the winter afternoon load rise period, designated as November to February, 4 – 6 PM, the load is rising while wind generation may be undergoing up-ramps or down-ramps. The distribution of hourly changes during these hours is shown in Figure 3-36 for load, and net load with 15 GW of wind generation capacity. The deltas for each three-hour afternoon load rise period from November to February were separated into 300-MW bins and plotted. Similar plots for other scenarios are included in Appendix C.4.

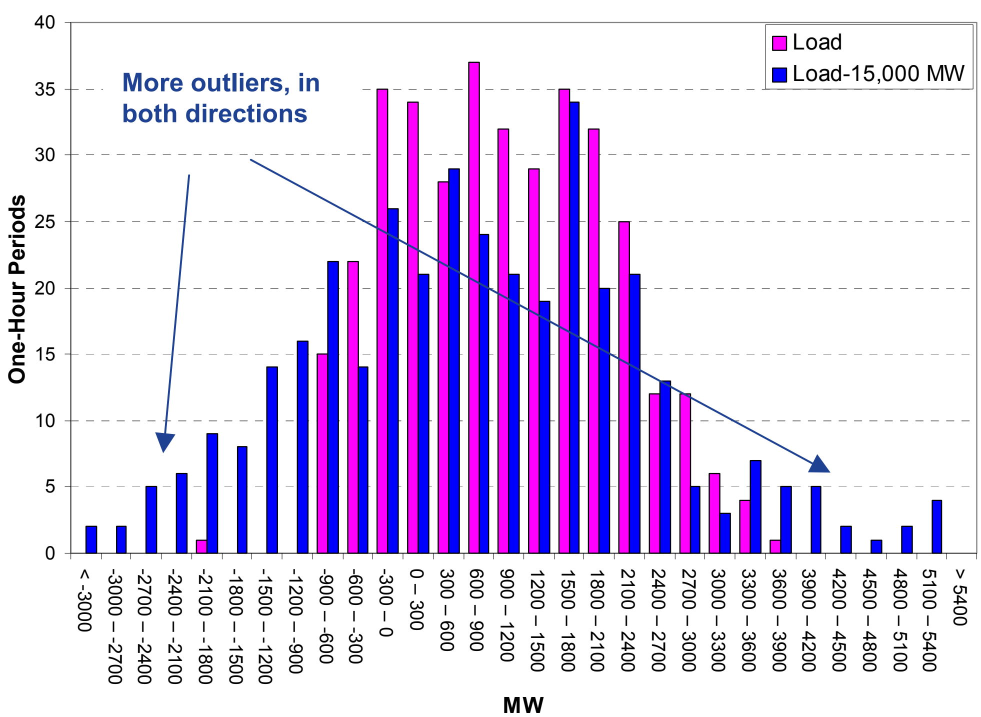

Figure 3-36 - Winter afternoon load rise hourly variability for load and net load (15 GW)

During this period, the hourly load changes are mostly positive (up-ramps), but with the incremental wind generation, there are additional large hourly changes in both directions. The number of one-hour rises greater than 3000 MW increases from 11 to 29 and the number of drops greater than 1500 MW increases from 1 to 32. Table 3-7 summarizes winter afternoon load rise variability for all the wind generation scenarios, and Figure 3-37 shows the trend with increasing wind output. Like the summer morning load rise period, the variability (sigma of the deltas) increases linearly, but the size of the extreme values tend to increase faster than the variability. Interestingly, the mean delta decreases, but this is due to the spread of net load deltas in the negative direction.

Table 3-7 - Summary of Winter Afternoon Load Rise Hourly Variability for Wind Scenarios

	Load	Load-5000 MW	Load-10,000 MW (1)	Load-10,000 MW (2)	Load-15,000 MW
Mean of Deltas (MW)	1018	895	776	823	722
σ of Deltas (MW)	1055	1232	1452	1405	1663
Max 1-Hour Drop (MW)	-1892	-1915	-2553	-2580	-3344
Max 1-Hour Rise (MW)	3678	4072	4694	4460	5190
Points ≥ ±2.5 * Load σ	1	6	12	10	19

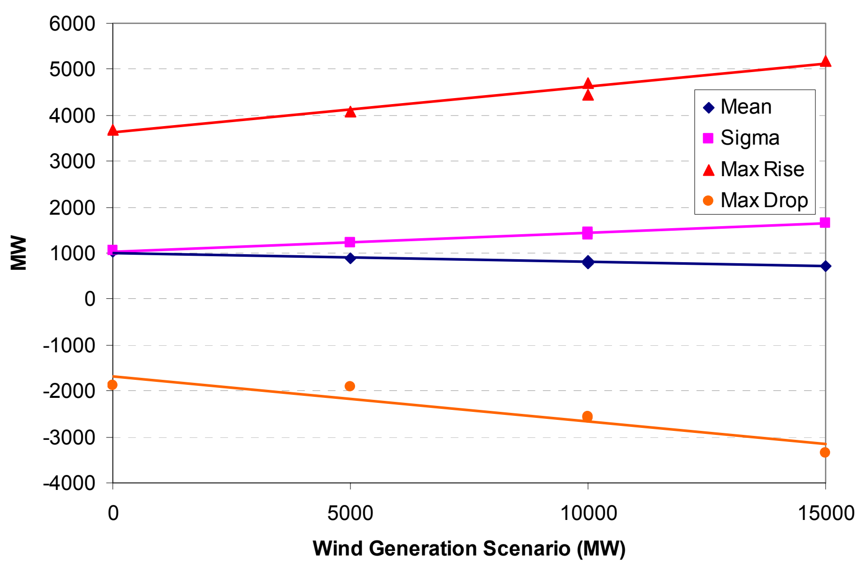

Figure 3-37 Trend in summer morning load rise variability for wind scenarios

3.5.3. Summer Evening Load Drop Period

Across the year, load generally drops in the evening while the wind generation tends to be ramping up. The charts in Figure 4-20 demonstrate that the net load variability increases and there are larger down-ramps. Since the largest one-hour net-load drops occurs in the summer, variability in the 8 PM to 12 Midnight period from June to September is examined. The deltas for each four-hour evening load roll-off period from June to September were separated into 200-MW bins and plotted on a frequency histogram. Figure 3-38 shows this plot for load, and net load with 15 GW of wind. Similar plots for the other wind generation scenarios are included in Appendix C.4.

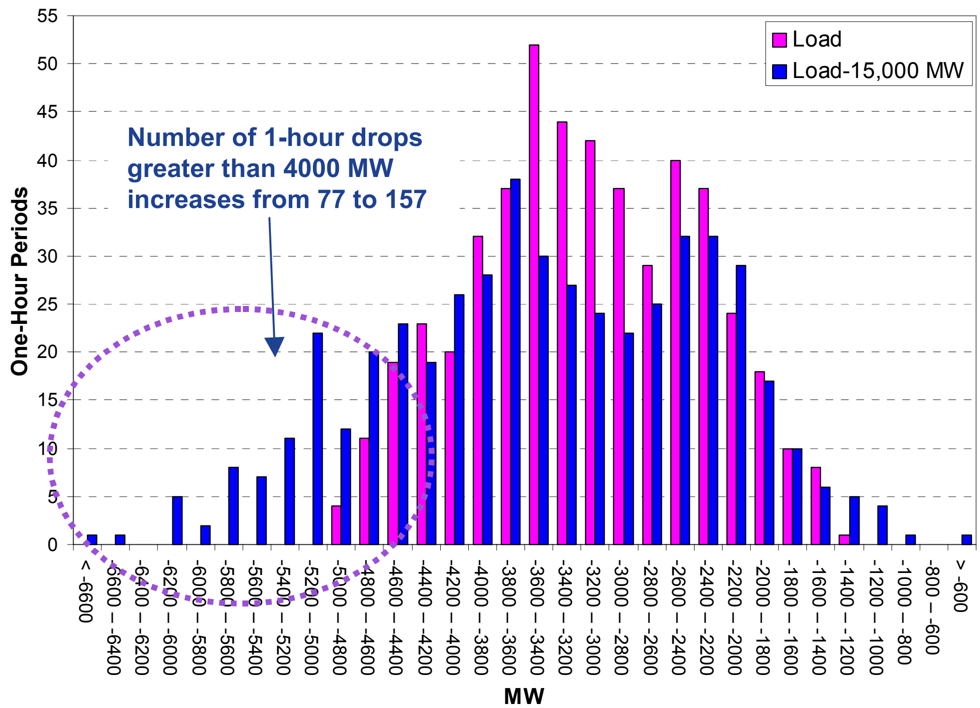

Figure 3-38 Summer evening load drop hourly variability for load and net load (15 GW)

As expected, the hour-to-hour load changes in the evening load-drop period are mostly negative and skewed to the left. With no wind, there are 77 periods (16% of the evening drop hours) when the load ramps down by more than 4000 MW/hr. With the addition of 15 GW of wind, there are 48 hours (or 32%) when net load-wind ramps down by 4000 MW/hr. Table 3-8 summarizes the evening load drop variability across all scenarios.

Table 3-8 - Summary of Summer Evening Load Drop Hourly Variability for Wind Scenarios

	Load	Load-5000 MW	Load-10,000 MW (1)	Load-10,000 MW (2)	Load-15,000 MW
Mean of Deltas	-3160	-3302	-3404	-3373	-3464
Std Dev (σ) of Deltas	795	927	1020	1025	1158
Max 1-Hour Drop	-4838	-5813	-6124	-6175	-6726
Max 1-Hour Rise	-1360	-1032	-837	-850	-565
Points ≥ ±2.5*Load σ	0	8	19	18	39

As wind penetration increases, the net load variability increases linearly, as shown in Figure 3-39. However the extreme values tend to increase faster than the variability, which is consistent with observations during other times of the day. A more complete discussion of extrema and their impact on operation requirements is included in Section 7.

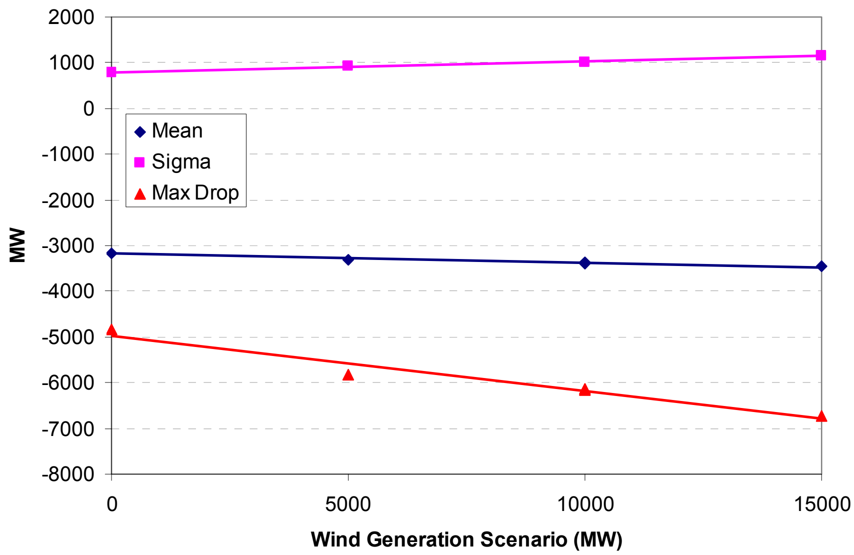

Figure 3-39 - Trend in summer evening load drop variability for wind scenarios

3.6. Summary

This section has discussed the variability of net-load (load-wind generation) from several different perspectives. The incremental variability due to wind has been assessed by comparing net load variability with load variability, rather than load and wind generation in isolation because experience has shown that some of the variation in load and wind output cancel each other. In order to perform credible analysis, load and wind generation time series must be time-synchronized to see the full impact of weather-related phenomena that affect both wind generation and load.

Over the months of the year, load and wind output vary considerably from day to day and throughout the day, but there is a distinct, observable diurnal cycle in the load. Wind output, on the other hand, does not exhibit strong periodic behavior, but correlation plots of load and wind series show that load peaks tend to coincide with wind generation valleys. The inverse-phase relationship appears to be stronger in the summer than during other seasons.

Other observations regarding load and wind coincidence include the fact that wind generation tends to drop sharply in the morning when load is rising quickly, wind generation generally increases sharply in the evening when load is dropping, and the winter afternoon load rise tends to coincide with a general increase in wind production, but there are times when wind is also ramping down in the period.

Using coincident load and wind generation time series, net load variability was examined in the one-minute, five-minute, fifteen-minute and one-hour timeframes. In all timeframes, incremental wind output linearly increased the overall net load variability (as measured by the standard deviation of the period-to-period changes, or deltas). The number and size of large and extreme deltas also increased with wind generation, but tended to grow faster than the variability.

A key observation is that in longer timespans (more than five minutes), net load variability is primarily driven by the long term ramp, but in shorter timespans there is an incremental component due to stochastic variation. The impact of the non-random ramp component can be seen in the frequency plots which become increasingly triangular in longer timeframes. With the same wind generating capacity, the incremental variability due to wind increases as the timespan becomes longer, but appears to taper off, and appears saturate at longer timeframes.

Seasonal trends in net load variability were examined using average yearly profiles and profiles of selected days. From an overall perspective, negative net load hour-to-hour changes (down-ramps) tend to be larger in the late spring, summer, and early fall, while the up-ramps are generally larger in late fall and winter. There tends to be larger differences between load deltas and net load deltas during spring and summer. The bottom line is that wind generation tends to have a greater overall impact on variability in the summer, late spring and early fall, but variations in winter and early spring may be more operationally significant due to the low net load levels.

Low load hours may present additional operational challenges because wind generation aggravates balance of generation ramp and range requirements. With regard to load level, variability is relatively constant, but tends to be greater during mid-range load levels than high and low load levels. Net load variability does increase significantly with wind penetration but the increment tends to be less at high and low load levels. However, low load periods are significant because net loads can be driven to extremely low levels with large wind penetration. The instantaneous wind penetration reaches 57% with 15 GW of wind and the minimum load point is reduced by 56%. Under these conditions additional measures may be needed to accommodate the net load variability.

From a system operation point of view, broad trends in variability are not nearly as important as variability during particularly challenging periods of the day. Considering time-of-day variability, wind generation is a large contributor to net load variability in the mornings and late evenings in most months (particularly in summer) and late afternoons during the winter. During the summer morning load rise period (June to September, 7-11 PM, wind generation increases variability in the period, creating more, and larger hourly up-ramps in net load. Where there were only nine hours when load rose by over 4000 MW/hr, there are 108 such instances with 15 GW of wind generation, and the maximum observed up-ramp increases by 41%. The general trend is the same in the winter afternoon load rise period (November to February, 5-7 PM) and the summer evening load drop-off period (June to September, 9 PM-12 Midnight). By all measures, the observed variability increases linearly with wind, as shown in, but the extreme values tend to increase faster.

The results of this analysis are important for a general understanding of the overall impact of wind generation on system, but also to assess the acute operation issues that arise during particular hours of the day and times of the year. Net load variability and extreme net load changes (in different timeframes) directly impact the requirements for regulation and responsive reserves. These are further discussed in Sections 6, 7 and 8..

The next section discusses net load predictability (or forecast accuracy) which has implications for non-spinning reserve requirements.

4. NET LOAD PREDICTABILITY

Day-ahead predictability of net load is important to the unit commitment process. Inaccuracies (large forecast errors) may compromise reliability, increase operating costs and may require greater ancillary service procurement.

For the purposes of this study, "forecast error" is defined as forecast minus actual. Therefore positive forecast error (forecasted quantity greater than actual) is defined as *over-forecast* and negative forecast error (forecasted quantity less than actual) is defined as *under-forecast*. Over-forecasting of load may lead to more generation being committed than needed (which has potential economic consequences), while under-forecasting of load may lead to under-commitment, which is a potential reliability problem. Therefore, from a system operation point of view, under-forecasting of load and net load is a more serious issue.

Several statistics are used in this study to characterize forecast accuracy. They include:

- **Mean Absolute Error** (MAE) – measures the average magnitude of the forecast errors, without considering their direction; mean of the absolute value of the errors.
- **Root Mean Square Error** (RMSE) – characterizes forecast error by measuring the "average" of the square of the deviations. RMSE will always be larger than MAE because it penalizes large deviations more.
- **Standard Deviation of Errors** (Sigma) – measures the spread of forecast errors around the mean; similar to RMSE but tends to be smaller.

The next few sections will discuss individual wind forecast accuracy, overall trends in load and net load forecast errors, and load and net load forecast accuracy during various months/seasons of the year and periods of the day.

4.1. Overall Wind Predictability

Actual load data and day-ahead forecasts were supplied by ERCOT from operations records, and scaled up to represent the study year, as discussed in Section 2. However, there were no actual wind generation data for the CREZ scenarios, for obvious reasons.[1] Therefore wind production data from AWS Truewind represents "actual" wind generation data in this study. AWS Truewind also provided simulated day-ahead wind output forecasts to accompany the "actual" wind production data. These data comprise the wind generation forecast for this study. A fuller discussion of the wind production

[1] Some existing wind output data was made available from operations, but not nearly the quantity and quality needed for even the smallest (5000 MW) scenario.

data and day-ahead forecast synthesis methodology is included in Section 2.2.1 and Appendix B.

Using the wind production data and simulated day-ahead forecasts for each scenario, several 8760 series of forecast errors were created. These data were organized into 300 MW bins and plotted on a frequency plot. Figure 4-1 below shows the distribution of wind generation forecast errors over the study year.

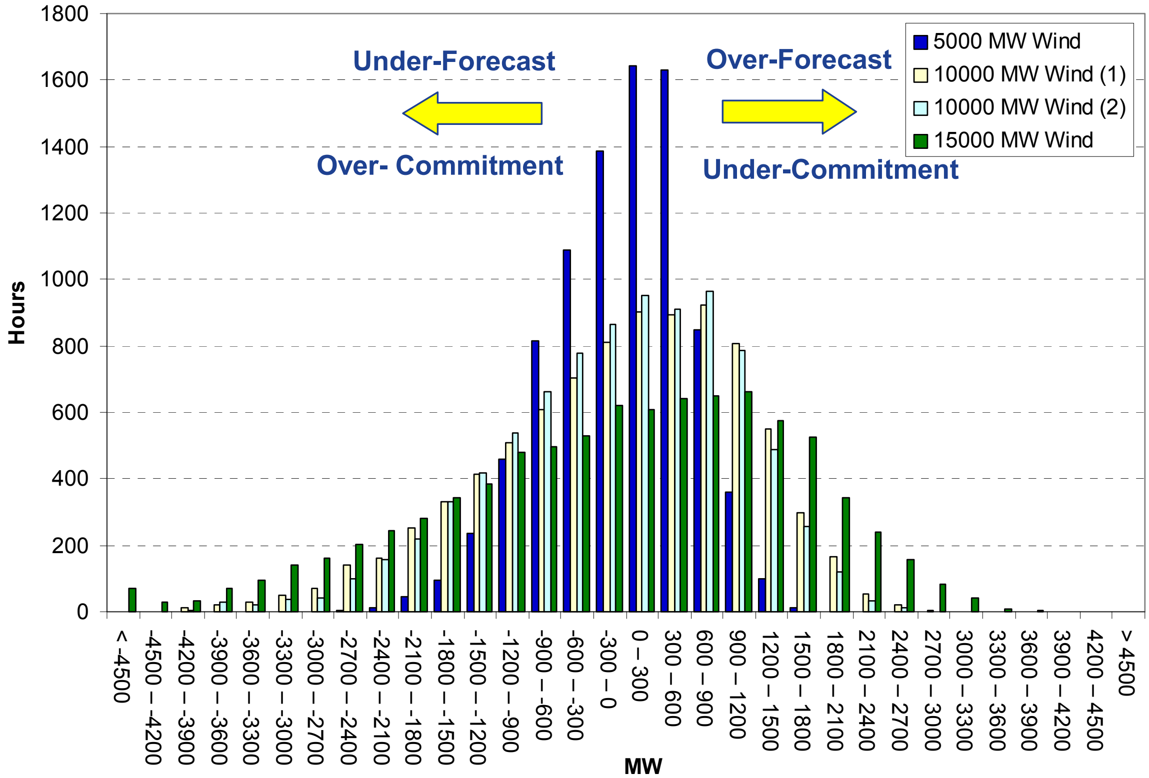

Figure 4-1 - Distribution of wind generation forecast errors over the study year

As wind penetration increases, the number and size of extreme forecast errors also increase. On both tails, there is a significant increase in extreme values going from the 10 GW case to the 15 GW case. The distribution of forecast errors becomes increasingly skewed to the left, which indicates that there is a clear tendency for the largest wind generation errors to be *under-forecast* errors. With 5 GW of wind generation capacity online, there are 30 under-forecast errors greater than 2000 MW, but with 15 GW online, there are 1164 such errors.

As discussed earlier, the real issue is whether forecast inaccuracies lead to unit under-commitment problems. Since wind generation is considered as negative load in the net load construct (load - wind), wind *under*-forecast errors actually manifest as *over*-forecast errors in net load. Therefore, the real operational concern is with wind generation *over*-forecasts, which ultimately show in net load as *under*-forecast errors. From the frequency plot, it appears that over-forecast is less of a problem in terms of severity. The number of wind over-forecast errors greater than 2000 MW increases from 0 in the 5 GW wind generation capacity scenario to 634 with 15 GW.

Table 4-1 summarizes some key measures of forecast accuracy as well the extreme errors. By all measures, there is a clear trend of decreasing forecast accuracy (increasing error) as wind penetration increases.

Table 4-1 - Summary of Wind Forecast Accuracy over the Study Year

Wind Scenario	MAE (MW)	RMSE (MW)	Sigma (MW)	Max Neg Error (MW)	Max Pos Error (MW)
5000 MW Wind	511	639	638	-2529	1744
10,000 MW Wind (1)	935	1169	1167	-4264	3032
10,000 MW Wind (2)	876	1096	1093	-4028	2671
15,000 MW Wind	1294	1614	1611	-5921	4052

Figure 4-2 shows that the MAE and RMSE actually increase linearly with wind generation capacity, with RMSE increasing faster, as expected. The measures of absolute forecast error (MAE and RMSE) and the maximum positive and negative errors are plotted against the left (MW) scale. MAE and RMSE as a *percentage of rated capacity* are plotted against the right (%) scale. The size of the maximum (extreme) over-forecast and under-forecast errors also increase linearly with wind penetration, with the extreme negative forecast error growing faster than the positive one.

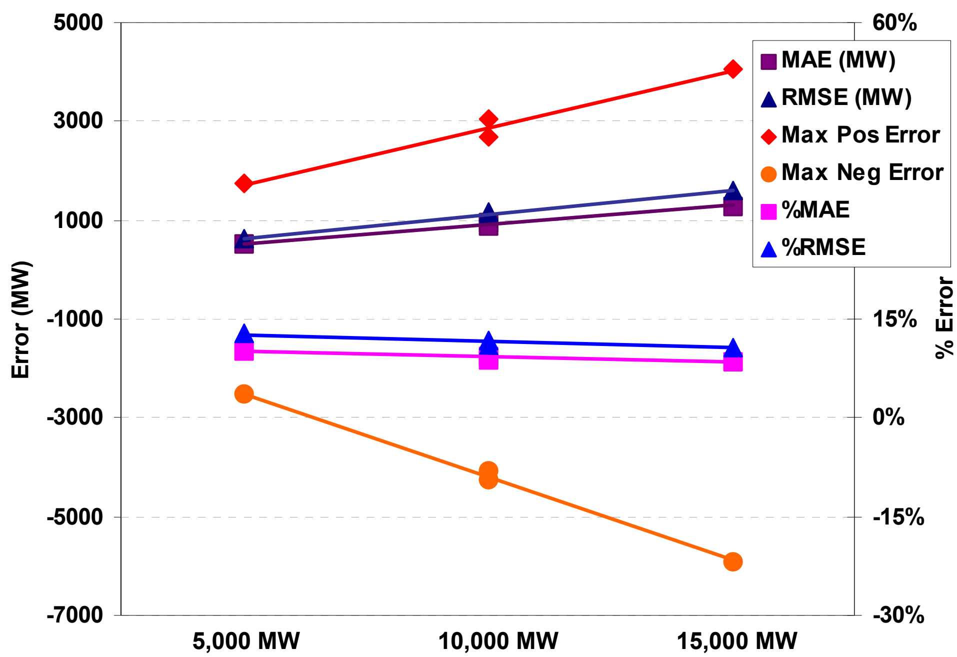

Figure 4-2 - Trend in wind forecast error accuracy and extreme errors

Interestingly, the percent error actually decreases with wind penetration, ostensibly because wind absolute error does not grow as fast as wind capacity. When capacity doubles from 5 GW to 10 GW, the absolute error does not double (increases 83%).

4.2. Overall Load and Net Load Predictability

Given day-ahead load forecasts and (simulated) next-day wind generation forecasts, next-day net load forecasts are generated by subtracting wind from load. These data are compared with the actual net load data to determine the net load forecast accuracy. In keeping with the defined convention, a positive forecast error is an over-forecast of net load and a negative forecast error is an under-forecast of net load. From an operations perspective, net load under-forecast errors are more significant because they can potentially lead to unit under-commitment.

Figure 4-3 shows the distribution of forecast errors, over the study year, for load and net load with 5000 MW and 15,000 MW of wind generation capacity. The first observation is that wind forecast errors do aggravate the overall net load forecast error, but this is more pronounced on the over-forecast side. The relative increase is greater around the inflection point, than on the tails of the distribution. Even so, there is still a definite increase in number of extreme errors as wind penetration increases. With no wind on the system, there are 210 instances where net load is over-forecasted by 4600 MW or more. With 15 GW of wind, this number grows to 316, a 50% increase, (but still less than 4% of all hours). On the negative side, the number of times when net load is under-forecasted at least 4600 MW goes from 26 with no wind, to 72 with 15 GW. Overall, there are more instances when load and net-load are over-forecasted than under-forecasted. The addition of wind skews the load-wind forecast toward the over-forecast side, because wind by itself tends to skewed toward being under-forecasted (as seen earlier in Figure 4-1).

Table 4-2 summarizes the broad measures of load and net load forecast accuracy, and Figure 4-4 plots the trend in overall error accuracy. In the plot, absolute error is on the left (MW) scale and error as a *percentage of the average net load* is on the left (%) scale. The plot demonstrates that there is a non-linear increase in absolute error and percent error as wind penetration increases. From the no-wind case to the 15 GW case, there is a 31% increase in MAE and a 23% increase in RMSE.

One non-intuitive observation is that the extreme positive forecast error actually *decreases* with additional wind generation., dropping by 5.4% from the no-wind case to the 15 GW case, in Table 4-2.

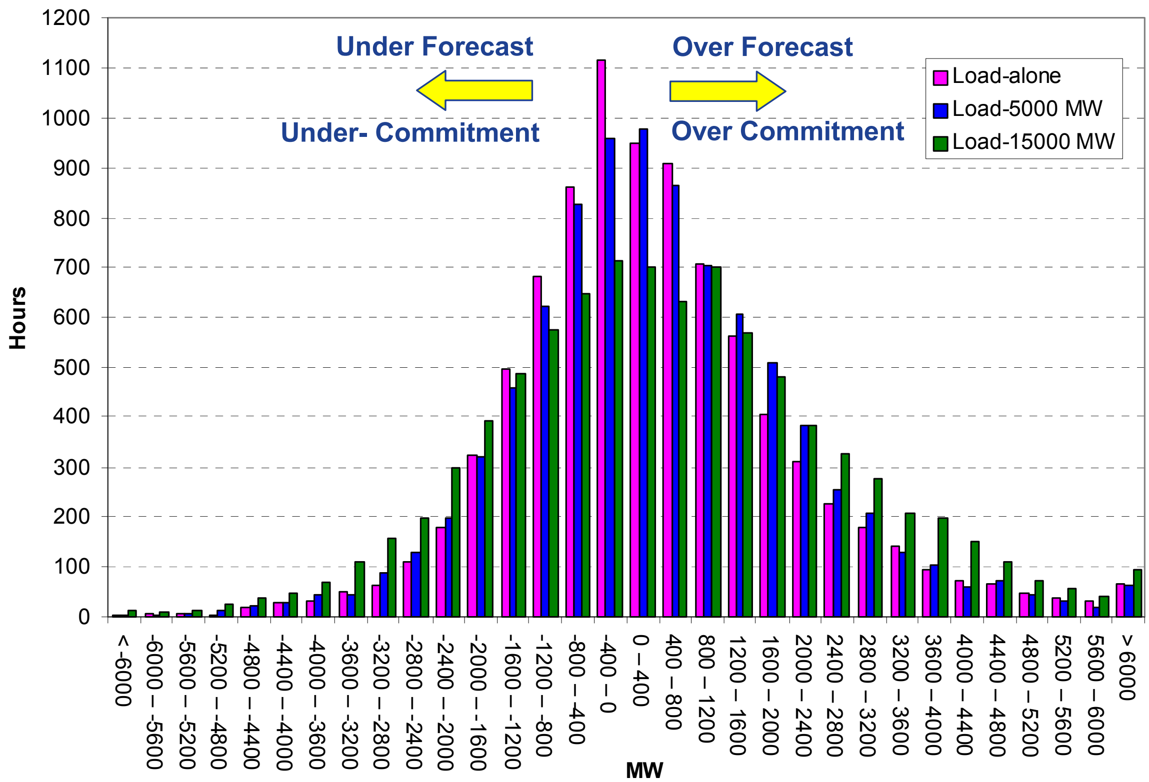

Figure 4-3 - Distribution of net load forecast errors over the study year

Table 4-2 - Summary of Net Load Forecast Accuracy over the Study Year

Scenario	MAE (MW)	RMSE (MW)	Sigma (MW)	Max Neg Error (MW)	Max Pos Error (MW)
Load-Alone	1296	1792	1755	-6291	10294
Load – 5000 MW	1338	1805	1762	-6574	9951
Load – 10,000 MW (1)	1505	1974	1928	-6724	9763
Load – 10,000 MW (2)	1467	1936	1887	-6803	9786
Load – 15,000 MW	1698	2199	2149	-7781	9765

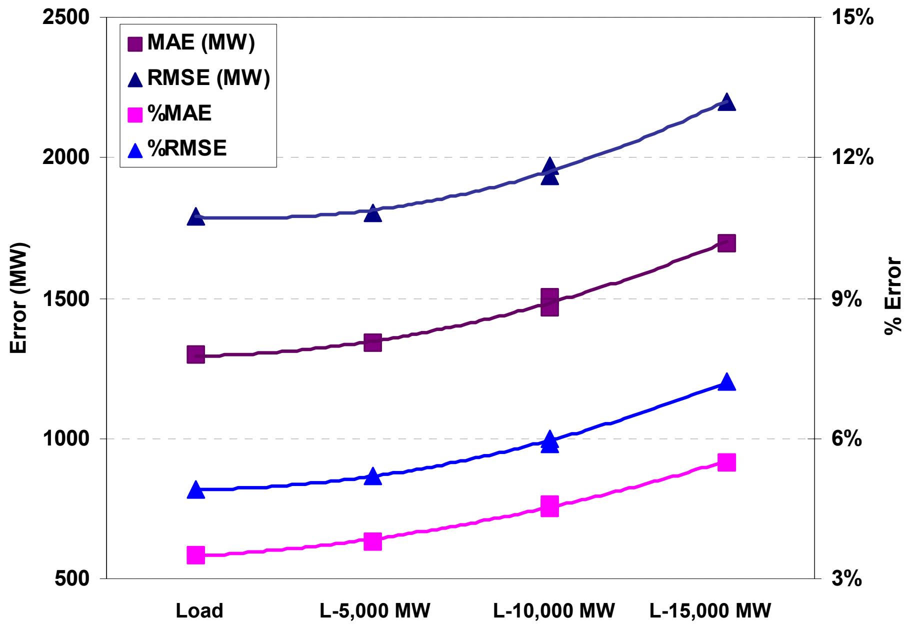

Figure 4-4 - Trend in net load forecast error accuracy

4.3. Net Load Forecast Errors by Time-of-Year

Load and wind generation vary over the year, from month to month and season to season. Therefore, one can reasonably expect some degree of variation in the ability to predict load and wind generation over the year. Figure 4-5 gives the profile of maximum daily load forecast errors, over the study year. This is to be compared with Figure 4-6 which plots the profile for maximum daily net load forecast errors for the 15 GW scenario.

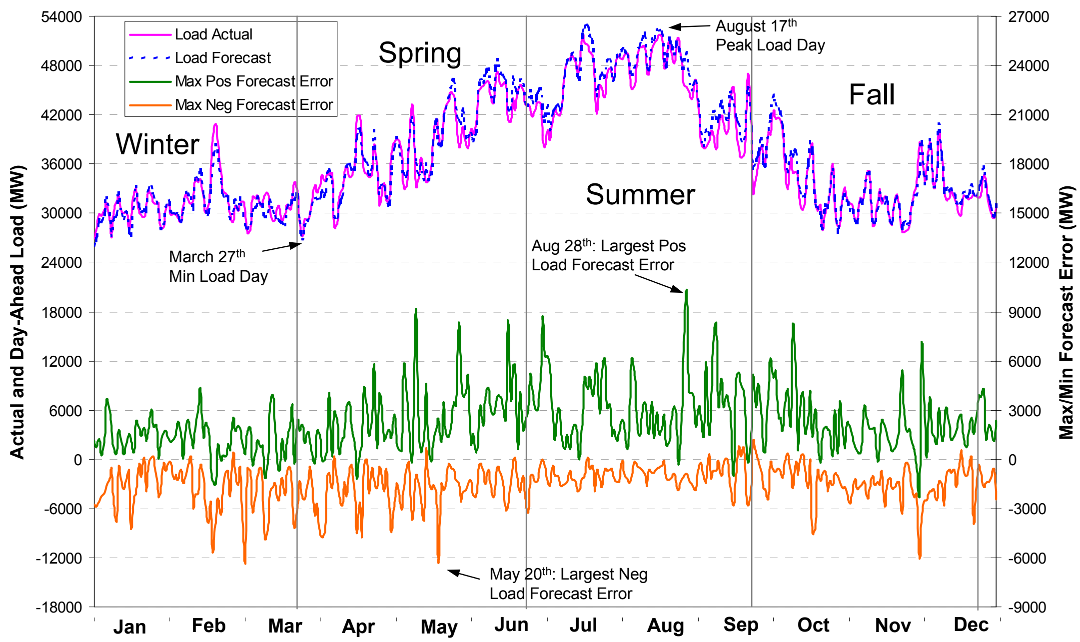

Figure 4-5 - Profile of maximum daily load forecast errors

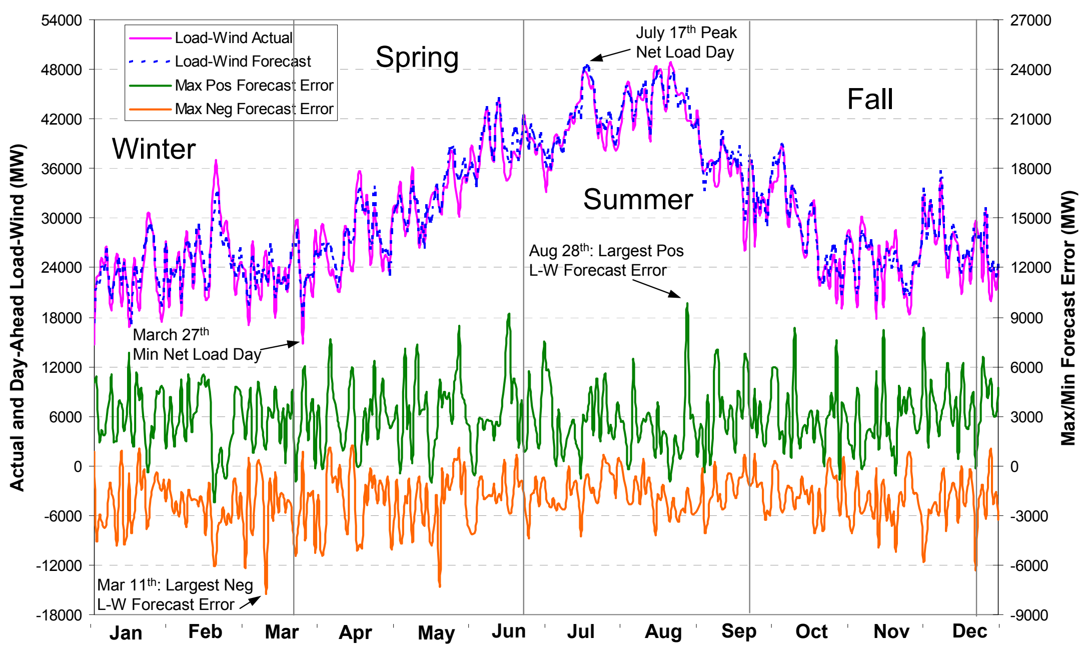

Figure 4-6 - Profile of maximum daily net load forecast errors (15 GW of wind)

The plots show *broad* trends in average daily forecast, and maximum daily forecast errors over the year, so by their very nature, they tend to mask the intra-day variability. Even so two general observations can be made regarding time-of-year forecast accuracy:

1. There is a greater tendency to accumulate large *load* over-forecast errors during the summer months and large load under-forecast errors during the winter months.
2. Extreme *net-load* forecast errors tend to be larger in non-summer months, than summer months.
3. Across the year net load forecast errors are generally larger than load forecast errors, but the increment may be greater for under-forecast errors in the summer.

These observations are confirmed and refined by additional analysis in the next sections.

4.3.1. Seasonal Forecast Errors

Figure 4-7 shows a scatter plot of load and wind generation forecast errors separated by season. Magenta diamonds represent load and wind generation forecast errors during winter hours, blue squares represent errors during spring hours, orange triangles represent summer hours, and green circles represent fall hours.

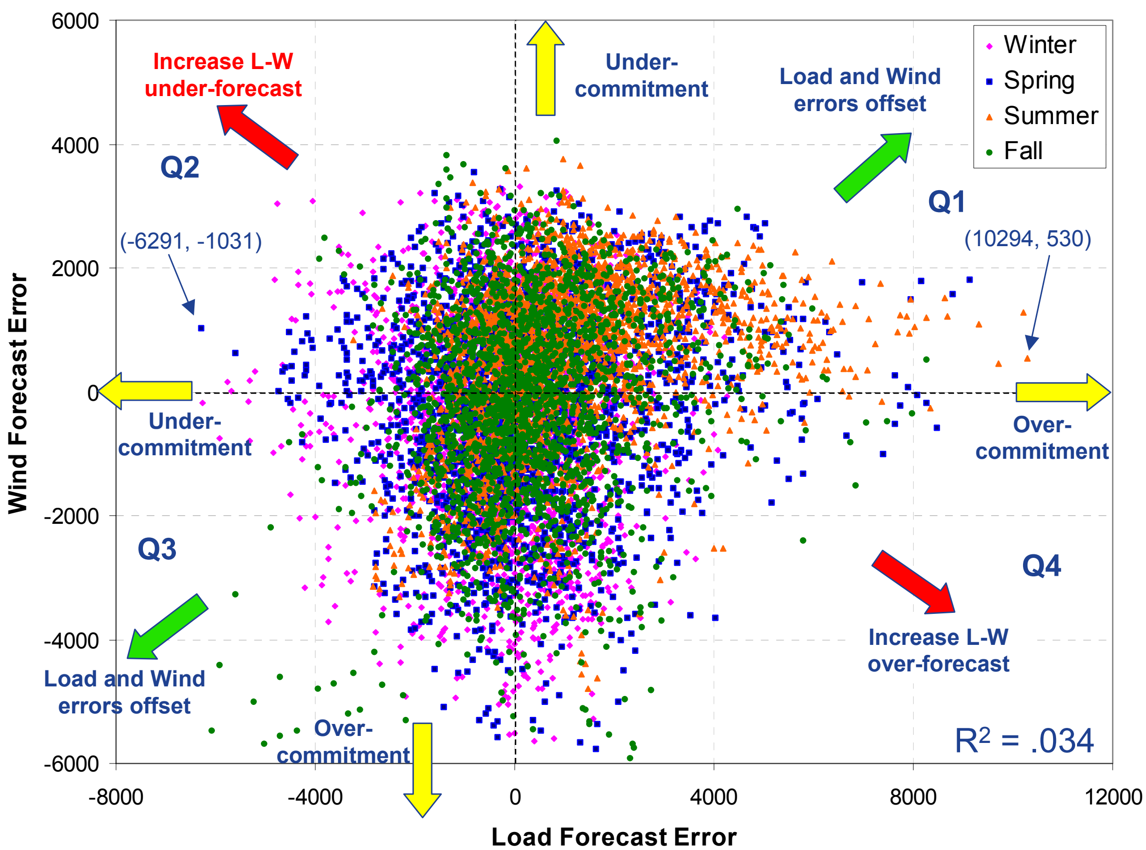

Figure 4-7 - Correlation of load and wind generation (15 GW) forecast errors by season

Overall, Figure 4-7 demonstrates that there is an extremely weak correlation between load forecast errors and wind forecast errors (R^2 = .034). This suggests that both errors are independent, not driven by the same factors, and are unlikely to coincide or reinforce each other. This exemplified by the data point in the first quadrant, Q1, corresponding to the largest load forecast error (10294 MW). During this same summer hour, the wind forecast error happens to be pretty modest (530 MW).

The scatter plot shows a very distinct spread in errors in the right-hand and downward directions. There are more large summer error-hours (orange triangles) along the positive x-axis (load over-forecast), than in other directions. Conversely, there are more non-summer error-hours along the negative x-axis (load under-forecast), than in other directions. This is completely consistent with the first observation made previously from the yearly profile of load forecast errors (Figure 4-5). The spread (and type) of points along the negative y-axis suggests that wind tends to be under-forecasted more in non-summer months, but as discussed below, this is may not be a significant operational issue.

The yellow arrows on Figure 4-7 show the forecast error directions that are consistent with unit commitment outcomes. For example, negative load forecast errors and positive wind forecast errors may individually lead to under-commitment of resources. On the other hand, positive load forecast errors and negative wind forecast are both consistent with over-commitment of resources.

The red diagonal arrows indicate the directions where load and wind errors combine (add) to increase net load forecast errors. All points in the second quadrant, Q2, represent hours during the year when load and wind errors combine to *increase* the net load *under*-forecast, which may lead to unit *under*-commitment problems. All errors in the fourth quadrant, Q4, potentially lead to over-commitment of resources -- so they are not as operationally significant (from a reliability standpoint) as errors in Q2.

The green arrows indicate directions in the off-diagonal quadrants, (Q1 and Q3), where load and wind forecast errors offset each other to reduce the net load forecast error -- so they are not generally as problematic as points in the diagonal quadrants.

In general, the points in Q2 and Q4 indicate that there are more extreme winter and spring errors (magenta diamonds, blue squares) than summer ones, *particularly in the under-commitment direction* (Q2). This is completely consistent with the second observation made earlier from the yearly profile of net load forecast errors (Figure 4-6). To expand on this point, Figure 4-8, separates the seasons into individual scatter plots and overlays the plots with equal-error lines. These are dashed lines that define the envelope where the sum of the load and wind forecast errors is the same.

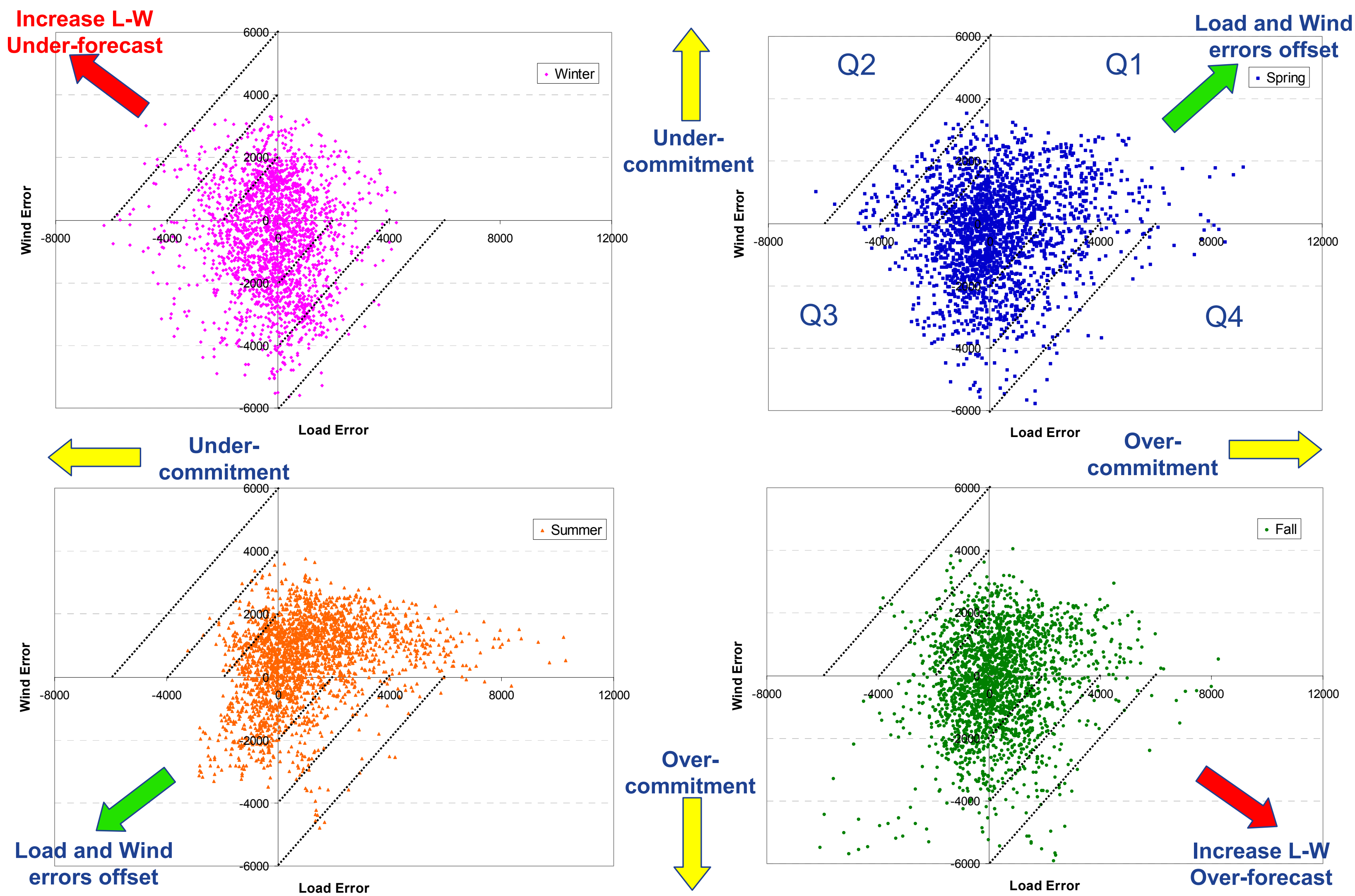

Figure 4-8 - Correlation of load and wind generation (15 GW) forecast errors in each season, with iso-error lines.

In Q2 and Q4, where load and wind forecast add, points outside the envelope lead to larger net load forecast errors, and points inside the envelope lead to smaller errors. For example, in Q2, which is consistent with net load under-commitment, very few points are beyond the 6000 MW bar, in all seasons. This means that in the winter, there are few hours when net load is under-forecasted by over 6000 MW, even less hours in spring and fall, and none in summer. In Q4, the pattern is weaker, but still discernable. This reinforces an earlier observation that it is improbable for the most severe load and wind errors to occur in the same hour -- or *the risk of simultaneous under-commitment error is small*.

Figure 4-9 shows time series plots and data on net load forecast accuracy during seasonally representative months, for the 15-GW wind generation scenario. The magenta trace is "actual" net load and the dotted blue trace is the day-ahead forecast. Both are plotted on the left scale. The orange trace is forecast error, plotted on the right scale. The plots and data confirm that *on average*, net load forecast accuracy is lower in the winter and spring months than during the summer.

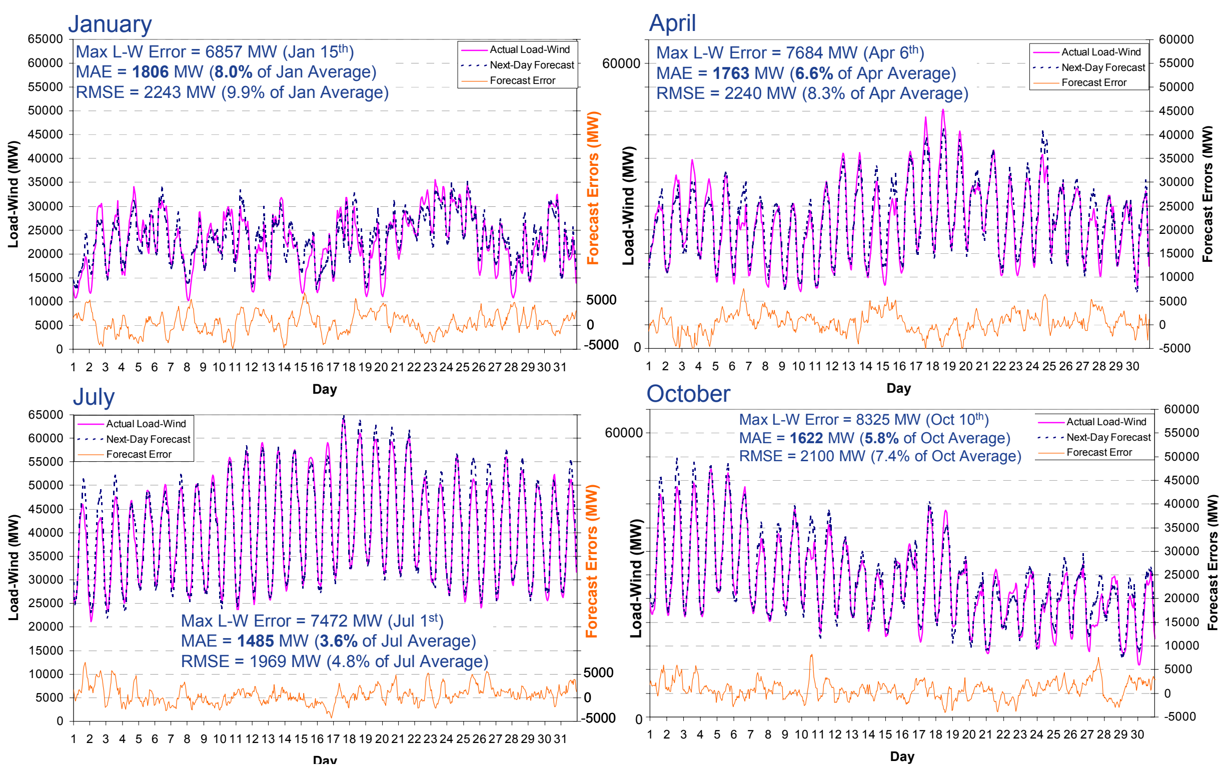

Figure 4-9 - Actual net load, day-ahead forecasts, and forecast error by seasonal month, 15 GW wind generation capacity scenario.

4.3.2. Forecast Errors for Selected Days

Based on Figure 4-6, there are some "interesting" days during the year where a closer examination of net load forecasts may give some additional insight. These include the days with the largest net load over- and under-forecast errors, the peak load day, minimum load day, and four typical, seasonally representative days.

Figure 4-10 shows the profile for the day on which the largest net load over-forecast occurs (August 28th), for the 15 GW wind generation scenario. The forecast error accumulates throughout the day, reaching a peak of 9675 MW (MAE is 4103 MW). However, the wind forecast error is consistently small, so the gross over-forecast is driven by the load forecast error.

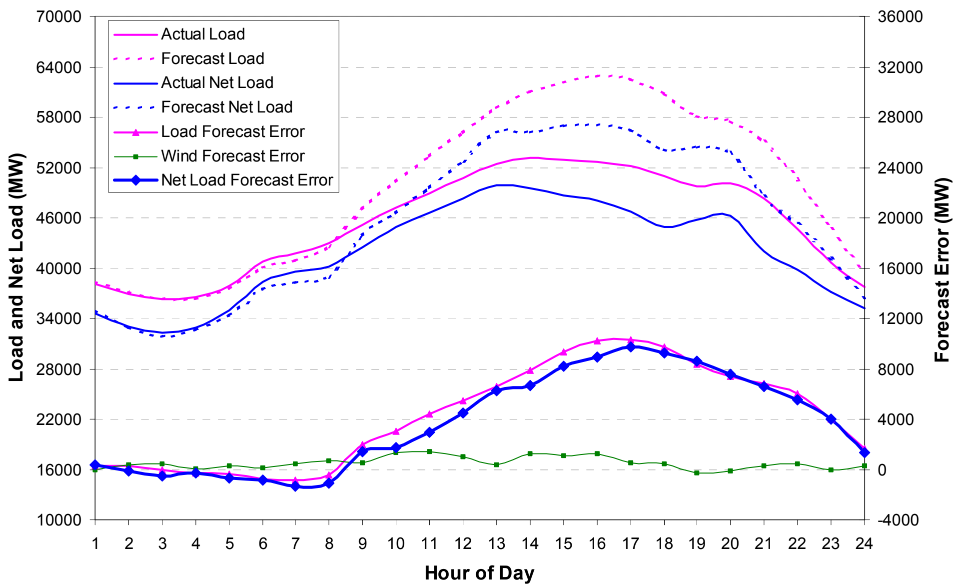

Figure 4-10 - Large positive net load forecast error day (Aug 28th), 15 GW wind scenario.

On the other hand, Figure 4-11 shows the profile for the day with the largest net load under-forecast error (March 11th), for the 15 GW wind generation scenario. In this case, the large net load under-forecast error (-7780 MW around 3 PM), is due to a simultaneous increase in wind over-forecast and load under-forecast errors at the time.

Figure 4-12 shows the daily profile for the peak load day (August 28th). This day is interesting if only for the lack of character. The load forecast is quite accurate, and the wind forecast error is uniformly small, creating relatively small net load forecast errors across the day. The largest forecast error is –2060 MW and the MAE is 886 MW.

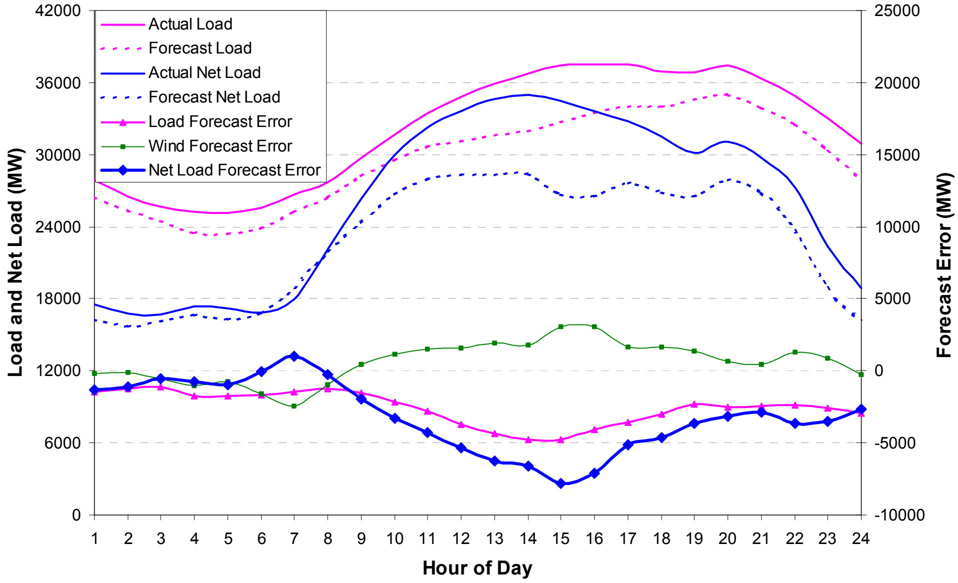

Figure 4-11 - Large negative net load forecast error day (Mar 11th), 15 GW wind scenario

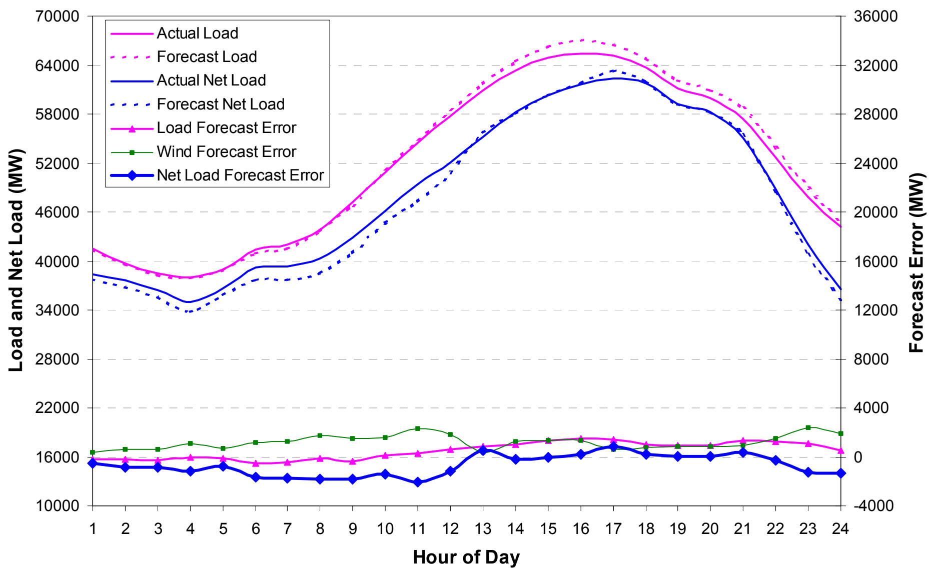

Figure 4-12 - Forecast errors for peak load day (August 17th), 15 GW wind scenario.

Figure 4-13 shows the minimum load day (March 27th). The plot exhibits some variation in net load forecast error across the day due to a combination of varying load and wind forecast errors. The largest over-forecast error, in the early morning, happens to coincide with the period when the least amount of resources are likely to be needed.

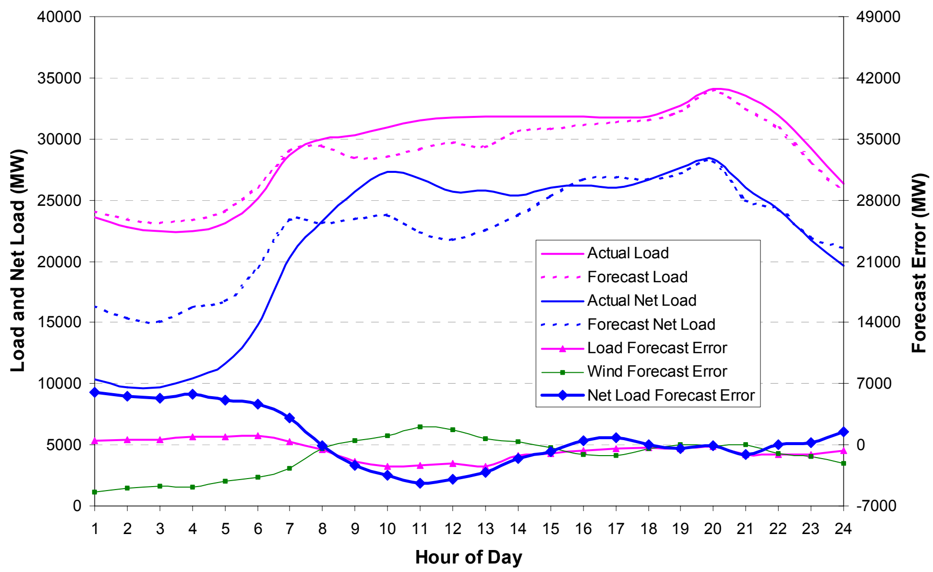

Figure 4-13 - Forecast errors for minimum load day (March 27th), 15 GW wind scenario.

The next four plots in Figure 4-14 show error profiles of typical days from each season. The representative seasonal days, January 27th, April 23rd, July 10th and October 25th were selected based on the fact that they did not significantly deviate from seasonal expected averages. On the plots, magenta traces are load-related, blue traces are net load-related, and the green trace is wind-related. Load and net load are on the left scale and the forecast errors are on the right scale. Note that some scales may vary among plots display purposes.

Since these typical plots are merely snapshots of the seasonal forecast accuracy, one should be careful when drawing broad inferences. However, from a macro perspective, the plots conform with the earlier observation that net load forecast errors show more separation from load forecast errors in winter, spring and fall days. To make any credible inferences about how forecast errors vary during the day, more data than just these four days need to be considered. Therefore, the next section will consider how forecast errors vary during the day, (hour to hour), across the entire year.

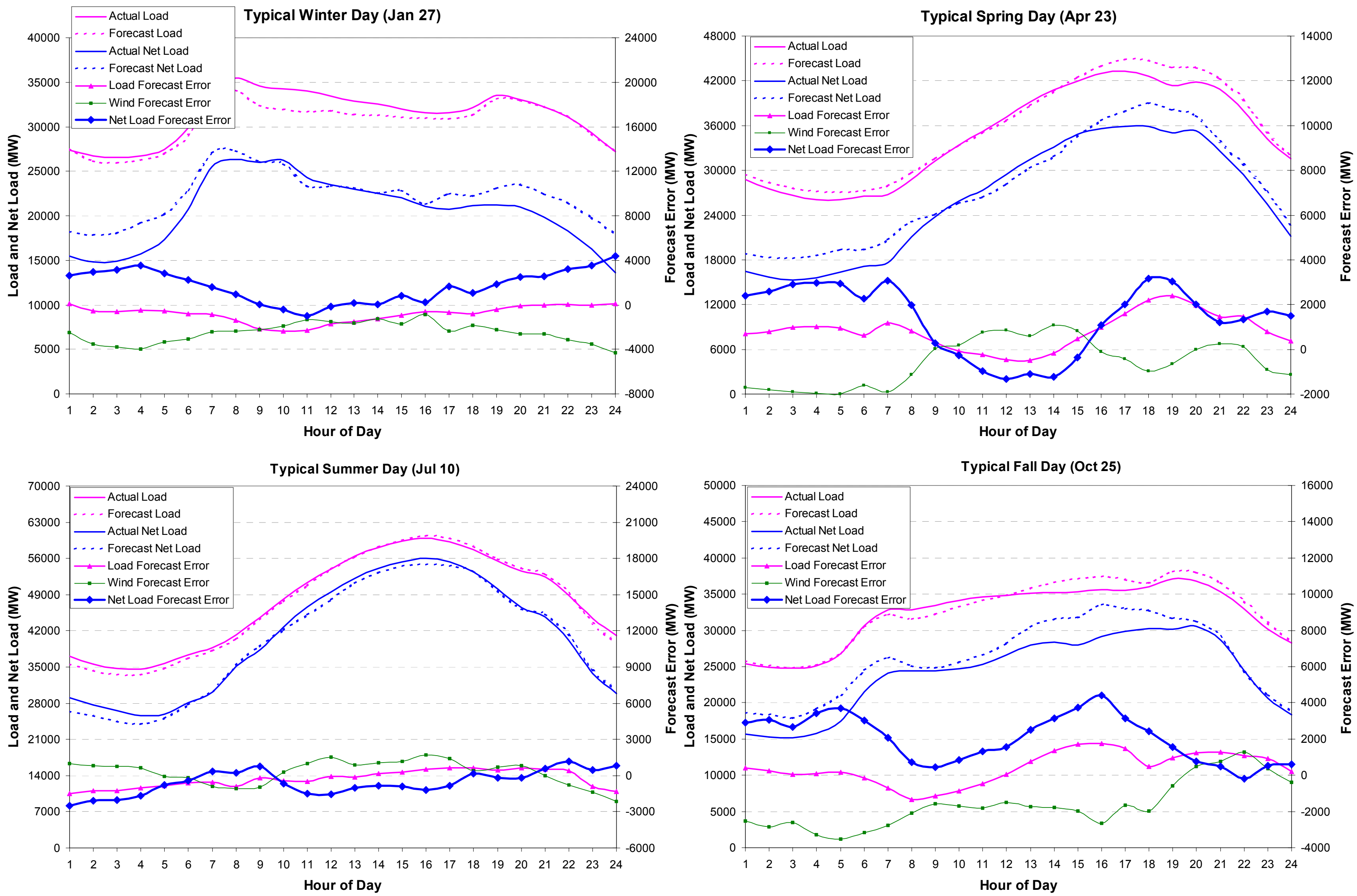

Figure 4-14 - Forecast errors for four seasonally representative days, (15 GW scenario)

4.4. Net Load Forecast Errors by Time-of-Day

From a system operation perspective, it is very important to understand the net load predictability during challenging periods of the day, such as when the system is stressed or resources are likely to be low. Since day-ahead forecast error is a key input to the unit-commitment decision-making process, this discussion is germane to the evaluation of non-spinning reserve requirements (further discussed in Section 8).

The time-of-day forecast errors will be examined in two ways: first, the daily time of extreme forecast occurrence will be examined over the twelve months and then the daily average error profile will be discussed in each season.

4.4.1. Timing of Forecast Errors

This section discusses the pattern of extreme forecast error occurrence over the hours of the day and months of the year. The data are presented in 24×12 surface plots using color intensity to represent the magnitude of the forecast errors.

The data for the surface plots were extracted from the forecast error time series. For each month of the year, the maximum positive and negative forecast errors where selected for each hour of the day. For example, in the month of January, there are thirty-one 6 AM hours (one for each day). Only the maximum errors from each of the 31 forecast errors was selected for the surface plot. Repeated for each month, this resulted in 24 positive error observations for each of the twelve months, and 24 negative error observation.

The next few surface plots illustrate the timing of positive and negative forecast errors, which highlight periods with the greatest risk of over- and under-commitment.

Figure 4-15 shows the surface plot for positive (over-commitment) load forecast errors. The legend indicates the level of the forecast error during a particular period. Periods with the largest errors are colored in red and orange. From the pattern, the largest load over-forecasts typically occur in late afternoons during the summer months. This is consistent with earlier observations.

With 15 GW of wind generation capacity (see Figure 4-16), there is generally an *increased* risk of over-commitment in mornings and afternoons during fall and winter. The risk is simultaneously reduced in the mid-summer afternoons.

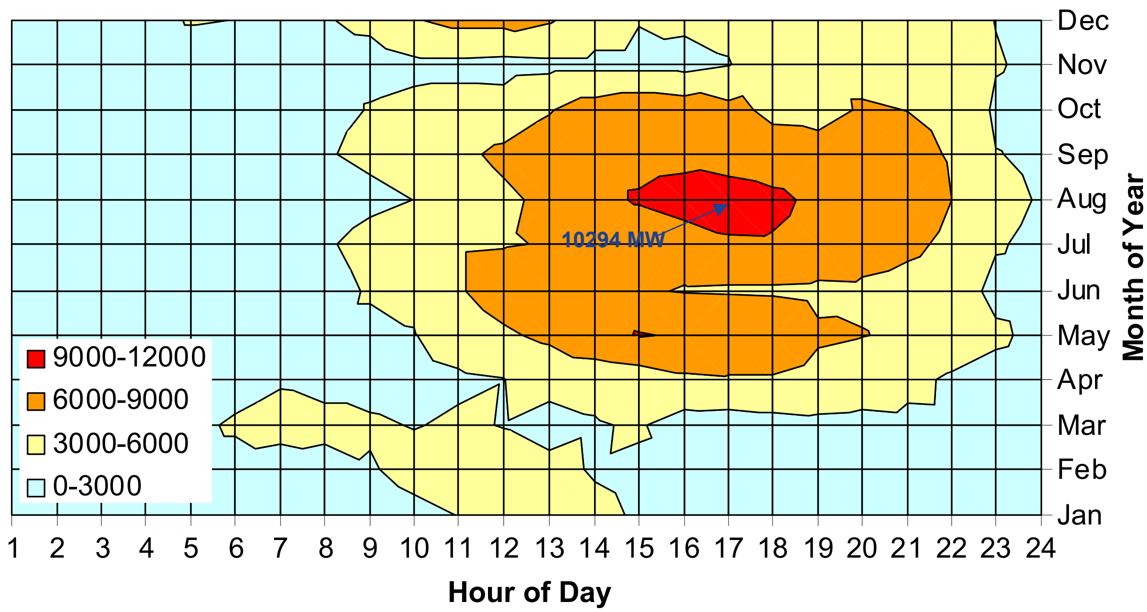

Figure 4-15 - Timing of maximum positive load forecast errors (over-commitment)

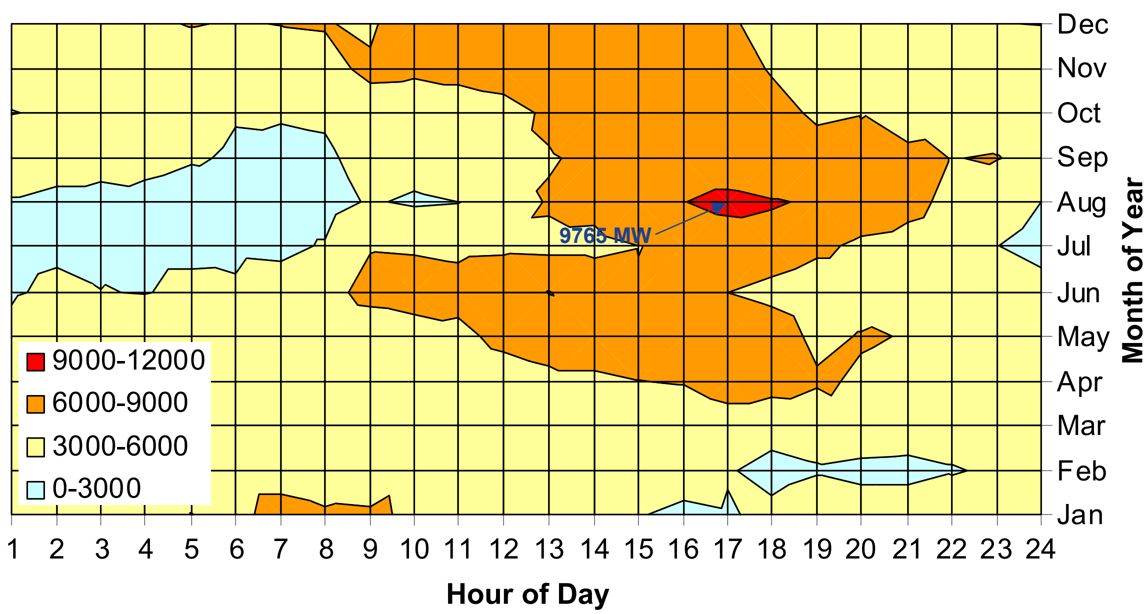

Figure 4-16 - Timing of maximum positive net load forecast errors (over-commitment), 15 GW wind generation capacity scenario.

Figure 4-17 shows the surface plot for negative (under-commitment) load forecast errors. With no wind on the system, the periods with the greatest risk of under-commitment are in the afternoon to early evening during winter and spring (red and orange areas). When 15 GW of wind generation is added, Figure 4-18 shows that the pattern of net load forecast errors changes appreciably. The extreme net-load under-forecasts (orange and red) are now much more spread over the day, and the magnitudes are greater (more red). The periods with the greatest risk of under-commitment occur in winter and spring.

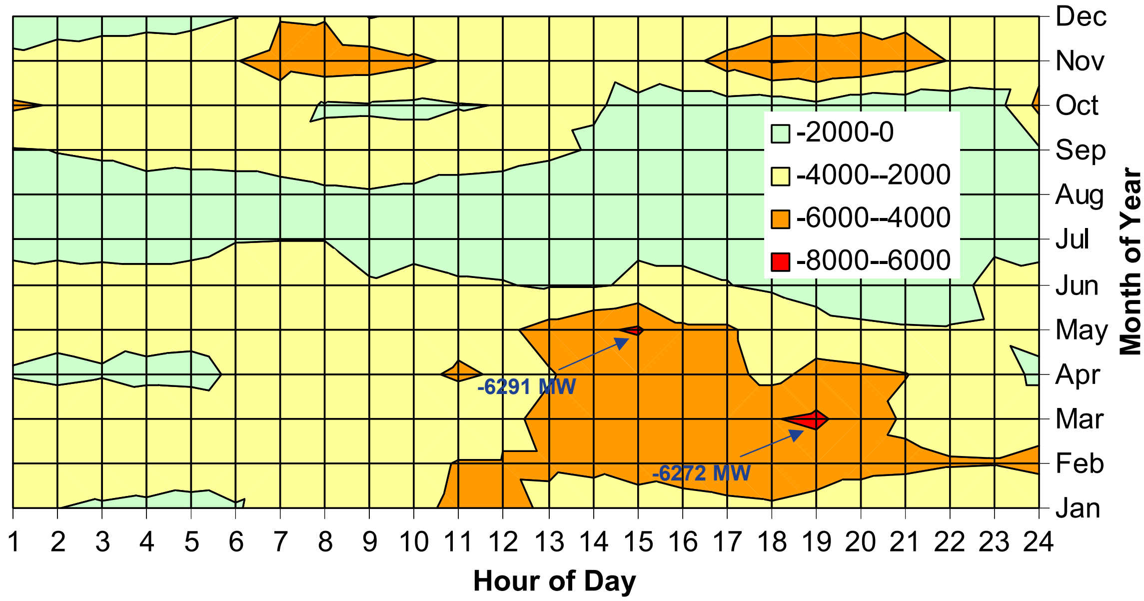

Figure 4-17 - Timing of maximum negative load forecast errors (under-commitment)

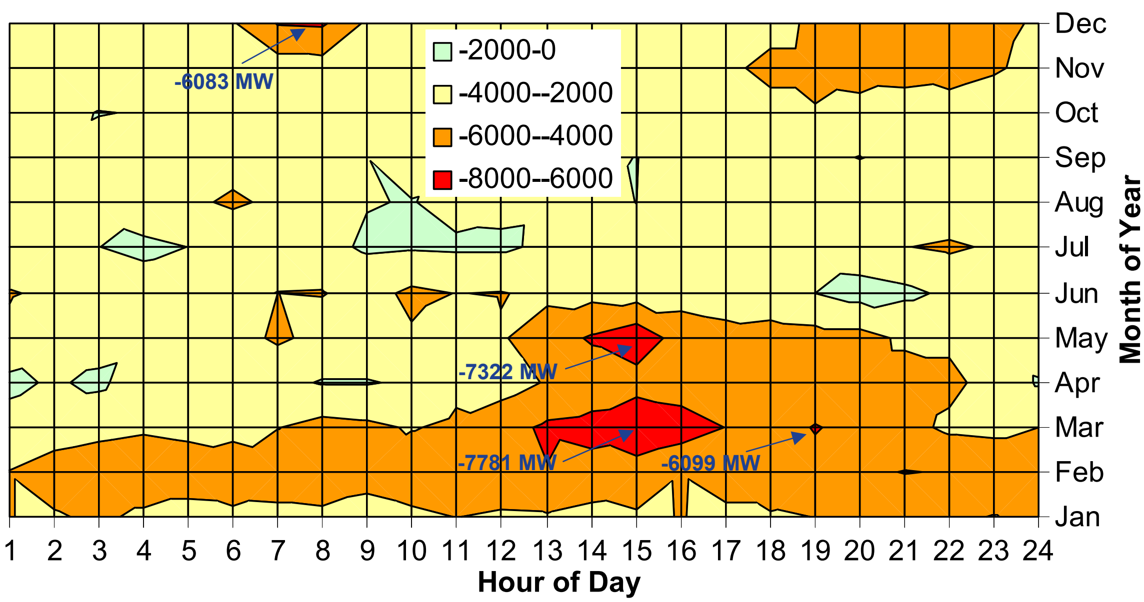

Figure 4-18 - Timing of maximum negative net load forecast errors (under-commitment), 15 GW wind generation capacity scenario.

The difference between Figure 4-17 and Figure 4-18 is the timing of the incremental large net load forecast errors due to wind, i.e. it highlights periods with incremental risk of under-commitment due to wind. This is shown in Figure 4-19 below. The pattern indicates that 15,000 MW of wind generation capacity would cause the risk of under-commitment to generally increase across all hours of the day and months of the year, with particularly acute increases in some periods. These include evening hours in summer and fall and early morning hours in the winter. This hourly risk is investigated further using daily profile plots in the next section.

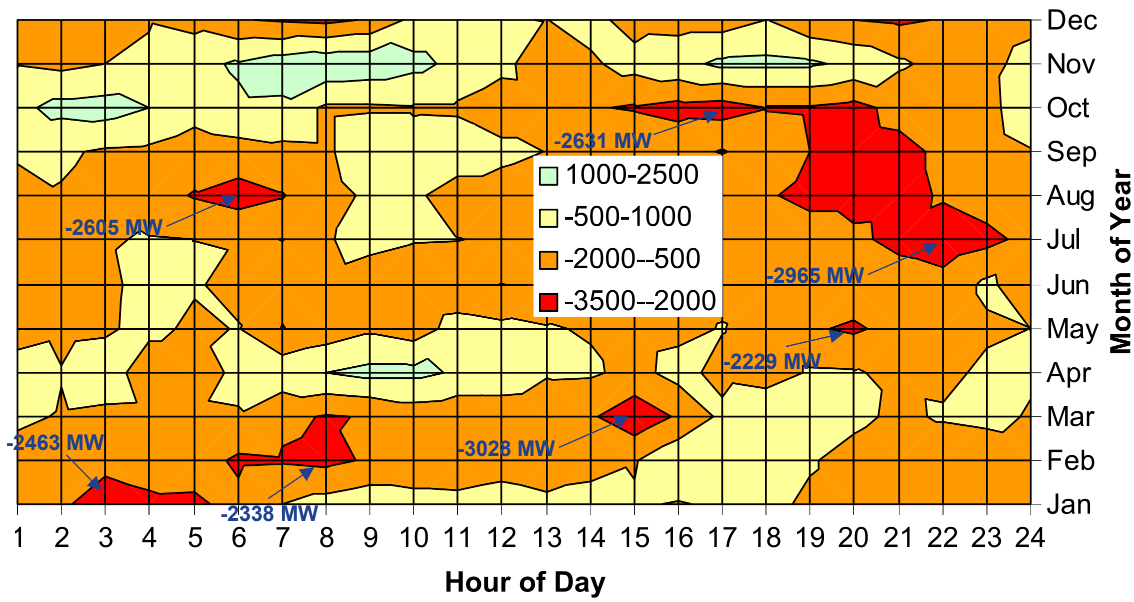

Figure 4-19 - Incremental maximum net load under-forecast errors due to wind

4.4.2. Daily Profiles of Forecast Errors

In order to assess how forecast error varies throughout a typical day, average daily profiles for four seasonally representative months are created and overlaid with the hourly forecast errors. Figure 4-20 shows these plots for load and net load with 15,000 MW of wind generation during January, April, July and October. Other plots, including complete traces of all profiles and forecast errors are available in Appendix D.

The dashed magenta and blue curves are average daily load and net load, plotted against the left scale. Average daily profiles are created by averaging all similar hours during a month to create a 24-hour profile. The forecast error at each hour of the day, across the month, is captured by the box and whisker plot. The length of the rectangular boxes represents a spread of one standard deviation (σ) around the mean of the day-ahead forecast error for a particular hour of the day. The whiskers show the maximum over-forecast and under-forecast errors over the month, for a particular hour of the day.

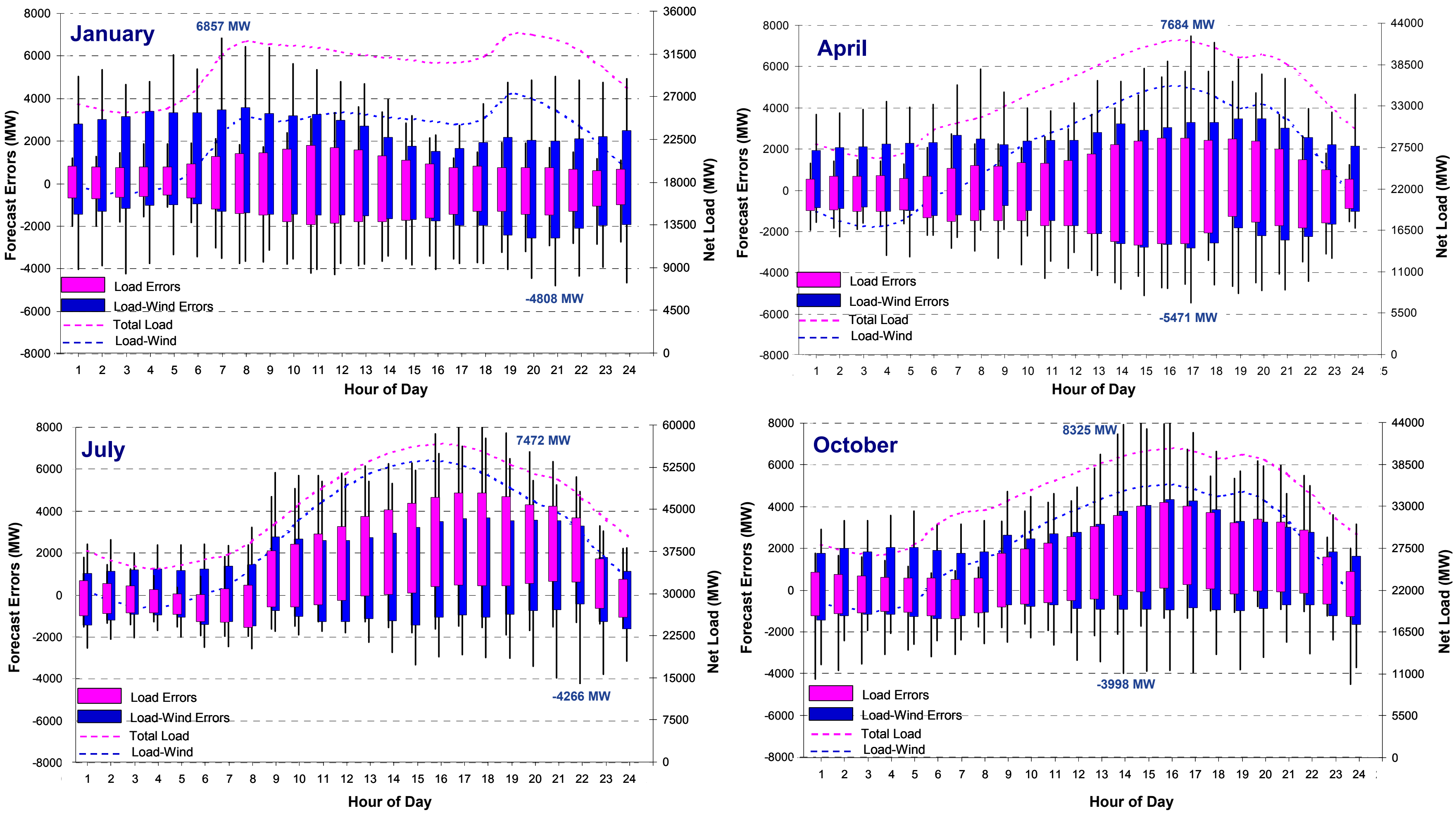

Figure 4-20 Average daily profiles and predictability for load and load-15,000 MW of wind generation (net load).

The length of the boxes in Figure 4-20 indicate the spread in forecast error, or the general forecast accuracy at a particular hour of the day. Considering the relative length of the magenta (load) and blue (net load) boxes, wind generation reduces forecast accuracy over most hours of the day, but particularly in early morning and late evening hours during winter, spring and fall.

Considering the trend in the average (center of the boxes), during the morning hours (corresponding with load-pickup), net load tends to be generally over-forecasted relative to load (positive bias). But during late afternoon to evening hours in summer and fall, net load tends to be under-forecasted relative to load (negative bias).

The whiskers in Figure 4-20 show the maximum positive and negative forecast errors. Considering the relative length of the whiskers for the load and net load boxes, we see that wind generation can drive extreme forecast errors in both directions. The late evening hours in summer and fall tend to see incrementally large net load under-forecast errors. This is consistent with the observation from the incremental surface plot in Figure 4-19. Large under-forecast errors during these hours may lead to under-commitment of resources, however, these are typically the hours when resource needs are low.

There are also incrementally large net load under-forecast errors in the early afternoon (peak) hours during the summer, (and fall to some extent). Note that the spread of the net load forecast errors (or general forecast accuracy) is not dramatically different from load alone, but there are significantly larger under-forecast errors with wind. This may potentially lead to under-commitment of resources during peak load times when they are most needed.

4.5. Summary

The predictability of net load is important to the unit commitment process because large errors in the day-ahead forecast may compromise reliability, increase operating costs and require greater ancillary service procurement.

Forecast error (forecast – actual) is defined as positive for over-forecast and negative for under-forecast. Over-forecasting may lead to more generation being committed than needed (which has potential economic consequences), while under-forecasting may lead to under-commitment, which is a potential reliability problem. From a system operation standpoint, under-forecasting is a more serious issue.

Considering wind generation in isolation, as penetration increases, the number and size of extreme wind forecast errors also increase. The distribution of forecast errors becomes more skewed to the left with additional capacity, which indicates that there is a clear tendency for wind generation to be under-forecasted. However, wind generation *under*-forecast errors show up in net load as *over*-forecast errors, which may lead to over-commitment (rather than under-commitment) problems.

Overall Net Load Trends - With coincident load and wind, there is an overall trend of decreasing forecast accuracy (increasing error) with increasing wind penetration. The incremental wind forecast errors tend to skew the net load forecast error toward the positive (over-commit) side. The size of the extreme forecast errors also increase with wind penetration, but the negative errors tend to grow faster than the positive ones.

Seasonal Trends - Seasonal trends in predictability were initially studied by comparing the profile of maximum daily load forecast errors with maximum daily net load forecast errors over the study year. The analysis revealed that

1. There is a greater tendency to accumulate large *load* over-forecast errors during the summer months and large load under-forecast errors during the winter months.
2. Extreme *net-load* forecast errors tend to be greater in non-summer months.
3. Across the year net load forecast errors are generally larger than corresponding load forecast errors, but the incremental increase may be greater for under-forecast errors in the summer.

These observations become even more pointed when the correlation of all load and wind forecast errors is examined by seasons. Overall, there is an extremely weak correlation between the errors, which suggests that both errors are independent, not driven by the same factors, and are unlikely to coincide or reinforce each other. Further inspection of the pattern of errors over different seasons led to the conclusion was that it is improbable for the most severe load and wind errors to occur in the same hour -- or *the risk of simultaneous under-commitment error is small*.

The scatter plots confirmed the earlier observation about net loads, (from the profile of maximum errors) -- on average, net load forecast accuracy is lower (errors are larger) in the winter and spring months than during the summer.

Time-of-Day Trends from Extreme Error Profiles - The time-of-day pattern for forecast errors was first investigated by looking at the time of occurrence of daily extreme errors across the months. The results showed that with no wind, the largest load *over*-forecasts typically occur in late afternoons during the summer months. With 15 GW of wind generation capacity, there is generally an *increased* risk of over-commitment mornings and afternoons in fall and winter. The risk is simultaneously reduced in the mid-summer afternoons.

Considering under-forecast errors, with no wind, the periods with the greatest risk of *under*-commitment are in the afternoon to early evening hours during winter and spring. With a large penetration of wind generation resources, the risk of net load under-commitment is more spread over the day, and the magnitudes are greater, particularly in spring afternoons.

The difference between negative load forecast errors and negative net load forecast errors gives the *incremental* risk of under-commitment due to wind generation. The resulting pattern indicates that the incremental risk (over load-alone) is increased across all hours of the day and months of the year, with particularly acute increases in some periods -- *evening hours in summer and fall and early morning hours in the winter*.

Time-of-Day Trends from Forecast Accuracy Profile - When the hourly risk is further investigated from the overall error profiles using box plots, the results conform with earlier observations. Wind generation reduces net load forecast accuracy (increases errors) over most hours of the day, but particularly in early morning and late evening hours during winter, spring and fall. With regard to time-of-day trends, there three major observations:

1. Across all seasons, during the morning load rise hours, net load tends to be generally over-forecasted relative to load (positive bias). These are the periods when ramping requirement is high, so resource over-commitment should not lead to reliability issues.
2. Late evening hours tend to have lower net load forecast (relative to load) and incrementally larger extreme net load under-forecast errors, which may lead to under-commitment of resources. However, these are typically the hours of the day when resource needs are low.
3. During afternoon to early evening (peak) hours during summer and fall, there are incrementally larger net load under-forecast errors (relative to load. The size of these errors, relative to load errors, are such that they may potentially lead to under-commitment of resources during peak load times when they are most needed.

5. PRODUCTION SIMULATION ANALYSIS

5.1. Introduction

An economic simulation was performed on the ERCOT system in order to determine the operational impact of various levels of wind generation on the balance of the system generation. In addition to seeing how thermal generation production might be expected to shift, the key values determined were the hourly spot prices, or marginal cost of energy, and the hourly value, or opportunity cost, of spinning reserves. The spinning reserve cost was used as a surrogate to estimate the impact of wind generation on the cost of ancillary services in general. Another key value determined was the amount of capacity available for regulation services. As more wind generation enters the system there is a tendency for less thermal generation to be committed, thereby reducing the amount of generation that would naturally be available to provide ancillary services.

Although these results were available as a natural by-product of the simulation, the primary purpose of the simulation analysis was NOT to determine the economic value of the wind generation but rather to determine the operational impact on the balance of the system. What type of generation is displaced, coal or gas? What is the impact on emissions? What is the spot price impact of introducing a large amount of "price takers" to the system? What is the ramping rate and range of the balance of the system for regulation services? These are the types of results addressed in the remainder of this section.

The operational analysis was performed using the GE Multi Area Production Simulation program (MAPS). This program has been used for years throughout North America to assist planners, developers and regulators in the analysis of electric power systems. MAPS is a highly detailed model that calculates hour-by-hour production costs while recognizing the constraints on the dispatch of generation imposed by the transmission system. When the program was initially developed over thirty years ago, its primary use was as a generation and transmission planning tool to evaluate the impacts of transmission system constraints on the system production cost. In the current deregulated utility environment, the model has been useful in studying issues such as market power and the valuation of generating assets operating in a competitive environment. The unique modeling capabilities of MAPS include a detailed electrical model of the entire transmission network, along with generation shift factors determined from a solved ac load flow, to calculate the real power flows for each generation dispatch. This enables the user to capture the economic penalties of redispatching the generation to satisfy transmission line flow limits and security constraints. The chronological nature of the hourly loads is modeled for all hours in the year. In the electrical representation, the loads are modeled by individual bus. In addition to the traditional production costing results, MAPS can provide information on the hourly spot prices at individual buses and flows on selected transmission lines for all hours in the year.

In this particular analysis the transmission constraints were ignored. The study was designed to examine the impact of the intermittent and uncertain characteristics of wind assuming that sufficient levels of transmission were available. The base year of interest was 2008. Chronological regional load data for 2006 were scaled up to the 2008 projections. These loads were then paired with generation outputs from various wind plants throughout the system based on actual 2006 hourly meteorological data, as has been described previously. It was important to have load and meteorological data from the same time frame in order to capture the correlation between them. Wind generation penetration levels of 5,000 MW, 10,000 MW and 15,000 MW were examined, with two slightly different 10,000 MW scenarios being considered. For each wind site two separate profiles were developed. The first profile estimated the hourly production that would be expected at each wind plant based on the actual meteorological data that had occurred. The second profile was an unbiased (mean, or 50% confidence level) wind generation forecast, representing a day-ahead forecast made on the previous day. These profiles are referred to as the “State-of-the-Art”, or S-o-A forecast and were used in the day ahead commitment process.

5.2. Simulation Results

The bars in Figure 5-1 show the generation by type for the various wind generation scenarios. These results are based on the 2008 (study year) simulation using a state-of-the-art wind generation forecast for the day ahead commitment. Only the generation types that changed are shown. These include combined cycle units (CC), peaking gas turbines (GT), steam coal units (STCOAL) and steam natural gas fired units (STNG). The wind generation is also shown for each scenario. As can be seen, the major generation displacement occurred on the combined cycle units. There was slight impact on the other types, with gas turbines increasing slightly for the 5,000 MW and 10,000 MW wind generation capacity scenarios.

One of the key factors examined was the impact of wind generation on the commitment and dispatch of the balance of the system. Figure 5-2 shows the hourly unit commitment by unit type for the peak load week in mid August assuming zero wind generation. The unit commitment took into account the operational characteristics of the individual generators, including minimum down time, start up costs and their ability to contribute to the spinning reserve. The combined cycle, steam gas and gas turbine varied the most throughout the week.

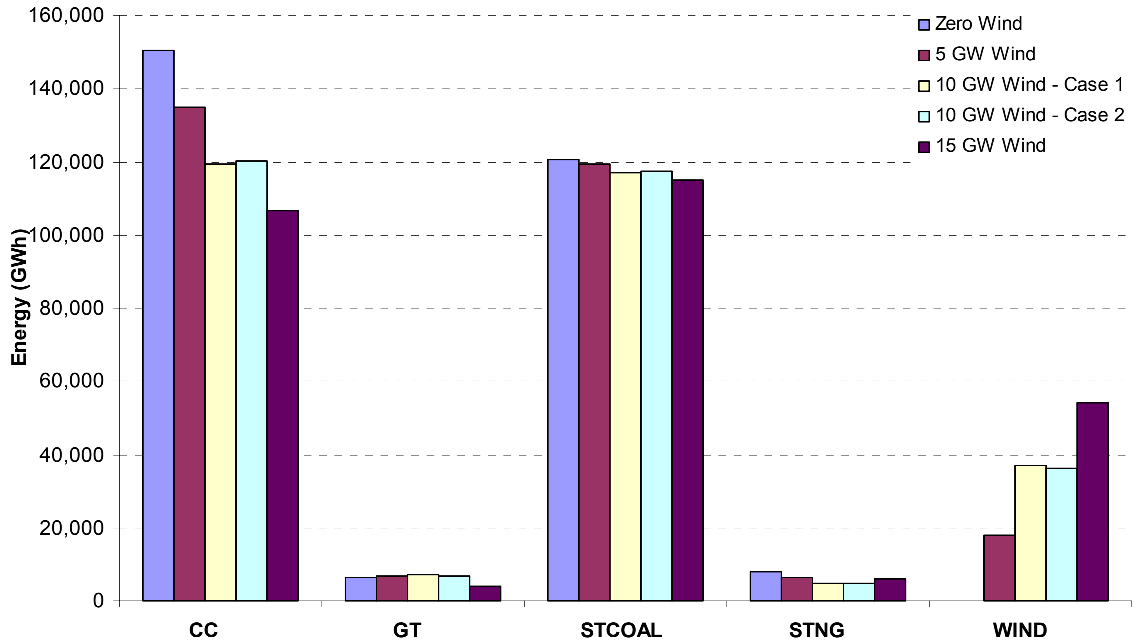

Figure 5-1 - Generation by type.

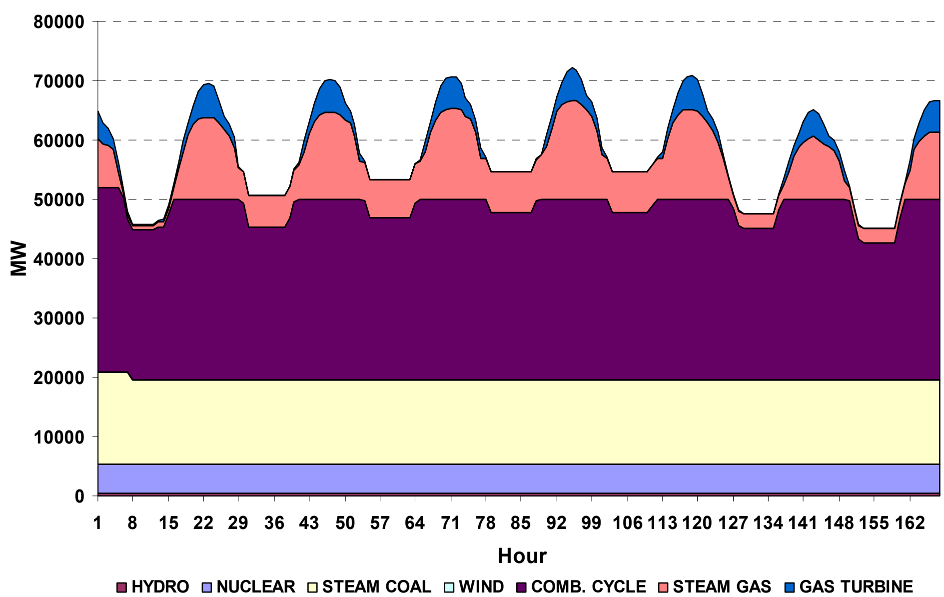

Figure 5-2 - Commitment for peak load week, zero wind generation.

The hourly dispatch for this week is shown in Figure 5-3. Here can be seen some variation in the hydro operation and more significant variation in the combined cycle and steam gas units. As will be shown later, this hourly unit commitment and dispatch information was used with the unit's ramping capability to determine the ramping (MW/minute) and range (MW) capability of the system on an hourly basis. This was then compared to the hourly regulation requirements of the system. Of particular importance was how this ramping and range capability changed as increasing amounts of wind generation were added to the system.

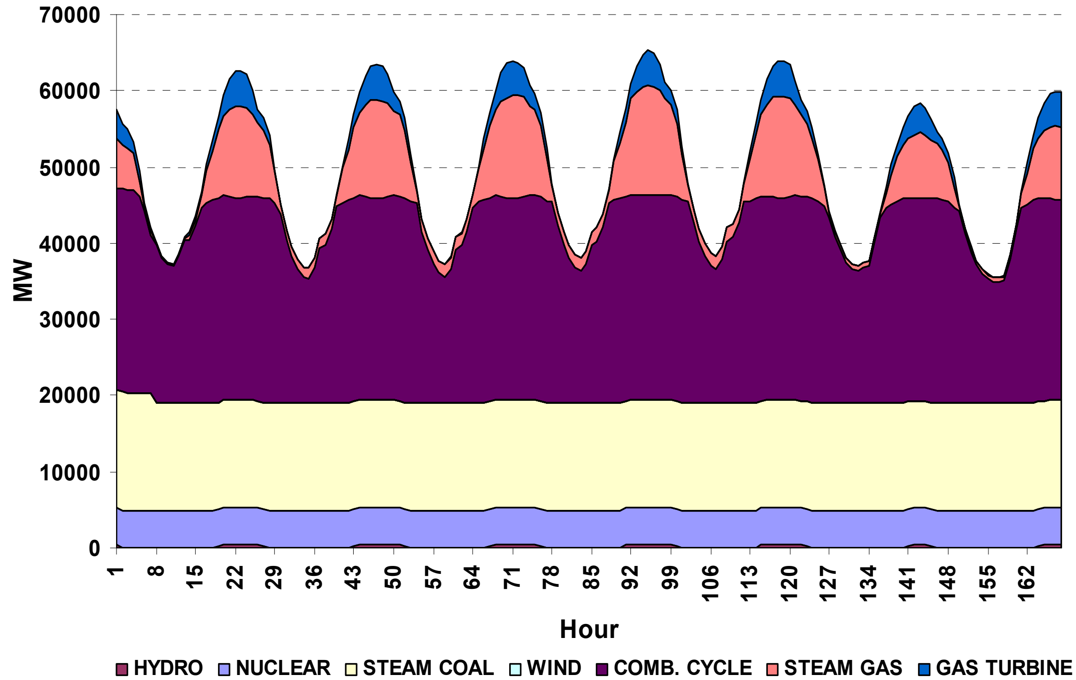

Figure 5-3 - Dispatch for peak load week, zero wind generation.

The plots in Figure 5-4 and Figure 5-5 show how the commitment and dispatch for this week change when 15 GW of wind generation capacity is added to the system. In this week it appears that the wind generation displaced peaking capacity on peak and combined cycle generation in the off-peak hours.

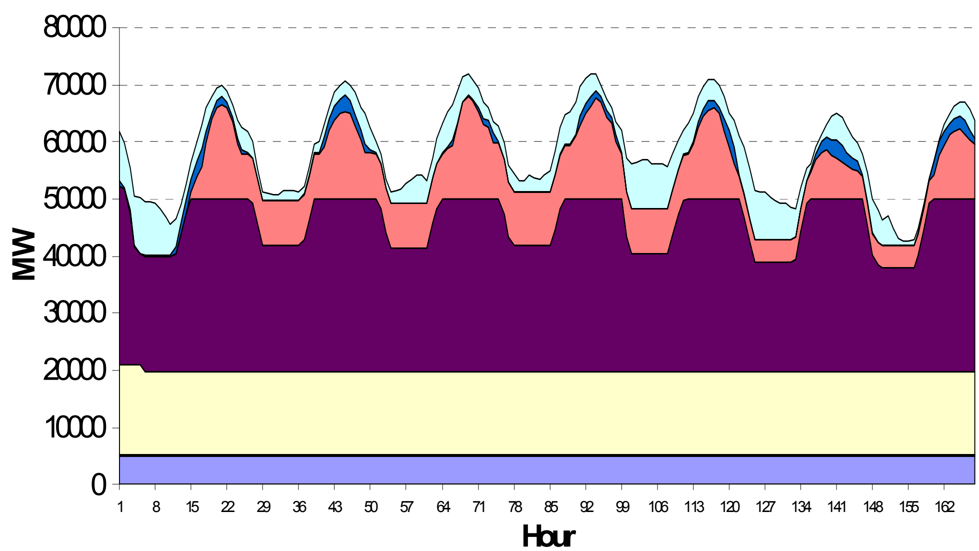

Figure 5-4 - Commitment for peak load week, 15 GW wind generation. (Same legend as Figure 5-3 applies)

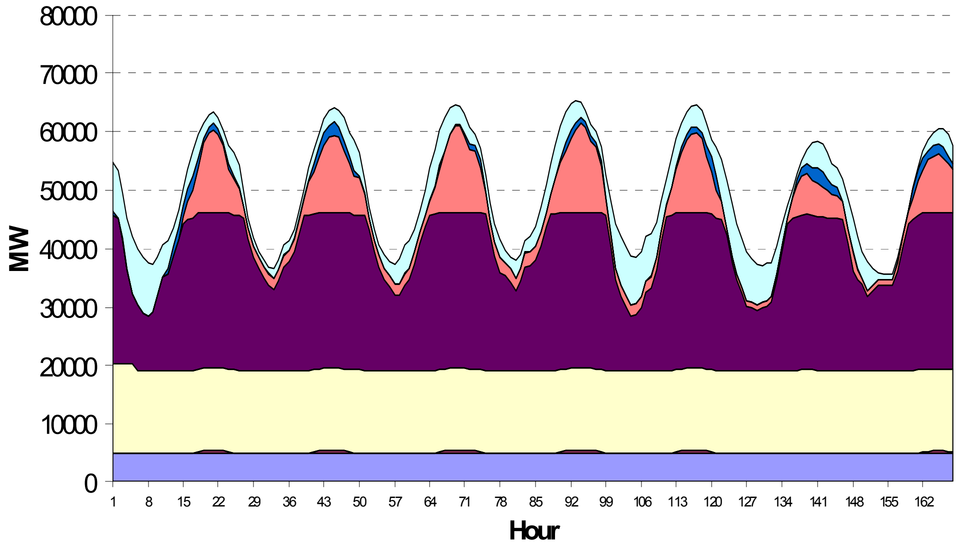

Figure 5-5 - Dispatch for peak load week, 15 GW wind generation capacity. . (Same legend as Figure 5-3 applies)

The next set of figures examines the system commitment and dispatch during the week with the highest amount of wind generation in early April. Figure 5-6 and Figure 5-7 show the hourly commitment and dispatch for this week for the zero wind generation scenario. Most of the variability in the loads is handled by the combined cycle generation. Figure 5-8 and Figure 5-9 show the impact of 15 GW of wind generation capacity added to the system. The committed combined cycle capacity is reduced to almost zero in some overnight periods and even the coal fired generation shows some deep turn downs in the overnight dispatch.

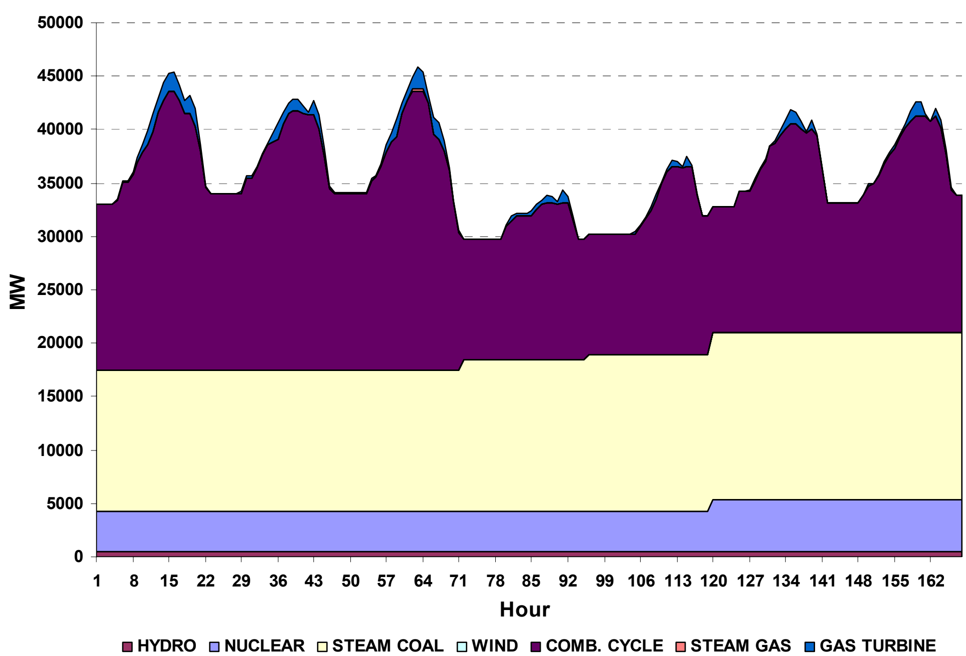

Figure 5-6 - Commitment for peak wind generation output week, zero wind generation.

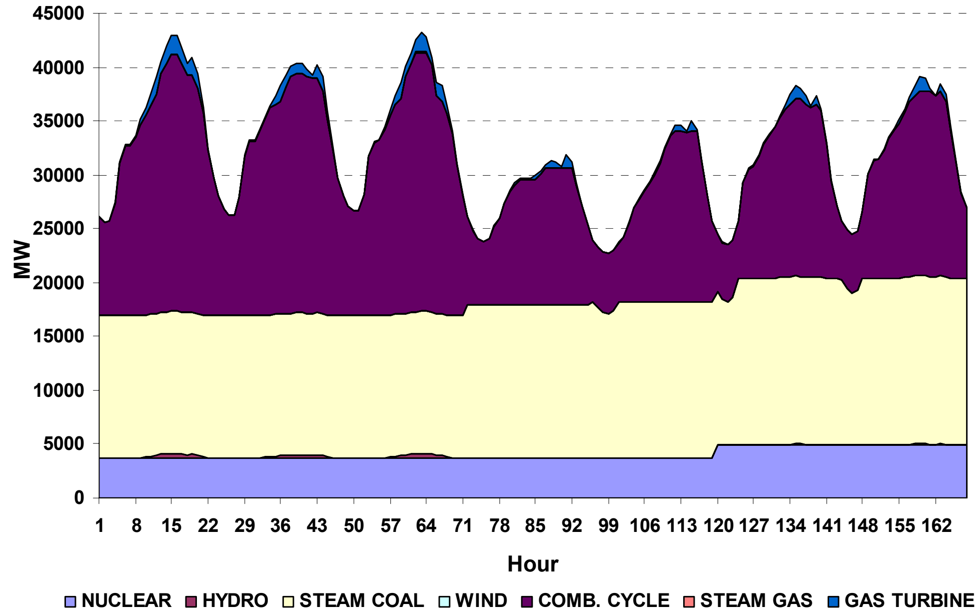

Figure 5-7 - Dispatch for peak wind generation output week, zero wind generation.

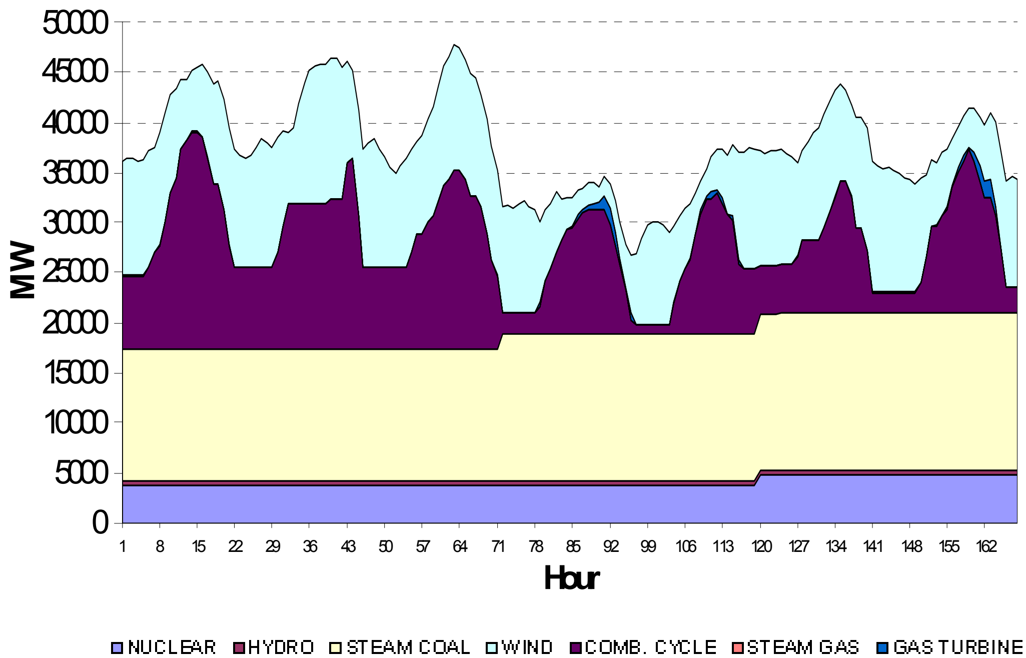

Figure 5-8 - Commitment for peak wind generation output week, 15 GW wind generation capacity.

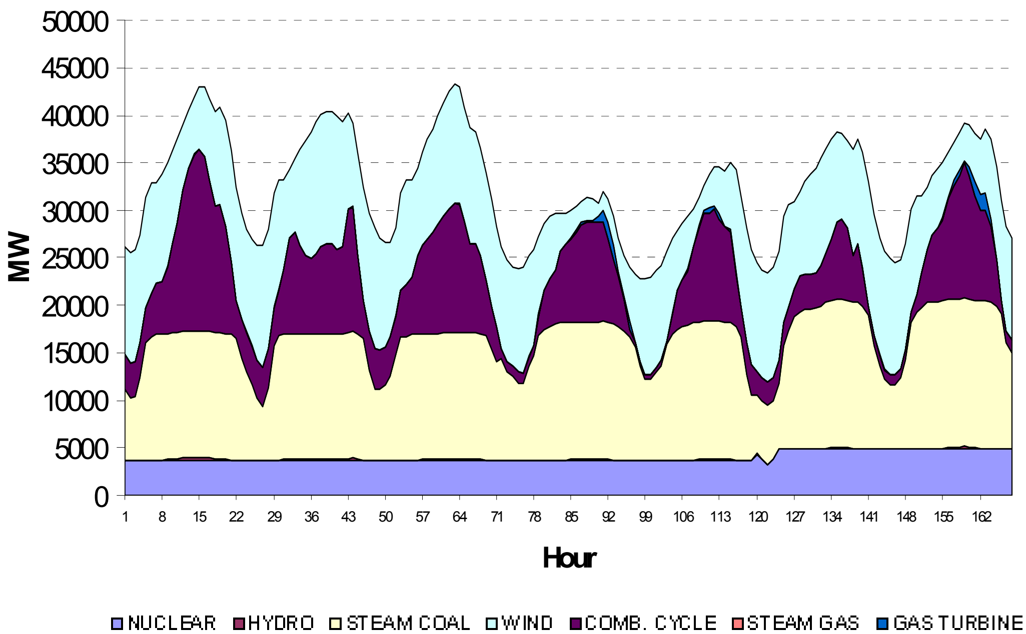

Figure 5-9 - Dispatch for peak wind generation output week, 15 GW wind generation.

The bars in Figure 5-10 show the reductions in the system production cost expressed on a megawatt hour of wind generation basis for the various wind scenarios. Based on this chart, the value of the wind does not drop significantly up through penetrations of up to 15 GW. These bars are consistent with the earlier chart showing that combined cycle generation bore the brunt of the displacement across all scenarios.

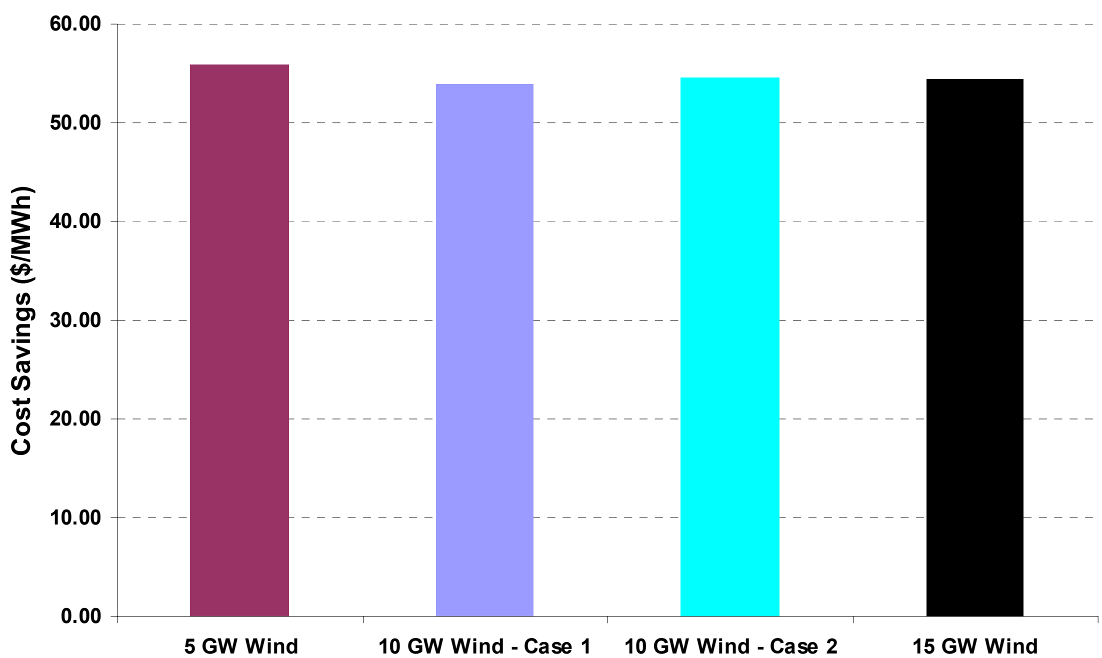

Figure 5-10 - Production cost reductions due to wind generation.

The charts in Figure 5-11 show how the total annual emissions decline as the wind generation penetration is increased.

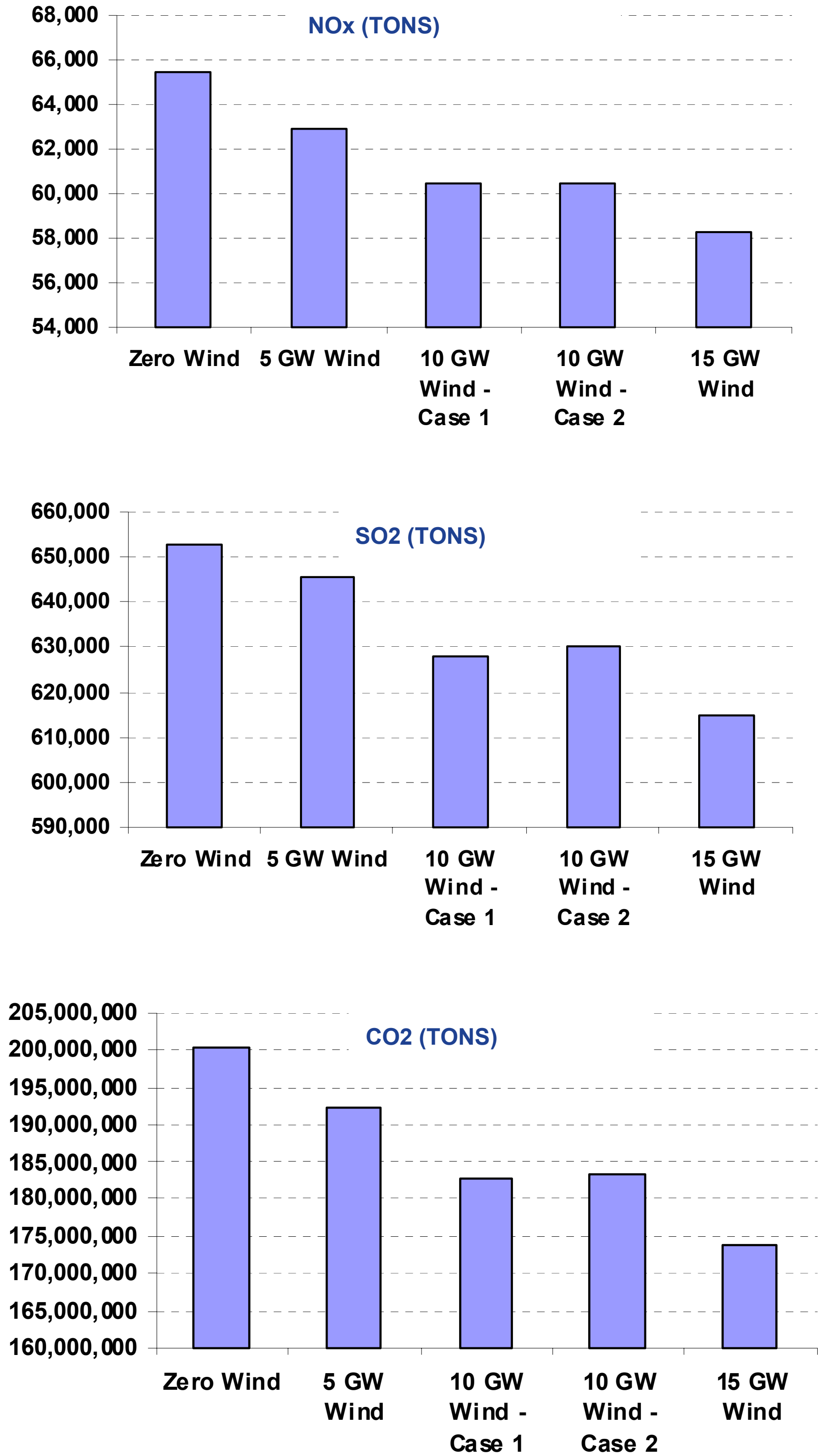

Figure 5-11 - Total annual emission.

5.3. Spot Price Impact

The curves in Figure 5-12 show the impact of increased wind generation on the system spot price, or incremental value of energy in $/MWh. The values were calculated on a chronological, hourly basis assuming a state-of-the-art wind generation forecast. They were then sorted individually for the plot.

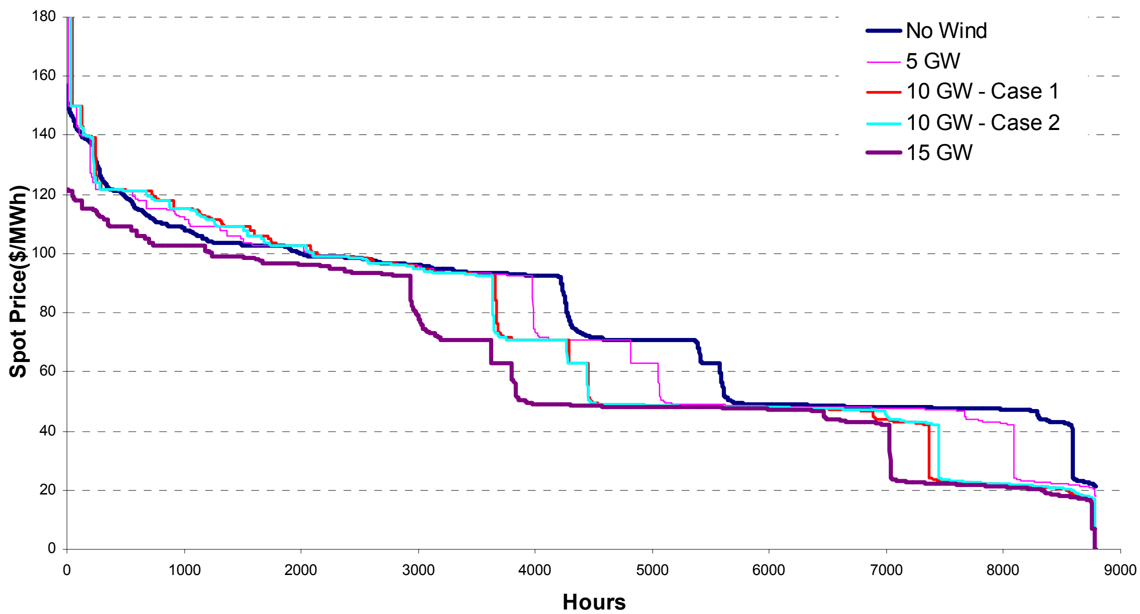

Figure 5-12 - Energy spot prices.

In general, as the wind generation penetration increases it displaces the higher cost thermal generation and reduces the overall cost of energy. In some cases the spot prices are slightly higher due to the imperfections in the state-of-the-art forecast used.

The curves in Figure 5-13 examine the impact of wind generation forecast on the resulting spot prices for the 15 GW penetration scenario. The perfect forecast drops slightly below the zero wind scenario for the first 3500 hours and then increases the separation for the rest of the curve. The spot prices calculated with the state-of-the-art forecast are slightly lower and then drop after about 3000 hours. The ”no forecast” case totally ignores the wind generation in the day ahead forecast and therefore significantly over-commits the system. This results in the spot prices dropping significantly all of the time.

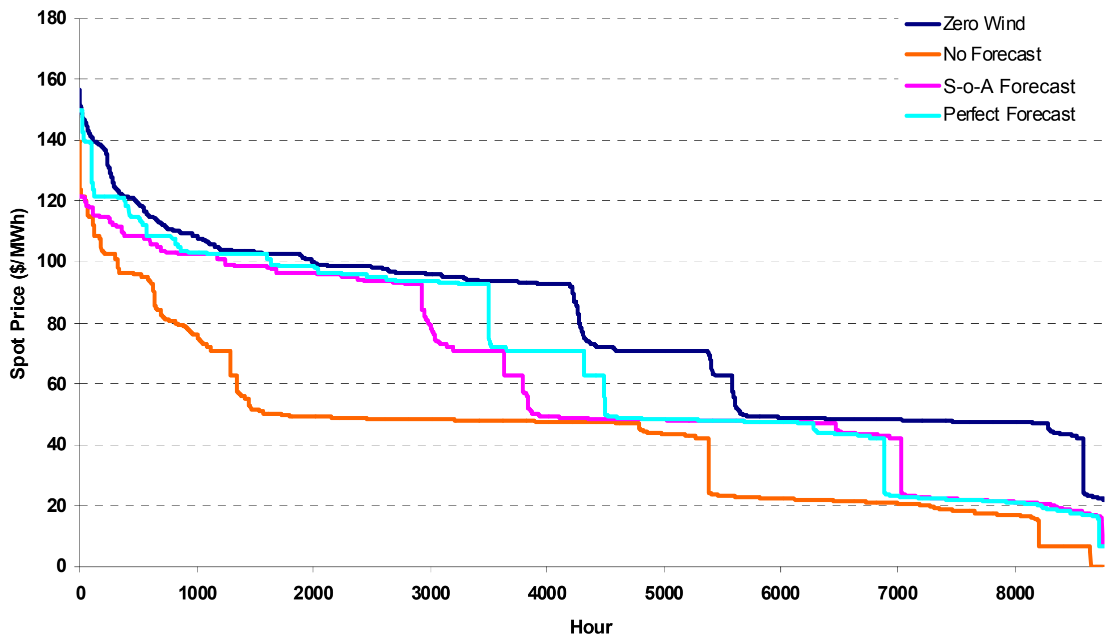

Figure 5-13 - Wind forecast impact on energy spot prices.

6. REGULATION REQUIREMENTS ANALYSIS

Section 3 provides the results of an extensive analysis of load and net load variability, over various timeframes, independent of specific ancillary services definitions or system operating practices. This section specifically analyzes the regulation ancillary service, as defined by ERCOT for use in the new nodal market structure.

This section includes extensive analysis of the deployed regulation for each of the wind generation scenarios, and correlation to temporal factors. The adequacy of ERCOT's present methodology to determine the amount of regulation to procure is assessed, and some improvements are suggested. Using production simulations for each scenario described in Section 5, the flexibility of the dispatchable generation fleet to provide the required regulation capability is assessed. Also using the production cost simulation results, the costs of procuring the regulation service are estimated.

6.1. Regulation in the Nodal Market

ERCOT plans to shift from a zonal market to a nodal market in 2009. In this transition, the methods of system operation and the nature of the regulation ancillary service will change. This study solely analyzes regulation as defined for the nodal market. However, there are details of the nodal market with regard to regulation that are still subject to refinement.

The ERCOT nodal market will use five-minute dispatch cycles. The dispatched generation setpoint for each period is the instantaneous value of load (or net load) at the beginning of the period, plus a heuristically-determined "tuning factor" times the expected change of net load over the period as determined by the short-term load forecast. The tuning factor will be between zero and one, and may vary with time of day and season.

Analysis of actual regulation requirements under the nodal market was beyond the scope of this study, as ERCOT has not yet made determination of the tuning factors that will be used. Any speculative choices made regarding the tuning factors are most likely to not be the same as the final values, and defining a quasi-optimal selection of tuning factor levels for different seasons and times of day would have required significant additional study outside of the study scope.

At the direction of ERCOT, the tuning factor was assumed to be zero. It is expected that optimizing the tuning factors on an hourly and seasonal basis will reduce the amount of regulation required to provide load-following service during periods of large system ramps (up or down). By proceeding with this analysis with the tuning factor set to zero, the study has purposely foregone an exact reflection of regulation requirements in the nodal market. But, by so doing, have allowed the development of an unbiased analysis of the incremental amounts of regulation required with increasing amounts of wind generation capacity on the system. The results of this study should not be considered as an absolute prediction of regulation requirements in the nodal market. But, this limitation does not invalidate what are the key results from this study - the incremental regulation requirements resulting from additional wind generation capacity. It is important that results shown in this report are not compared with historical zonal regulation requirements.

In this study, regulation has been defined to be the deviation of the net load from the economic dispatch setpoint, unadjusted by the short-term net load forecast. as illustrated in Figure 6-1. Up-regulation (indicated in this report as +REG) is the positive difference between actual load and dispatched generation output, and is used when load exceeds the generation . Down-regulation (indicated in this report as –REG) is used when load is less than the dispatched generation output. Throughout this report, up-regulation is shown as a positive number and down-regulation is shown as a negative number.

Figure 6-2 shows the regulation deployments using the nodal algorithm, for one typical day (April 1). The regulation is strongly influenced by the load ramp rate, with large up-regulation requirements during periods of load rise, with little or no down-regulation required for the same period, and large down-regulation requirements during load drop. The impact of load ramp rate has a greater influence on regulation than does the random variation of load.

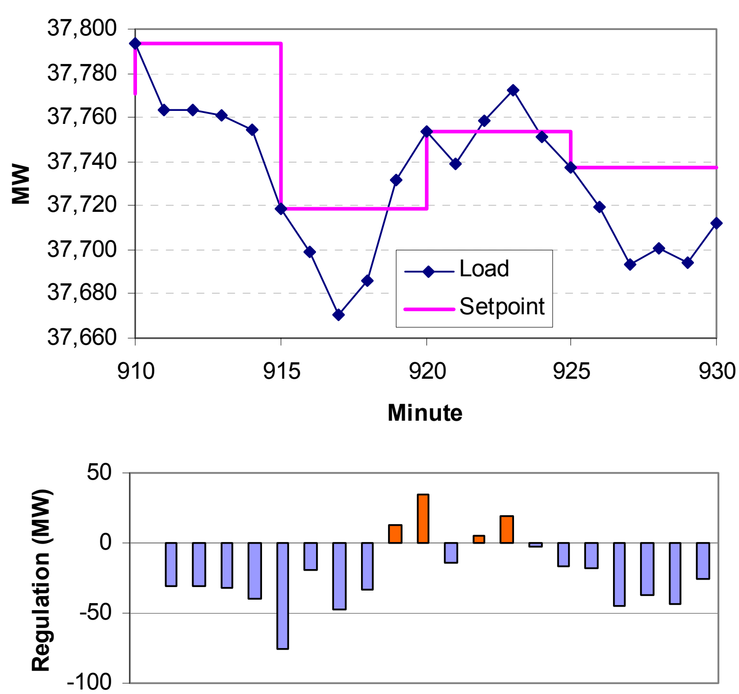

Figure 6-1 - Illustration of regulation as defined for the ERCOT nodal market

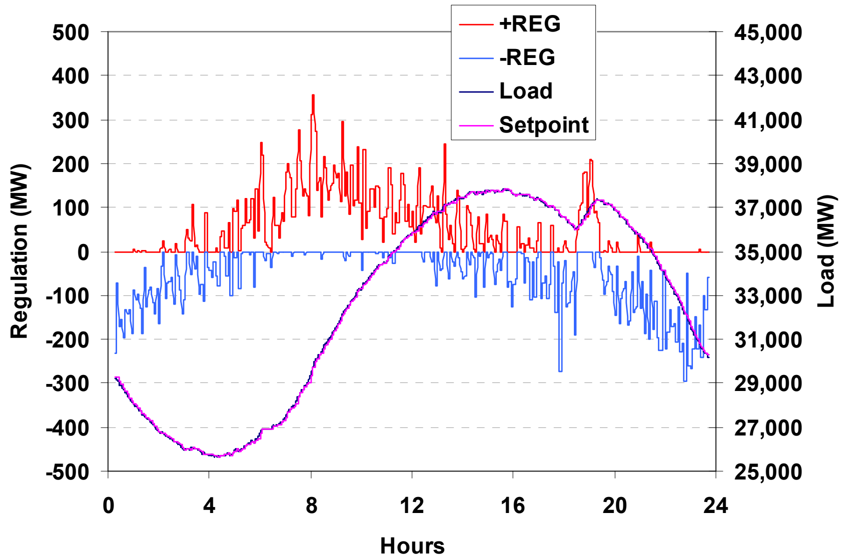

Figure 6-2 Regulation deployments for the same spring day as Figure 6-1.

6.2. Impact of Wind on Regulation

The nodal regulation algorithm was modeled on a minute-by-minute basis for the entire "study year", and for the "prior year, for each of the wind generation scenarios. Figure 6-3 plots the maximum up-regulation and down-regulation[1] requirements for each hour in a 100-hour (approximately four day) sample from January of the study year. Similar plots for the months of April, July, and October, representing the seasons of the year, can be found in Appendix E.1. In these plots, the lines above zero represent up-regulation, plotted as a positive number, and the lines below zero represent down-regulation, plotted as a negative number. These plots illustrate several observations which can be made regarding the impact of wind generation on regulation deployments, which are:

- The general nature of the regulation requirement is not greatly altered by the addition of wind generation.
- Some extrema are driven entirely by the wind. An example is seen at Point A of the expansion in Figure 6-3, where there is no significant peak in regulation requirements at this hour without wind generation, and the peak becomes progressively more significant as wind generation is added.
- The largest peaks in the plot are driven by the load behavior such as at Point B, and addition of wind makes only a very incremental increase in severity.

[1] Maximum in the absolute value sense. Because the down-regulation is recorded as a negative number, the most severe down-regulation requirement is, mathematically speaking, the minimum regulation.

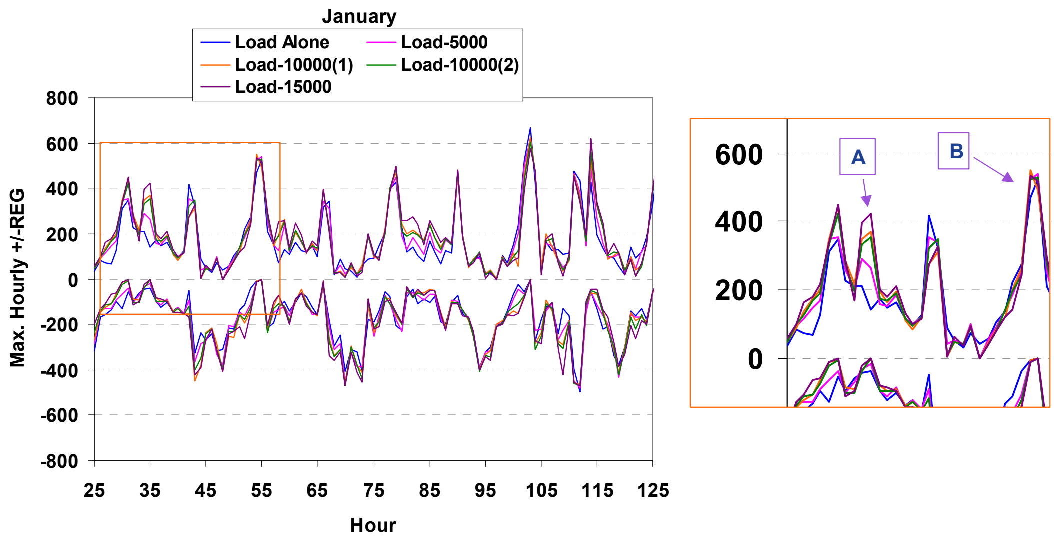

Figure 6-3 ***Maximum hourly regulation deployments for a 100-hour sample from January of the study year, for the wind generation scenarios. (Plot to the right is an expansion of the boxed area shown in the plot on the left).***

6.2.1. Statistical Description of Regulation Deployment

The cumulative distributions of hourly regulation maxima shown in Figure 6-4 to Figure 6-9 illustrate the incremental impact of increased wind penetration on regulation deployments. Figure 6-5 and Figure 6-8 expand the plot for the lower values of maximum regulation that pertain to 90% of the annual hours. Most important to system operations are the extreme values of regulation deployment[2]. Figure 6-6 and Figure 6-9 expand the cumulative distribution plots for the most severe 100 hours, or 1.14% of the year, and indicate that the increase in extreme regulation deployments between zero and 15,000 MW of wind is on the order of 100 MW. Throughout all of these plots it can be seen that the impact of wind penetration on regulation is quite incremental, and approximately proportional to the amount wind generation capacity of the scenario.

It should be noted that the cumulative distributions, plotted in Figure 6-4 to Figure 6-9, use data separately sorted and ranked for each scenario. Therefore, points at the same location on the independent axis (x-axis) are not necessarily associated with the same hour in the year. Another way to view the relative impact of wind penetration on regulation requirements is by the frequency distribution of changes in regulation

[2] In this report, the difference between net load and dispatch setpoint are always considered “deployed” regulation, even if this amount exceeds the procured regulation service for that hour. In such a case, when the procured regulation reserves are exhausted, responsive reserves are used to fulfill the regulation deployment required.

requirements, due to wind, on an hour-by-hour basis. Such a distribution is plotted in Figure 6-10, and statistics of the hour-by-hour comparison are summarized in Table 6-1.

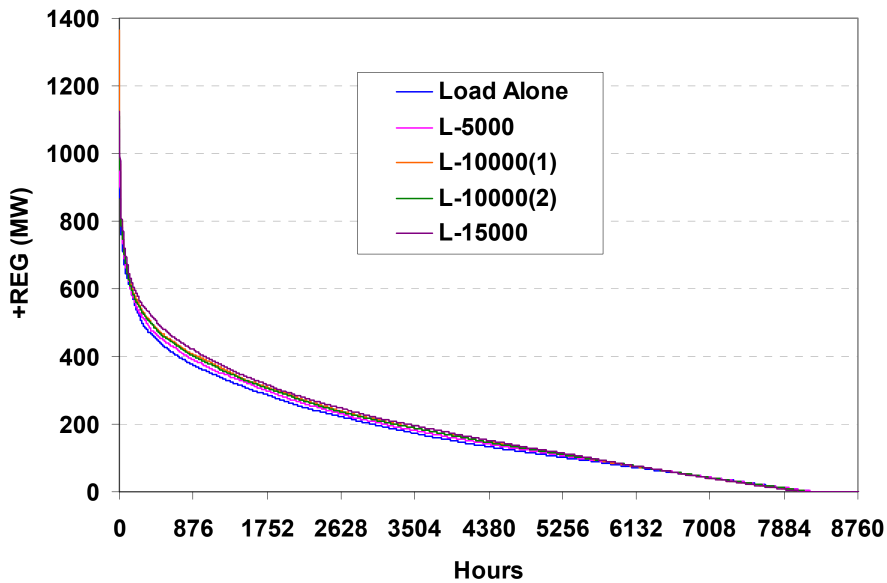

Figure 6-4 Cumulative distribution of hourly up-regulation maxima.

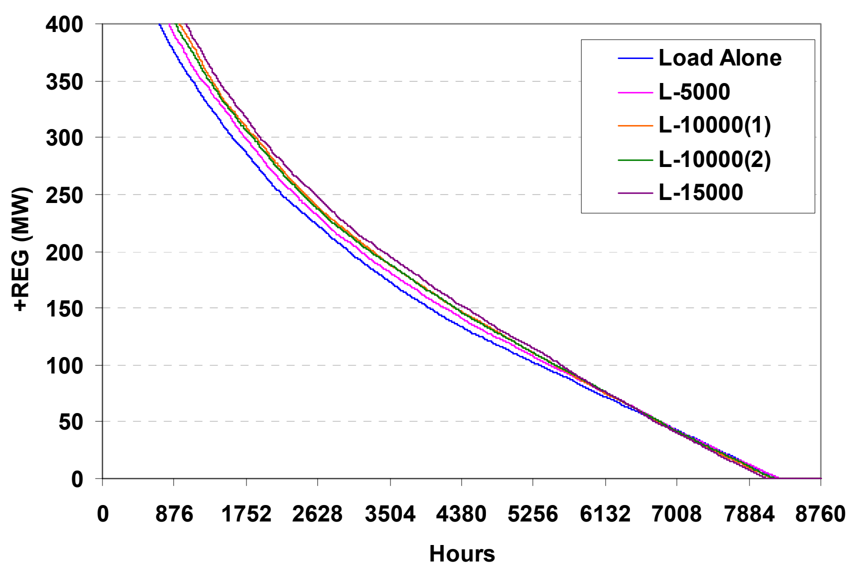

Figure 6-5 Expansion of Figure 6-4 for the range of 0 to 400 MW up-regulation.

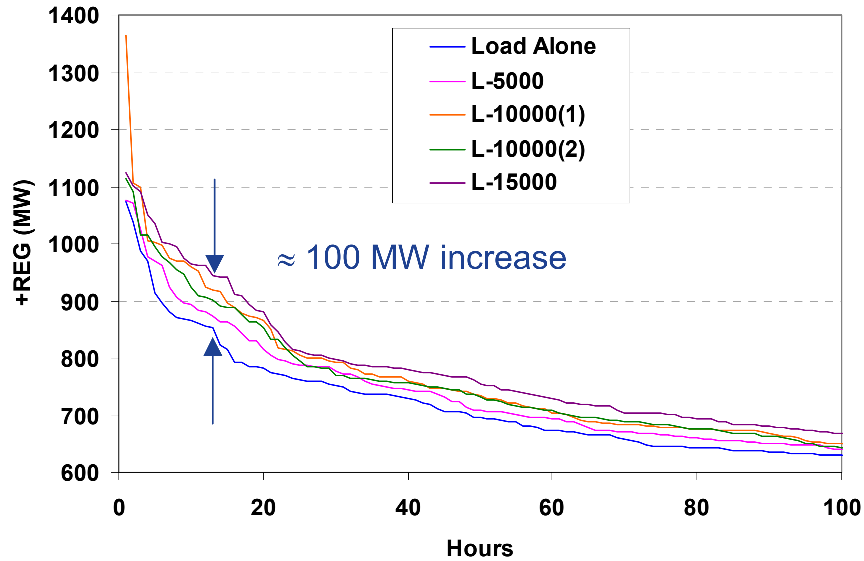

Figure 6-6 ***Expansion of Figure 6-4 for the 100 hours with the greatest up-regulation deployments***

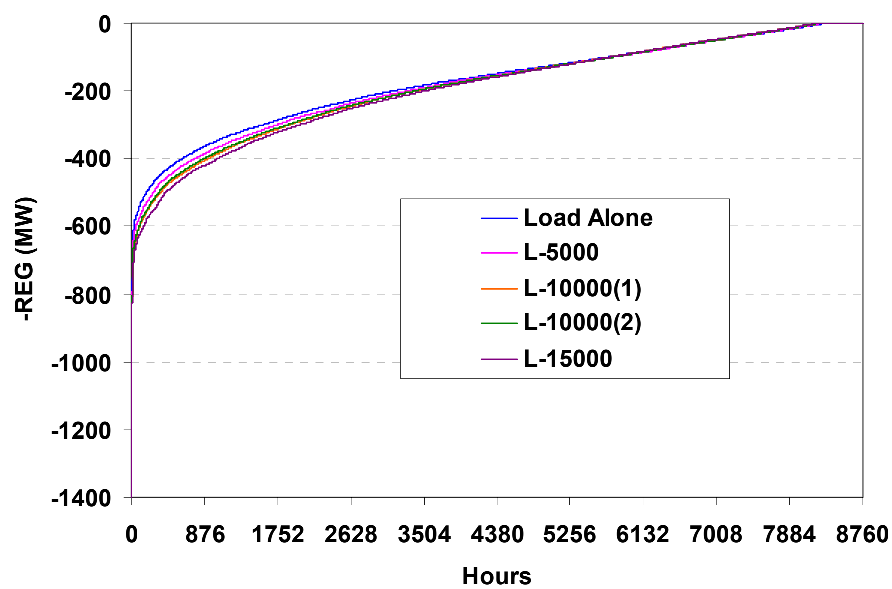

Figure 6-7 ***Cumulative distribution of hourly down regulation maxima.***

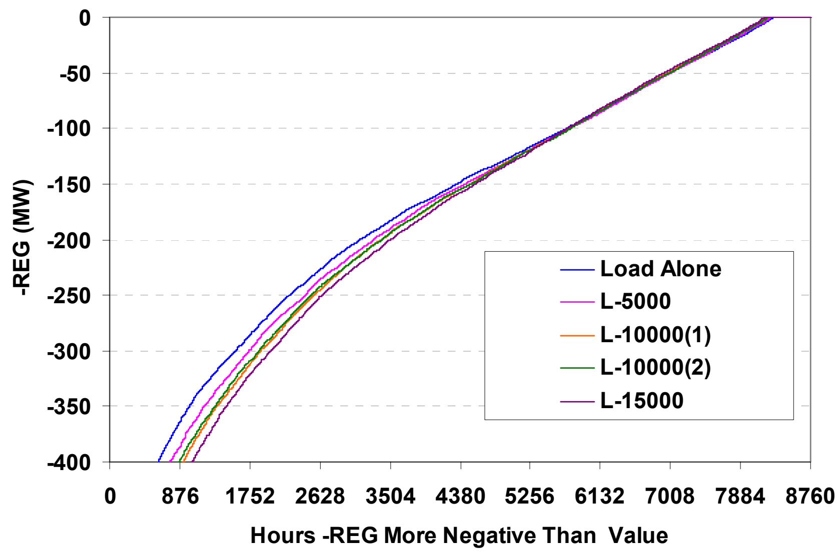

Figure 6-8 ***Expansion of Figure 6-7 for the range of 0 to 400 MW down-regulation.***

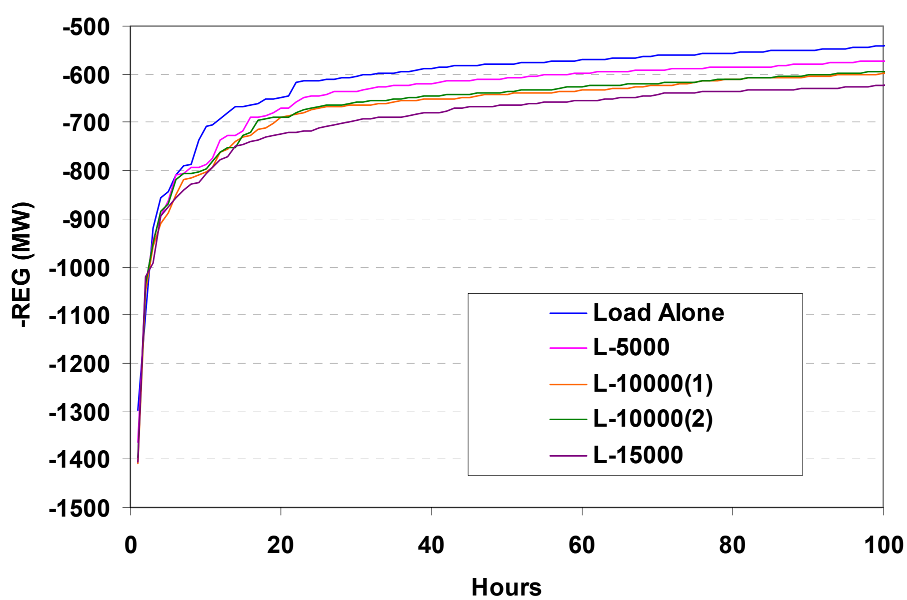

Figure 6-9 ***Expansion of Figure 6-7 for the 100 hours with the most severe down-regulation deployments***

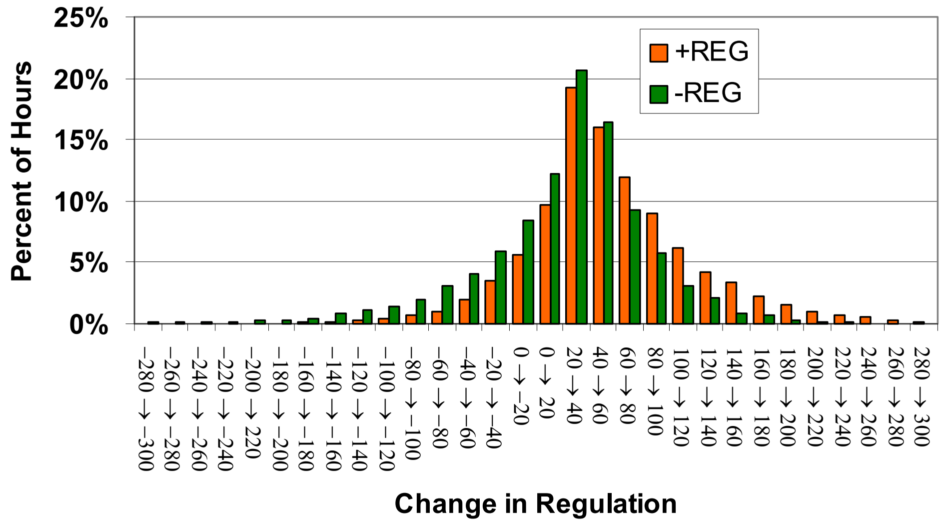

Figure 6-10 ***Frequency distribution of changes in hourly maximum regulation deployments between the 15,000 MW wind scenario and the zero wind scenario.***

Table 6-1 ***Statistical Summary of Changes in Hourly Maximum Regulation Deployments, Between No Wind to 15,000 MW of Wind Generation Capacity***

	+REG	-REG
Mean	17.7	-18.2
Sigma	64.9	65.1
Maximum	444.2	265.3
Minimum	-287.2	-453.1

There are a number of observations which can be made with regard to this frequency distribution and statistical summary:

- For any given hour, the magnitude of regulation can be either increased or decreased by having more wind capacity in the system.
- The mean increase in absolute value of hourly regulation extrema is approximately 18 MW for both up- and down-regulation.
- The mode (value range with the highest frequency) is a positive value for both the up-regulation and the down-regulation, even though the down-regulation is analyzed as a negative number. This means that a small increase in up-regulation, and a small decrease in down-regulation absolute value, are the most common changes caused by wind.

- The standard deviation of the relative regulation change is nearly equal for both up- and down-regulation, but there is a very obvious skew in the distributions toward the direction of increased regulation requirements (positive for up-regulation, and negative for down-regulation as a negative value).
- The most severe changes are symmetrical for up-regulation and down-regulation. The maximum up-regulation is nearly equal to the minimum, or most negative (most severe) down regulation. Also, the greatest changes in the direction of most severity were about 150%-170% of the greatest change toward reduced regulation severity (minimum, or most negative, change for up-regulation and maximum, or most positive change for down-regulation).

6.2.2. Regulation Service Procurement

ERCOT presently procures regulation services based on statistical analysis of historical deployments. For each month, procurements are determined for each hour of the day, with the same daily procurement pattern applying to all days of the month. Historical deployments considered are for the same hour of day in the prior month, and for the same month in the prior year. To perform the statistical analysis, ERCOT starts by determining the maximum regulation deployment within 5-minute periods for the hour in consideration. Maximum deployment data for the hour are combined for all days in the month, yielding a total of 336 to 372 periods (12 periods per hour times the number of days in the month). The 98.8th percentiles of these points are determined for the data pools for the same month in the prior year and for the prior month, and the greater of these is used as the basis for regulation procurement.

Thus, the statistical description of regulation deployments in terms of the 98.8th percentile is most relevant, and is indicative of the changes in regulation service procurements which will need to be made with increased wind penetration.

Table 6-2 summarizes the average, 98.8th percentile[3], and extrema[4] of the 5-minute regulation deployments for each wind generation scenario. The 98.8th percentile data

[3] This value is the average of the 98th percentiles of the maximum regulation in five-minute periods for each hour for each month, which is a metric indicative of the annual average amount of regulation service that would need to be procured. The process for determining this value is as follows: 1) Maximum up-regulation, or most negative down-regulation, is determined for each five minute period. 2) The 98th percentile of these maxima are determined for each hour-of-day within a month (population of 336 to 372 samples). 3) The average of the 98th percentiles are determined for all hours-of-day within the month (24 values). 4) The annual weighted average of the months, weighted by the number of days per month, yields the final value.

[4] Mathematically, the maximum of the up-regulation deployments and the minimum of the down regulation deployments.

increases, relative to the zero wind case, by 20.7% and 23.1% for up-regulation and down regulation, respectively. Interestingly, this correlates closely with the relative increase in net load variability as presented in Section 3. Also of note is the fact that the regulation extrema do not increase as much as the mean and 98.8th percentile values. This implies that the distributions are better behaved with increasing wind, with outliers less severe relative to the magnitude of the mean and 98.8th percentile.

Table 6-2 - Deployed Regulation Statistics

Up-Regulation

Wind (MW)	Average Max of 5-min Periods	% Change	98th Percentile of 5-min Periods	% Change	Maximum	% Change
0	73.8 MW		232.1 MW		1072.5 MW	
5,000	78.1 MW	5.8%	247.0 MW	6.4%	1075.9 MW	0.3%
10,000 (1)	82.5 MW	11.7%	265.2 MW	14.2%	1105.6 MW	3.1%
10,000 (2)	81.4 MW	10.2%	261.5 MW	12.7%	1112.7 MW	3.7%
15,000	86.1 MW	16.5%	285.8 MW	23.1%	1124.9 MW	4.9%

Down-Regulation

Wind (MW)	Average Min of 5-min Periods	% Change	98th Percentile of 5-min Periods	% Change	Minimum	% Change
0	-74.3 MW		-233.0 MW		-522.2	
5,000	-78.6 MW	5.8%	-246.7 MW	5.9%	-538.9	3.2%
10,000 (1)	-83.0 MW	11.7%	-262.7 MW	12.8%	-554.9	6.3%
10,000 (2)	-81.5 MW	9.7%	-260.4 MW	11.8%	-565.9	8.4%
15,000	-86.6 MW	16.5%	-281.2 MW	20.7%	-566.4	8.5%

6.2.3. Temporal Trends

Figure 6-11 shows plots of the maximum and 98.8th percentile of regulation deployments for four months of the year, representing each season. The solid lines represent the 98.8th percentile of the maximum regulation deployments for the five-minute periods, with the magenta line representing load alone, and the blue line representing the net load for the 15,000 MW wind scenario. The dotted lines represent the extrema for the two scenarios plotted here.[5] Plots above zero indicate up-regulation, and plots below zero represent down-regulation, plotted as a negative number.

The contour plots in Figure 6-12 and Figure 6-13 compare the temporal characteristics of the up-regulation deployment 98.8th percentiles for no wind and the 15,000 MW wind scenario, respectively. The x-axis indicates the hour of day, and the y-axis indicates the month of year. The colors, according to the legend, indicate the 98.8th percentile of the

[5] For plotting clarity, only the maximum (15,000 MW) and zero wind penetration results are shown in many plots of this report. These results bracket the results for all the scenarios, and results of this study show the intermediate scenarios providing results which are generally proportional to the wind penetration.

maximum regulation deployments in all the 5-minute periods for the particular hour, over all the days in the month. Figure 6-14 and Figure 6-15 are equivalent contour plots for down-regulation. Appendix E.2 provides these contour plots for all wind scenarios.

The temporal characteristics of the differences in 98.8th percentile regulation deployments, between zero and 15,000 MW of wind scenarios, are shown in Figure 6-16 and Figure 6-17.

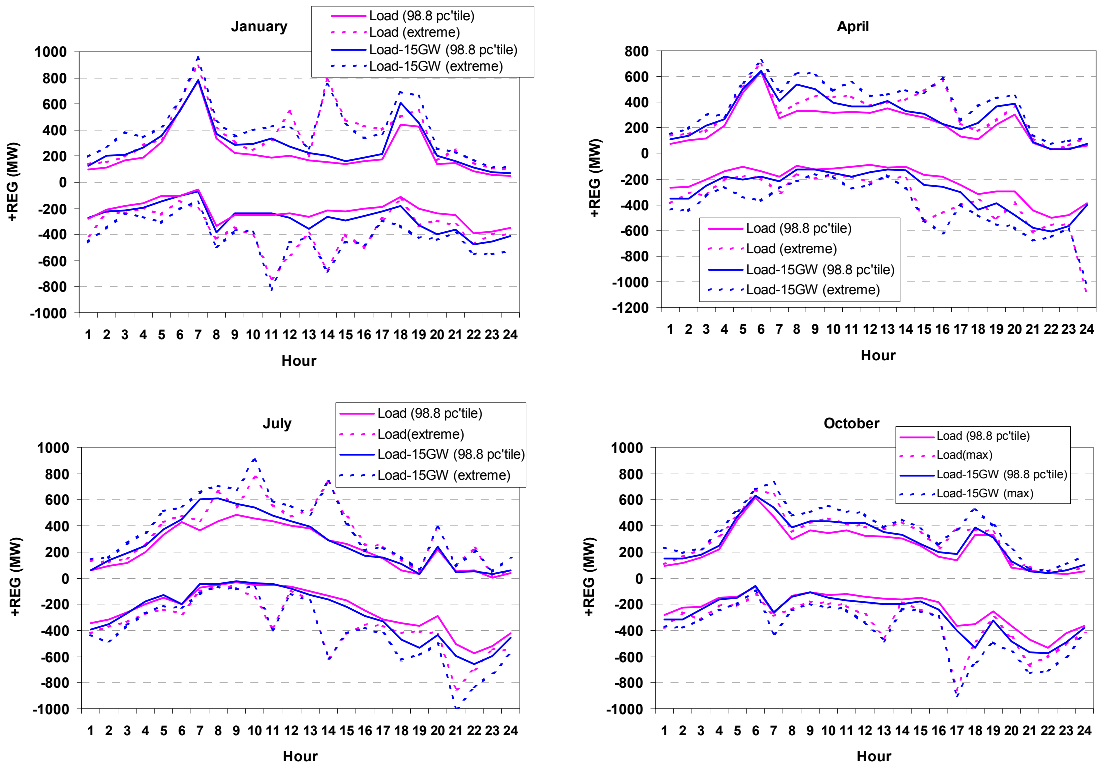

Figure 6-11 - Maximum and 98.8th percentile regulation deployments by hour of day for months representing the four seasons.

Regulation procurements are currently based on the greater of the 98.8th percentile of deployments for the same month in the prior year and the prior month in the same year. Because wind generation capacity is presently increasing very rapidly in ERCOT, the prior month value may be controlling most of the time if measures are not taken to adjust the prior year data for the wind capacity growth. Basing regulation procurement only on the prior month, by default, may result in under-procurement in months where the regulation requirements exceed the prior month. A methodology adjustment to account for year-to-year wind capacity additions is discussed later in Section 6.3.2.

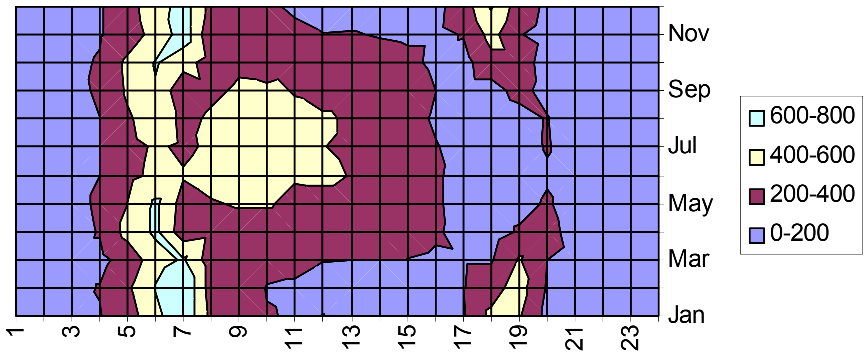

Figure 6-12 98.8th percentile of up-regulation deployments for the zero wind scenario.

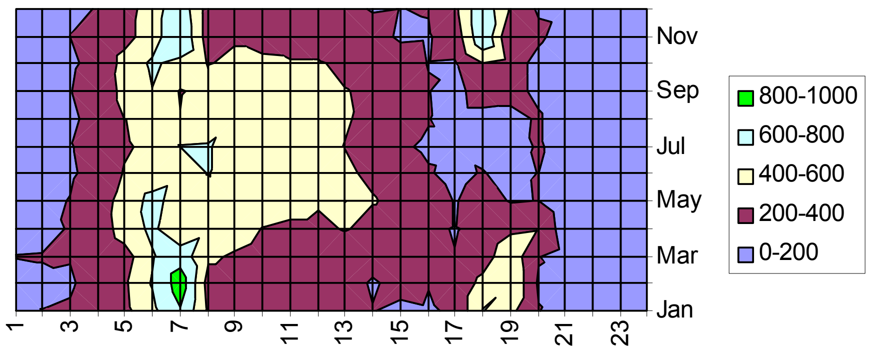

Figure 6-13 98.8th percentile of up-regulation deployments for the 15,000 MW wind scenario.

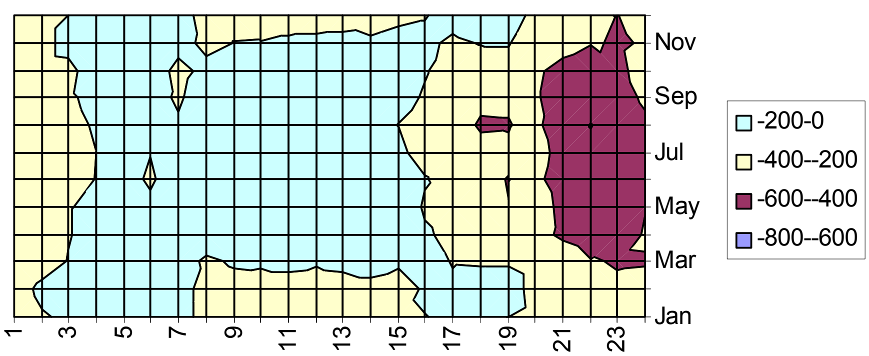

Figure 6-14 98.8th percentile of down-regulation deployments for the zero wind scenario.

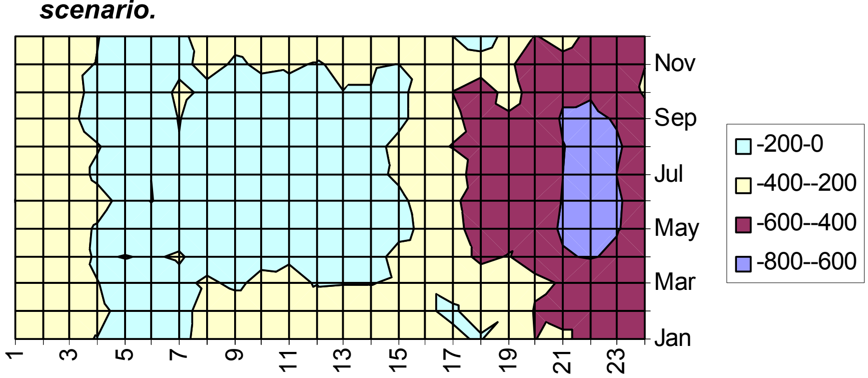

Figure 6-15 98.8th percentile of down-regulation deployments for the 15,000 MW wind scenario.

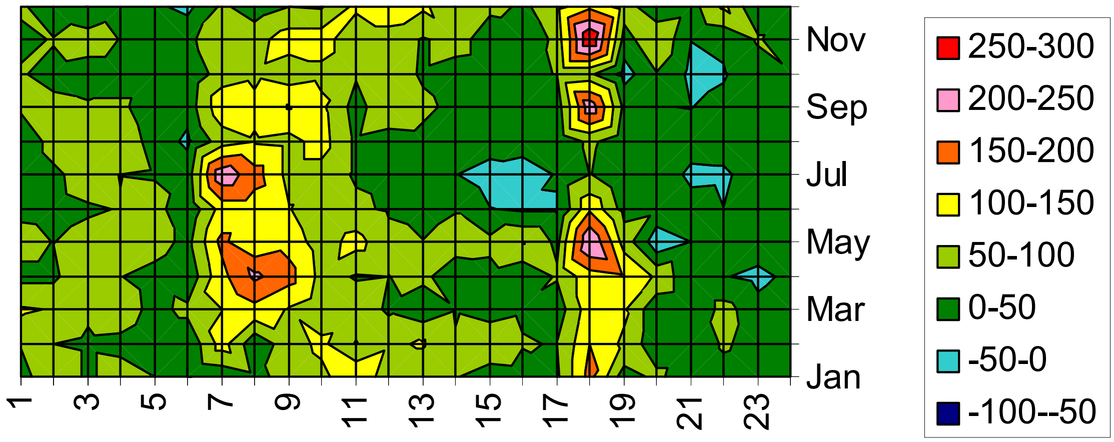

Figure 6-16 ***Difference in 98th percentile of up-regulation deployments between 15,000 MW wind scenario and zero wind scenario.***

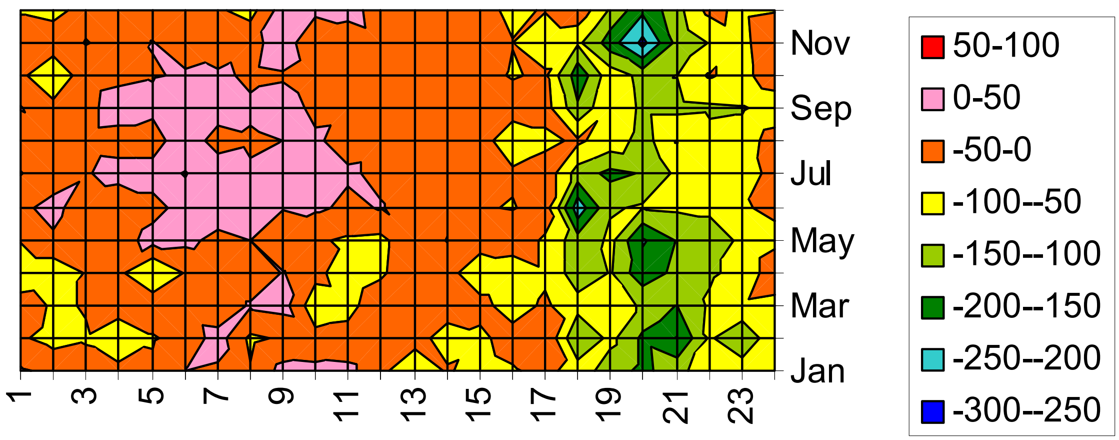

Figure 6-17 ***Difference in 98th percentile of down-regulation deployments between 15,000 MW wind scenario and zero wind scenario.***

The following observations regarding the changes in the 98.8th percentile of regulation deployments, due to wind, can be derived from these plots:

- Up-regulation requirements are most significantly increased during the morning load rise period, particularly during spring and summer, when winds tend to drop.
- Up-regulation requirements also increase significantly during the evening, for all seasons except summer.
- Down-regulation deployments increase during the evening, all year round.
- Down-regulation requirements tend to decrease, with increasing wind, during the morning hours, particularly during the period from late spring through early fall.

The relative changes in regulation are not consistent over the temporal space. Selected periods of significant regulation change are plotted as a function of the wind penetration in Figure 6-18.

The relative changes in regulation deployments vary greatly for different time periods. However, all the changes are nearly perfectly linear with wind capacity. This attribute can be applied to adjusting ERCOT's regulation procurements during periods of significant year-to-year wind capacity growth. This is discussed later in Section 6.3.2.

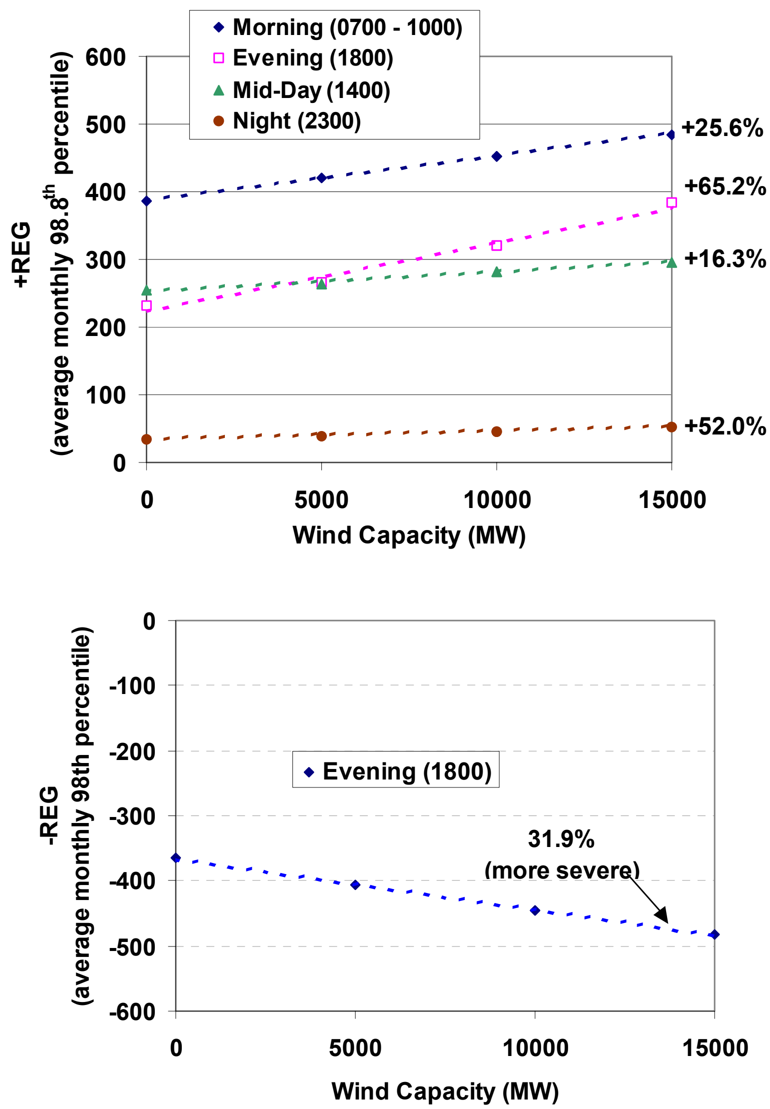

Figure 6-18 *Regulation deployment (average 98.8th percentile) as a function of wind generation capacity.*

6.2.4. Comparison of Regulation Deployments in 10,000 MW Scenarios

This study considered two 10,000 MW wind generation scenarios, with different allocations of generation capacity to the CREZs. The first 10,000 MW case, denoted as the 10,000(1) scenario, has 1,500 MW of wind generation in CREZ 4, located in the Texas Panhandle. The second 10,000 MW case, denoted as the 10,000(2) scenario, substitutes 1,500 MW of wind generation in CREZ 24, located on the coast of South Texas, for the CREZ 4 generation. Table 6-3 compares the regulation deployments for these two scenarios. These results indicate that the improved geographic diversity of the wind generation portfolio, in the 10,000(2) scenario, slightly decrease regulation service requirements. Figure 6-19 and Figure 6-20 show the temporal distribution of the regulation deployment differences.

Table 6-3 Comparison of Regulation Deployments for the 10,000 MW Wind Generation Capacity Scenarios

	Case 10,000(1)	Case 10,000 (2)
Up-Regulation (MW)		
Mean	82.5	81.4
Sigma	64.9	64.1
98.8th Percentile	265.2	261.5
Maximum	1105.6	1112.7
Down-Regulation (MW)		
Mean	-83.0	-81.5
Sigma	63.7	63.1
98.8th Percentile	-262.7	-260.4
Maximum	-554.9	-565.9

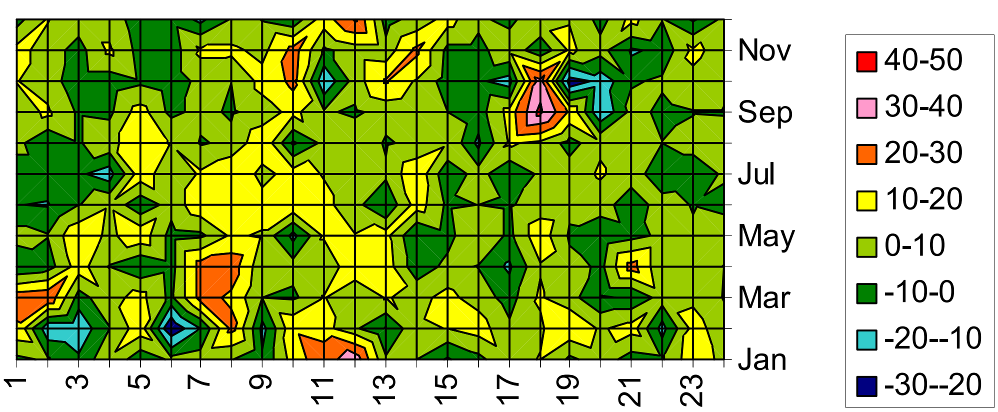

Figure 6-19 Difference in up-regulation (Case 10,000(1) minus Case 10,000(2))

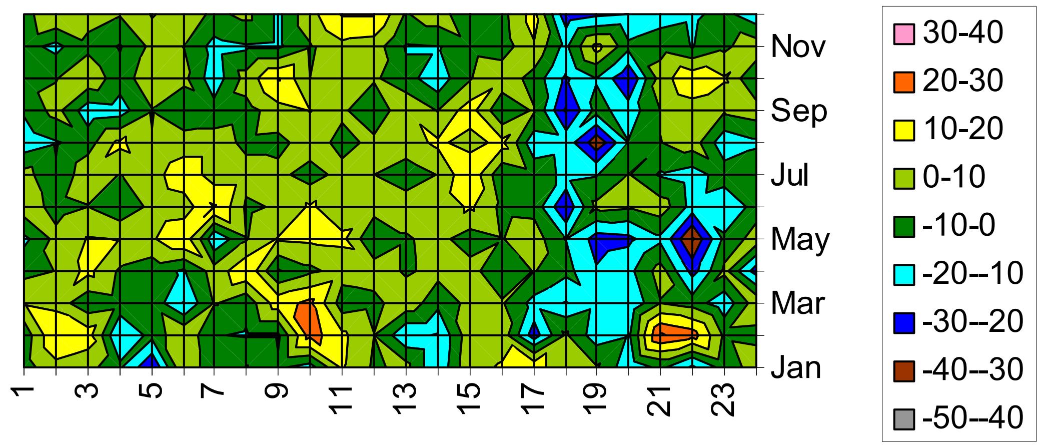

Figure 6-20 Difference in down-regulation (Case 10,000(1) minus Case 10,000(2))

6.2.5. Correlation of Regulation to Wind Generation Output

The previous correlations of regulation are to temporal parameters; hour of day and month, for various levels of wind generation capacity. In this section, regulation deployments are correlated to the real-time output of the wind generation portfolio for the respective hour. The analysis focuses on the incremental regulation requirement for the 15,000 MW wind generation capacity scenario, compared to the zero-wind capacity scenario.

The incremental hourly maximum up-regulation and down-regulation deployments are plotted as a function of the average wind generation output for the respective hour in Figure 6-21. Note that, in a given hour, wind generation output may increase or decrease regulation requirements. Figure 6-22 plots the maximum of the absolute value of up- and down-regulation for each hour, plotted versus wind generation output. The solid line in this plot is a quadratic curve fit of the scattered points, indicating that the impact of wind on regulation is most pronounced at the mid levels of output of the installed capacity (15,000 MW in these plots).

Figure 6-23 plots a typical wind turbine's power output versus wind speed characteristic, as well as a probability density function for wind speeds at a typical site. When the output of the entire wind generation portfolio is midway between zero and the rated capacity, most wind turbines are operating on the steep portion of the wind turbine output curve, where small wind velocity changes yield large power changes. This amplifies variability in output due to wind variations, and is the probable explanation for the increased incremental regulation requirements at mid-levels of wind generation output.

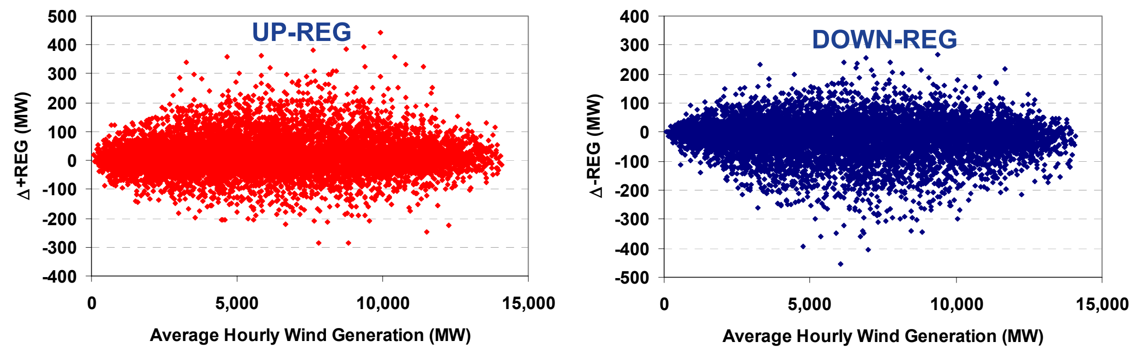

Figure 6-21 ***Incremental hourly maximum up- and down-regulation due to wind, versus average hourly wind generation output***

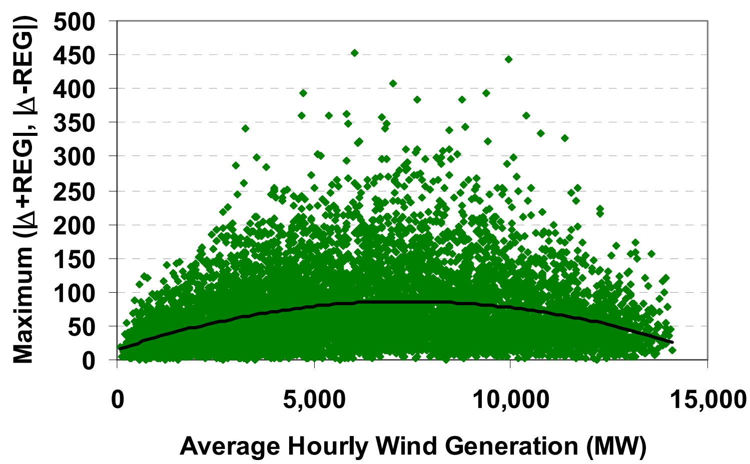

Figure 6-22 ***Incremental hourly maximum -regulation due to wind, versus average hourly wind generation output. Maximum of up- and down-regulation.***

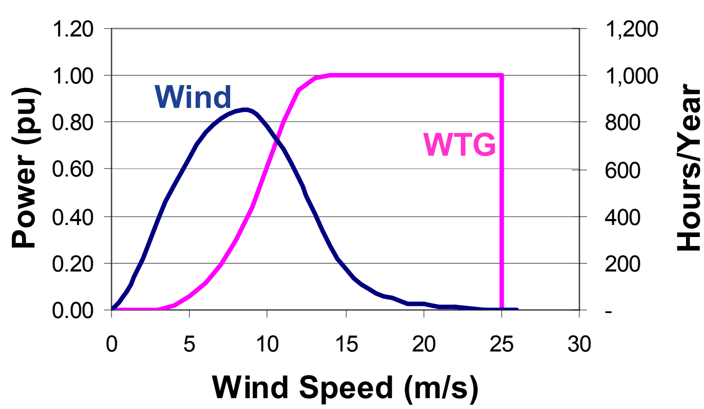

Figure 6-23 ***Typical wind turbine power output curve and wind probability density function for a typical wind plant site.***

Figure 6-24 shows a very strong correlation between the incremental regulation maximum, due to wind, and the long-term ramp rate of the wind generation output. The wind ramp rate used here is the delta between successive hours' integrated wind power output (current hour minus previous hour). As discussed earlier, the ERCOT definition of regulation results in the regulation requirements being strongly affected by the ramping of the net load, and the wind output is one component of the net load. The solid lines in these plots indicate the amount of power change in one five-minute dispatch period, which is the hourly ramp rate divided by twelve. The plotted points clearly trend along these lines. This correlation is applied later in Section 6.3.2 to possible improvements to the regulation procurement methodology.

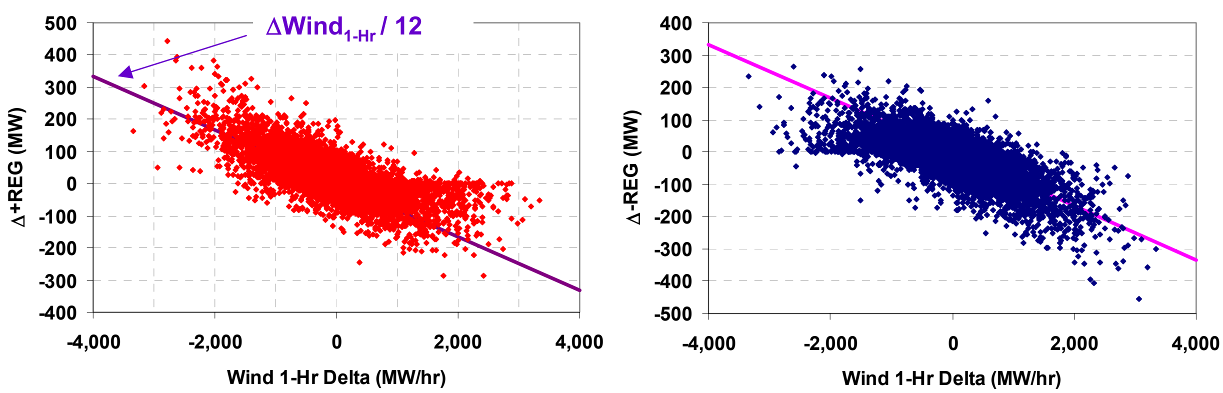

Figure 6-24 Incremental hourly maximum regulation versus wind generation ramp rate.

6.3. Adequacy of ERCOT Regulation Procurement Methodology

Regulation procurements were calculated for each hour of each month of the study year using regulation deployments calculated for the prior month of the study year and the same month of the prior year, applying ERCOT's present methodology. This process was performed for each wind scenario, with the installed wind generation capacity assumed to be constant from year to year. Deployments for each hour and month were compared to the procurements to determine the adequacy of the methodology with increased, but constant (steady-state), wind penetration. Later, in Section 6.3.2, suggestions will be given for modifying the regulation procurement process to properly account for year-to-year wind generation capacity increases when penetration is increasing rapidly.

Figure 6-25 plots up-regulation procurements and deployments over a fifty-hour interval, illustrating several under-deployment periods. Figure 6-26 compares up-regulation deployments and procurements, for scenarios with 15,000 MW of wind generation and without wind generation. This example shows periods where the addition of wind generation results in an under-procurement, and other periods where the margin between wind procurement and wind deployment is increased. Similar plots for example periods in each season are in Appendix E.3.

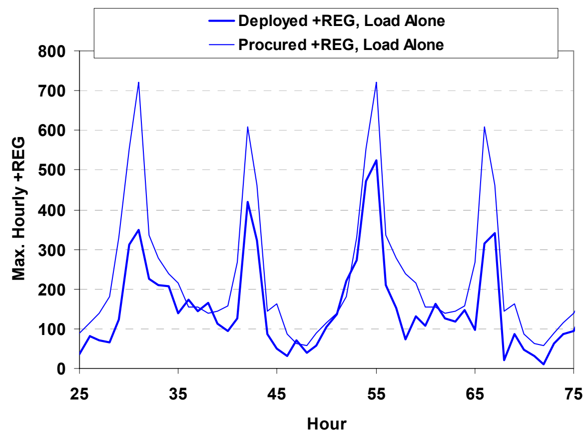

Figure 6-25 Illustration of up-regulation procurement and deployment

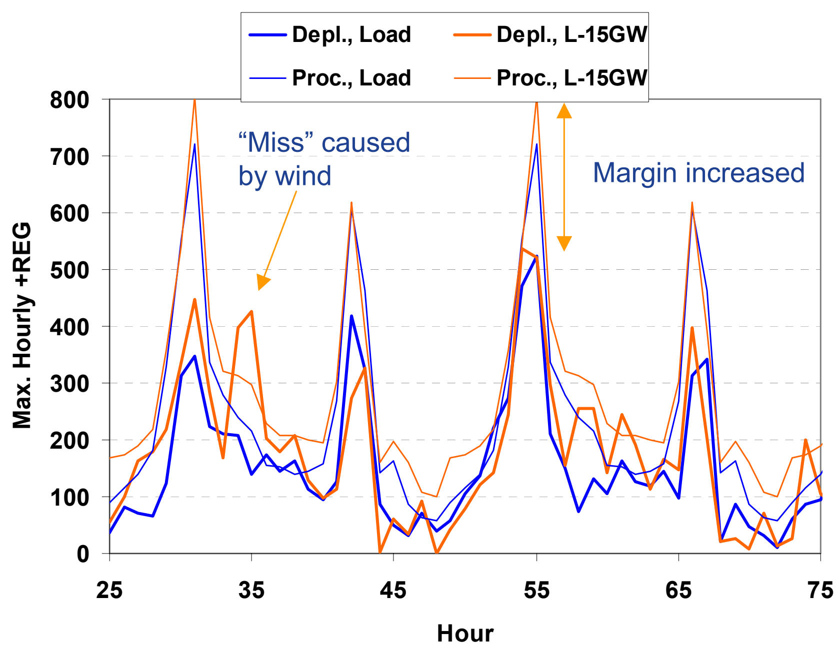

Figure 6-26 Up-regulation deployments and procurements, with 15,000 MW of wind generation and without wind generation, for an example period.

Figure 6-27 plots the mean and maximum regulation procurement and deployment as a function of the installed wind capacity. Again, it is seen that results are nearly perfectly linear. The slope of the extreme procurements are greater than that of the extreme deployments, meaning that the under-deployment gap narrows with more wind capacity.

(Note that down regulation is considered to be a negative number, so minimum down-regulation is a more severe requirement.)

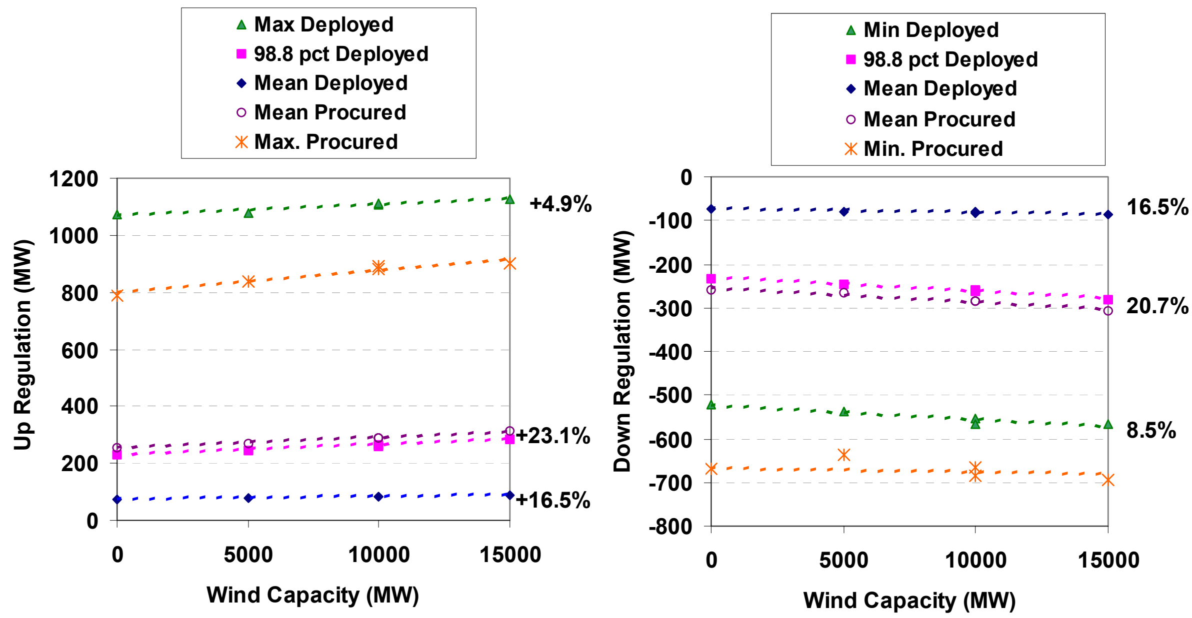

Figure 6-27 Regulation procurement and deployment as a function of wind capacity.

6.3.1. Analysis of Under-Procurements

The adequacy of the regulation procurement methodology can be quantified by analysis of the under-procurements — periods where the algorithm does not procure sufficient regulation services to cover the regulation deployment. There are various metrics that can be placed on under-procurement that indicate the frequency and the severity of the under-procurements. It should be noted that the procurement methodology is not intended to be perfect; procurement of sufficient regulation such that deployment needs are always met would be uneconomical. Instead, the responsive reserve service is relied upon to cover infrequent excesses, with the expectation that an unusually large regulation requirement will not coincide with a worst-case generation trip. ERCOT has determined that procuring sufficient regulation service for 98.8% of the five-minute periods reduces the risk to an acceptable level.

Table 6-4 summarizes regulation under-procurement metrics for the wind generation scenarios. The data columns are explained as follows:

Percentage of Periods – Percentage of five-minute periods in the study year with regulation requirements exceeding the amount procured.

Total MWh Under-Proc. – Sum of the products of amount that regulation requirements exceed procurement for each period, times the duration of each period, (1/12 of one hour for each period). Periods where regulation requirements do not exceed the procured value count as zero.

Average Under-Proc. – Average amount of the under-procurement, considering only periods where regulation requirements exceed procurement.

RMS of Under-Proc. – Root-mean-square of under-procurements, considering only periods where regulation requirements exceed procurement. This value of this metric is that it gives greater weighting to larger under-procurements, which tend to be more operationally significant.

Extreme Under-Proc. – The most severe under-procurement (maximum of up-regulation under-procurements, and minimum of down-regulation under-procurements, with down-regulation expressed as a negative number).

The results in this table indicate that ERCOT's current regulation procurement methodology provides essentially equivalent accuracy with, or without, significant wind penetration. The very slight increase in under-procurement rate for up-regulation is not significant, and the down-regulation under-procurement rate is less for the 15,000 MW wind scenario, relative to the zero-wind scenario. The increase in average up-regulation under-procurement, between zero and 15,000 MW of wind generation, is 23%, nearly identical to the increase in the average up-regulation procured. Thus, the relative under-procurement is essentially invariant. The increase in down-regulation under-procurement (12.8%), is substantially less than the increase in down-regulation procurement, so the relative under-procurement decreases with wind generation capacity additions. The increase in the root-mean-square of under-deployment, for both up-regulation and down-regulation, increase much less on a percentage basis than the average under-procurement. This implies that the more extreme magnitudes of under-procurement occur less frequently with greater wind capacity. The most severe up-regulation under-procurements actually decrease, and the down-regulation under-procurement extrema increase only slightly.

Table 6-4 Regulation Under-Procurement Metrics

Up-Regulation

Wind Scenario	Percentage of Periods	Total MWh Under-Proc.	Average Under-Proc.	RMS of Under-Proc.	Extreme Under-Proc.
0	1.29%	5,141	45.5 MW	80.1 MW	653 MW
5000	1.26%	5,320	48.2 MW	82.1 MW	634 MW
10,000 (1)	1.36%	6,201	52.0 MW	85.0 MW	638 MW
10,000 (2)	1.35%	6,004	50.8 MW	84.2 MW	643 MW
15,000	1.37%	6,712	55.9 MW	88.5 MW	632 MW

Down-Regulation

Wind Scenario	Percentage of Periods	Total MWh Under-Proc.	Average Under-Proc.	RMS of Under-Proc	Extreme Under-Proc.
0	1.18%	5,011	48.5 MW	89.2 MW	886 MW
5000	1.12%	5,148	52.5 MW	90.4 MW	911 MW
10,000 (1)	1.20%	5,439	51.7 MW	87.9 MW	946 MW
10,000 (2)	1.16%	5,301	52.2 MW	89.2 MW	940 MW
15,000	1.16%	5,562	54.7 MW	90.1 MW	927 MW

Figure 6-28 and Figure 6-29 show two example frequency distributions of up-regulation deployments for particular hours and months. The dotted lines indicate the procured regulation, and very few deployment periods exceed the procured values. The most severe under-procurement in Figure 6-28 is due to a single very large deployment outlier near 800 MW. In this particular example, the magnitude of the maximum deployment for the 15,000 MW scenario is slightly less than that for the zero-wind scenario. Because the procurement is greater for the case with 15,000 MW of wind capacity, the magnitude of under-procurement is actually less in the high-wind penetration case.

A different situation is illustrated in Figure 6-29. In this case, the up-regulation deployments are more widely scattered, and there are many deployments exceeding the procured values for both scenarios. The wide distribution is probably due to the volatility of weather, and consequently load behavior, in this spring month. The procured regulation does not cover anywhere near 98.8% of the deployments. Evidently, the variability was not present in the prior month, nor in the same month of the prior year, resulting in insufficient procurement for the highly volatile study year conditions. The number of periods exceeding the procured value is significantly greater for the 15,000 MW wind scenario. The magnitude of the under-deployments is not as extreme as in the prior example.

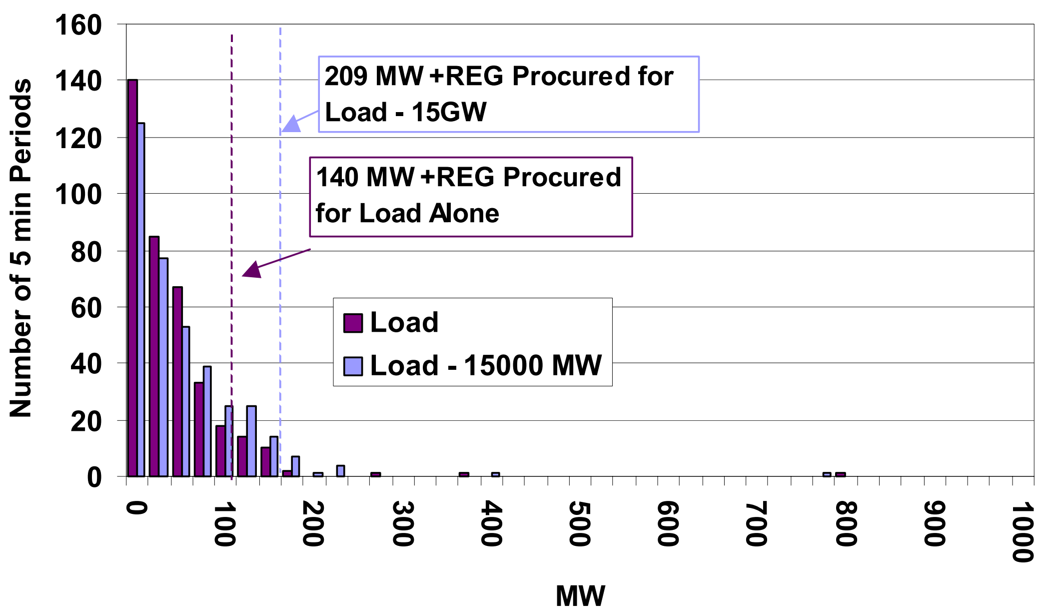

Figure 6-28 ***Frequency distribution of up-regulation deployments for 2 p.m. in January, for scenarios with no wind capacity, and with 15,000 MW of wind capacity.***

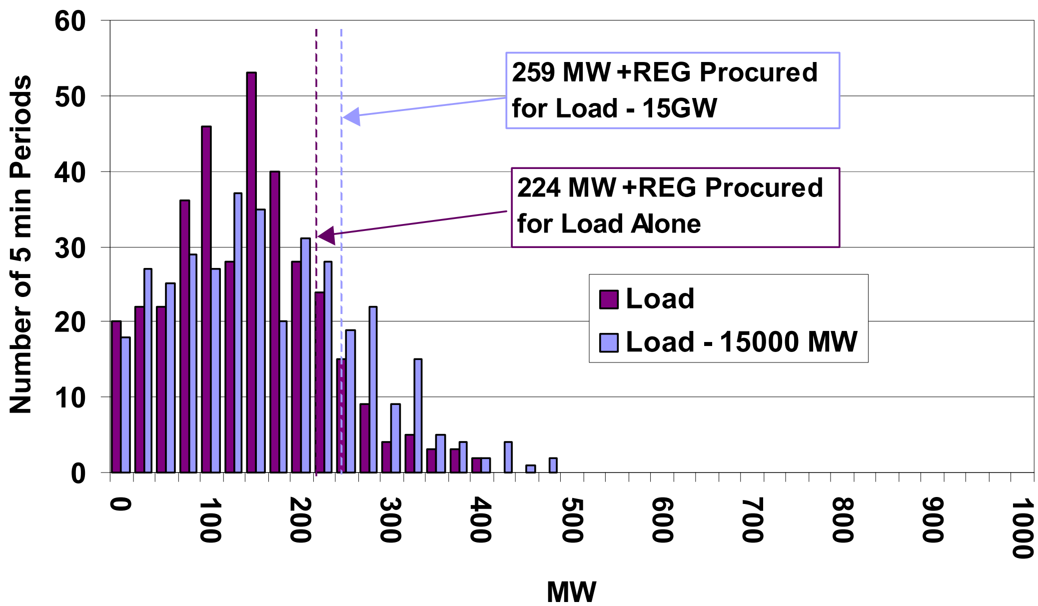

Figure 6-29 ***Frequency distribution of up-regulation deployments for 1 p.m. in April, for scenarios with no wind capacity, and with 15,000 MW of wind capacity.***

The next group of figures indicate the temporal characteristics of the regulation under-deployments. The contour plots of Figure 6-30 to Figure 6-37 show the regulation under-procurement rates for the zero-wind and 15,000 MW wind generation capacity scenarios. Maxima in these contour plots tend to be narrow spikes, so peak values are shown numerically as indicated by the arrows. Without wind generation, the up-regulation procurement methodology falls short relatively frequently during the late morning through mid-day in the spring, and in the evening in the fall. With 15,000 MW of wind generation capacity, under-procurements are less frequent for many of the morning hours. The peak under-procurement rate, however, is greater. Without wind generation capacity in the system, the regulation procurement methodology under-predicts down-regulation needs most severely in the evenings in the early spring. This peak of under-procurement frequency, however, is greatly reduced in the 15,000 MW wind scenario.

Figure 6-34 to Figure 6-37 show the temporal characteristics of the differences in regulation under-procurement magnitudes between the scenarios with 15,000 MW wind generation capacity and zero wind generation capacity. These differential contour plots show both up- and down-regulation under-procurements expressed in terms of MW×hours and root-mean-square of deficiency. In general, the differences in regulation deficiencies are well scattered about the temporal space. An exception is the sharp peak in the MWh metric for up-regulation, pertaining to autumn evenings. The fact that this peak is created by the data for one hour-month pairing, rising from a rather benign plateau raises question if this peak is an anomaly of the study year data, or if is consistent on a year-to-year basis. ERCOT is encouraged to continuously monitor these trends as wind capacity is developed to apply as much data as possible to operating decisions.

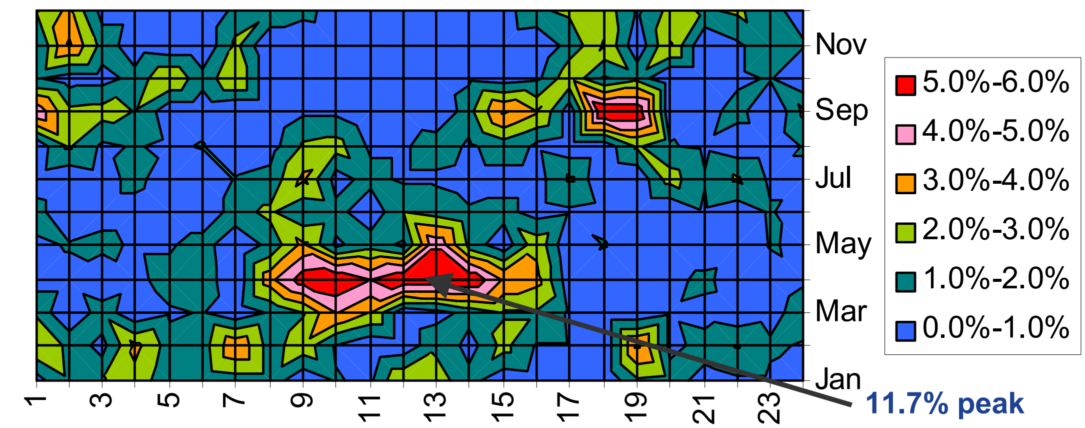

Figure 6-30 Percentage of 5-minute periods with up-regulation under-deployments for the zero-wind generation capacity scenario.

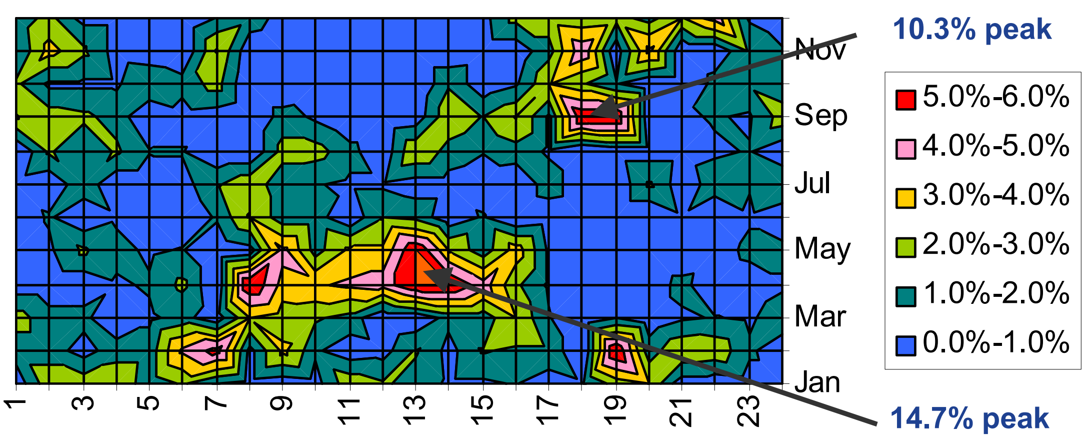

Figure 6-31 Percentage of 5-minute periods with up-regulation under-deployments for the 15,000 MW wind generation capacity scenario.

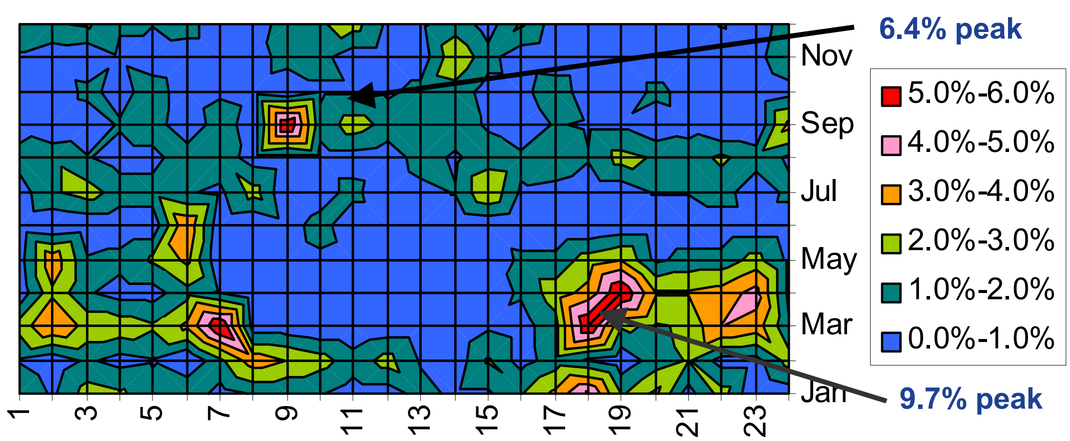

Figure 6-32 Percentage of 5-minute periods with down-regulation under-deployments for the zero-wind generation capacity scenario.

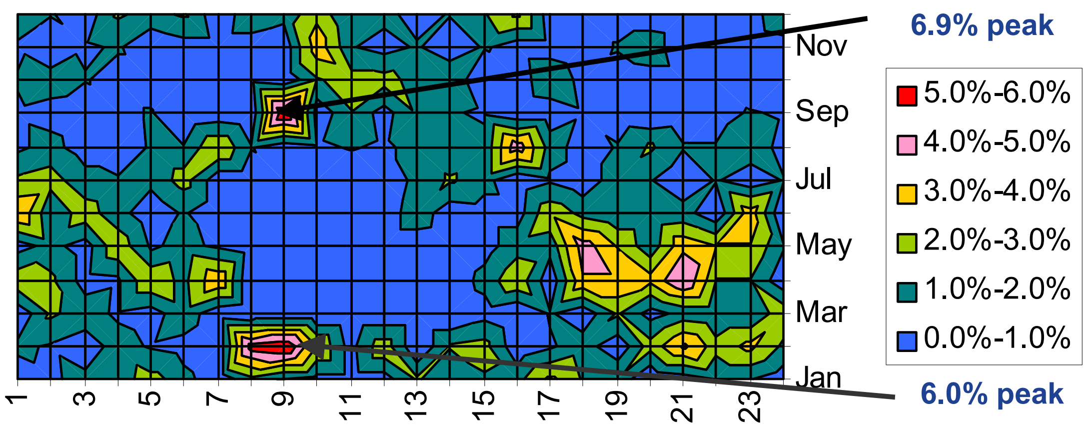

Figure 6-33 ***Percentage of 5-minute periods with down-regulation under-deployments for the 15,000 MW wind generation capacity scenario.***

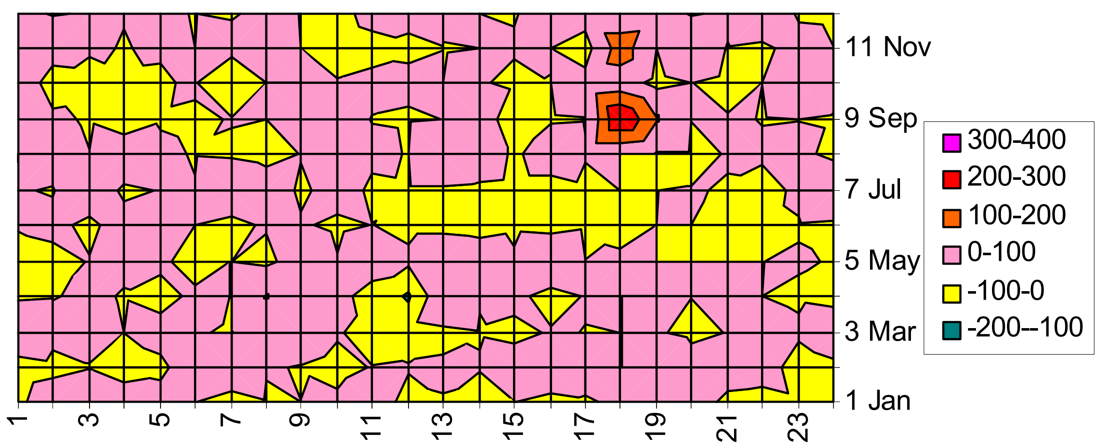

Figure 6-34 ***Differential MWh of up-regulation under-procurement; 15,000 MW wind generation capacity scenario minus the zero-wind generation scenario.***

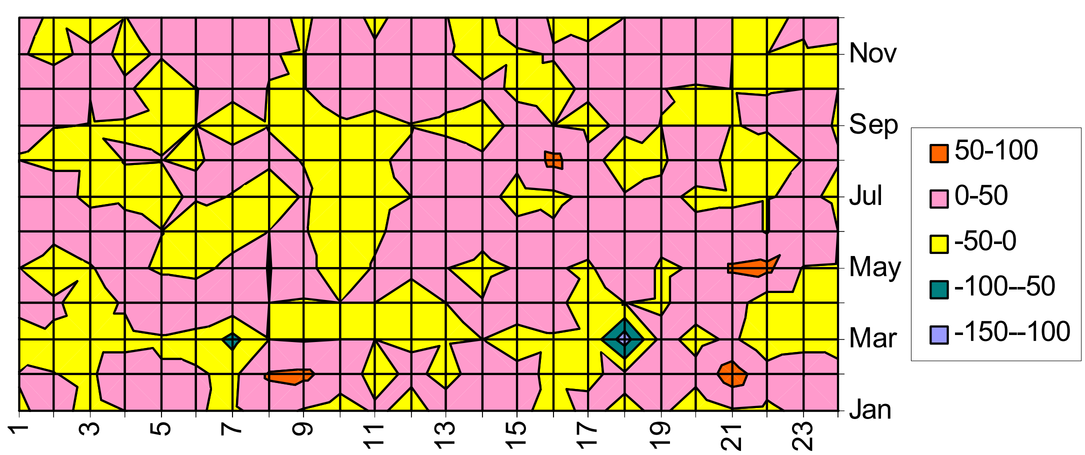

Figure 6-35 ***Differential MWh of down-regulation under-procurement; 15,000 MW wind generation capacity scenario minus the zero-wind generation scenario.***

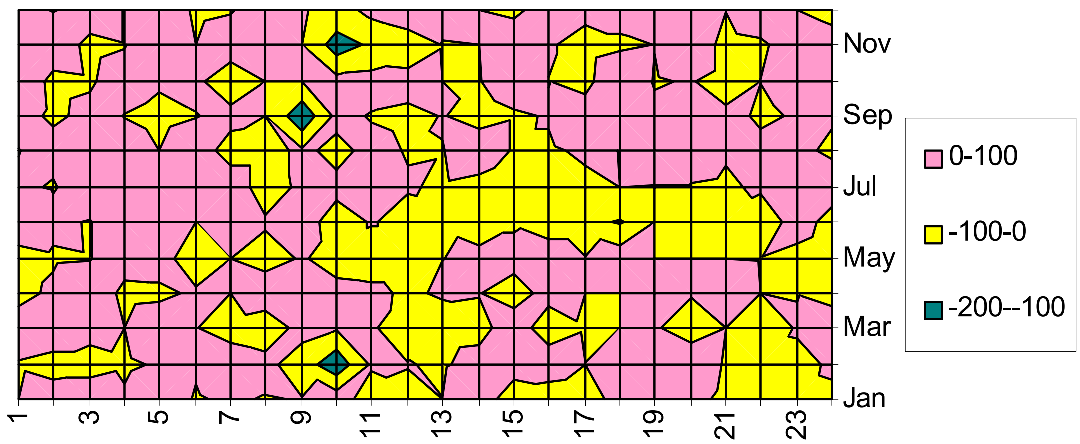

Figure 6-36 ***Differential RMS of up-regulation under-procurement; 15,000 MW wind generation capacity scenario minus the zero-wind generation scenario.***

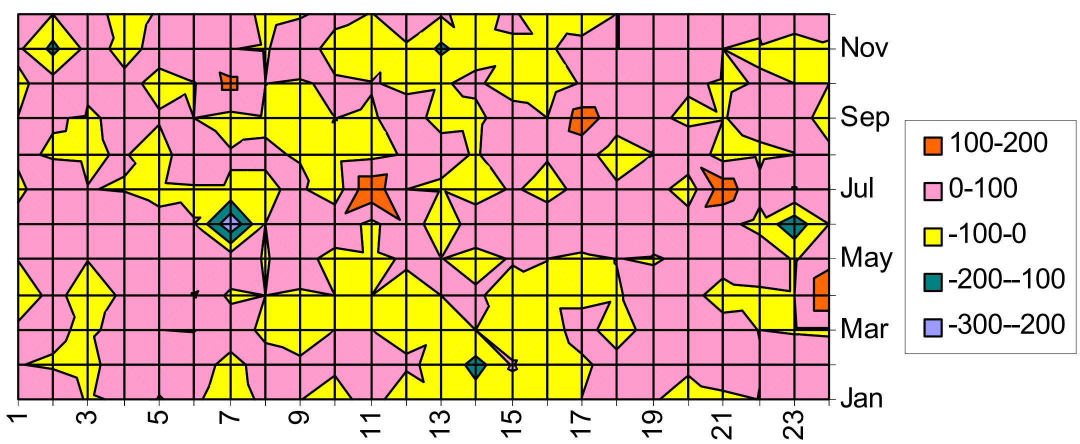

Figure 6-37 ***Differential RMS of down-regulation under-procurement; 15,000 MW wind generation capacity scenario minus the zero-wind generation scenario.***

6.3.2. Possible Methodology Improvements

Year-to-Year Wind Capacity Growth

Wind generation capacity has been added to the ERCOT system at a very fast pace over the past few years, and this pace is expected to accelerate. The present ERCOT regulation procurement methodology, applied to the net load, does not take into account year-to-year wind capacity growth when using prior-year regulation deployments to predict present-year procurement needs. The results of this study show a near-perfectly linear correlation between regulation requirements for any period of time, and the amount of installed wind capacity. Therefore, it is reasonable to apply adjustment factors to prior-year regulation deployment 98.8th percentile values to account for increases in wind capacity over the prior year. These factors depend on the time of day and month of year.

The tables in Appendix F show additive adjustments, in units of MW of regulation requirement (98.8th percentile of deployment) per GW of incremental wind capacity since the same month of the prior year. These adjustments are the smoothed differential between 98.8th percentile regulation deployments in the 15,000 MW case minus the zero-wind case, divided by fifteen. The smoothing function uses 50% of the differential for the respective month and time of day, plus 12.5% each of the differentials for the same hour in the prior and following months, and for the same month and the prior and following hours (i.e., the four "adjacent" points in the hour-of-day and month spaces). This process smoothes extreme hour-to-hour and month-to-month variations in the differential that may not be realistic.

Incorporation of Wind Forecasts

ERCOT's present methodology for regulation procurement correlates regulation requirements to time of day and month of year. This is a reasonably good assumption for system load.[6] Loads have a distinct daily cycle, and short-term variations around this diurnal cycle are not greatly influenced by weather. Although wind does have diurnal and annual patterns, wind generation output also follows multi-day cycles of weather system movement. Incorporating day-ahead wind generation forecasts can improve regulation procurement accuracy and lower costs. This results in a regulation procurement for a particular hour of day over a month that is composed of a fixed component, constant throughout the month for the particular hour, plus a positive or negative adjustment component that varies for each day depending on the forecast wind generation volatility.

One forecastable wind generation characteristics is the long-term (multi-hour) ramp rate. Subtracting the influence of long-term wind ramp rate (hourly delta divided by twelve) on the maximum regulation deployments yields the plot shown in Figure 6-38. Comparing this plot with Figure 6-22 reveals a decreased scattering of points. These results imply that the precision of regulation procurement might be increased by factoring the effects of wind generation output ramping into the regulation procurement.

[6] It is quite possible that the present methodology could be improved if regulation requirements were segregated between weekdays and weekends. This hypothesis was not investigated as the scope of this study is focused on the impacts of wind on ancillary services procurement.

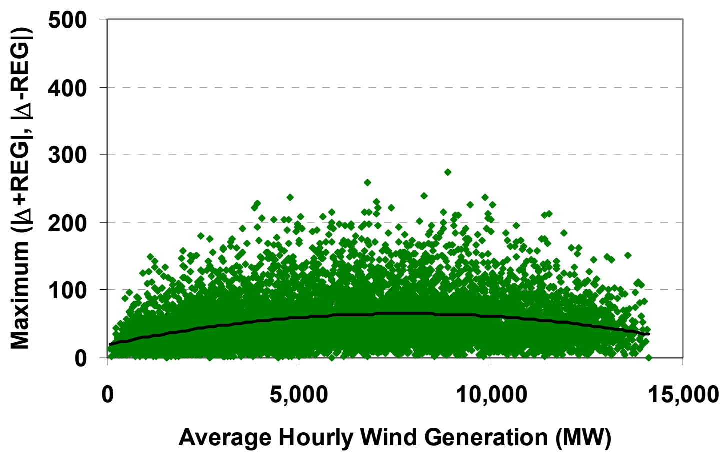

Figure 6-38 ***Incremental hourly maximum -regulation due to wind, minus the effect of wind ramp rate, versus average hourly wind generation output.***

Wind output ramping is present in both the historical data used to determine procurements, and in the real-time requirements for regulation. An algorithm that removes the influence of wind output ramping on historical regulation data, but then re-inserts the predicted influence of wind output ramping on a day-ahead basis, may be more accurate than the present methodology. This can result in an improved procurement at reduced cost.

This approach requires use of day-ahead wind forecasts to determine wind ramp rates on an hourly basis to include this influence in regulation procurements. The steps of the suggested methodology are summarized as follows:

1. Factor out wind multi-hour wind generation output ramp-rate contributions (hourly change divided by twelve) to historical deployed regulation data.
2. Determine the maximum of 98.8th percentiles for the previous month and previous year, as in the present methodology, but using these adjusted data.
3. Use the day-ahead wind forecast to determine the expected hourly wind ramp rates.
4. Adjust the regulation procurement on a day-ahead basis, applying the forecast wind ramp rates.

Another forecastable wind generation characteristic is the expected operating points on the wind turbine performance curves. Figure 6-38 shows that, with the influence of ramp rate removed, there is a visible non-linear correlation between regulation requirements and the average hourly wind generation, relative to the capacity. When the aggregate wind generation is at approximately 50% of capacity, the regulation requirements are maximized. The apparent cause is that many wind turbines are operating on the steep part of their performance curves when the aggregate output is at the intermediate levels.

Rather than adjust ERCOT regulation procurements based on the aggregate output level, greater accuracy in regulation procurement adjustments might be obtained by a more detailed analysis. Day-ahead wind generation forecasts are based on meso-scale weather models, from which calculated wind speeds at wind plants are applied to wind generator performance curves to determine expected hourly energy output. This process can also be applied to determine the expected variability on a site basis, depending on the forecast turbulence at the site and the mean operating point on the wind turbine performance curve. An aggregate variability can be determined for the entire ERCOT wind generation portfolio using a capacity-weighted combination of these variability factors. Because the intra-hour variabilities should be generally uncorrelated between sites, root-sum-square combination of the factors would be appropriate.

This is a marked departure from ERCOT's present regulation procurement practice, for which an identical daily pattern of regulation procurement levels is repeated for each day of the month. The suggested methodology would adjust this daily pattern on a day-ahead basis, using wind forecasts. ERCOT needs to consider the implications for market operations. One possibility to minimize market changes is to determine a base regulation requirement that repeats in a constant daily cycle for each day of a month, as is the current practice. An additional regulation adjustment service could be created and procured on a day-ahead basis to include the expected effect of wind ramp rates and forecast variability.

The four-step algorithm for adjusting for wind ramp rate was tested using this study's model data, including synthesized wind generation forecasts. Results of this test do not confirm the value of the hypothesized approach, but further investigation reveals that the synthesized day-ahead wind generation forecasts used in this study have ramp rates containing much more hour-to-hour variational "noise" than the wind generation output data for the same periods. The application of the synthesized wind forecasts to predict ramp rates was not considered in the design of the synthesis process.

As ERCOT begins to use wind generation forecasting in system operations, data points of actual wind generation forecasts, power outputs, and regulation deployments will provide ERCOT the opportunity to evaluate this suggested methodology modification on an off-line basis. If ongoing analysis of the real data indicates that the methodology changes would allow regulation procurements to be decreased, while maintaining adequate procurement precision (at least 98.8% of periods covered), then this methodology change can be implemented in the ERCOT market.

6.4. Available Regulation Range

In addition to increasing the amount of regulation required, the presence of wind generation tends to diminish the amount of regulation service available from the dispatchable generation resources. This is because the wind generation displaces dispatchable generation units from the commitment schedule, and often the higher-cost units displaced are the most flexible providers of regulation service. Regulation capacity of the system becomes most constrained under conditions of low served load and high wind generation output.

Figure 6-39 shows the amounts of regulation capability, measured in MW per minute ramping capability, by generation type from MAPS analysis for the week in the study year having minimum load. This is for the zero-wind generation capacity scenario. The same week is shown for the 15,000 MW wind generation capacity scenario in Figure 6-40. Note that there are several periods when the only regulation available is provided by normally base-load coal-fired units. In one period between hours 93 and 99, there is no regulation ramping capability available using an economic unit commitment and dispatch. To provide regulation, either the unit commitment schedule and dispatch would need to be modified, or the wind generation curtailed.

The correlations of regulation down-ramping capability to system load level are shown in Figure 6-41 for the 15,000 MW wind generation capacity scenario. The hours without down-ramping available (without deviating from economic unit commitment and dispatch) coincide with the extreme low-load periods.

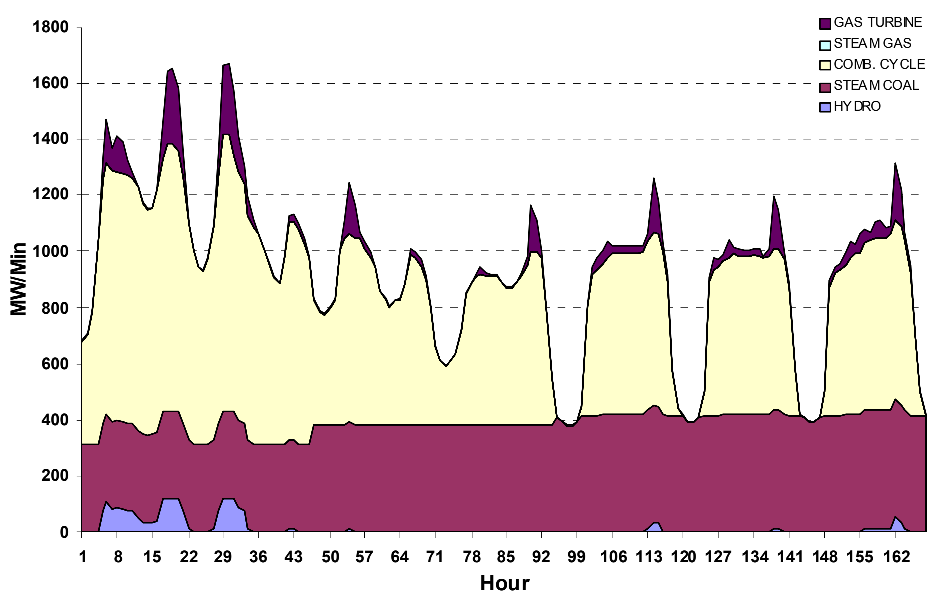

Figure 6-39 Regulation capacity provided, by generation unit type, for the minimum-load week in the zero-wind generation capacity scenario.

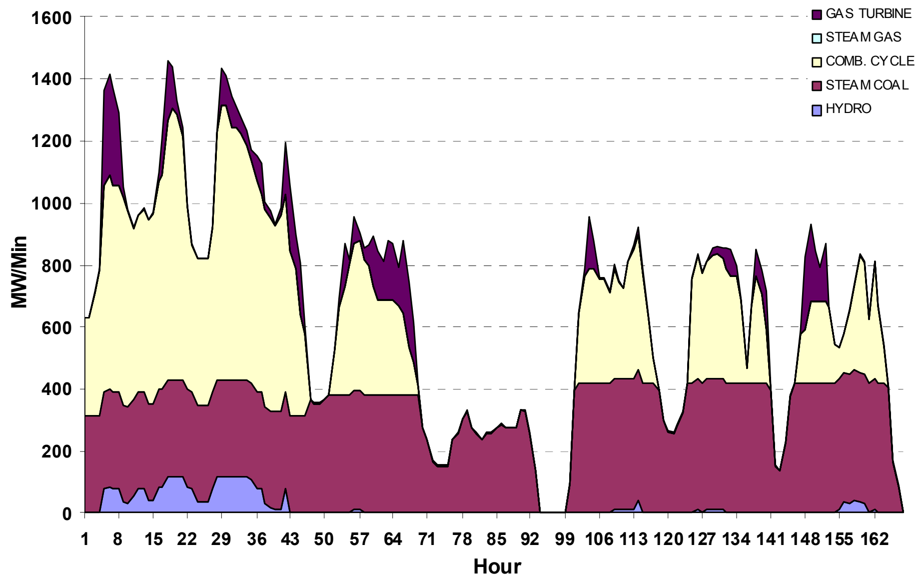

Figure 6-40 Regulation capacity provided, by generation unit type, for the minimum-load week in the 15,000 MW wind generation capacity scenario.

Currently, in the zonal market design, the ramping capability of regulation service is defined as being one-tenth of the procured regulation. This is for a dispatch period of fifteen minutes. In the nodal market, the dispatch periods are five minutes long. The ramping capability of units supplying regulation service must be such that the procured amount of regulation can be realized in five minutes or less. Therefore, in this study, the amount of regulation available, in units of MW, is assumed to be constrained by the available ramp rate in MW per minute, times five.

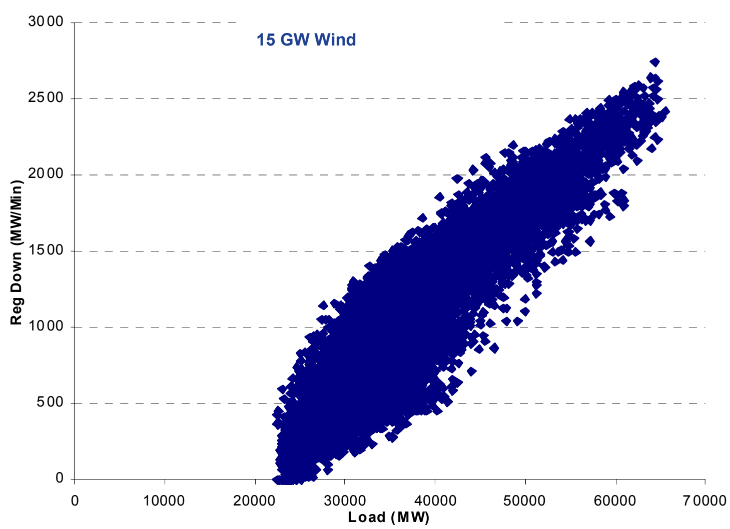

Figure 6-41 – Correlations of down-ramping capability with system load level.

Figure 6-42 shows hourly regulation procurement requirements for the study year, shown by the red (up-regulation) and blue (down-regulation) bands. Available regulation capacity, defined by the ramping capability times five, is shown by the magenta and teal bands. With load alone, in the zero-wind capacity scenario, there is ample margin between procurement requirements and available capacity. The margin is greater for up-regulation than for down-regulation. With 5,000 MW of wind generation capacity, up-regulation capacity margin is ample, but the down-regulation capacity margin is small for isolated hours. In the 10,000 MW and 15,000 MW wind generation capacity scenarios, there are hours where down-regulation capacity is insufficient for the procurement requirements. Figure 6-43 shows an expansion of the time scale for the 15,000 MW scenario. This shows that some apparent intersections of regulation procurement requirements and capacity seen in the time scale of Figure 6-42 are not actually under-capacity situations. An example is at hours 577 and 700. Up-regulation capacity remains sufficient for all the wind generation capacity scenarios investigated.

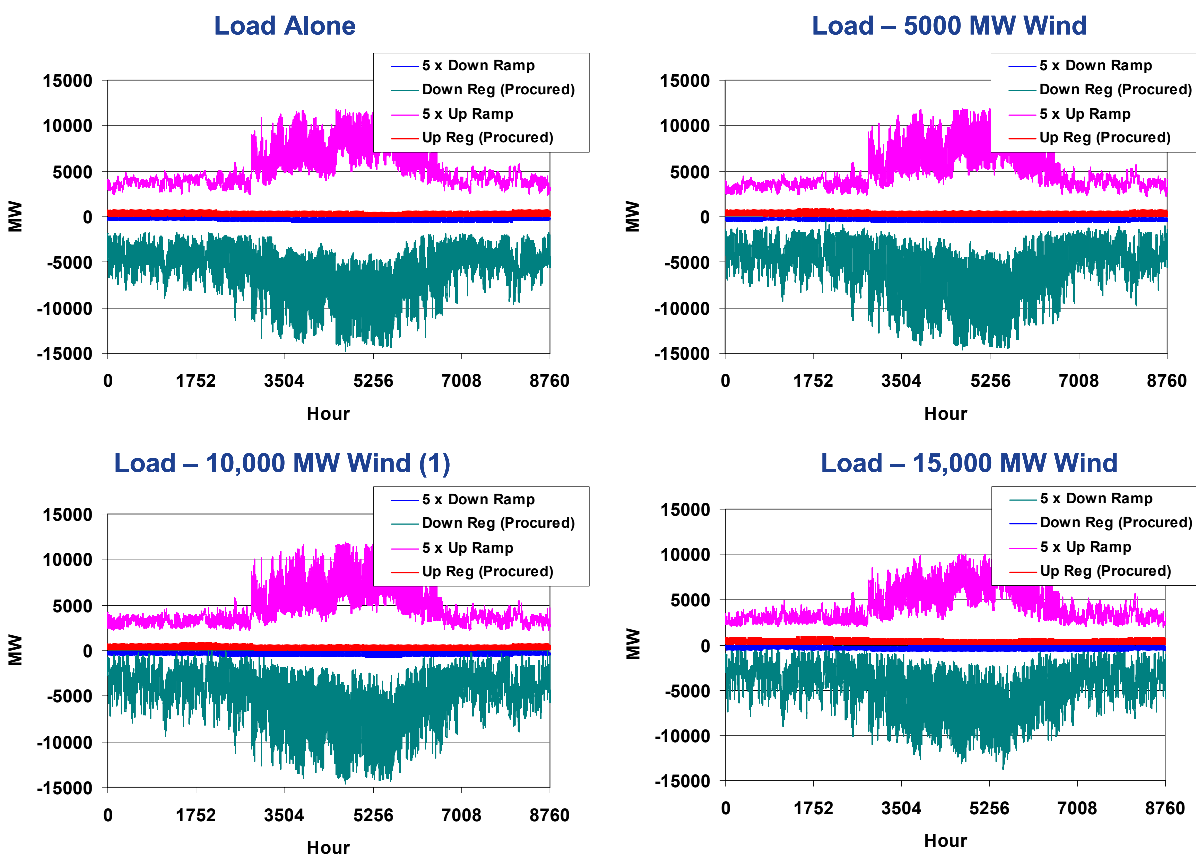

Figure 6-42 Regulation procurement requirements compared with regulation capability.

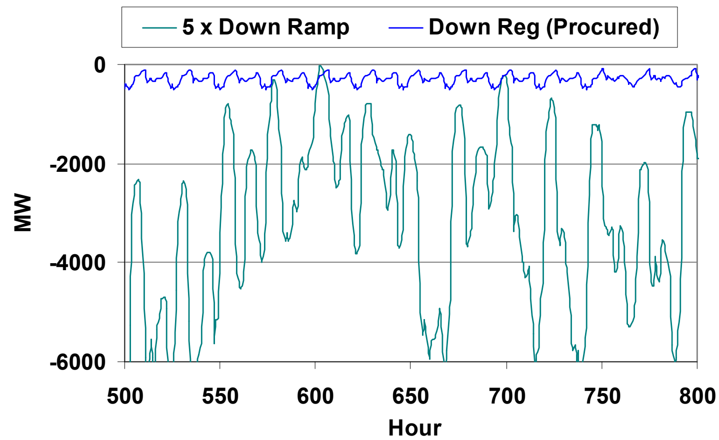

Figure 6-43 Expansion of the time scale of Figure 6-42 for down-regulation in the 15,000 MW wind generation capacity scenario.

Table 6-5 summarizes the regulation shortfalls for each wind generation capacity scenario. Even in the 15,000 MW scenario, the total number of hours where regulation capacity, based on an economic unit commitment and dispatch, is relatively small (51 hours). Of the two 10,000 MW scenarios, the second case, which has 1,500 MW of capacity in coastal South Texas substituting for an equal capacity in the Panhandle, has less frequent and less severe regulation capacity shortfalls.

Table 6-5 Regulation Capacity Shortfalls

Wind (MW)	Hours Deficient	Total MWh Deficient	Average Deficiency (MW)	Maximum Shortfall (MW)
0	0	0	0	0
5,000	0	0	0	0
10,000 (1)	11	2709	246	482
10,000 (2)	7	1097	157	316
15,000	51	10308	202	712

6.5. Costs of Regulation Service

Penetration of wind generation capacity affects both the requirements for regulation service procurement, as well as the unit price for the balance of generation (non-wind generation) to provide that service. Figure 6-44 shows the total amount of regulation service procured as a function of wind generation capacity.

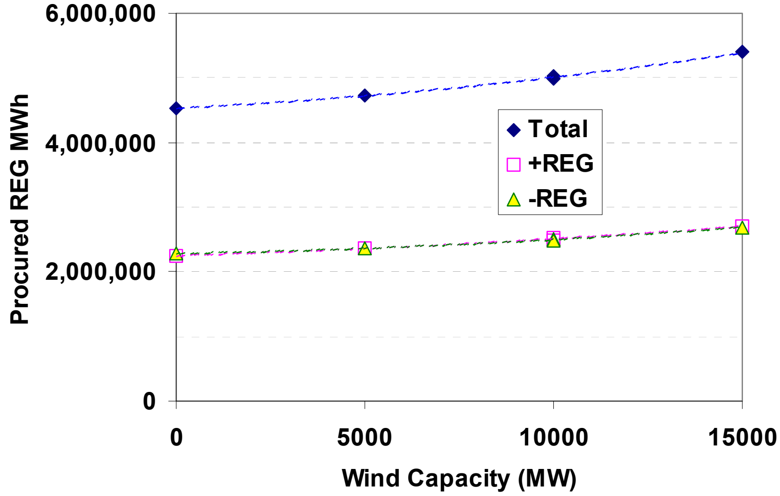

Figure 6-44 – Total annual procured regulation service as a function of wind generation capacity.

6.5.1. Per-Unit Costs of Regulation Service

The MAPS models predict the hourly opportunity costs for providing spinning-reserve services, including regulation and responsive reserve. MAPS does not, however, predict the bidding behavior of generation owners bidding into the ancillary services market. Actual hourly ERCOT ancillary services prices were obtained and analyzed, and it was found that up-regulation and down-regulation prices did have an approximate correlation with spinning reserve costs. MAPS shows many hours in a year where the opportunity costs for spinning reserve are zero. Actual regulation prices, however, do not fall to zero in these time periods. Instead, regulation prices tend to reach a "floor" of approximately $5/MWh.

In general, with increasing wind generation capacity, the unit price per MWh of spinning reserve decreases due to several factors. First, the balance of generation is provided by units with lower variable costs as wind generation capacity is increased. Second, because of the daily variability of wind generation, thermal units with long start-up times and minimum-run times tend to be scheduled for hours where their dispatch levels are reduced by wind output. This provides regulating range with virtually no opportunity costs for these high-wind hours. Third, the accuracy of wind forecasting used in day-ahead unit scheduling plays a role. If wind generation forecasts are not considered at all, or are heavily discounted, the balance of generation will tend to be over-committed.

Figure 6-45 shows the cumulative cost-duration curve for spinning reserve, as modeled in MAPS, for the wind generation capacity scenarios. For this figure, it is assumed that the day-ahead unit commitment schedule makes use of the mean value (50^{th} percentile confidence level) wind forecast, based on current wind forecasting accuracy levels. For a few hours per year, the spinning reserve opportunity cost spikes to as high as $240/MWh, beyond the scale indicated here. This is due to under-commitment, in turn due to under-forecast of net load.

Figure 6-46 shows the same curve where the wind forecast is perfect in accuracy. There is less over-commitment of units and the opportunity cost for providing spinning reserve is increased (overall system operating costs are decreased, however). At the opposite extreme, Figure 6-47 shows the spin cost curve where wind forecasts are ignored in the day-ahead unit commitment (i.e., wind generation output assumed to be zero). Over-commitment of the balance of generation yields to a collapse in spinning reserve prices as the amount of wind generation capacity increases.

For the purposes of evaluating the impacts of wind generation penetration on regulation procurement costs, the hourly per-unit costs of regulation are the greater of:

- Opportunity cost of spinning reserve, as determined by MAPS, or
- An estimated floor of $5/MWh

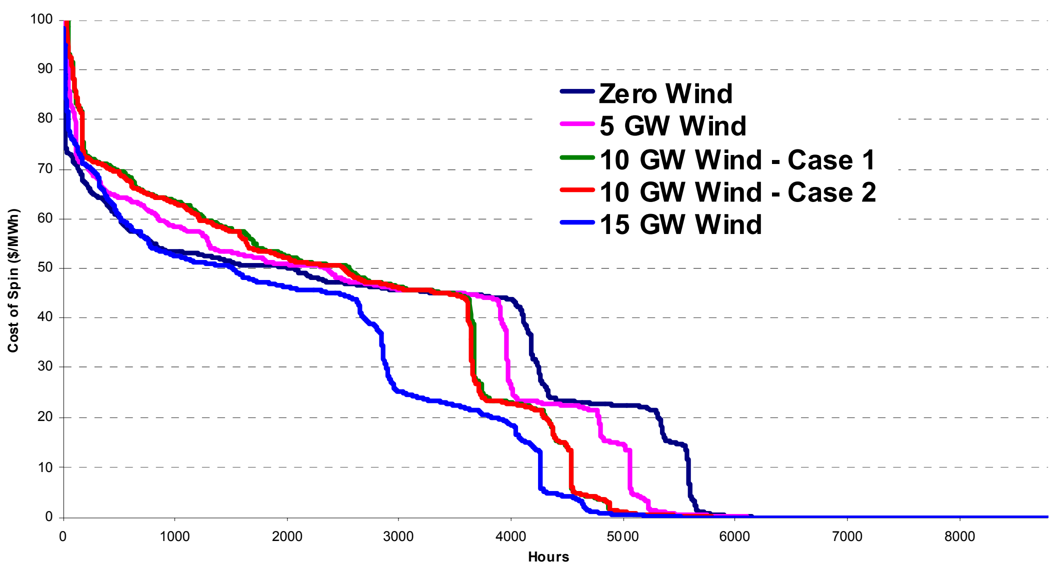

Figure 6-45 – Cost-duration curve for spinning reserve, assuming a "state-of-art" wind generation forecast (50th percentile confidence level) is used in the day-ahead unit commitment.

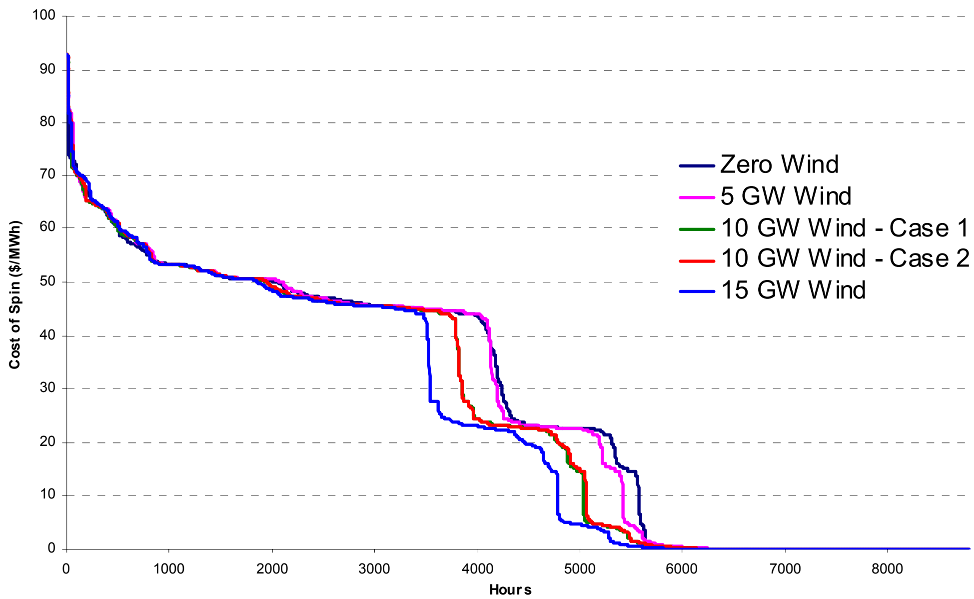

Figure 6-46 - Cost-duration curve for spinning reserve, assuming a perfect wind generation forecast is used in the day-ahead unit commitment.

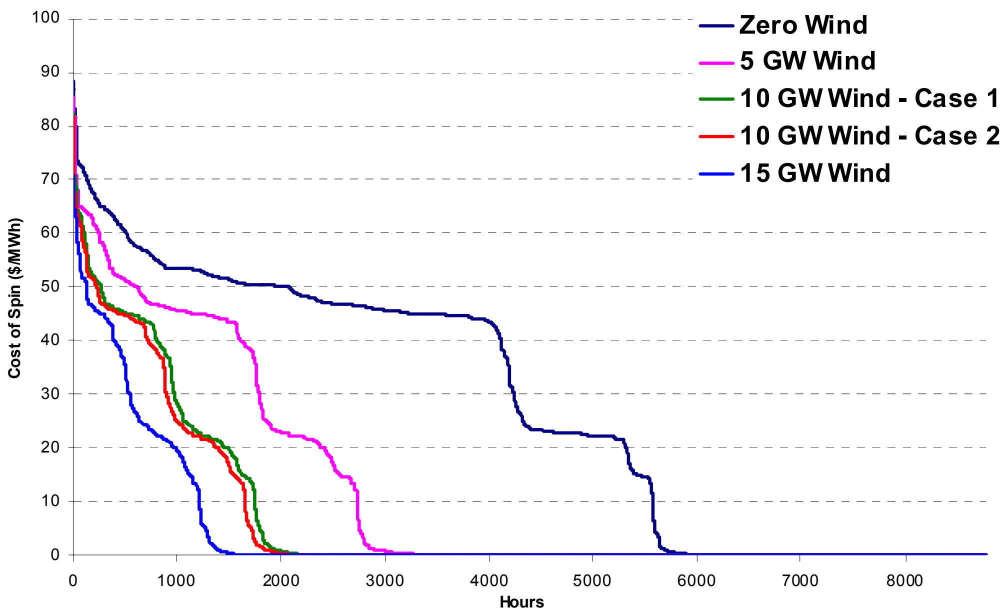

Figure 6-47 - Cost-duration curve for spinning reserve, with wind generation forecast ignored in the day-ahead unit commitment.

If any hour's economic dispatch does not provide sufficient regulating range to meet the procurement requirements, the dispatch must obviously be revised to provide the needed range. There are costs associated with this re-dispatch. The upper limit to the re-dispatch costs are the costs of curtailing wind generation equal to the amount that the regulation procurement requirements exceed the available range in the economic dispatch. The cost of this energy, priced at the hourly spot price, was added to the regulation costs as determined above. These assumptions are deemed adequate for evaluating the relative cost impacts of the wind generation scenarios.

Hourly costs of up- and down-regulation were multiplied by the regulation procurement requirements for each hour. Figure 6-48 shows the average annual per-unit costs of up- and down-regulation for each wind scenario, for both the "state-of-art" and perfect wind generation forecasts used in unit commitment. These costs are shown relative to the costs for the load-only scenario. With the "state-of-art" wind generation forecast used in unit commitment, the average cost of regulation decreases slowly through the 10,000 MW wind generation capacity scenarios, and then collapses at the 15,000 MW level. With unit commitment based on perfect forecasting of the wind, the per-unit regulation cost decreases in a more regular fashion as wind generation capacity increases.

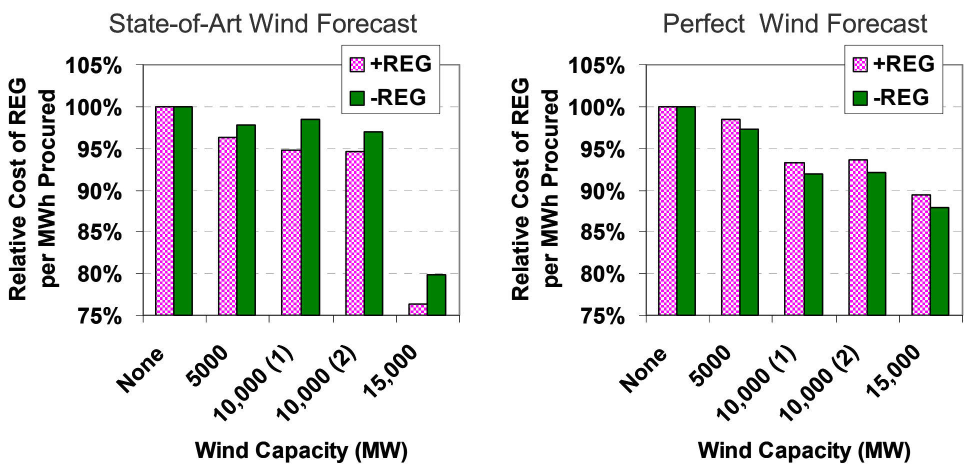

Figure 6-48 – Average per MWh costs of procured regulation.

6.5.2. Total Costs of Regulation

The tendency for regulation requirements to increase with wind generation capacity is offset by the tendency for per-unit regulation costs to decrease. As a result, the total annual costs for regulation tend to rise slightly until the 10,000 MW wind generation capacity scenarios, and then drop at the 15,000 MW level due to the collapse in per-unit costs, with the state-of-the-art wind generation forecasting applied to unit commitment. This is shown in Figure 6-49. If the wind generation forecast were perfect, the total annual regulation costs increase steadily, but very slightly, as wind generation capacity is increased as shown in Figure 6-50. The rate of regulation cost increase with wind generation capacity additions is far less than the relative increase in regulation MWh procured.

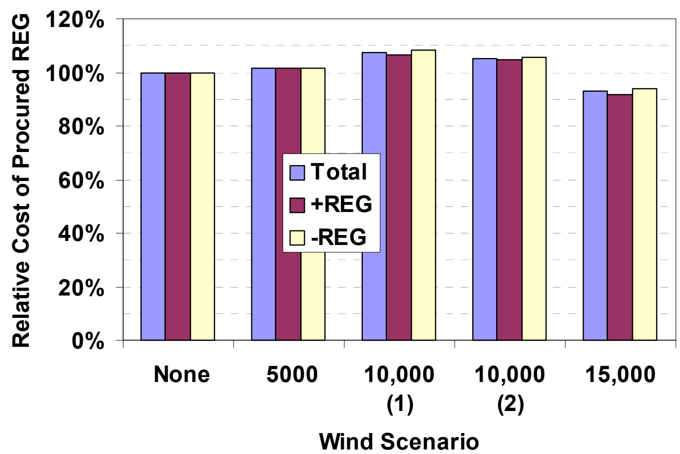

Figure 6-49 – Relative total annual cost of procured regulation, based on state-of-the-art wind generation forecast used in day-ahead unit commitment.

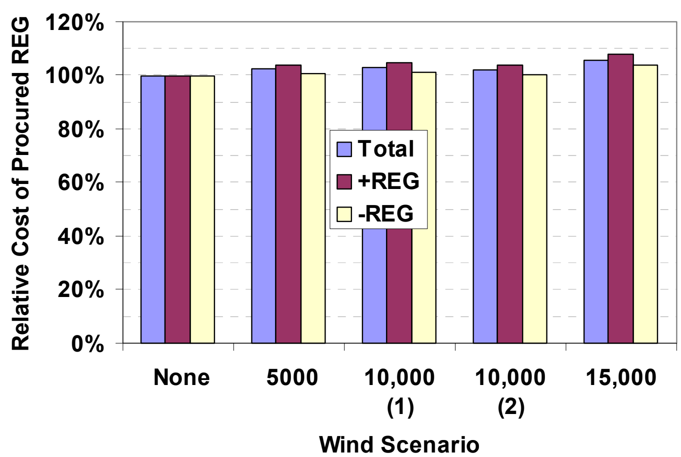

Figure 6-50 - Relative total annual cost of procured regulation, based on a perfect wind generation forecast used in day-ahead unit commitment.

Table 6-6 summarizes the total regulation costs for each wind generation capacity scenario, and shows results for both the "state-of-the-art" and perfect wind forecasts used in day-ahead unit commitment. Figure 6-51 shows the incremental cost of regulation per MWh of wind energy produced.

The incremental costs of regulation appear volatile, subject to differences in sign due to differences in forecast accuracy. The fact is, however, that the incremental per MWh regulation costs are small in all cases and the changes are not of practical significance.

Table 6-6 – Summary of Total Regulation Costs

Wind Capacity (MW)	Reg-Up Cost ($MM)	Reg-Down Cost ($MM)	Total Reg. Cost ($MM)	Total Wind Generation (MWh)	Inc. Cost of Regulation ($/MWh)
0	$66.88	$72.21	$139.09	0	
State of Art Wind Generation Forecast					
5,000	$67.90	$73.21	$141.11	17,940,311	$0.112
10,000 (1)	$71.22	$78.14	$149.35	37,037,236	$0.277
10,000 (2)	$70.12	$76.21	$146.33	36,180,453	$0.200
15,000	$61.44	$67.94	$129.37	53,933,379	-$0.180
Perfect Wind Generation Forecast					
5,000	$69.54	$72.76	$139.09	17,940,311	$0.179
10,000 (1)	$70.12	$72.93	$142.30	37,037,236	$0.107
10,000 (2)	$69.36	$72.49	$143.05	36,180,453	$0.076
15,000	$72.01	$74.83	$141.85	53,933,379	$0.144

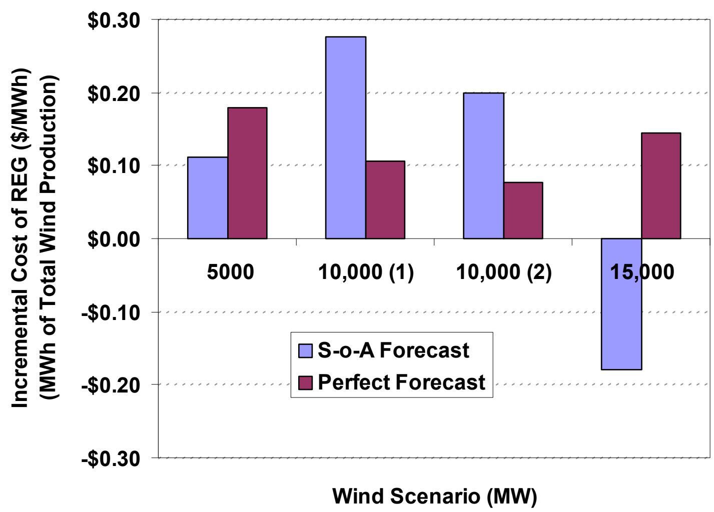

Figure 6-51 – Incremental cost of regulation, relative to the no-wind scenario, per MWh of wind energy produced.

6.5.3. Temporal Characteristics of Regulation Costs

Changes in the costs of regulation, due to wind generation capacity increases, are not uniform across the year. Figure 6-52 show costs of up-regulation by hour of day and month of year for the load-alone and 15,000 MW wind generation capacity scenarios. The differential cost, in percentage of the load-alone value, is shown in Figure 6-53. Similar plots for down-regulation are shown in Figure 6-54 and Figure 6-55. All of these plots assume that a state-of-the-art wind generation forecast is used in the day-ahead unit commitment. This analysis was also performed assuming a perfect forecast, and the resulting plots are provided in Appendix G.

•

a)

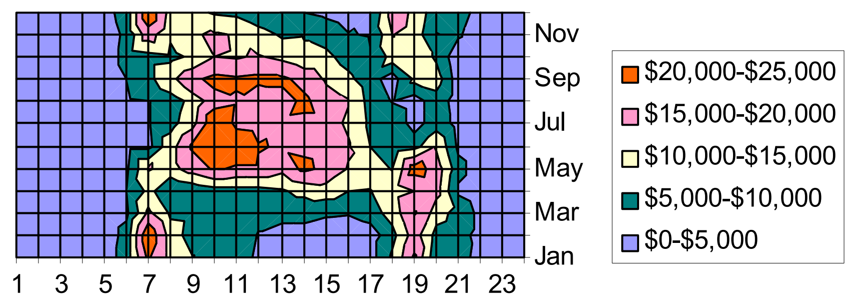

b)

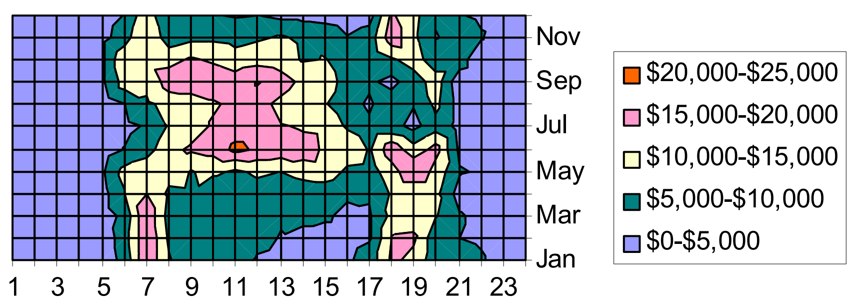

Figure 6-52 – Costs of up-regulation (average $/hr) by hour of day and month of year for the scenarios with load alone (a) and with 15,000 MW of wind generation capacity (b).

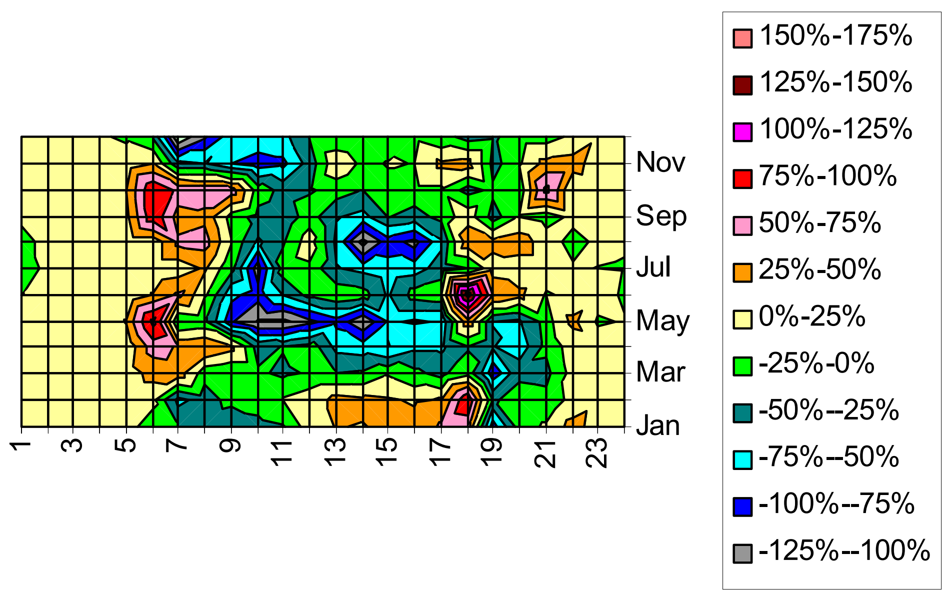

Figure 6-53 – Change in average up-regulation costs, by hour of day and month of year, from the load-alone scenario to the 15,000 MW wind generation capacity scenario. The percentage base is the respective hour and month up-regulation cost for the load-alone scenario.

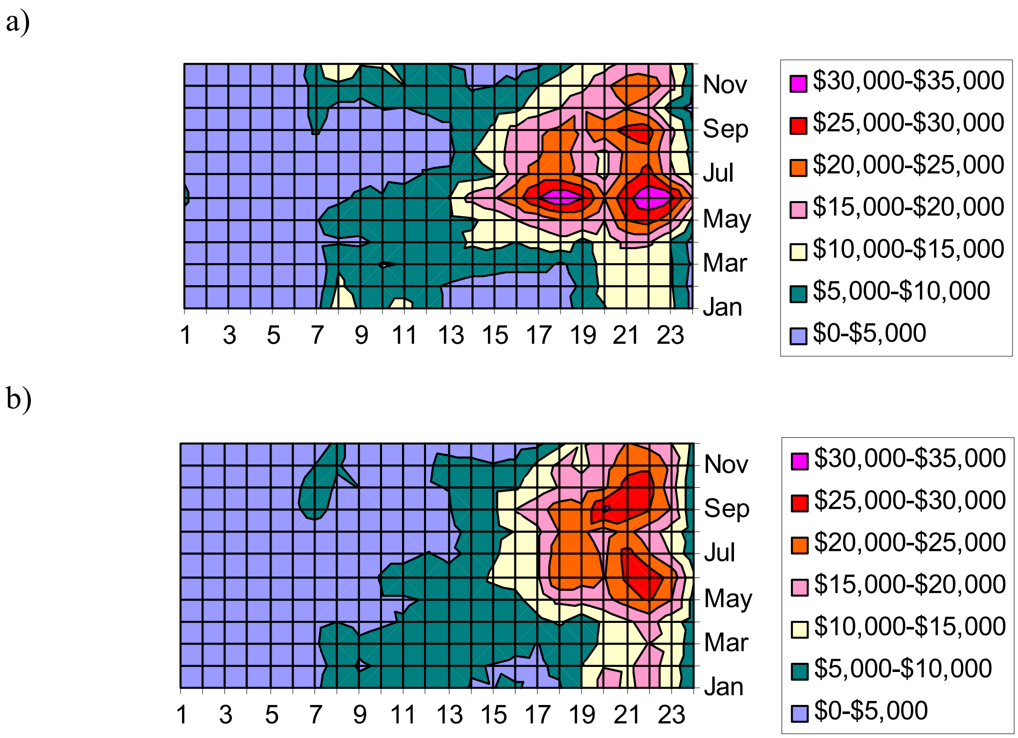

Figure 6-54 - Costs of down-regulation (average $/hr) by hour of day and month of year for the scenarios with load alone (a) and with 15,000 MW of wind generation capacity (b).

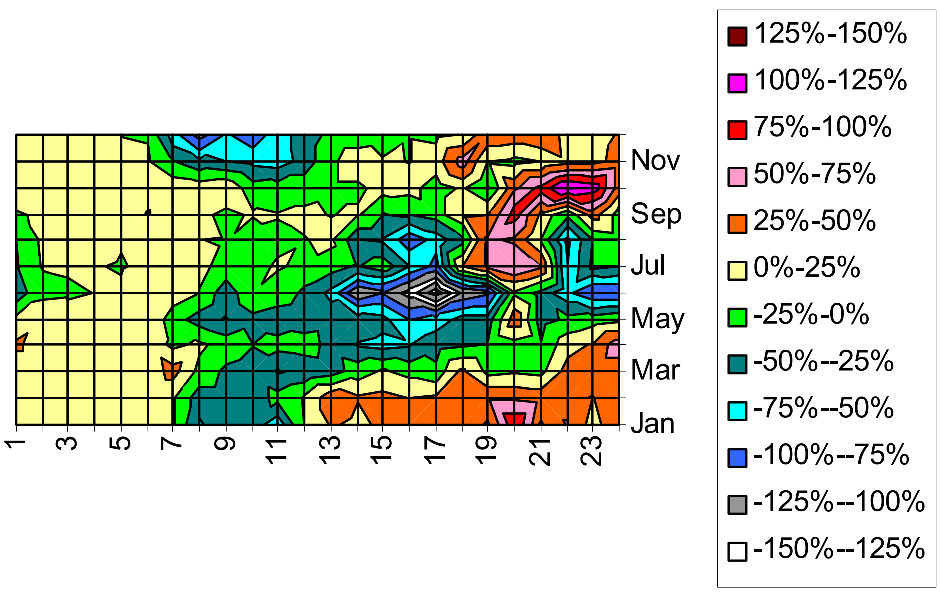

Figure 6-55 - Change in average down-regulation costs, by hour of day and month of year, from the load-alone scenario to the 15,000 MW wind generation capacity scenario. The percentage base is the respective hour and month down-regulation cost for the load-alone scenario.

6.6. Alternatives to Meet Regulation Requirements

There are various means to obtain sufficient regulation range when the economic dispatch does not inherently provide enough. These are:

- Adjust the dispatch of non-wind generation. For example, to increase down-regulation range, a unit can be de-committed and the remaining units dispatched to a higher level to provide more range to their lower limits.
- Allow wind generation units to participate in the regulation market, particularly down-regulation. Because wind units are subject to un-ordered power changes, the definitions and rules of regulation would need to be adapted, and perhaps a unique regulation service defined specifically for wind generation.

Require up-ramp limits on wind generation for the affected hours. Some wind plant control systems already provide this function.

7. EXTREME WEATHER

ERCOT's present ancillary services protocols define extreme weather on the basis of unusually hot or cold weather in the major Texas load areas. This temperature-based definition is relevant to load, but a system with high wind penetration is also stressed by severe changes in wind generation output due to different types of extreme weather.

In this section, the propensity of the system to experience unusually large and rapid changes of net load, due to wind variations, is explored using two different approaches; one based on meteorological analysis and the other based on outlier analysis of the modeled wind generation data. The information derived from the analysis of extreme wind generation changes is used later in Section 8 to define requirements for the responsive reserve and non-spinning reserve ancillary services.

7.1. Meteorological Analysis

As a key part of the analysis of extreme weather, with respect to wind generation output changes, AWS Truewind (AWST) was tasked to perform an analysis of extreme wind generation changes in Texas and the underlying meteorological basis. Their report is included, in entirety, as Appendix H. In this main body of the study report, key findings of the AWST work are briefly summarized.

The concentration of AWST's work was on analysis of historic events causing more than a 200 MW change in wind generation output over a thirty minute period. Thirty minutes was chosen as a criterion because ERCOT presently requires that units bidding into the Non-Spinning Reserve Service be able to start in thirty minutes. The 200 MW change is on a base of 970 MW of wind generation capacity located at a limited number of sites for which ERCOT could provide historical minute-by-minute wind generation data from 2005 and 2006. Thus, the changes constitute more than 20% change of the somewhat limited sampling of wind generation sites.

Both increases and decreases in wind generation output were considered. Extreme wind generation decreases are more operationally significant to the power system. However, increases in wind velocity can also cause sharp decreases in wind generation output due to wind turbines going into high-wind cutout. Thus, rapid wind velocity increase incidents are equally significant.

7.1.1. Underlying Weather Phenomena

For the extreme wind generation change events identified by AWST, the underlying causes were determined by evaluation of available meteorological observations. Several weather phenomena are identified in AWST's report as causes for significant wind changes:

- **Frontal system, trough, or dry line**. These fronts can extend for over 600 miles, and the frontal line can advance with speeds in excess of 34 mph. These fronts typically cause a rapid increase of wind speed, followed by a slower decay of wind speed.
- **Thunderstorms and convection-induced outflow**. These storms are generally more local in extent, and can move with considerable speed. They can form rapidly and are sometimes difficult to predict.
- **Low-level jets** are a common weather feature in Texas, and can form due to radiational cooling at sunset, or due to a cold front.[1]
- **Weakening pressure gradients** cause rapid decrease of wind speed over a potentially large area.
- **Strengthening pressure gradients**, developing high winds that can potentially cause widespread wind turbine cutouts.

7.1.2. Probability and Predictability of Wind Events

AWST's analysis of wind events in Texas is summarized in Table 7-1. In this table, "Ramp up/Ramp down" indicates the number of events in the actual wind plant output data where wind generation output change up or down at least 20% of capacity in thirty minutes. Note that this is for a limited number of wind generation sites, and this sampling does not have the geographic diversity of the CREZ scenarios. The typical events per year is the number of times per year that the given weather event can be expected to occur, but not necessarily with any particular severity.

7.1.3. Extrapolation to the 15,000 MW Scenario

AWST used the historic weather analysis, along with the geographic descriptions of the CREZs and the proposed wind generation capacities in each CREZ, to make an informed estimate of maximum wind generation change events in the 15,000 MW wind generation scenario. The results of this extrapolation are shown in Table 7-2. In this table, the column marked "CREZs affected" indicate the estimated worst-case scenario of adjacent CREZs that could be involved simultaneously in each type of event. The aggregate capacity is the capacity of wind generation in each of the affected CREZs for the 15,000 MW wind generation capacity scenario.

---

[1] Investigation of large ramp events detected no direct evidence of the involvement of low-level jets as a significant cause. Given the lack of observations needed to directly detect the presence of a low-level jet near a wind farm, at best we can infer the potential for low-level jets since there is only one station in Texas that continuously measures the vertical wind profile in the lower boundary layer. Low-level jets, while potentially significant to the variability of a specific plant, may not be as important to the aggregate production.

Table 7-1 - Summary of weather phenomena associated with ramp events[2]

	Ramp up/Ramp down	Typical Events per year	Preferred time of day/season	Forecast Lead Time
Frontal Passage	12/3	Around 50	Winter, followed by Spring or Fall, no preference for time of day, although pre-frontal convection usually occurs during evening.	Can usually be forecast days in advance with better accuracy of timing as event approaches. More precise frontal timing can be accurately forecast with a few hours lead time on a given day. Within 2-5 hours of anticipated frontal passage they can be forecast to perhaps within 30 minutes.
Dry Line	4/0	40-50	Spring, Summer. The dryline generally advances east by day, retreats by night	Dry line formation can typically be anticipated a day or so in advance. When formed, dry line passage can be forecast on the local scale a few to several hours in advance.
Troughs	5/1	Around 50	Anytime, no strong seasonal preference, no hourly dependency	Similar to frontal passages, above.
Weakening Pressure Gradient	0/14	80/100	Anytime, no strong seasonal preference, no hourly dependency	Large scale gradients similar to “fronts”; smaller scale gradients related to small scale pressure couplets similar to “convection”.
Convective Outflow	14/5	40-60 days in the project area at a given point. Can have multiple outflows from one event.	Spring or Summer, afternoon and evening	Occurrence can be “nowcast” using current data, with a few hours lead. Individual outflows perhaps 20-30 minutes in advance of arrival at a particular site. Probabilities in a region may be forecast a few (2-3) days in advance with good confidence
Stabilization	0/1	unknown	Around sunset	Can be anticipated perhaps a day or two in advance for probabilities.
High Wind	1/1	1	Anytime, preference for cold season	A few hours to several days

2 From AWS Truewind Report, *Analysis of West Texas Wind Plant Ramp-up and Ramp-down Events*, included as Appendix H to this report.

Convective events can range from an isolated thunderstorm to a large cluster of storms. While a single storm can be of devastating potential to a small number of wind turbines, the impact on ERCOT-wide wind generation impact cannot be large. A cluster of thunderstorms can affect wind generation sites over a moderate area. AWST estimates that a single such event could affect CREZ 5 and 9 within a thirty-minute period. Severe events can be expected two to four times per year. Fronts and troughs can affect a wider area. The most widespread wind generation impact can be caused by strengthening of pressure gradients between weather systems. The resulting high winds can potentially result in widespread wind turbine cutouts. Such a phenomenon was responsible for the February 24, 2007 event causing rapid wind generation output changes in ERCOT. For the 15,000 MW scenario, AWST conceived a worst-case scenario of this phenomenon affecting nine different CREZs. Given an event of similar severity as the February 24, 2007 event in the 15,000 MW scenario, AWST forecasts that a 2836 MW drop in wind generation could occur over a thirty-minute period. Events of this severity can be expected less often than once per year; AWST estimates a mean recurrence of once in three to five years. . As indicated in Table 7-1, these events can generally be predicted several days in advance.

Table 7-2 - Extreme Events Summary: 15,000 GW Scenario[3]

Weather Event	CREZs Affected	Aggregate Rated Capacity (MW)	Maximum 30-Minute Ramp (MW)	Frequency (# times approaching max ramp per year)
Convective	5, 9	3251	+1300	2 - 4
Frontal/dry line/trough	5, 6, 9	4529	+1324	2 - 4
Weak gradient	5, 6, 9	4529	-1313	2 - 4
High Wind	2, 4, 5, 6, 7, 9, 10, 12, 14	12,329	-2836	< 1

7.2. Analysis of Modeled Wind and Net Load Data

Large rates of change in wind generation output and net load were identified in the modeled scenario data and analyzed to provide indications of the severity and frequency of occurrence of extreme changes.

7.2.1. Wind Generation Diversity

Similar to the way system load exhibits diversity, the variations of the wind generation portfolio are mitigated by spatial diversity. In Table 7-3, the maximum one-hour drop in

[3] *Ibid.*

wind generation output for each scenario is compared with the sum of the non-coincident maximum drops for all the wind sites[4]. The ratio is a coincidence factor. Note that this coincidence factor decreases as the total wind generation capacity increases, due to greater diversity. The second 10,000 MW scenario has a smaller coincidence factor than the first because it has 1,500 MW of capacity in CREZ 24 (South Texas Coast) substitute for the same capacity in CREZ 4 (Panhandle), again, illustrating the value of geographic diversity of the wind generation assets.

Table 7-3 – Coincidence of Wind Generation Output Drops

	Wind Generation Capacity Scenario			
	5,000 MW	10,000 MW (1)	10,000 MW (2)	15,000 MW
Observed max drop for scenario	-1507	-2418	-2242	-3340
Sum of max drops for all sites	-2418	-4979	-4883	-7320
Coincidence factor	0.62	0.49	0.46	0.46

On January 28, 2006, a significant wind generation drop event was observed in ERCOT. Because this is the year on which the study year data were based, the models used to derive the wind generation model reflect the meteorological phenomena that occurred on that date. Figure 7-1 and Figure 7-2 plot the modeled wind generation output for the 15,000 MW capacity scenario, as a function of time, for this date. Figure 7-1 shows wind plant output aggregated by CREZ. Because this event was the result of frontal activity, it affected a number of CREZs in West Texas over a short period of time. CREZ 9 and 10 had the steepest drops. CREZ 24, in South Texas, actually had an increase of wind output for the same period as the West Texas CREZs were dropping, providing partial mitigation. A key observation is that, although this was a severe event, the aggregate effect of such an event is a fast ramp of power, not an abrupt drop such as occurs with the trip of a large thermal generating unit. In Figure 7-2, the modeled outputs of sites in CREZ 10 are plotted. For sites within a CREZ, the output drops for a severe weather event are a near-simultaneous ramp-down.

[4] Individual actual wind plant sites plus hypothesized sites identified by AWS Truewind for use in constructing the wind generation scenarios.

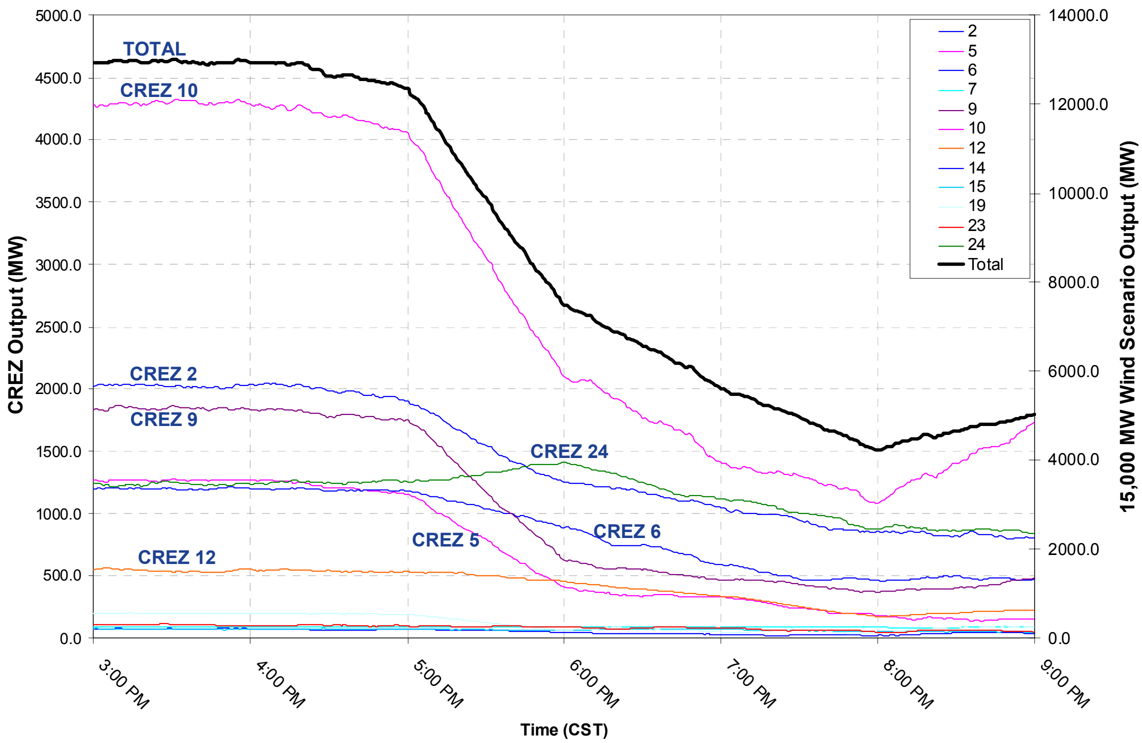

Figure 7-1 – Aggregate CREZ outputs for wind ramp-down event of January 28, 2006.

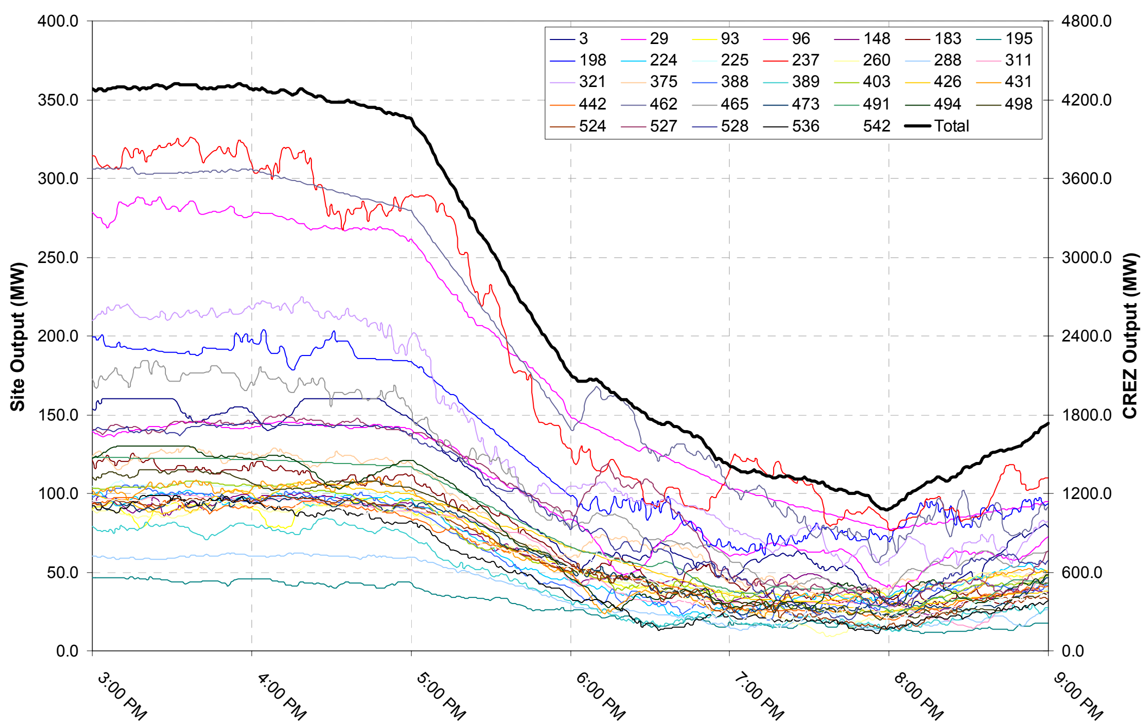

Figure 7-2 - Aggregate wind plant outputs in CREZ 10 for wind ramp-down event of January 28, 2006.

7.2.2. State Transition Matrices

Changes of wind generation output, from one 15-minute period to the next for the entire study year, were processed to define the state transition matrix shown in Table 7-4. This state transition matrix is for the 15,000 MW wind generation capacity scenario. Rows in this matrix indicate the level of average wind generation output at any given period, and columns indicate the average output at the next 15-minute period. Elements in the matrix indicate the probability that the wind generation output will change from the value given by the row to the value indicated by the column.

The elements of the diagonal of this matrix, highlighted in yellow, indicate an average probability of more than 85% that the generation output will remain nearly the same (within the same band of 10% width). Wind generation output is actually most stable when the portfolio is operating close to the maximum capacity. At operating points greater than 80% of capacity, the probability of the wind remaining in the same band is more than 90%.

The elements highlighted in green are the probabilities of the wind generation output increasing to the next higher band, and the elements highlighted in blue indicate probability of dropping to the next lower band. The average probability of the wind generation output decreasing by one 10% band in fifteen minutes are less than seven percent. Changes of more than one band are less frequent than once in 5,000 hours.

Table 7-4 – Fifteen-Minute State Transition Matrix – 15,000 MW Scenario

Next State (Output, % rated capacity)

Current State (Output)	0-10%	11-20%	21-30%	31-40%	41-50%	51-60%	61-70%	71-80%	81-90%	91-100%
0-10%	0.8386	0.1614	0.0000	0.0000	0.0000	0.0000	0.0000	0.0000	0.0000	0.0000
11-20%	0.0225	0.8602	0.1173	0.0000	0.0000	0.0000	0.0000	0.0000	0.0000	0.0000
21-30%	0.0000	0.0486	0.8445	0.1069	0.0000	0.0000	0.0000	0.0000	0.0000	0.0000
31-40%	0.0000	0.0000	0.0598	0.8232	0.1170	0.0000	0.0000	0.0000	0.0000	0.0000
41-50%	0.0000	0.0000	0.0000	0.0655	0.8176	0.1169	0.0000	0.0000	0.0000	0.0000
51-60%	0.0000	0.0000	0.0000	0.0000	0.0667	0.8079	0.1253	0.0000	0.0000	0.0000
61-70%	0.0000	0.0000	0.0000	0.0000	0.0000	0.0641	0.8495	0.0864	0.0000	0.0000
71-80%	0.0000	0.0000	0.0000	0.0000	0.0000	0.0000	0.0514	0.8701	0.0785	0.0000
81-90%	0.0000	0.0000	0.0000	0.0000	0.0000	0.0000	0.0000	0.0516	0.9134	0.0350
91-100%	0.0000	0.0000	0.0000	0.0000	0.0000	0.0000	0.0000	0.0000	0.0791	0.9209

A similar state transition matrix, for changes in 30-minute periods, is shown in Table 7-5. There is an 80% probability that the wind generation output will remain within ±750 MW of the current output. The probability of a 3000 MW (20% of capacity) decrease is small. When the wind generation portfolio is operating at an aggregate output of 60%-70% of capacity (9,000 MW to 10,500 MW), there is one chance in more than 900 that wind generation will drop by more than 3000 MW in the next half hour. At other operating points, the probability is too small to be indicated by the decimal places carried in the matrix.

Table 7-5 – Thirty-Minute State Transition Matrix – 15,000 MW Scenario

Next State (Output, % rated capacity)

Current State (Output)	0-10%	11-20%	21-30%	31-40%	41-50%	51-60%	61-70%	71-80%	81-90%	91-100%
0-10%	0.8139	0.1861	0.0000	0.0000	0.0000	0.0000	0.0000	0.0000	0.0000	0.0000
11-20%	0.0199	0.8094	0.1707	0.0000	0.0000	0.0000	0.0000	0.0000	0.0000	0.0000
21-30%	0.0000	0.0595	0.7698	0.1699	0.0008	0.0000	0.0000	0.0000	0.0000	0.0000
31-40%	0.0000	0.0000	0.0820	0.7324	0.1835	0.0021	0.0000	0.0000	0.0000	0.0000
41-50%	0.0000	0.0000	0.0000	0.0916	0.7247	0.1832	0.0005	0.0000	0.0000	0.0000
51-60%	0.0000	0.0000	0.0000	0.0000	0.0939	0.7209	0.1847	0.0005	0.0000	0.0000
61-70%	0.0000	0.0000	0.0000	0.0000	0.0011	0.0879	0.7840	0.1270	0.0000	0.0000
71-80%	0.0000	0.0000	0.0000	0.0000	0.0000	0.0013	0.0583	0.8362	0.1042	0.0000
81-90%	0.0000	0.0000	0.0000	0.0000	0.0000	0.0000	0.0000	0.0477	0.9019	0.0503
91-100%	0.0000	0.0000	0.0000	0.0000	0.0000	0.0000	0.0000	0.0000	0.0658	0.9342

Table 7-6 shows a one-hour state transition matrix for the 15,000 MW wind generation capacity scenario. The average persistence of the wind generation output, the probability of remaining within the same 1500 MW-wide band of the current output, drops to 66%. Persistence, however is significantly greater at the upper and lower end of the power output range. The probability of a -1,500 MW change is less than 18%.

Table 7-6 – One-Hour State Transition Matrix – 15,000 MW Scenario

Next State (Output, % rated capacity)

Current State (Output)	0-10%	11-20%	21-30%	31-40%	41-50%	51-60%	61-70%	71-80%	81-90%	91-100%
0-10%	0.7244	0.2742	0.0014	0.0000	0.0000	0.0000	0.0000	0.0000	0.0000	0.0000
11-20%	0.0590	0.6881	0.2419	0.0103	0.0007	0.0000	0.0000	0.0000	0.0000	0.0000
21-30%	0.0000	0.1398	0.6106	0.2250	0.0246	0.0000	0.0000	0.0000	0.0000	0.0000
31-40%	0.0000	0.0043	0.1845	0.5527	0.2355	0.0221	0.0009	0.0000	0.0000	0.0000
41-50%	0.0000	0.0000	0.0066	0.1915	0.5315	0.2357	0.0347	0.0000	0.0000	0.0000
51-60%	0.0000	0.0000	0.0000	0.0161	0.1847	0.5432	0.2390	0.0171	0.0000	0.0000
61-70%	0.0000	0.0000	0.0000	0.0000	0.0149	0.1943	0.5934	0.1890	0.0085	0.0000
71-80%	0.0000	0.0000	0.0000	0.0000	0.0000	0.0039	0.1399	0.7242	0.1320	0.0000
81-90%	0.0000	0.0000	0.0000	0.0000	0.0000	0.0000	0.0077	0.1231	0.8077	0.0615
91-100%	0.0000	0.0000	0.0000	0.0000	0.0000	0.0000	0.0000	0.0286	0.1429	0.8286

7.2.3. Extrema Analysis

Figure 7-3 shows the frequency distribution of wind generation output 30-minute deltas (changes). Superimposed is a normal distribution curve, for reference. Note that this curve is slightly skewed to the positive direction, indicating the propensity for wind generation output to rise faster than it declines. Wind generation output deltas for fifteen minutes and one hour are included in Appendix I.

Power system operations, however, are predominately focused on managing the extreme events rather than the average system behavior. Figure 7-4 and Table 7-7 focus on the negative fringes of the wind delta distribution; indicating the frequency of large drops in wind generation output in thirty-minute periods. The focus of the analysis on the thirty-minute change is based on ERCOT's present ancillary services practices. Responsive Reserve Service (RRS) is used as the backstop to extreme change events exceeding the procured regulation service. For unanticipated changes over a longer period, Non-Spinning Reserve Service (NSRS) units can be placed in service. The startup time for NSRS units is defined as thirty minutes. Changes in less than thirty minutes are assumed to drive RRS requirements, unless the start-up time requirement for NSRS is shortened. Appendix I contains plots similar to Figure 7-4 for 15-minute and one-hour changes.

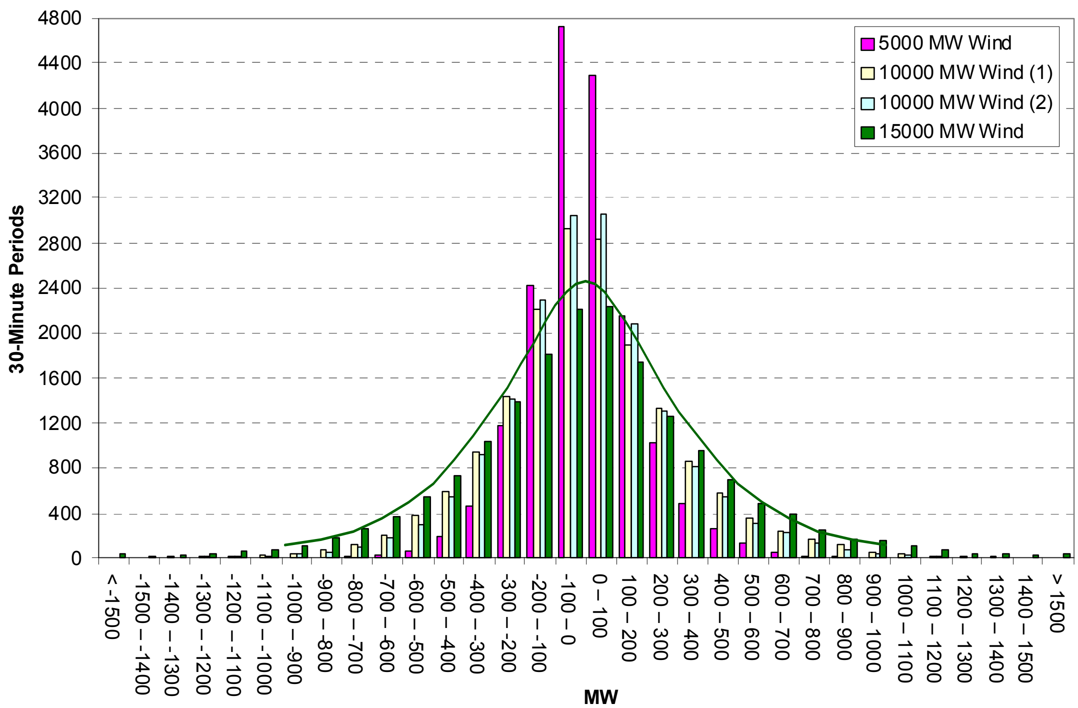

Figure 7-3 – Frequency distribution of 30-minute wind generation output deltas.

Table 7-7 – Extreme 30-Minute Wind Generation Output Drops

	5000 MW Wind	10,000 MW Wind (1)	10,000 MW Wind (2)	15,000 MW Wind
Max Pos Delta	1079	1611	1629	2370
Max Neg Delta	**-1167**	**-2053**	**-1771**	**-2563**
No. Drops > 1000 MW	5	63	36	249
No. Drops > 2300 MW	**0**	**0**	**0**	**3**

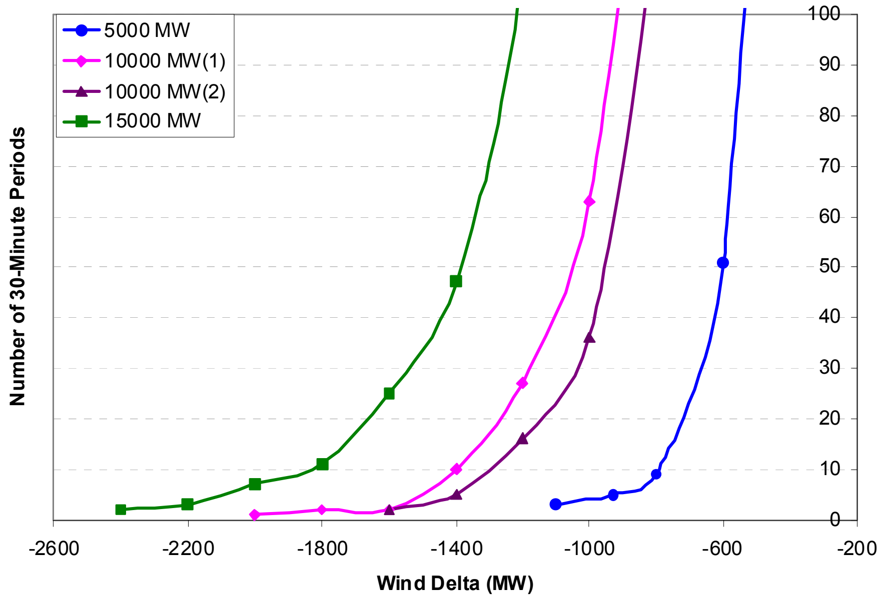

Figure 7-4 – Number of 30-minute periods where wind generation output drops are more severe than the x-axis value.

At the same time that wind changes, however, system load is also changing. The salient impact on the system is defined by the change in net load. Figure 7-5 shows the cumulative frequency of extreme thirty-minute increases in net load, and Table 7-8 provides related statistics. Appendix I shows similar plots for extreme 15-minute and one-hour net load rises. The vertical dashed line in Figure 7-5 indicates the maximum thirty-minute increase for load alone, 3101 MW. Of particular operational significance is that the frequency of exceeding this threshold increases nonlinearly with addition of wind generation capacity. Figure 7-6 plots this increase in frequency as a function of wind generation capacity. Although it is statistically risky to fixate on the absolute extrema (worst case) from a limited data set of one year, there is also an apparent non-linear increase in worst-case net load thirty-minute deltas with increasing wind generation capacity.

Although statistically defined metrics of the wind generation impact on net load, such as mean values, standard deviations, etc., vary linearly with wind penetration, it is observed that the severity and frequency of extreme conditions increase at a much faster rate.

Table 7-8 – Extreme 30-Minute Net Load Increases

	Load-alone	L-5000 MW Wind (1)	L-10,000 MW Wind (1)	L-10,000 MW Wind (2)	L-15,000 MW Wind
Max Pos Delta	**3101**	**3271**	**3928**	**3805**	**4502**
Max Neg Delta	-2756	-3138	-3360	-3300	-3612
No. Rises > 1000 MW	2557	2769	2986	2916	3092
No. Rises > 2300 MW	**78**	**114**	**191**	**168**	**289**

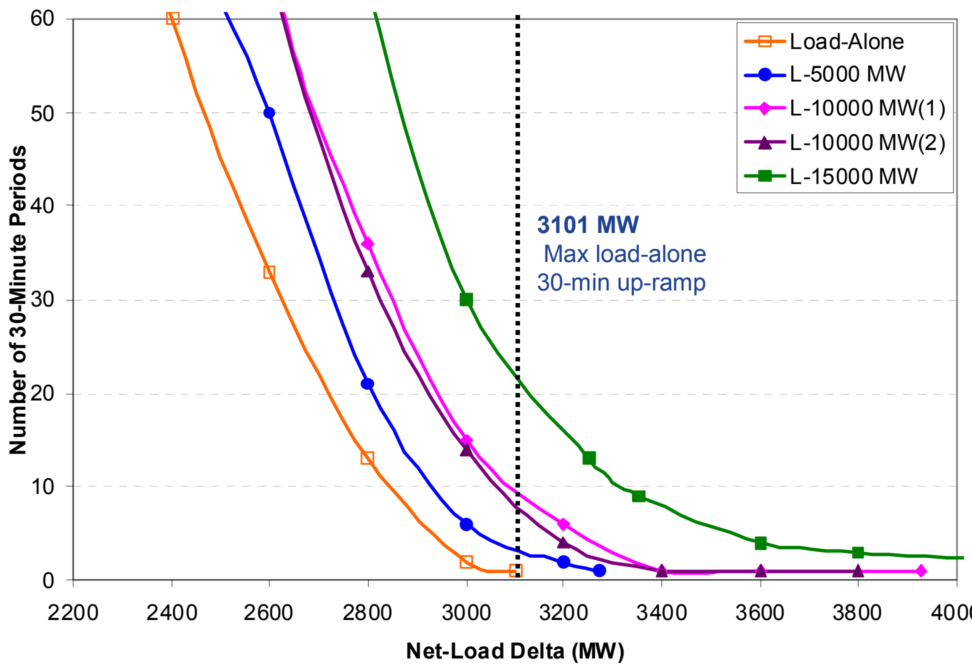

Figure 7-5 - Number of 30-minute periods where net load increase exceeds x-axis value.

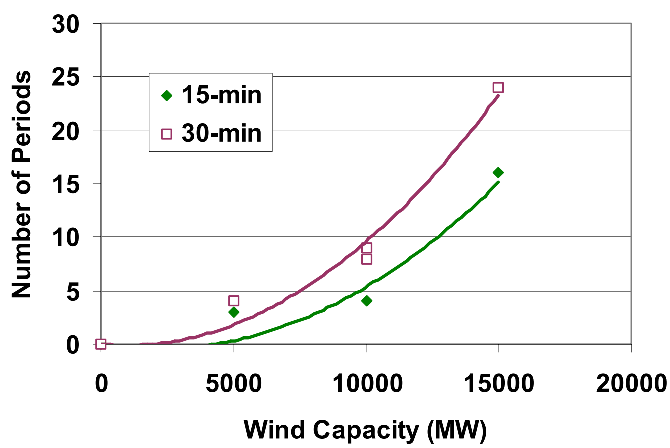

Figure 7-6 – Number of periods where the net load increase, over 15 and 30 minute periods, are greater than the worst case for load alone.

These results clearly show that the extreme changes in net load are less severe than the extreme changes in its components: wind generation output and system load. For example, the extreme 30-minute change decrease wind generation output, for the 15,000 MW wind scenario, is 2563 MW. The maximum 30-minute increase in system load is 3101 MW, yet the largest increase in net load for this scenario is 4502 MW, which is less than 80% of the sum of the component extrema.

7.2.4. Temporal Characterization of Extrema

The timing of the maximum thirty-minute decreases in wind generation output, for the 15,000 MW wind generation capacity scenario, is plotted in Figure 7-7. The most severe decreases tend to be in the morning, and in the evening in winter, spring, and fall. The morning decreases of wind coincide with load pickup, shown in Figure 7-8, compounding the increase in net load rise as shown in Figure 7-9. The severe evening wind generation output drops tend to offset load drops in the summer. However, in the winter, there is a load rise in the evening that is aggravated by the wind generation drops.

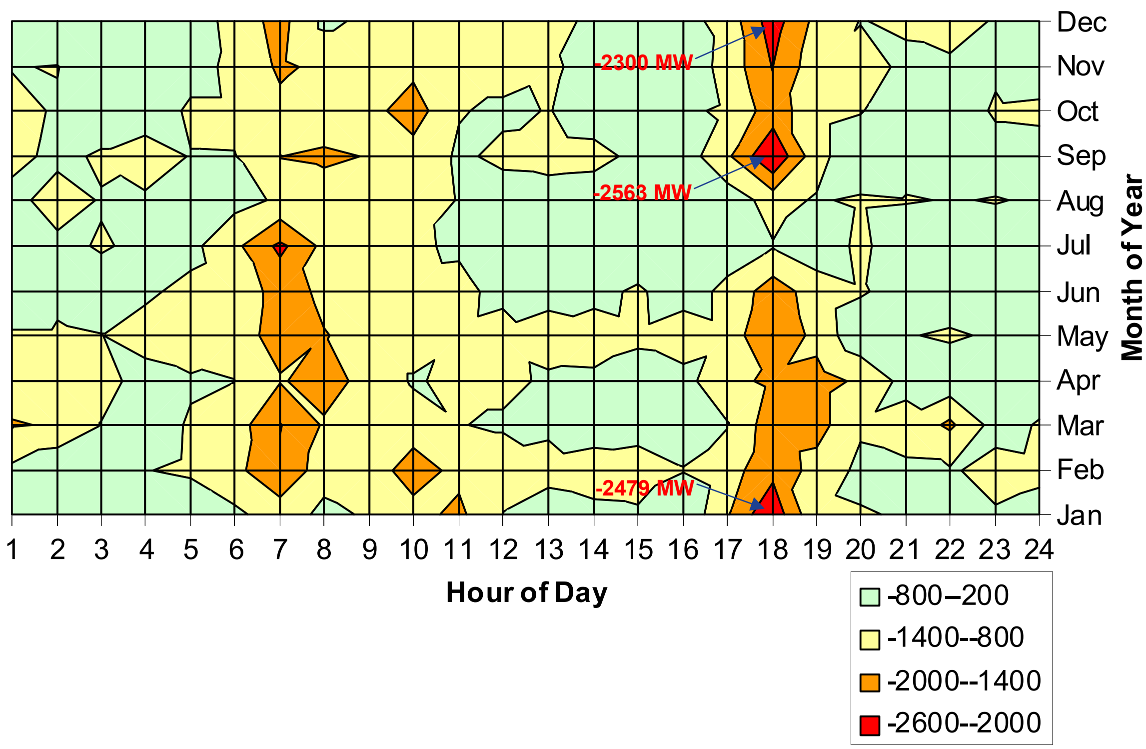

Figure 7-7 – Timing of extreme 30-minute decreases in wind generation output for the 15,000 MW wind generation capacity scenario.

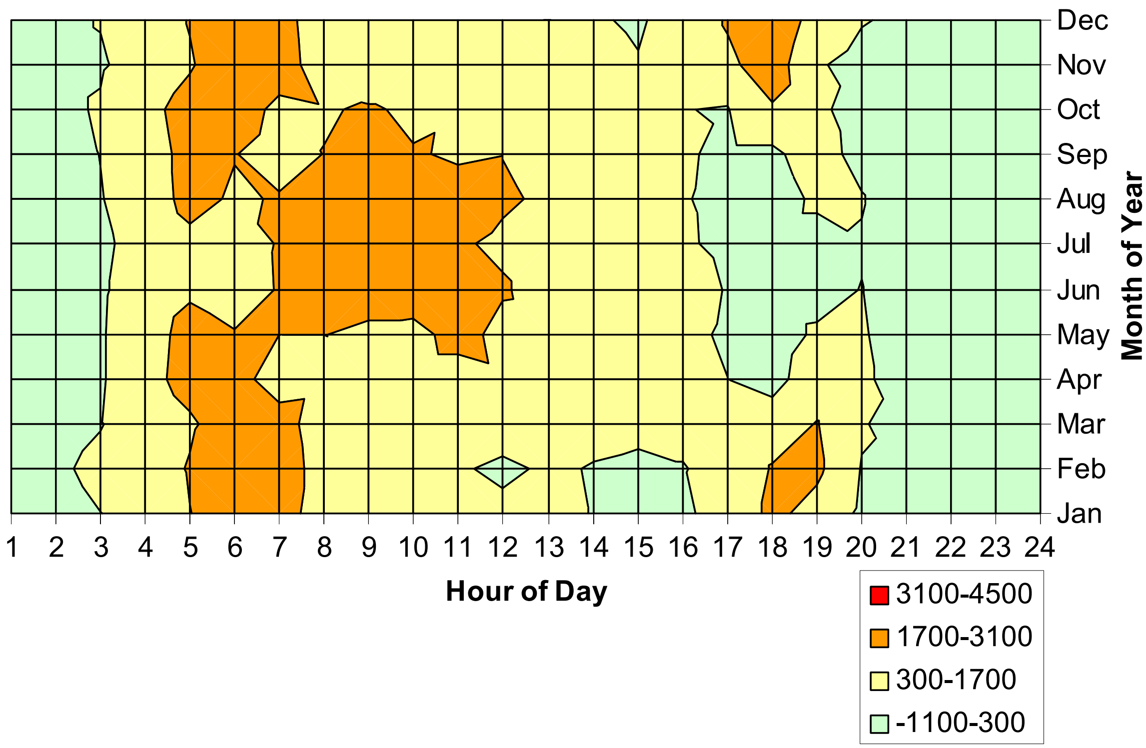

Figure 7-8 - Timing of extreme 30-minute increases in load.

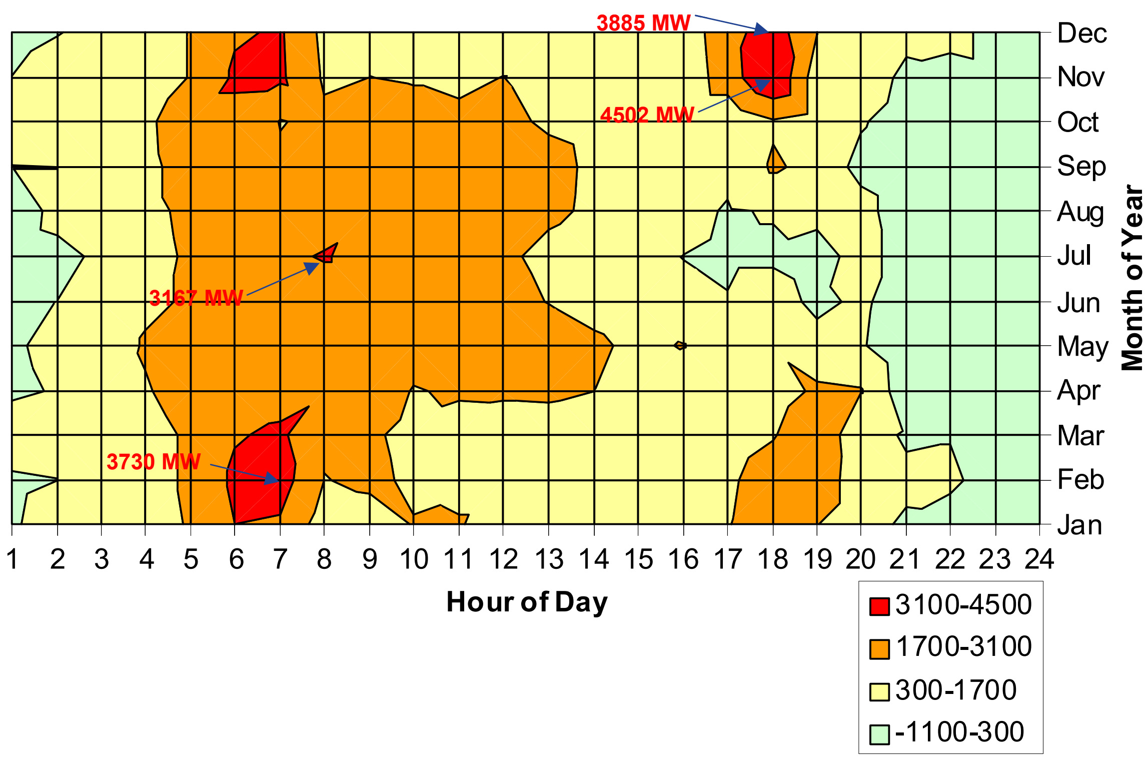

Figure 7-9 - Timing of extreme 30-minute increases in net load for the 15,000 MW wind generation capacity scenario.

8. RESPONSIVE AND NON-SPIN RESERVE SERVICES

ERCOT's present operating practice is to procure sufficient regulation to cover 98.8 percent of changes in net system load. When changes occur that are beyond the regulation procurement, the Responsive Reserve Service (RRS) is called upon to maintain system frequency. RRS is also used to cover generation plant trips, and the present amount of RRS procured, 2300 MW, is based on near-simultaneous trips of the two largest generating units in ERCOT. Thus, RRS has been employed both for load changes and generation contingencies.

These two fundamental needs for RRS, distinct in a system of conventional loads and generation, effectively merge together when non-dispatchable wind generation is added to the system. Individual wind generator units are of insignificant size with respect to the whole ERCOT system. While entire wind plants can trip, e.g., due to an interconnection substation fault, the capacity rating of an individual wind plant is much less than the largest thermal power plant units. Wind plants are becoming ever larger, but the practical aspects of collector system design will tend to cause future "mega-plants" to have multiple interconnections to the transmission system and are thus not prone to single-contingencies. Wind generation, however, is subject to uncontrollable output decreases in the same way that system load is subject to uncontrollable increases. Both wind generation decrease and load increase are continuous (i.e., ramping) events, not abrupt changes like generation trips. Thus, wind generation extreme output drops are like a positive load change, despite the fact that they are a generation "contingency".

Unpredicted load changes, occurring over a period longer than thirty-minutes, can be accommodated by calling up Non-Spinning Reserve Service (NSRS) units. ERCOT does not presently procure NSRS for all hours, but limits this procurement to periods identified as "high risk". ERCOT presently defines "high risk" as periods when "hot weather, cold weather, or uncertain weather is expected, and when amounts of spinning reserve less than 4,600 MW (including that used for RRS) are projected". These criteria are focused on the load behavior. Increased penetration of wind generation, acting as a "negative load", suggests that additional criteria for wind variability need to be included in the high-risk period definition.

8.1. RRS Requirements

RRS requirements are driven by system reliability, and must consider the probability and severity of events causing unanticipated changes in generation or load over a short period of time. Because the present ERCOT RRS requirement of 2300 MW is based on loss of the two largest generating units, the present standard is implicitly based on the joint probability of two such trips. Unlike large plant trips, which are discrete events, there is a continuous relationship between the magnitude and probability of unanticipated wind generation output changes, just as there is a similar relationship for load changes.

With significant wind penetration, RRS requirements should be determined considering the joint probabilities of generation trips and unanticipated changes in load and wind generation output. Because load and wind generation changes are fast ramps, their magnitude for determining RRS requirements are relevant only up to the power change that can occur within the time until other resources, such as NSRS or re-dispatch of committed units, can respond.

The detailed system reliability study required to determine the RRS needed is beyond the scope of this study, but this study provides ample characterization of wind generation variability needed to support such an investigation. Unlike thermal generation trips, which are essentially uniform in probability throughout the year[1], wind generation extreme changes are concentrated into particular times of day and seasons. Thus, RRS requirements with high wind penetration should be temporally variable, on an hourly and seasonal basis, to minimize system operating cost while maintaining reliable operation. Information provided in previous sections provide a great deal of information to guide establishment of standing temporal patterns of RRS requirements. In addition to standing patterns, the RRS procurement should be adjusted for periods of specific risk, as discussed later in Subsection 8.3.

Presently, ERCOT allows 50% of the RRS to be provided by Loads Acting As Reserves (LAARS). The willingness of loads to accept an interruptible service depends on the frequency that they are called upon. This factor needs to be considered in determining the appropriate proportion of LAARS in the RRS with high wind penetration.

8.2. Tradeoffs Between RRS and NSRS

Generating plant trips, causing imbalances exceeding the regulation range, must necessarily be compensated by RRS. Fast drops in wind generation output are a fast ramp event more equivalent to an anomalous load rise and RRS need only be procured to cover these events to the degree that they cannot be covered by NSRS. The shorter the NSRS startup time, the smaller the RRS procurement required. ERCOT presently has an NSRS startup time requirement of thirty minutes. Other operating areas have shorter startup times for non-spinning reserves, often ten or fifteen minutes. There are thermal generating technologies, typically single-cycle gas turbines and reciprocating engines, that can easily achieve these faster starting times. In addition, demand response can be a very effective tool in achieving a rapid correction of unanticipated generation shortfalls.

[1] The largest thermal units presently defining RRS needs are base-load units which are almost always on line.

There is an inherent tradeoff between the amount of RRS required and the NSRS startup time. It is possible that a change in NSRS startup time requirements could be economically attractive. However, a change of ERCOT's NSRS startup time requirement may be disruptive as existing units participating in the NSRS market are likely to have been configured assuming the present thirty minute startup time. A possible solution is to develop an additional "quick-start non-spinning reserve" service with a shorter startup criterion. Units that are capable can participate in this market, and this will incent future generating unit additions or modifications that permit quick starting.

8.3. Periods of Risk

Extreme wind generation changes are generally caused by weather conditions that are forecastable. Although wind generation forecast might not predict the timing and magnitude of events with total precision, forecasters are able to indicate periods of risk when weather conditions are prone to severe wind generation output changes. Therefore, RRS requirements should be adjusted based on forecast risk. ERCOT's present Operating Guides allow RRS to be increased for periods of "extreme conditions". With high wind generation penetration, it is important that identified periods of wind volatility should be included in the definition of extreme conditions.

ERCOT's ancillary services methodology calls for procurement of NSRS for defined system conditions related to month of year and ambient temperature conditions in the large load areas. Wind generation forecast uncertainty needs to be added to this list of conditions where NSRS is required. On a day-ahead basis, the wind forecasters should be able to assess the uncertainty in their forecasts and ERCOT can procure NSRS accordingly.

Because present commitment schedules are based on the mean (50% confidence level) forecast for system load, and both load and wind are subject to forecast error, it is not consistent to use the mean forecast for load and a biased forecast (e.g., 80% confidence level) for wind generation. The system would be more efficiently operated if the mean, unbiased forecast were used for both wind generation and load, and the appropriate reserves procured according to the total uncertainty.

9. CONCLUSIONS

9.1. General Observations

Uncertainty and variability are an inherent part of power system operations; power system infrastructure and operating practices have developed around the requirement to accommodate variability and uncertainty. Addition of wind generation capacity increases both, but does not greatly change their nature. The tools of operation used to address these attributes for load alone are expandable to address the net load resulting from wind generation partially offsetting connected system load.

An overall observation in this study is that through 5,000 MW of wind generation capacity, approximately the level of wind capacity presently in ERCOT, wind generation has limited impact on the system. Its variability barely rises above the inherent variability caused by system loads. At 10,000 MW wind generation capacity, the impacts become more noticeable. By 15,000 MW, the operational issues posed by wind generation will become a significant focus in ERCOT system operations. However, the impacts can be addressed by existing technology and operational attention, without requiring any radical alteration of operations.

While ERCOT's present regulation procurement methodology is adequate in terms of procuring sufficient regulation service, there are improvements that can be made which are expected to reduce the amount of procurement while maintaining sufficiency. Most notable is the inclusion of wind generation forecast information. Also, adjustments are advisable to accommodate year-to-year wind generation capacity growth.

Proper use of wind generation forecasting is of critical importance to reliable and efficient operation of the system. In addition to making efficient unit commitment decisions, wind forecasts allow ancillary services procurements to be adapted to actual conditions. The risks of extreme weather events are generally very predictable, and appropriate operating decisions can be made to pre-emptively reduce their impact.

High penetration of wind generation reduces loading on thermal units while increasing the requirements for these units to provide ancillary services. Beyond ERCOT's present level of wind generation capacity, there will be infrequent periods when unit dispatch and commitment may need to be altered to provide ancillary services. Through the 15,000 MW wind generation capacity scenario investigated, these events become progressively more frequent.

9.2. Summary of Findings

9.2.1. Variability of Net Load

- Wind generation in Texas has a diurnal component of variation that tends to be anti-correlated, or out-of-phase, with the daily load curve. Wind generation output tends to be the greatest at night and least in the daytime. The inverse-phase relationship appears to be stronger in the summer than during other seasons.
- Wind generation tends to drop sharply in the morning when load is rising quickly, and increase sharply in the evening when load is dropping. The winter afternoon load rise tends to coincide with a general increase in wind production, but there are times when wind is also ramping down in this period.
- The instantaneous wind generation penetration reaches 57% of served load during low-load periods with high wind, when the wind generation capacity reaches 15,000 MW. The minimum net load, served by the non-wind generation, is reduced by 56% during this period. The 15,000 MW of wind generation capacity is 23% of the peak system load.
- The variability of net load (served load minus wind generation) is much less than the sum of the variabilities of load and wind generation considered in isolation. This is true for both extreme values as well as mean values. Nevertheless, the incremental variability of net load at high wind penetrations is substantial.
- Both wind generation and load are affected by the same weather-related phenomena. Correct analysis of net load variability requires use of time-synchronized wind generation and load data.
- Wind generation tends to have a greater overall impact on variability in the summer, late spring and early fall, but variations in winter and early spring may be more operationally significant due to the low net load levels. When segregated by load level, variability is relatively constant, with a tendency to be somewhat greater during mid-range load levels than high and low load levels.
- Net load variability increases linearly with wind generation capacity. The number and size of large and extreme changes from one time period to the next also increase with wind generation, but tend to grow faster than a linear rate.
- For longer time spans (more than five minutes), net load variability is primarily driven by the long term ramp, but in shorter time spans there is an incremental component due to stochastic variation. The impact of the non-random ramp component can be seen in the frequency plots which become increasingly triangular in longer timeframes. With the same wind generating capacity, the incremental variability due to wind increases as the time span becomes longer, but appears to taper off, and appears to saturate at longer timeframes.

9.2.2. Predictability of Wind Generation and Net Load

- Load and wind generation forecast errors are virtually independent; they do not systematically coincide or reinforce each other. It is improbable for the most severe load and wind errors to occur in the same hour.
- Net load forecast accuracy decreases with increasing wind penetration. The larger wind forecast errors tend to be under-forecast errors, which skew the frequency distribution of the net load in the direction of generation over-commitment. This results in an operating cost penalty, in contrast to under-under-forecast errors which result in decreased system security.
- Extreme net-load forecast errors tend to be larger in non-summer months, than summer months.
- Across all seasons, during the morning load rise hours, net load tends to be generally over-forecasted relative to load alone.
- With wind generation, late evening hours tend to have lower net load forecast accuracy (relative to load-alone forecast accuracy) and incrementally larger extreme net load under-forecast errors, which may lead to under-commitment of resources. However, these are typically the hours of the day when resource needs are low.
- During afternoon to early evening (peak) hours during summer and fall, there are incrementally larger net load under-forecast errors with wind generation. The size of these errors, relative to load errors, are such that they may potentially lead to under-commitment of resources during peak load times when they are most needed.

9.2.3. Regulation Requirements

- The overall tendency is for average up and down regulation deployments to increase 18 MW with 15,000 MW of wind generation capacity. The 98.8th percentiles of deployment, however, increase 54 MW (23%) for up-regulation and 48 MW (20%) for down-regulation.
- Regulation deployment changes, due to wind, vary greatly for different times of day and seasons. The impact of wind generation on up-regulation procurement is greatest in the summer mornings and evenings all year. Between zero wind and 15,000 MW of wind generation capacity, up-regulation in the evening (1800) increases 65%. On a percentage increase basis, the overnight hours have a large regulation increase 52% over the small amount required without wind. The period with the greatest regulation requirements for load alone (zero wind), mornings, has an increase of 26% when 15,000 MW of wind is added to the system. Down-regulation procurement requirements are increased in the evening all year, increasing 32% between the zero wind and 15,000 MW scenarios.

- Of the two 10,000 wind generation capacity scenarios investigated, the scenario with wind sites in coastal South Texas in place of 1,500 MW of capacity in the Panhandle required somewhat less regulation.
- The incremental regulation requirements due to wind generation are highly correlated to the multi-hour ramp rate of wind generation. This ramping impact is more significant to regulation than the increase in stochastic "noise".
- The incremental impact of wind generation on regulation requirements is greatest when the wind generation output is at about half of the installed capacity.

9.2.4. Regulation Procurement Methodology

- By and large, the present ERCOT regulation procurement methodology continues to be adequate with a large penetration of wind capacity in the system, from the standpoint of procuring sufficient regulation service. Procurements continue to cover 98.6% to 98.8% of the deployment requirements, as planned for in the methodology. There are no periods where the wind generation causes a significant increase in under-procurement frequency.
- The average and root-mean square measures of under-procurement magnitudes, the amount of regulation required that exceeds the amount procured, increase on a MW basis with wind capacity. However, when viewed relative to the amount of regulation procured, the under-deployment magnitude remains the same for up-regulation and decreases for down-regulation.
- The study assessed steady-state levels of wind generation penetration. The present regulation procurement methodology may maintain accuracy when there are large year-to-year increases in wind generation capacity. An improved approach to factor in this growth has been detailed in the report.
- Incorporation of day-ahead wind forecast information into the regulation procurement methodology may also be able to reduce the amount of regulation procured, while retaining the accuracy of procurement. These improvements require a break from the current practice of procuring a constant amount of regulation service for a given hour of day for a month. Adjustments can be made to the regulation procured based on the forecast wind generation ramp rate and forecast wind variability.

9.2.5. Regulation Availability and Cost

- There appears to be sufficient up-regulation range available for all hours with all of the wind generation scenarios investigated. There are a limited number of hours per year, at wind generation capacities greater than 10,000 MW, when there is insufficient maneuverability of committed generation to meet down-regulation requirements. There are various ways that the down-regulation can be provided, including modification of unit commitment and dispatch for these periods.

- The total regulation service procured in a year increases with wind generation capacity. However, increased wind capacity tends to reduce the per-MWh costs for non-wind generating units to provide regulation service. The increased requirement for regulation service is more or less offset by the decreasing per-MWh price, yielding a cost of regulation per MWh of wind generation that is very small, ranging between –\$0.18/MWh to +\$0.27/MWh, depending on the wind capacity scenario and wind forecast accuracy assumptions.

9.2.6. Extreme Weather

- Geographic diversity of the wind generation limits the rate at which wind generation output can change. Extreme changes in wind occur as rapid ramps, not as abrupt changes like occurs for a conventional power plant trip.
- Extreme wind generation output changes are almost always due to predictable weather phenomena.
- The frequency and severity of extreme short-term (15 minute to one hour) wind generation output changes increases at a faster than linear rate with increasing wind generation capacity.
- Based on meteorological analysis, the maximum 30-minute drop in wind generation is predicted to be 2836 MW for the 15,000 MW wind generation capacity scenario, with a mean recurrence of once in three to five years. Based on analysis of the modeled wind production data, a 30-minute drop of approximately 2400 MW might occur once per year.
- For the 15000 MW wind scenario, a 30-minute change in net load, greater than the maximum 30-minute change for load alone, occurs approximately 24 times per year. The maximum 30-minute rise in net load is 4502 MW for this wind generation capacity scenario, compared to 3101 MW for load alone. This maximum net load rise is less than 80% of the sum of the maximum load rise and the maximum wind generation decrease (absolute value).
- Large, abrupt increases in net load are more likely in the morning, and in the evening during winter.

9.2.7. Impacts of Wind Generation on Energy Production

Indirectly related to ancillary services, *per se*, but as a by-product of the economic production simulations performed to determine availability and costs of ancillary services, a number of observations were made:

- Energy production from wind tends to be offset primarily by reduction in production from combined-cycle natural gas plants.
- For the maximum wind penetration studied (15,000 MW capacity), combined cycle plant commitment and dispatch levels are reduced to near zero during the overnight hours having high wind levels. Even coal plants see significant turn-downs in these periods.

- In general, as the wind generation penetration increases, it displaces the higher cost thermal generation and tends to reduce the overall spot price of energy.
- Wind generation decreases total system energy production cost, per MWh of wind energy produced, by $53/MWh to $55/MWh for the 5,000 MW through 15,000 MW wind generation capacity scenarios.
- The accuracy and utilization of day-ahead wind generation output forecasts has significant impact on spot prices. Compared to the present "state-of-the-art" wind forecast accuracy, a perfect forecast tends to raise spot prices for nearly all hours. If wind forecasting is totally ignored in the day-ahead unit commitment, spot prices are decreased dramatically due to over commitment of thermal units.

9.3. Other Observations

Beyond the information developed from this study, it has been observed that economic factors, plus the inherent maneuverability of wind generation plants, can result in rapid wind generation changes that become operational problems. Modern wind plants can intentionally change their power production very rapidly anywhere between near zero and the maximum possible for the existing wind conditions. There is little to no incremental costs associated with starting and stopping wind plants, beyond the obvious energy revenue costs. Consequently, price signals to reduce or increase wind plant output can and will be acted upon much faster than for thermal plants. Recent events, both within ERCOT and elsewhere, involving swings of prices into the negative domain and back, have demonstrated that this agility can cause some surprising and undesirable behavior. On the other hand, this high level of agility also presents an opportunity for creative applications to make the system both more reliable and economic.

A recent operational incident in ERCOT resulted in dropping of interruptible loads (LAARs). Wind generation ramping was a contributor to this event, which coincided with a sharp load rise and issues with dispatched generation. The wind generation change was forecast, but the ERCOT operating procedures had not been revised to employ the wind forecast at that time.

9.4. Recommendations

Wind generation forecasts are essential to efficient and secure operation of power systems with large wind power penetration. ERCOT is encouraged to obtain, and integrate into system operations and ancillary services procurement, wind generation forecasts that not only assess the predicted wind generation for each hour, but also the degree of uncertainty in each hour's forecast and a forecast of the expected wind variability on a sub-hourly basis. Wind generation forecast accuracy improves significantly as the time horizon shortens. ERCOT should consider introducing a step between the day-ahead and hour-ahead commitments. The one to six hour ahead timeframe is critical to providing better system reliability and to assure sufficient unit commitment during those periods when the uncertainty of wind forecasts may cause operational problems. Many thermal units can respond to a four-hour ahead schedule adjustment, for example, based on revised load and wind forecasts.

Wind generation has characteristics resembling load, but with a negative sense. ERCOT presently uses a 50% confidence level load forecast in system operations. To be consistent, 50% confidence level (unbiased) wind forecasts should be used as well to calculate the net load forecast to which non-wind generation is committed and dispatched. There is no fundamental difference in the nature and development over time of wind and load forecast errors; both evolve. Although wind forecast error are greater than load forecast errors, on a percentage basis, uncertainty in the wind forecast is more appropriately addressed by procuring ancillary services than by distorting unit commitment. For example, non-spin reserves could be procured to cover the difference between the unbiased wind production forecast and the forecast wind production at a more conservative confidence level. Using a biased forecast would force more dispatchable generation to be committed, removing the operational flexibility to address the wind forecast inaccuracy with less-expensive NSRS instead of what is functionally an increase in spinning reserve.

Conservative levels of responsive and non-spinning reserves, broadly applied over all times, can provide a secure but inefficient system. The risks to system security from large, rapid decreases in wind generation output are not uniformly distributed over time. System efficiency is improved if the procured amount of these reserves is adjusted commensurate with risk factors. Information in this report provides a great deal of information on the general temporal (seasonal and time of day) trends in this risk. These general trends can be used to guide longer-term ancillary service procurement planning (e.g., month ahead). However, day ahead forecasts, and possibly shorter term forecasts, should be used as the basis of ancillary service procurement.

ERCOT should consider introducing a new non-spin reserve service with a startup time of ten to fifteen minutes. This can significantly reduce the amount of responsive reserves needed for identified periods of wind generation drop risk.

The regulation services are presently in amounts that vary over the hours of each day, but with the pattern repeated for all days of the month. Using forecast data, with both wind ramping influence and wind variability (turbulence) considered, the regulation service procurements should be adjusted for each hour on a day-ahead basis.

The results reported here assume that the amount and mix of conventional thermal generation, relative to load growth, will remain constant. It is important that the amount and character of generation capable of delivering ancillary services be tracked. Exit from the market of significant participants could have adverse impacts on the availability and price of ancillary services. A consideration of market design should be providing sufficient incentives to maintain the availability of ancillary services.

The rules and definitions of ancillary services should be continuously reviewed and refined in order to encourage and include a broad range of participants in the competitive ancillary service market. In so far as it is consistent with system reliability, all technologies should be given an opportunity to participate and prove their economic value. This could include load control with sufficient response to provide regulation, energy storage, and wind generation. Wind generation can be very effective in providing down-regulation, when the value of that regulation service exceeds the opportunity value of the wind energy not delivered.

While the pace of wind generation growth in ERCOT is rapid, there is an opportunity for ERCOT to gather data, evaluate potential changes, and implement changes based on real operational data before wind generation capacity reaches the maximum levels investigated in this study. ERCOT is encouraged to collect, analyze, and act on this evolving stream of data. Particular attention should be given to monitoring system operations during periods of low load combined with high wind generation output.

Particular attention should be devoted to thorough analysis of major operational events related to wind generation variability and imprecise predictability. Frequency of such events should be determined and compared to the projections in this study. A meteorological root-cause analysis should be performed for each major event, and reasons for deviations between forecast and actual behavior should be ascertained. As necessary, ancillary services procedures should be updated as actual long-term statistics evolve.

APPENDIX A – TABLE OF FIGURES

APPENDIX B - AWS TRUEWIND REPORT: *WIND GENERATION AND FORECASTING PROFILES*

A Report to

GE Energy Consulting

WIND GENERATION AND FORECASTING PROFILES

Submitted by:

AWS TRUEWIND, LLC
263 NEW KARNER ROAD
ALBANY, NEW YORK

Michael Brower
Chief Technical Officer
Tel: 978-749-9591
Fax: 978-749-9713
mbrower@awstruewind.com

October 23, 2007

A REPORT ON THE CREATION OF WIND GENERATION AND FORECASTING PROFILES FOR TEXAS

1 INTRODUCTION

As input to a study of the ancillary services requirements for wind generation in Texas performed by GE Energy consulting for the Electric Reliability Council of Texas (ERCOT), AWS Truewind produced model-derived wind plant output and forecast data for two continuous years, 2005-2006. Four sets of data were produced: one-hour plant output, one-hour forecasts looking four hours ahead, one-hour forecasts looking one day ahead, and one-minute output. The data were generated for each of 716 project sites in 25 Competitive Renewable Energy Zones (CREZs) selected by AWS Truewind in a previous project.[1] This report describes the methods used to generate the data.

2 METHODS

The methods used to generate the wind data were adapted from those developed in previous projects to assess the impacts of wind generation on the New York, North and South Dakota, and California power grids.[2]

2.1 Hourly Wind Generation Profiles

For each wind project site identified in the previous project, AWS Truewind created two historical years (2005-2006) of hourly simulated wind generation data. The procedure was very similar to that used in the previous project. The main difference was the time period for which the data were produced (two continuous years rather than 366 days sampled from a 15-year period).

In the first stage of the process, the MASS model, a numerical atmospheric simulation model that is part of AWS Truewind's MesoMap system, was run in continuous one-month blocks throughout the period. The initial conditions and lateral boundary conditions for the simulations were taken from the NCAR/NCEP reanalysis data set, a global, gridded data base of historical weather conditions every 6 hours for the past 60 years. Additional data for the simulations were obtained from rawinsonde (instrumented balloon) observations. The simulations were performed in a nested grid configuration, with the innermost grid having a horizontal spacing of 10 km.

During the simulations, hourly samples of wind speed, direction, temperature, pressure, and other atmospheric parameters were stored for each grid cell at 25 heights from the surface to the top of the atmosphere. The wind, temperature, pressure, and turbulent kinetic energy (TKE) were then interpolated to the location of each project site and the presumed 80 m hub height of the turbines.

---

[1] AWS Truewind, LLC, "Wind Generation Assessment," Report to ERCOT, January 2007.

[2] See, e.g., GE Power Systems Energy Consulting, "The Effects of Integrating Wind Power on Transmission Planning, Reliability, and Operations," Report to the New York State Energy Research and Development Authority, Appendix A (2005). The Dakotas work was performed in conjunction with ABB for the Western Area Power Administration. The California work is being performed for GE and the California Energy Commission.

The wind speed, direction, and temperature data were then converted to plant output. The method accounted for variations in speed, air density, wake loss (as a function of direction), and other losses (such as electrical losses), as well as random fluctuations related to turbulence. For each site, the following steps were carried out:

- The diurnal average speeds were adjusted to match observed patterns at 11 tall towers in the state.
- A direction-dependent loss factor was then subtracted from the speed in each hour to represent the effect of wake interference between turbines as well as other, non-direction-dependent losses such as blade soiling. The loss factor ranged from 4% to 9% depending on the direction of the wind relative to the prevailing (most frequent) direction.
- The speed was adjusted up or down by a random factor related to the turbulent kinetic energy (TKE) predicted by the model for that hour. The TKE is a measure of the gustiness of the wind, and, thus, this adjustment allowed the output to fluctuate according to how gusty the conditions were expected to be.
- The speed was transformed to power using a generic power curve, which had been adjusted to the predicted air density for each hour. The power curve was a composite of three leading turbine power curves chosen to match the IEC class of the site.[3] The turbine models for each class were as follows:

  Class I (>8.5 m/s): GE 1.5sl, Vestas V80, Gamesa G80

  Class II (7.5-8.5): GE 1.5sle, Vestas V82, Gamesa G87

  Class III (<7.5 m/s): GE 1.5xle, Vestas V100, Gamesa G90

  (The speed ranges are defined for the standard sea-level air density of 1.225 kg/m^3.)
- The output was adjusted by a random loss factor ranging from 0% to 8%, with an average of 4%, representing fluctuations in losses associated with turbine down time. The combined wake and non-wake losses averaged about 14% for all projects and ranged from 12% to 16%.

The output data were provided to GE Energy Consulting in one comma-delimited file for each CREZ. Within each file, a time series of data was provided for each project site in the CREZ. This approach allowed GE Energy Consulting to select any number of sites in a CREZ, up to the maximum, to create a variety of wind generation scenarios.

2.2 Next-Day and Four-Hour Forecasts

After producing the hourly generation data, AWS Truewind simulated forecasts for the existing and future wind project sites. The aim was to reproduce the dynamic behavior and error patterns of state-of-the-art wind forecasts. Two types of forecasts were provided: four-hour-ahead and next-day forecasts. Four-hour-ahead forecasts are defined as the predicted generation from 2.75

[3] Turbines are designed for sites that fall within a range of wind conditions defined by the IEC class. At a standard sea-level air density of 1.225 kg/m^3, a site is Class I if its mean speed exceeds 8.5 m/s, Class II if it exceeds 7.5 m/s, and Class III if it is below 7.5 m/s. The speed threshold is adjusted according to the air density: a lower air density means the speed threshold for a particular IEC class can be increased, so that, for example, a Class II turbine could be used at a site that, at standard density, would be Class I.

hours to 3.75 hours after the time of delivery of the forecast, which is 15 minutes after every hour. Day-ahead forecasts are defined to occur early in the morning and cover from midnight to midnight of the following day, in one-hour intervals.

Normally, mesoscale numerical weather modeling would be a key input for wind forecasts. However, since such modeling was already employed to simulate the “actual” generation, it was necessary to apply a purely statistical model to reproduce the error patterns and dynamic behavior of real forecasts. Otherwise, the forecasts would appear to be too good.

For each time horizon, we derived from forecast performance data in other regions a set of error distributions as a function of forecasted generation and previous forecast error.[4] Following a Markov chain approach, the statistical model stepped through time, drawing randomly from the error distributions to construct a forecast based on the simulated generation. Finally, a bias correction was applied to ensure accurate prediction of the mean.

2.3 One-Minute Plant Output

In the final task, AWS Truewind simulated one-minute plant output data for the two-year period for the same sites. To produce the data, AWS Truewind employed a computer program to sample four-hour windows of historical one-minute data from existing wind projects. The source of the samples was two years of one-minute plant output data provided by ERCOT for 17 substations serving seven Texas wind projects.[5] The program removed one-hour trends from the data and added the residuals to the simulated hourly output for each site. It did not allow the same window of residuals to be applied to two different sites in the same time period, as this would have resulted in perfect correlation of the one-minute fluctuations between those sites, whereas in reality one-minute fluctuations between wind projects are entirely uncorrelated. The program excluded from the training data one-minute changes greater than 5% of the plant rated capacity, as they correspond to plant outages, curtailments, and restarts unrelated to the wind. (Such events are discussed in section 3.4.)

3 RESULTS AND VERIFICATION

3.1 Representativeness of 2005-2006

The first question we addressed was whether the mean wind resource for the two-year period was typical. We obtained hourly wind speed measurements from four National Weather Service (NWS) stations in northern and central Texas (Amarillo, Abilene, Lubbock, and Midland) and one (Corpus Christi) on the southern Texas coast. These stations are fairly representative of the wind climate where most Texas wind projects have been built or proposed. We found the average speeds at each station for 2005 and 2006, and compared those values with the average speeds from July 1996 to June 2007.

---

[4] Although AWS Truewind has provided forecasts for wind projects in Texas, confidentiality agreements prevented the use of these data to define the probability distributions for this study. Instead, we relied on forecasts generated for several California wind projects.

[5] The files provided by ERCOT contained data for 32 substations. However, 17 of these did not have valid data. Of the remaining 15 substations, several represented different parts of the same project.

The results, shown in Table 1, indicate that 2005 was well below normal (as defined by the 1996-2007 average) at all stations, whereas 2006 was slightly above normal at all stations except Midland. The average for the two years ranges from 3.9% below the 1996-2007 average to 0.3% above normal. If the stations are plotted on a map, it is apparent that the degree of departure from normal conditions depends on latitude. The station farthest north, Amarillo, experienced the closest to normal conditions in 2005-2006; Lubbock, which is the next station to the south of Amarillo, was below normal by 1.6%, whereas all the other stations were at least 2% below normal. Most existing wind projects are located in two clusters, one between Midland and Abilene and the other south of Midland. For these projects, 2005 in particular was a rather poor wind year, with mean speeds more than 5% below the 1996-2007 average.

Table 1. Annual mean wind speeds in meters per second (m/s) for representative National Weather Service stations in Texas.

Weather Station	*2005*	*2006*	*2005-2006 Average*	*1996-2007 Average*	*Difference*
Abilene	4.59	4.94	4.77	4.86	-2.0%
Amarillo	5.54	5.79	5.67	5.65	0.3%
Corpus Christi	4.73	5.11	4.92	5.05	-2.5%
Lubbock	5.10	5.38	5.24	5.32	-1.6%
Midland	4.54	4.68	4.61	4.80	-3.9%

3.2 Hourly Wind Generation Profiles

Figure 1 presents typical examples of the simulated hourly wind generation data superimposed on the concurrent actual generation for a wind project at the same location. Although there are discrepancies, which may be caused by such factors as the finite mesoscale grid resolution and possible curtailments or low availability of the wind project,[6] the simulated and actual generation exhibit similar behavior. Similar results are found for other projects and months. For the seven projects for which data were available, the r^2 correlation coefficient between actual and predicted generation ranged from 0.35 to 0.6.[7]

[6] We noted that the average capacity factor of some of the seven wind projects was relatively low in 2005-2006. The average for the two years was 0.35, whereas for the same sites and period, the simulated net capacity factor averages 0.42. The difference may be indicative of performance problems at some projects, such as low availability, or transmission curtailments, as well as the use of different turbine models.

[7] These results and others presented in this section are for 2005. Similar results were obtained for 2006.

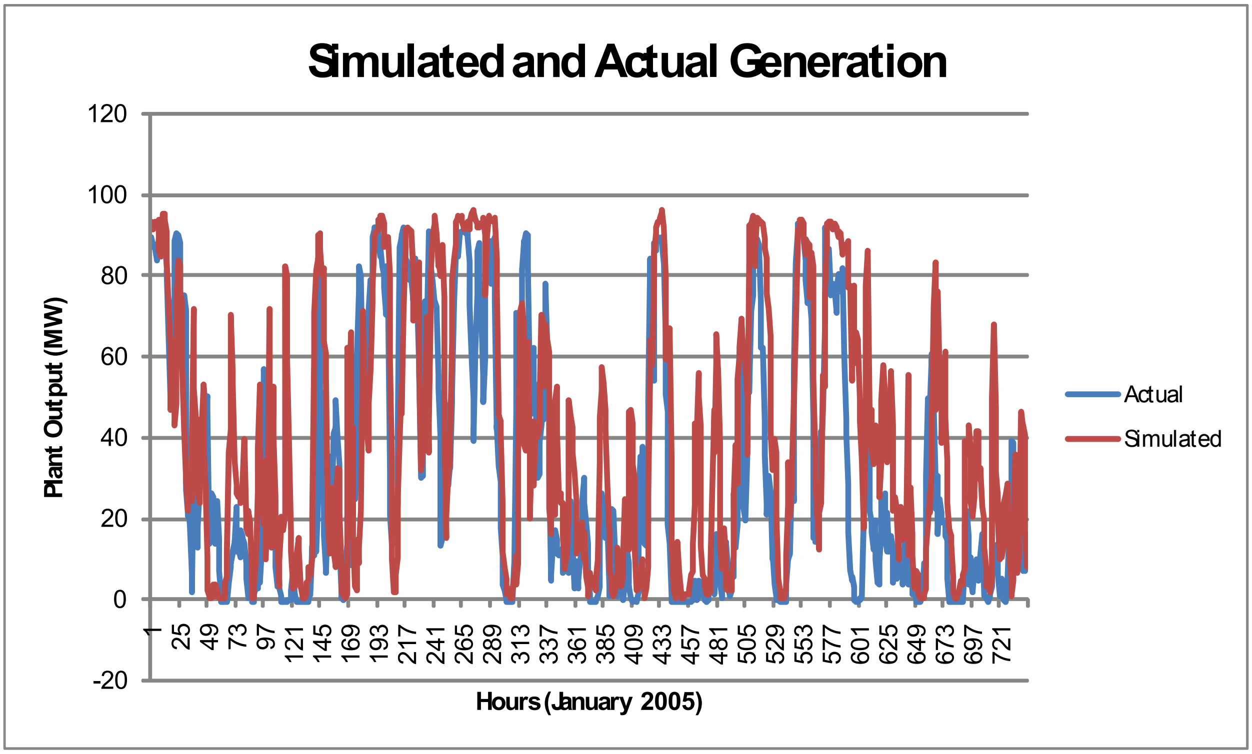

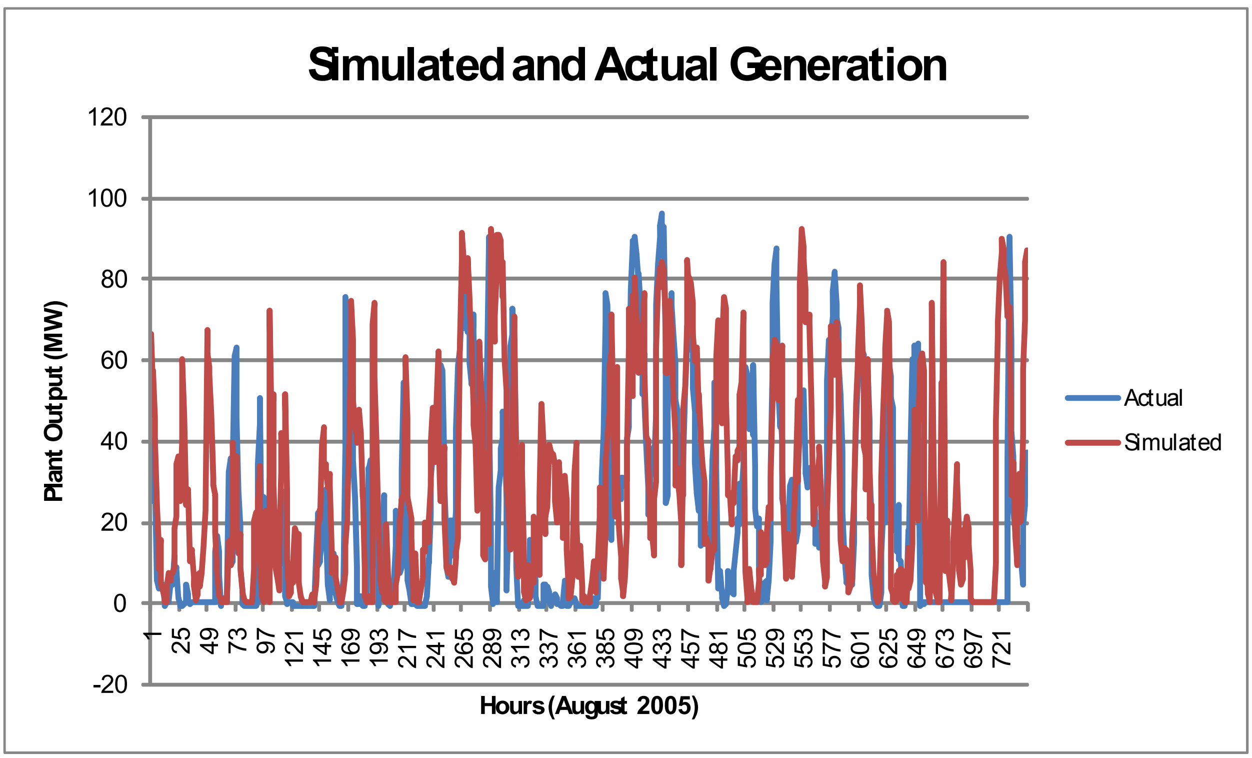

Figure 1. Comparison of actual and simulated hourly wind generation for a wind project in Texas for (a) January 2005 and (b) August 2005.

Another measure of the similarity of the actual and simulated wind generation is the rate of change of plant output. This is relevant for the analysis of ancillary services such as load following, which requires generation to respond to changing net load. Figure 2 compares the simulated and actual mean absolute deviation (normalized to the annual average output) averaged over the seven projects for time lapses of one to nine hours. The two curves follow very similar trajectories.

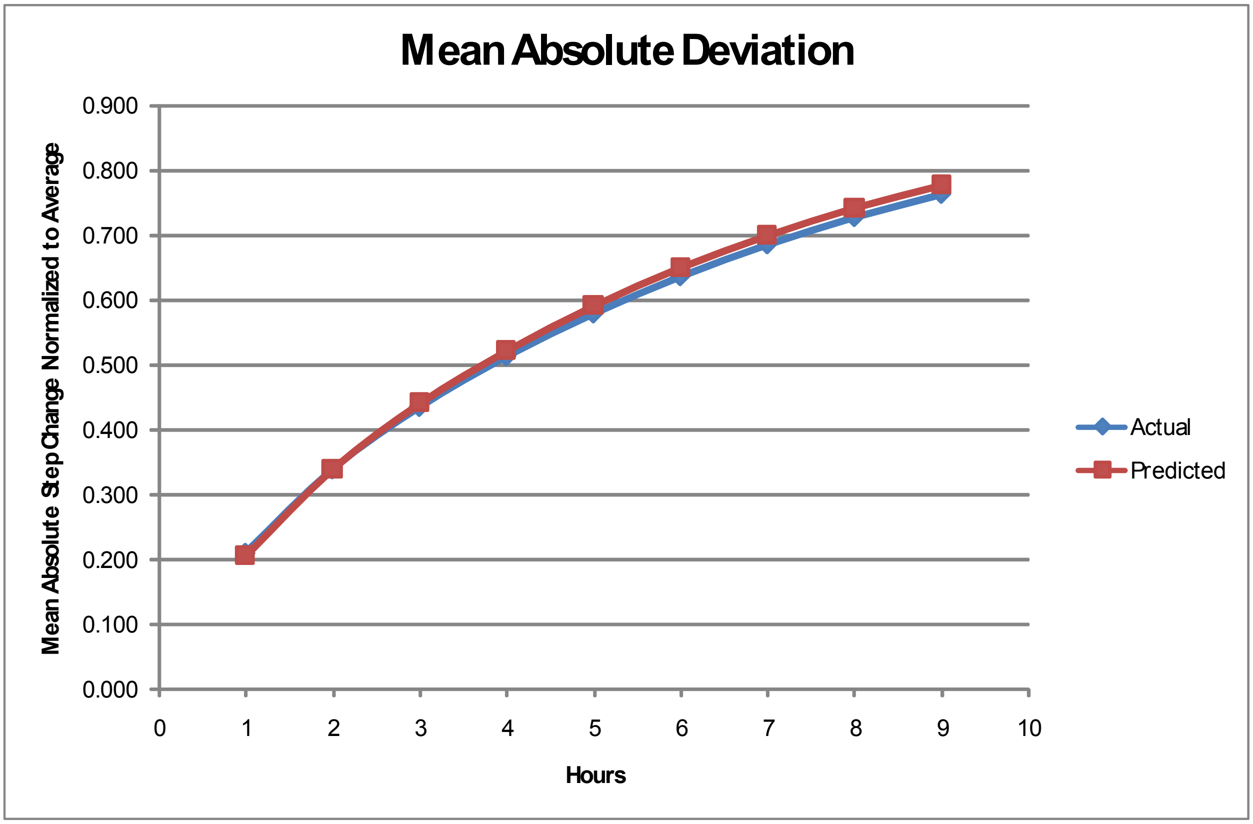

Figure 2. Relationship between the mean absolute change of the simulated and actual generation in 2005, averaged over seven wind projects, and the time lapse in hours.

Figure 3 illustrates the distribution of simulated and actual one-hour step changes in 2005 for the seven projects. This allows both small and large step changes to be compared in detail. Overall, the two patterns are very similar. The frequency of changes less than +/- 0.1 (i.e., less than 10% of the average annual output) is slightly greater for the real projects than for the simulated projects, a difference that is made up by a slightly smaller frequency of changes between +/- 0.3 and +/- 0.1. Such differences have little significance for ancillary services, however. Of greater interest are the large changes, greater than, say, +/- 0.9, which, for an average capacity factor of 40%, corresponds to about 36% of rated capacity. Overall, the actual projects exhibit a slightly greater chance of a large step change than the simulated projects. The total frequency for changes greater than 0.9 is 2.75%, according to the actual data, compared to 2.17% for the simulated data.

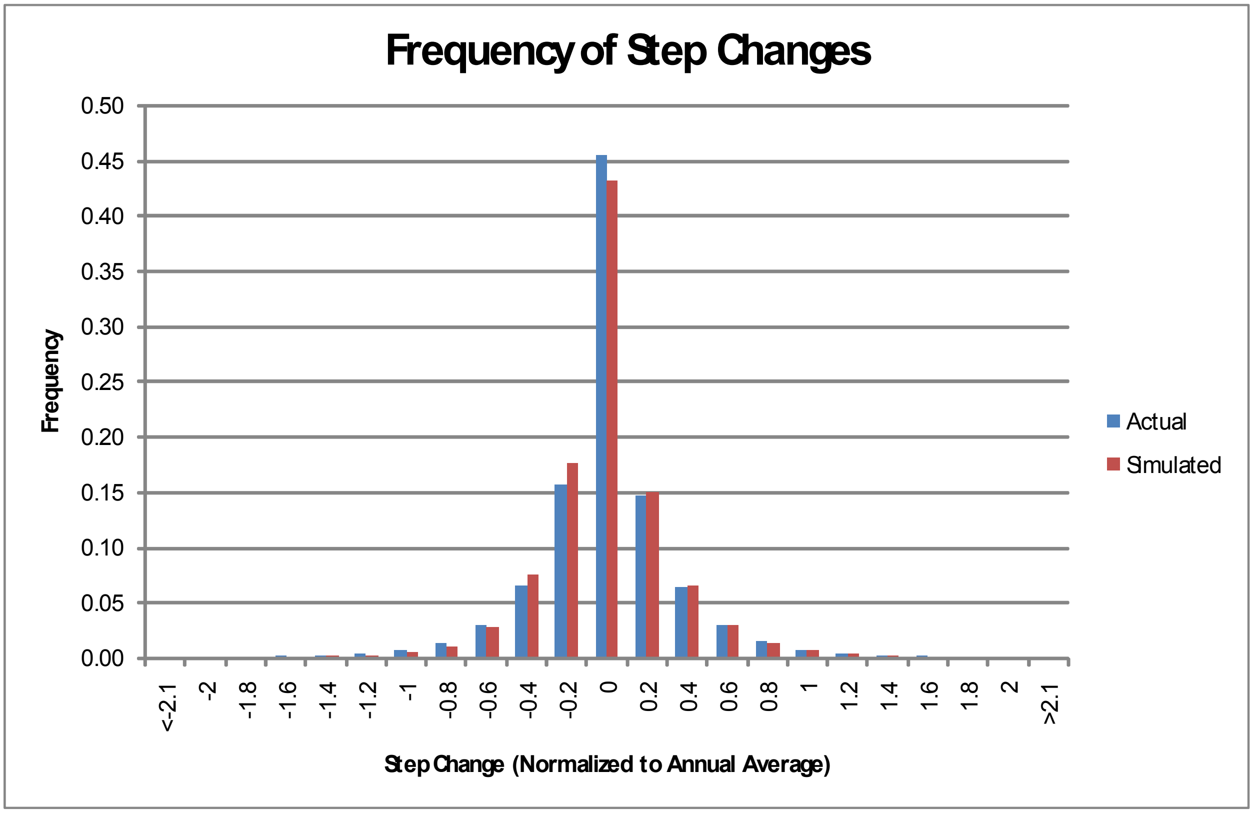

Figure 3. Frequency of one-hour step changes for the ensemble of seven projects and corresponding simulated projects. The step changes are normalized to the average annual output of the projects.

The largest actual one-hour change in 2005 was a drop of 4.5 times the annual average output, whereas in the simulated data, the largest drop was 2.1 times the annual average. However, we suspect that such large changes in the observed output are caused by plant or grid outages or mandated curtailments rather than by fluctuations in the wind. The largest single proportionate drop in 2005 was observed at a substation where the reported output fell from 38 MW to 1 MW in two minutes. This represents almost certainly a forced shutdown. The pattern of output at such times is clearly indicative of partial or complete outages, curtailments, and restarts. One example is shown in Figure 4.

For the aggregated plant output, which is not very sensitive to anomalous events at individual projects, the simulations appear to capture the frequency and magnitude of step changes very well. The largest observed step change in aggregated output in 2005 was 1.13 times the annual average output; for the simulated data, it is 1.10.

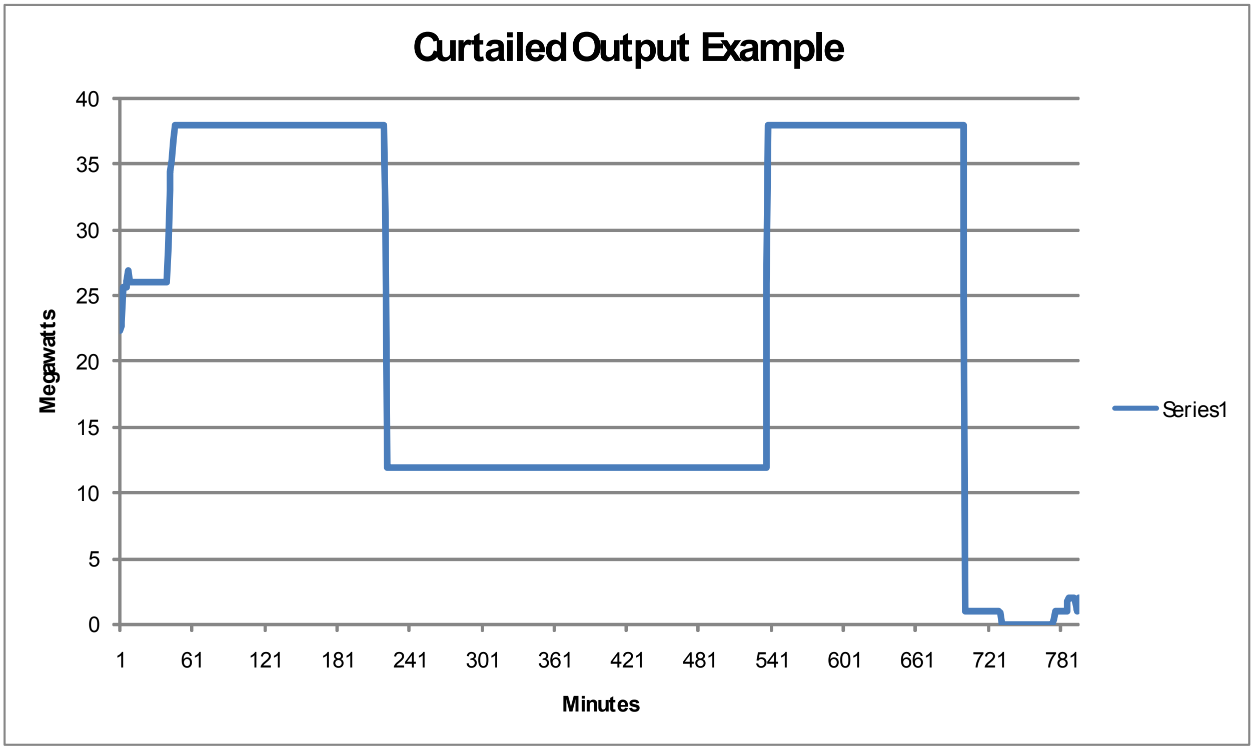

Figure 4. An example of a wind project whose output has been partially curtailed. Such curtailments may be due to a grid capacity constraint or the outage of a string of turbines. At the end of the period, it appears the plant is completely shut down.

Another important aspect of the behavior of wind projects is the time correlation of the output of different projects. If output variations are highly correlated between projects, then there is little proportionate reduction in the variability of the aggregated output; in other words, the geographic diversity benefit is small. Conversely, a small degree of correlation between projects confers a large diversity benefit.

To determine if the simulated data faithfully capture such correlations, we compared the observed and simulated correlation coefficients (r values) of the seven projects. Tables 2 and 3 present the actual and simulated correlations between the projects. Figure 5 shows the correlations between one of the seven and each of the other six. The correlation coefficients agree well, with the exception of project no. 2, whose actual output is not as well correlated with that of the other projects as the simulated output.

Table 2. Correlation coefficients of hourly average observed plant output for seven wind projects

	1	2	3	4	5	6	7
1	1.00	0.14	0.58	0.54	0.74	0.80	0.49
2		1.00	0.01	0.15	0.16	0.14	0.04
3			1.00	0.78	0.57	0.61	0.83
4				1.00	0.53	0.54	0.80
5					1.00	0.89	0.47
6						1.00	0.49
7							1.00

Table 3. Correlation coefficients of hourly average simulated plant output for seven wind projects

	1	2	3	4	5	6	7
1	1.00	0.26	0.55	0.54	0.77	0.78	0.52
2		1.00	0.20	0.25	0.25	0.23	0.22
3			1.00	0.87	0.63	0.57	0.79
4				1.00	0.60	0.52	0.79
5					1.00	0.93	0.53
6						1.00	0.50
7							1.00

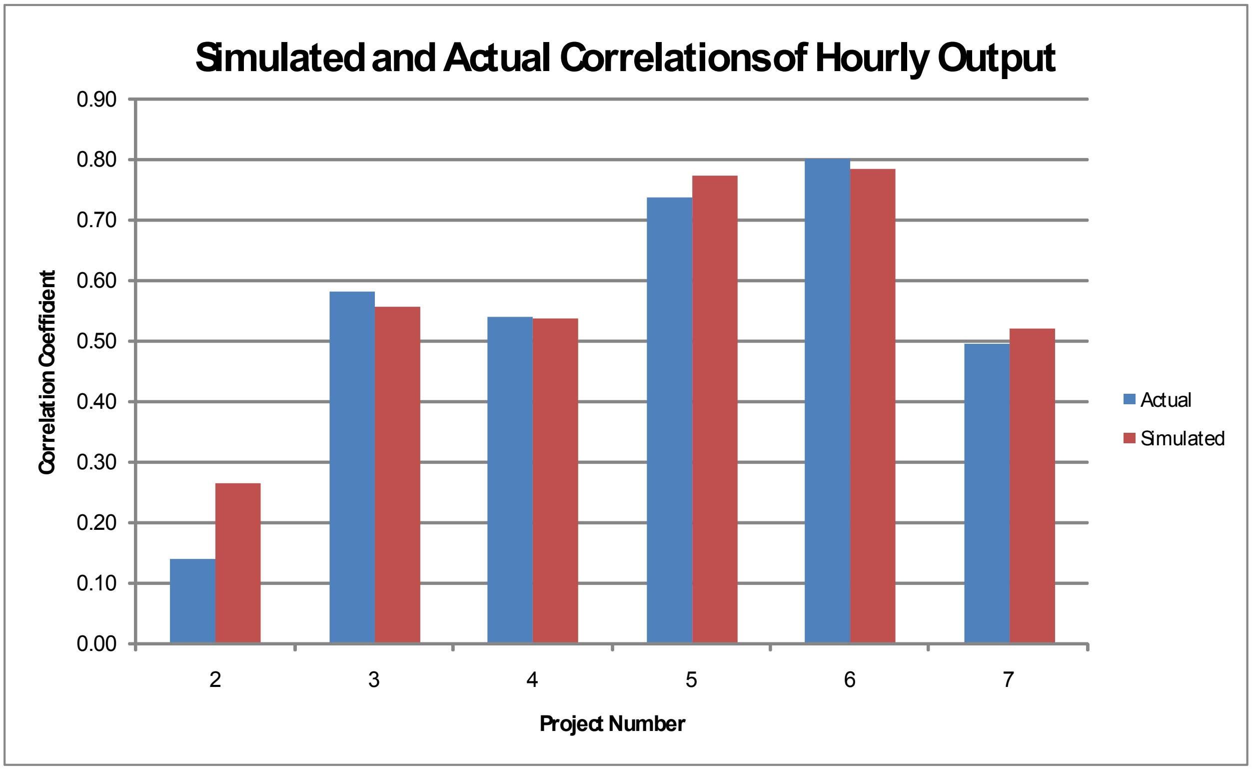

Figure 5. Correlation coefficients between the hourly average output in 2005 of wind plant no. 1 with each of the other six projects.

The seasonal and diurnal patterns of generation influence the capacity value of wind (the reliable output during peak load periods) as well as average transmission flows and the mix of non-wind electricity generation sources. Figure 6 compares the simulated and actual diurnal average plant output for one of the seven projects. The curves, which are typical for Texas projects,[8] agree closely. Figure 7 compares the simulated and actual monthly averages for the same project for the 24 months starting January 2005. The two curves clearly follow a very similar pattern, although there are some discrepancies, most notably the surge in plant output observed in June,

[8] In Texas, as in most other regions, the output of a wind project – assuming a turbine hub height of around 60 m or greater – is typically at a maximum at night because of the decoupling of the surface layer from the upper atmosphere under thermally stable, nighttime conditions.

2005, which is only partly matched by an increase in the simulated generation. These discrepancies follow no apparent pattern.

On the basis of these comparisons, we conclude that the model reproduces the dynamic behavior of wind plants in Texas with acceptable accuracy. It is not expected that the simulated winds will match the actual exactly at any given time or place. Some of the discrepancies we have noted may be caused by limitations in the numerical weather modeling, such as the finite grid resolution. Others may be caused by differences in the assumed turbine models or problems with the wind plant performance (including low availability, curtailments and outages). Considering that the dynamic behavior is realistic and the mean seasonal and diurnal patterns are captured reasonably well, the data appear to provide a solid basis for the hourly grid impact simulations.

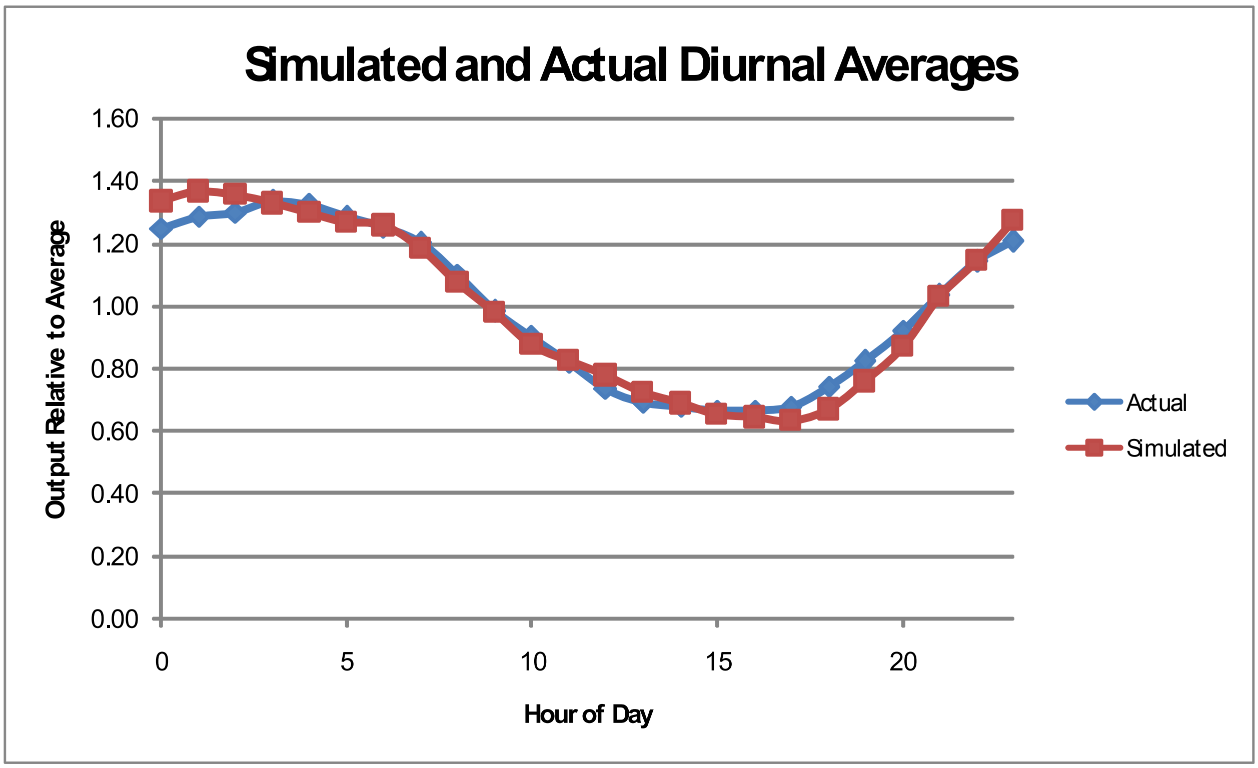

Figure 6. Comparison of the simulated and actual average output in 2005 as a function of time of day, for one project.

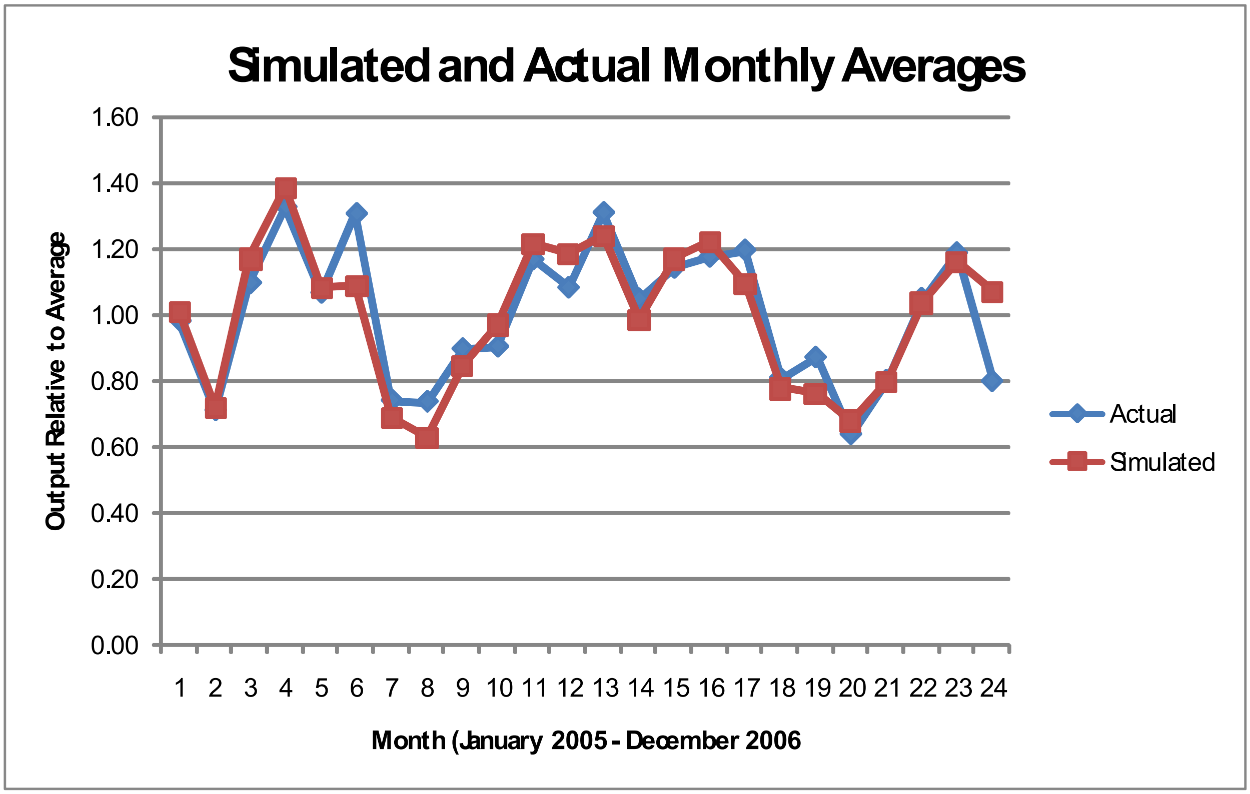

Figure 7. Comparison of the simulated and actual monthly average output in 2005-2006 for one project.

3.3 Forecasts

Figure 8 presents an example of both next-day and four-hour forecasts for a two-week period in January 2005, for a site in west-central Texas. The "actual" generation in this case is that simulated by the AWS Truewind model. Although the forecasts follow the actual to a considerable degree, there are significant errors in some hours. These errors tend to be larger for the next-day forecasts than for the four-hour forecast. Such discrepancies are normal for wind forecasts, since weather forecasting models do not have perfect prediction accuracy, and errors tend to grow with the forecast time horizon.

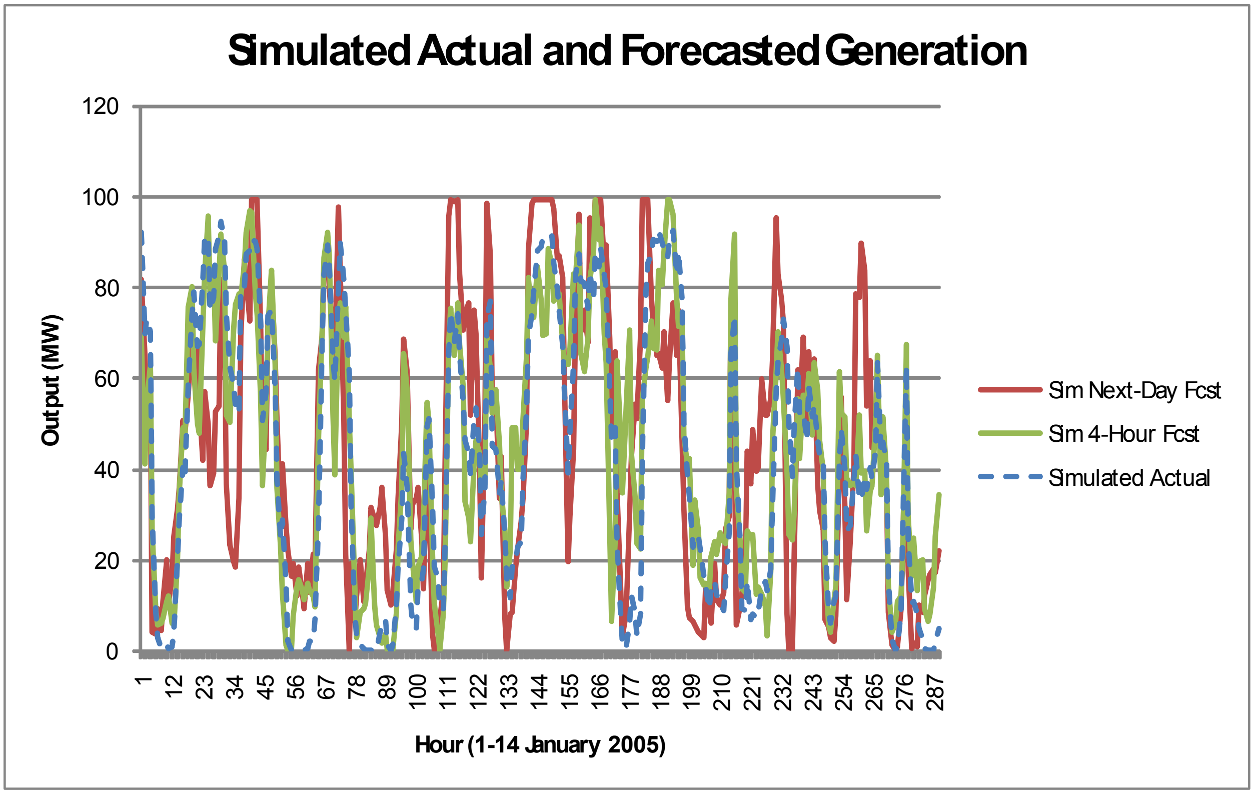

Figure 8. Typical four-hour and next-day wind forecasts for a two-week period in January 2005, compared to the simulated "actual" generation, for a site in west-central Texas.

The error characteristics of these simulated forecasts are similar to those of actual state-of-the-art forecasts. The statistical model used to create the forecasts was based on eWind forecasts for southern California wind projects, as sufficient forecasting data for Texas projects were not available. As noted earlier, it was necessary to employ a statistical model rather than a standard weather forecasting model (which would be used in real forecasts) because such a weather model was already used to simulate the "actual" output of the Texas wind projects. Were the same type of model to be used, the forecasts and actual generation would be too similar, resulting in much smaller errors than are typically encountered in real forecasts. The statistical model gets around this problem by mimicking the error patterns.

In 2005, the mean absolute deviation (MAD) of four-hour eWind forecasts averaged 9.2% of rated capacity at both Tehachapi and San Gorgonio passes; for next-day forecasts the range was 13.1% to 16.1%. A comparable level of next-day forecast performance was achieved in a 12-month wind forecasting test conducted in Texas by the Electric Power Research Institute (EPRI).[9] For the 75-MW project that was the subject of that test, the MAD of AWS Truewind's forecasts averaged 17.5%. In the present study, the MAD for Texas forecasts averaged 11.4% and 16.7% for four-hour and next-day forecasts, respectively, in CREZ 1. Thus, the errors for both the actual and synthesized forecasts in Texas were somewhat larger than the errors of the California forecasts. This difference arises because the Texas forecasts were for individual

[9] Electric Power Research Institute, "Texas Wind Energy Forecasting System Development and Testing: Phase 2: 12-Month Testing," Report #1008033, August 2004.

projects, whereas the California forecasts were numerous projects totaling hundreds of megawatts in each resource area. Forecast errors generally decrease with larger numbers of projects. For example, for a sample of eight projects in CREZ 1, the MAD for next-day forecasts is 14.1%.

We did not account for potential improvements in wind forecasts. Significant improvements are possible, particularly with the advent of new remote sensing platforms (including satellites) that can provide more precise and high-resolution weather data for forecasting models.

3.4 One-Minute Plant Output

Figure 9 presents a typical one-minute sample of simulated plant output data for a single site overlaid on the simulated hourly data for the same site. The sample shows the wide deviations that can occur within an hour due to the passage of weather fronts and turbulent fluctuations in wind speed. Figure 10 shows the same extracted from actual data for an existing wind project.

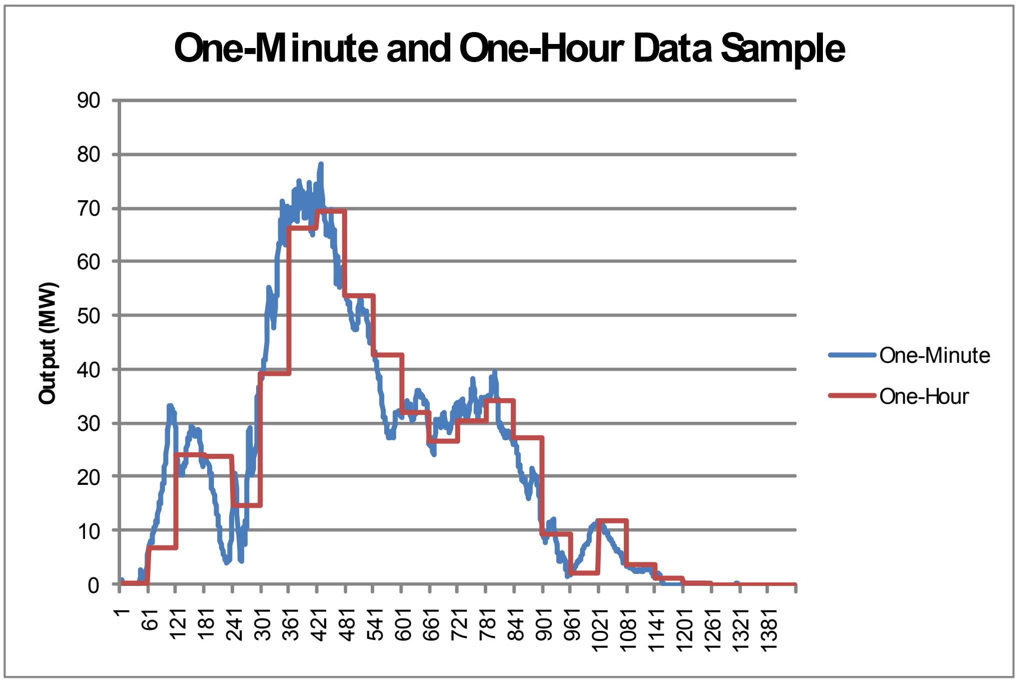

Figure 9. Sample of one-minute data for a single wind project site, overlaid on the corresponding one-hour data, for a 24-hour period beginning 6 PM on October 13, 2005.

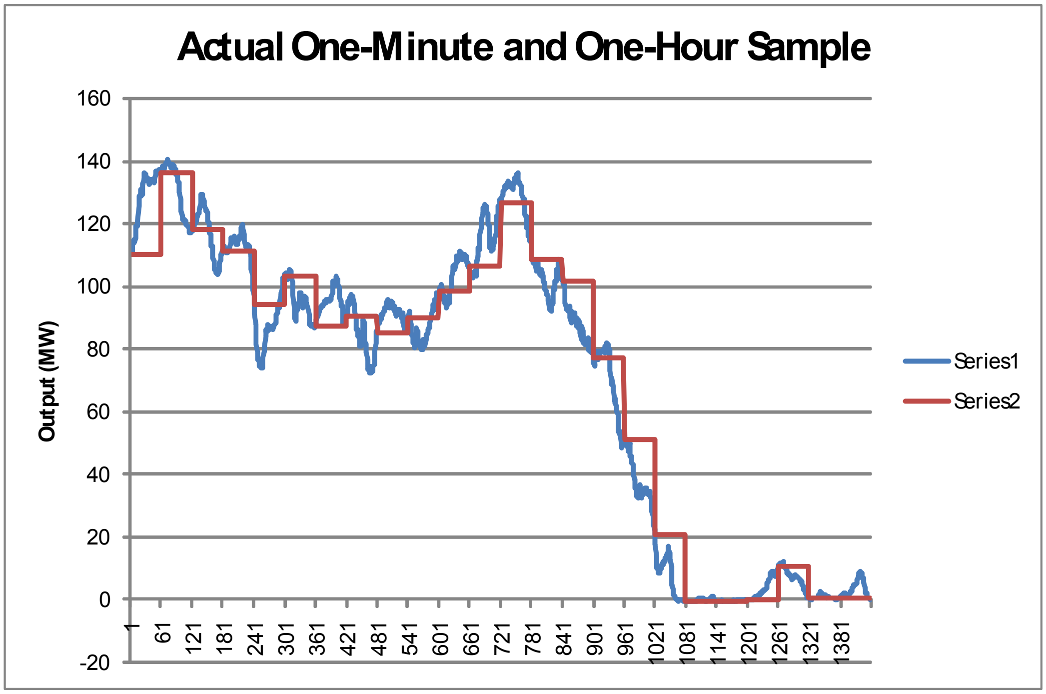

Figure 10. Sample of one-minute data for a single wind project site, overlaid on the corresponding one-hour data, for a 24-hour period beginning 6 PM on August 13, 2005.

Figure 11 compares the distribution of step changes of one-minute plant output for an existing project in Texas and for the simulated data for the same location. As with the one-hour step changes, the distributions are superficially very similar. A closer examination shows that the actual plant output rose or dropped in one minute by amounts greater than 5% of the rated capacity of the project much more often than a normal distribution of changes would allow.[10] In the largest such change at this project, the output increased from zero to 80.5 MW in one minute. Almost certainly this indicates the restoration of the grid connection after an outage or curtailment rather than a surge of production caused by a project-wide wind gust. Analysis of the output data suggests that almost one-minute step changes greater than 5% of rated capacity are not caused by wind fluctuations but by some other factor, such as strings of turbines going on or off line. Such events were therefore excluded from the training sample in creating the one-minute wind output data, as described in section 2.3.

[10] At this project, the standard deviation of step changes, as a fraction of rated capacity, is about 0.9%. A 5% change is therefore more than 5 standard deviations. The probability of such an event occurring by chance, assuming a normal distribution of changes, is about 1×10^{-7}, implying one such event in 20 years. Approximately 1300 such changes were actually observed at this project in 2005.

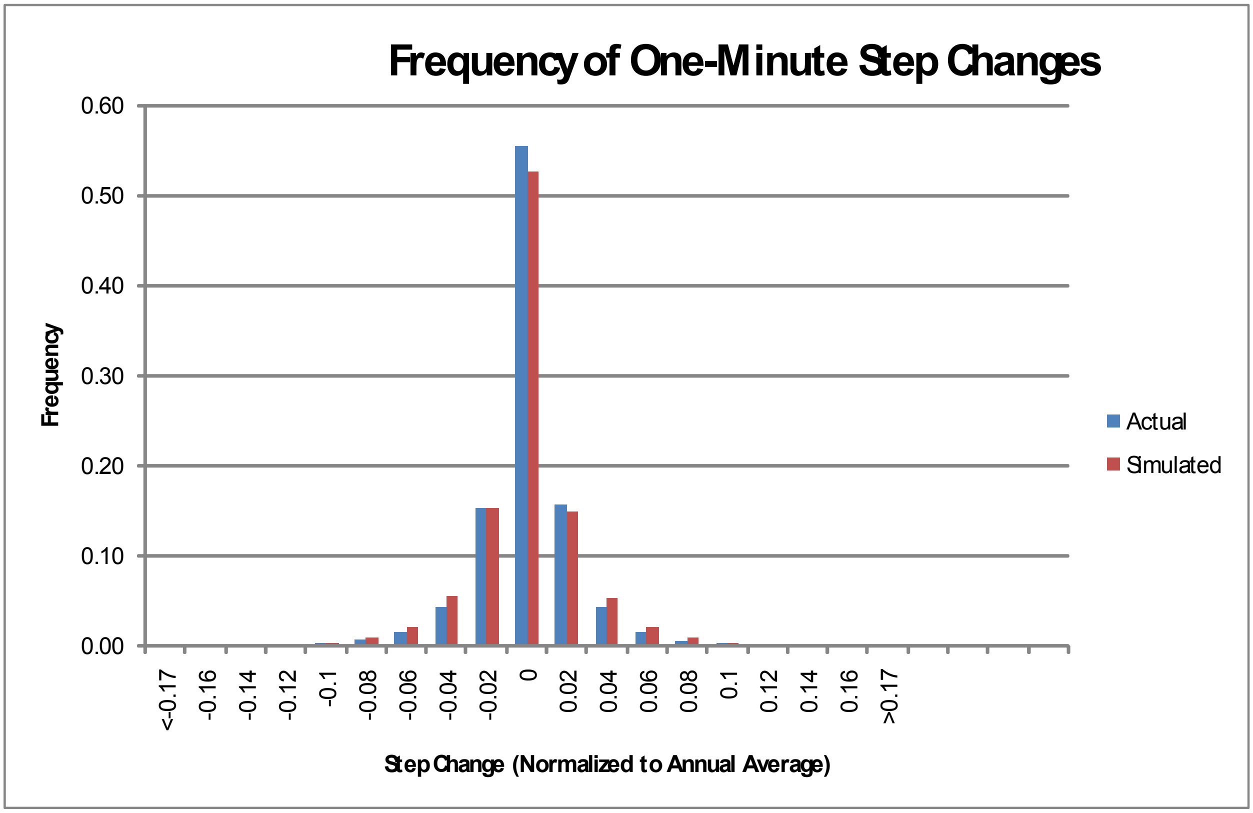

Figure 11. Frequency distribution of step changes of simulated and actual one-minute output for a single wind project.

4 CONCLUSIONS

AWS Truewind employed its MesoMap system and a variety of other tools to produce data files characterizing the hourly output of up to 4000 MW of capacity in each of 25 CREZs for two continuous historical years. The simulated output values were adjusted to match observed diurnal patterns using tall tower data obtained by AWS Truewind from various parts of the state. AWS Truewind also simulated next-day and four-hour forecasts, as well as one-minute plant output data, for the same sites and time period. The results have been verified through comparisons with one-minute data from existing wind projects as well as other sources of information. In general, the seasonal and diurnal patterns, rates of change, and distributions of step changes match the behavior of existing wind projects very well, and the accuracy of the simulated forecasts is consistent with actual forecasts in California and Texas. The data therefore appear to provide a sound basis for the study of ancillary service requirements for wind energy projects in Texas.

APPENDIX C – SUPPLEMENTAL VARIABILITY PLOTS

C.1 Time Series Plots and Average Daily Profiles

Load-5000 MW of Wind Capacity (Study Year)
Time Series Plots

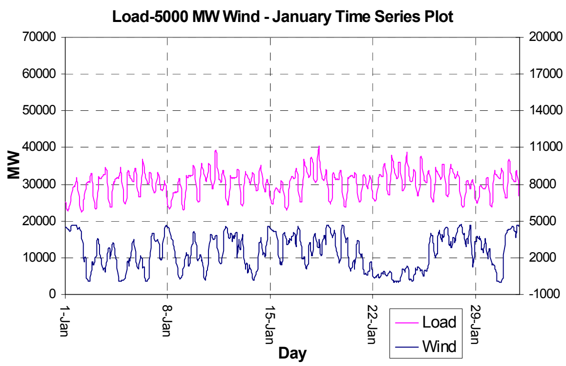

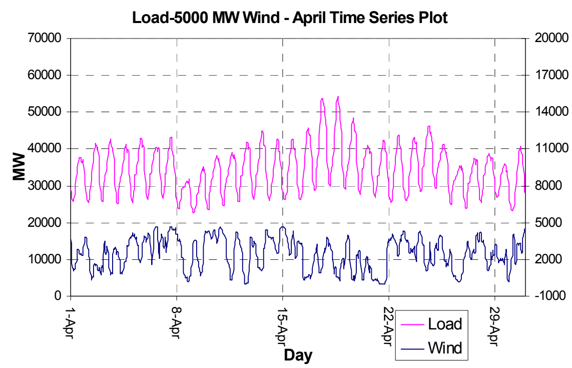

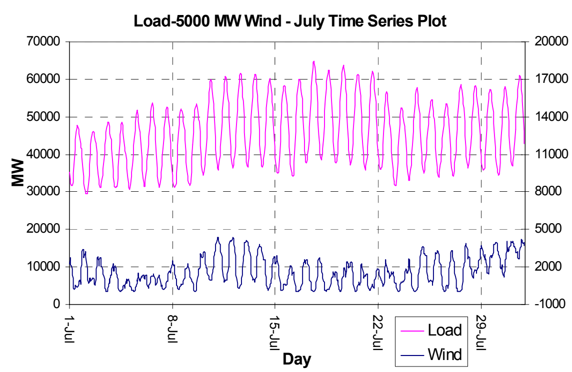

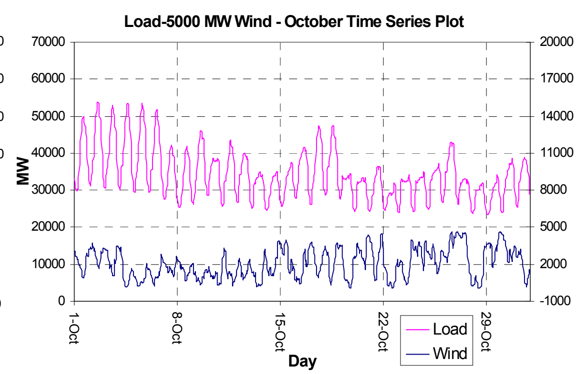

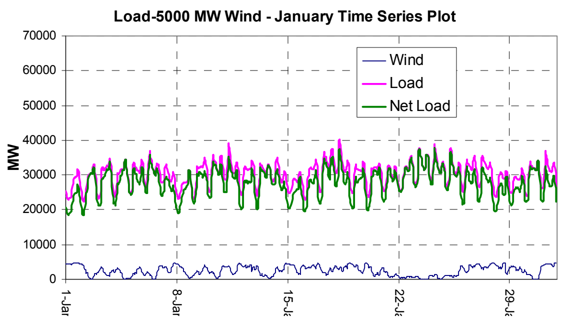

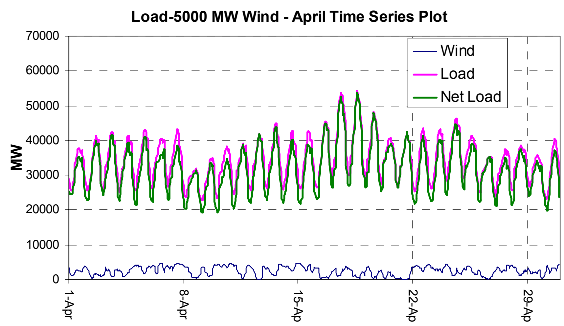

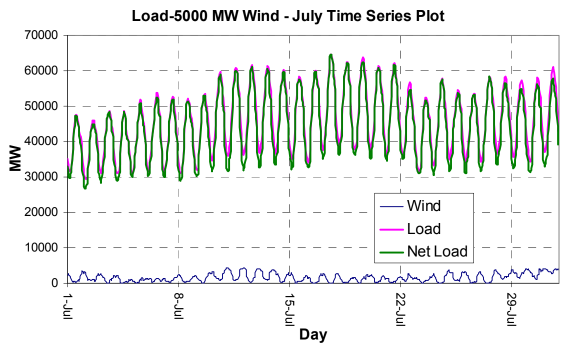

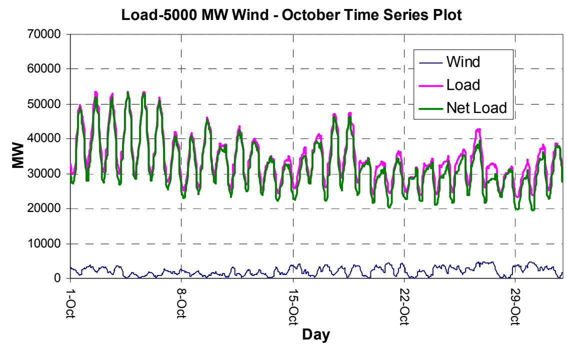

Average Daily Profiles

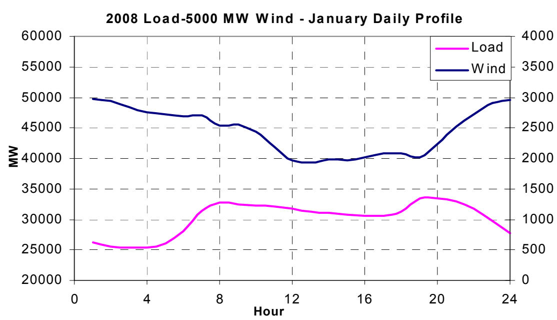

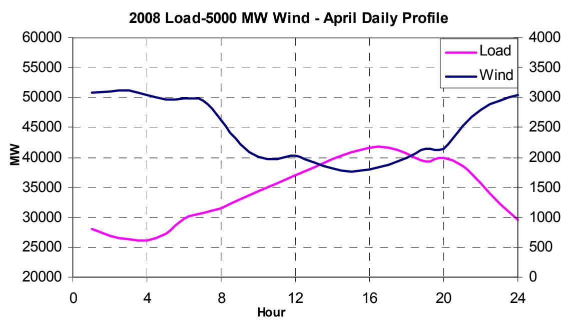

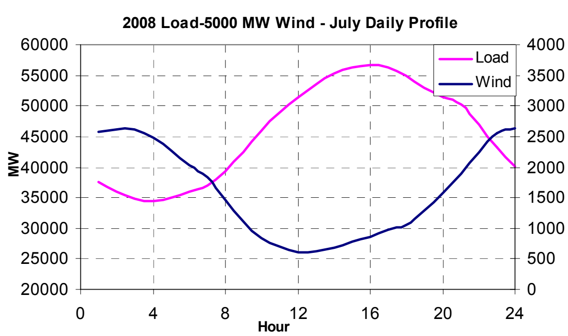

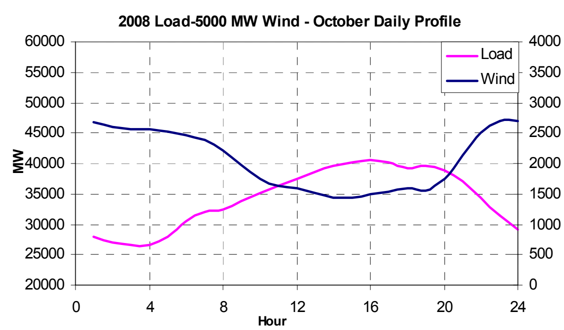

Load-10,000 MW of Wind Capacity, Case 1 (Study Year) Time Series Plots

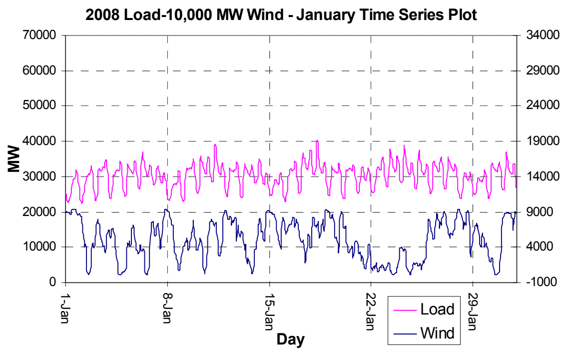

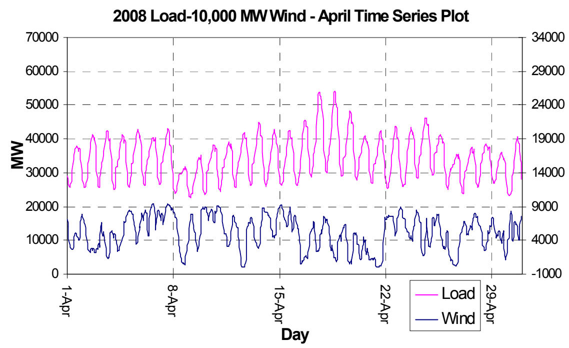

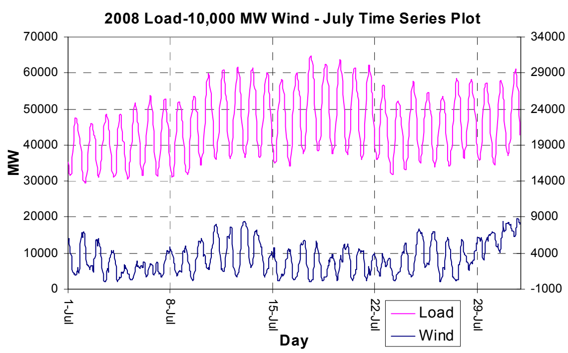

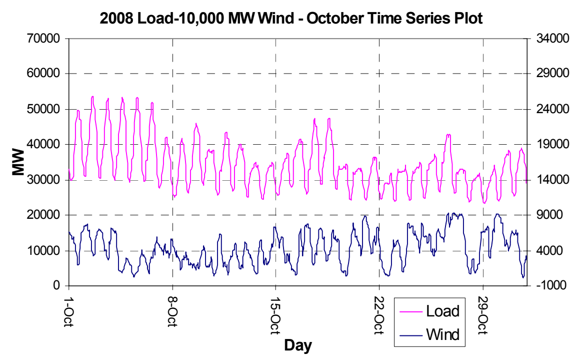

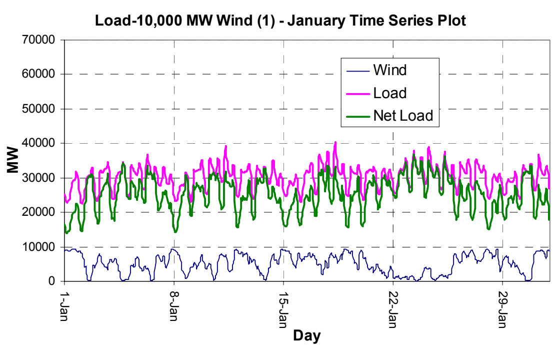

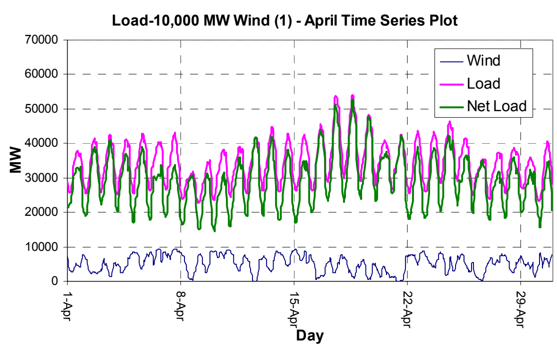

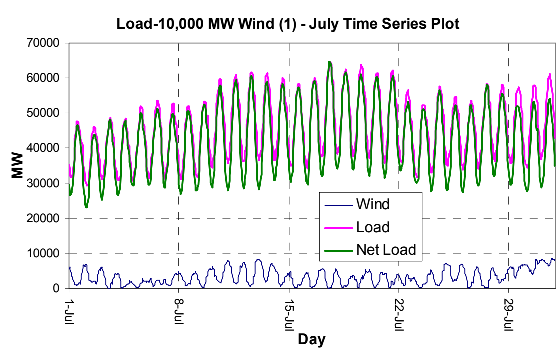

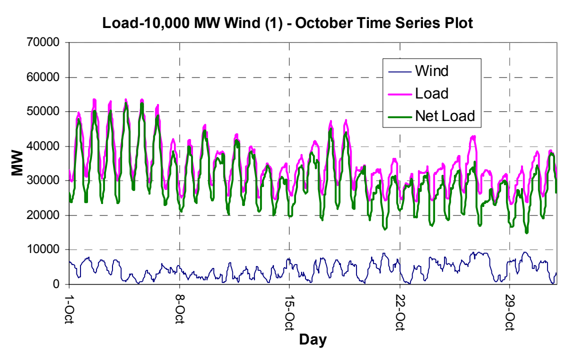

Average Daily Profiles

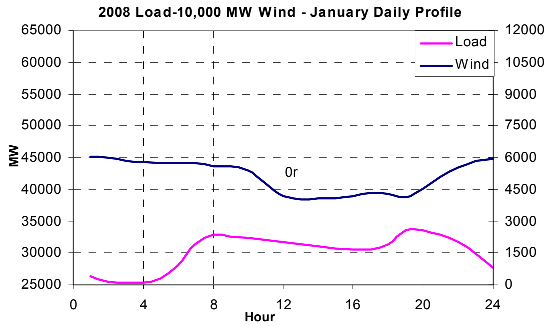

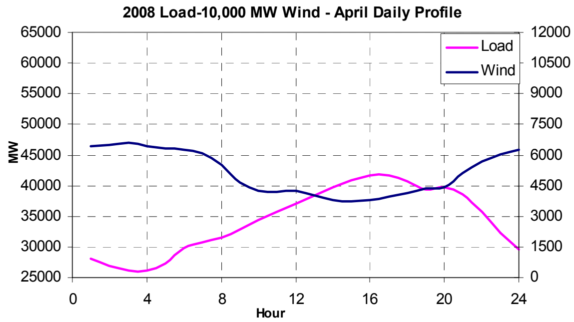

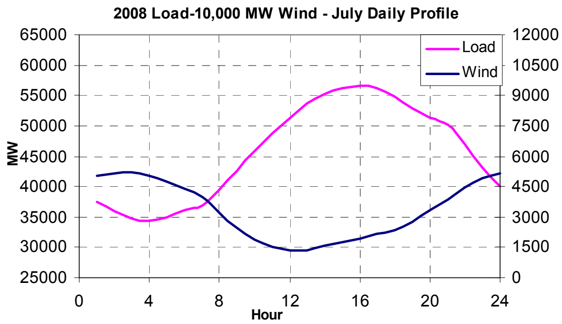

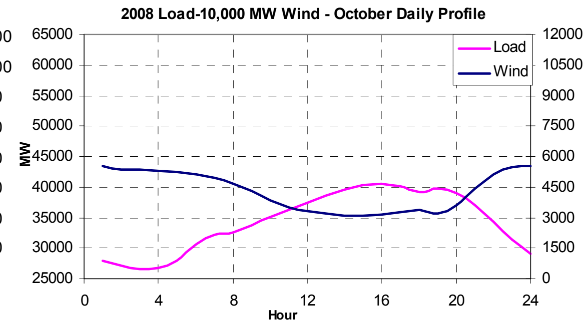

Load-10,000 MW of Wind Capacity, Case 2 (Study Year) Time Series Plots

2008 Load-10,000 MW Wind (2) - January Time Series Plot

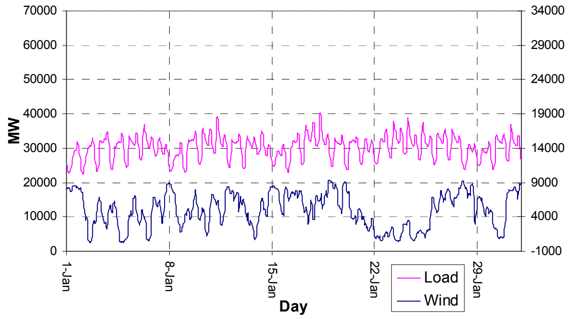

2008 Load-10,000 MW Wind (2) - April Time Series Plot

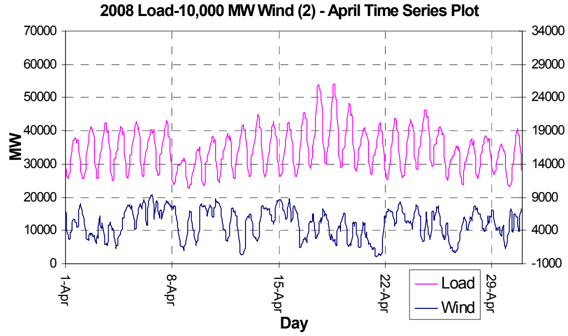

2008 Load-10,000 MW Wind (2) - July Time Series Plot

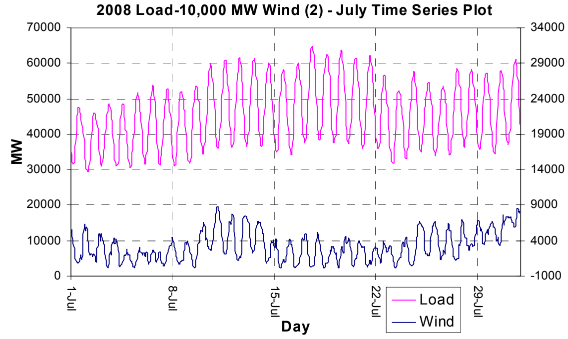

2008 Load-10,000 MW Wind (2) - October Time Series Plot

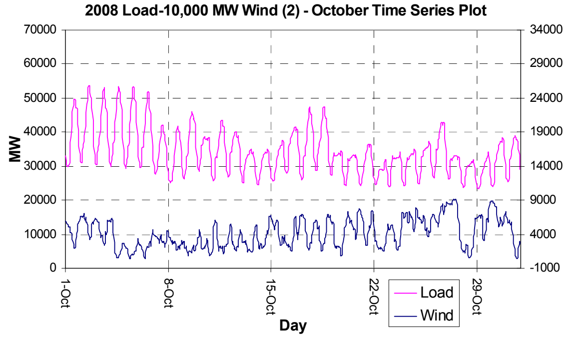

Load-10,000 MW Wind (2) - January Time Series Plot

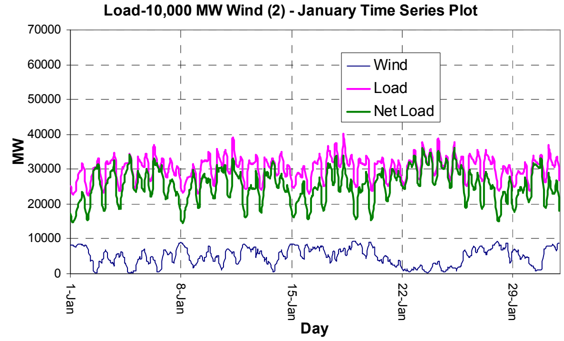

Load-10,000 MW Wind (2) - April Time Series Plot

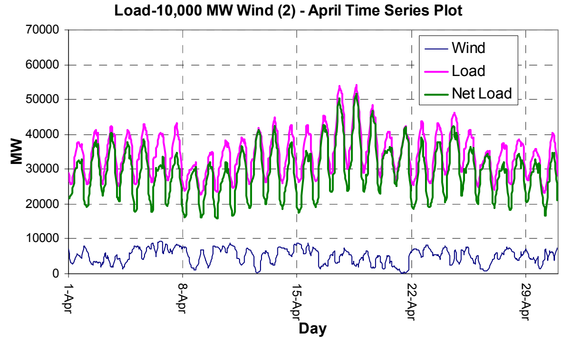

Load-10,000 MW Wind (2) - July Time Series Plot

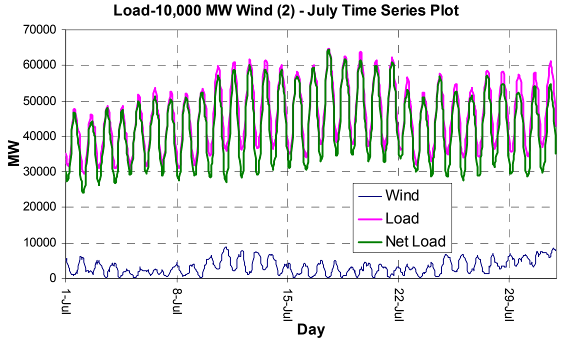

Load-10,000 MW Wind (2) - October Time Series Plot

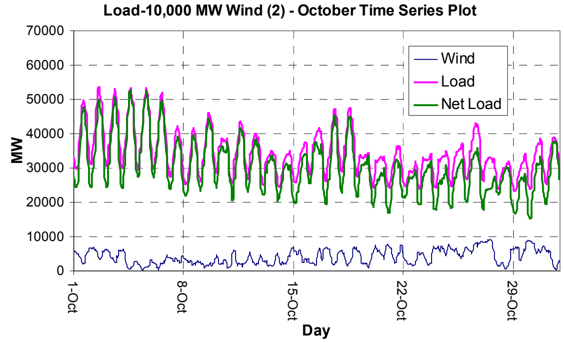

Average Daily Profiles

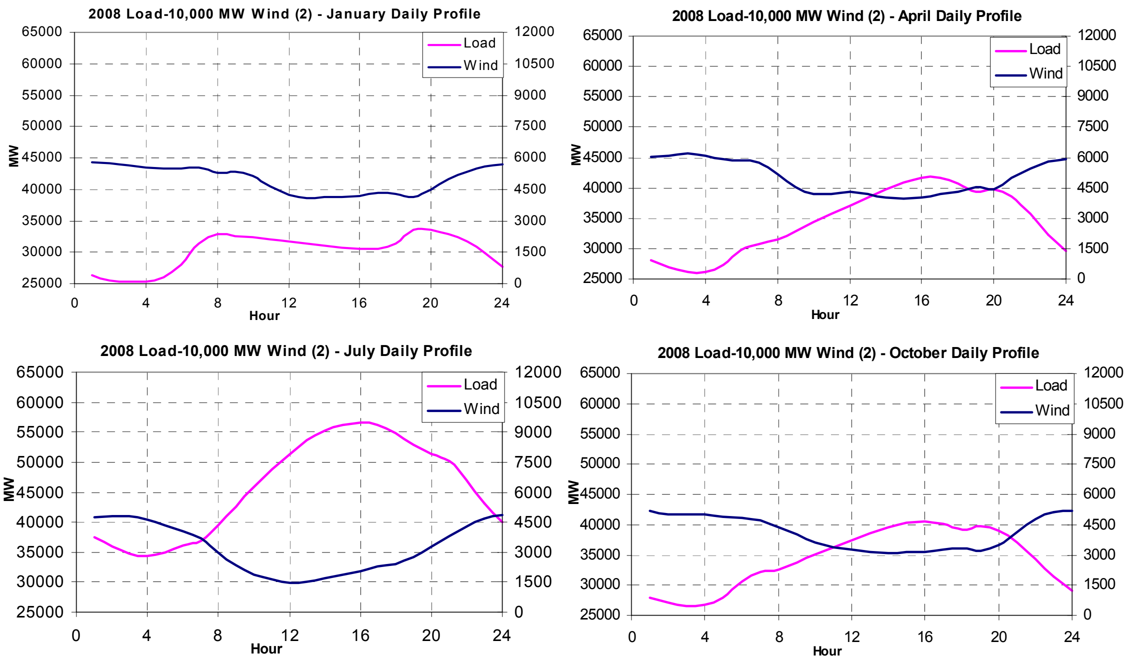

Load-15,000 MW of Wind Capacity, (Study Year)
Time Series Plots

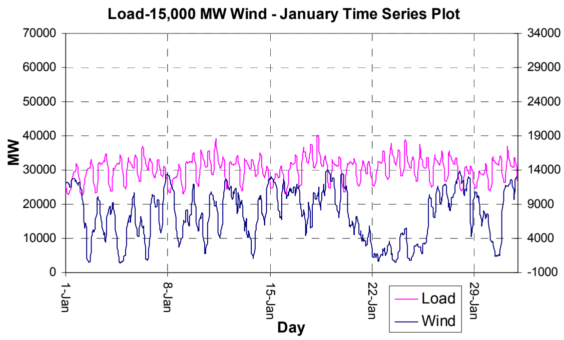

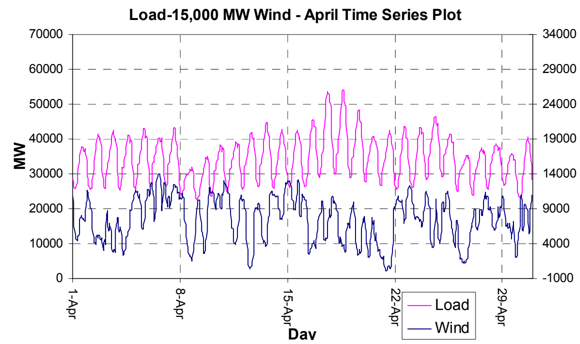

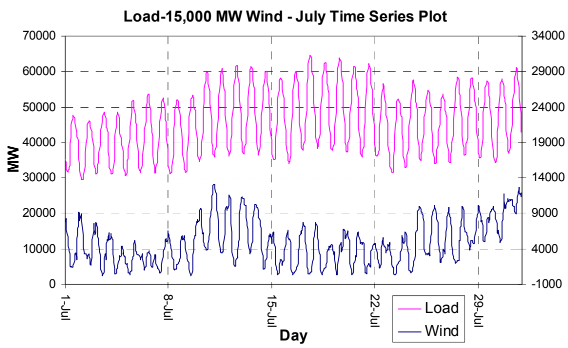

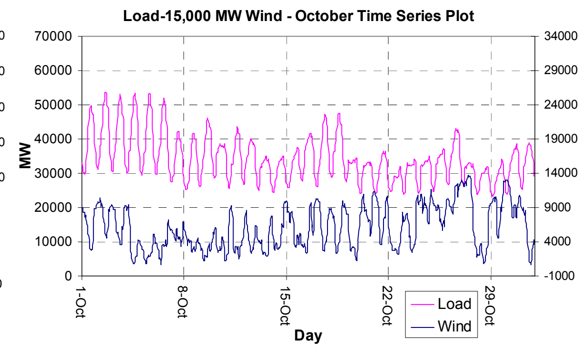

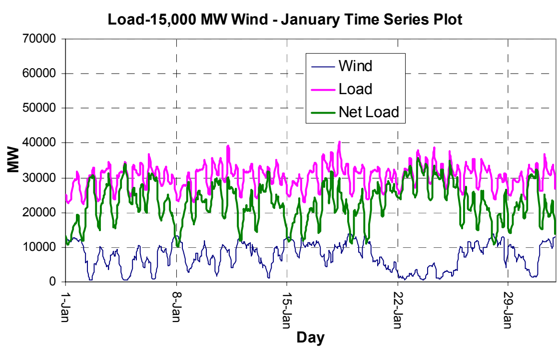

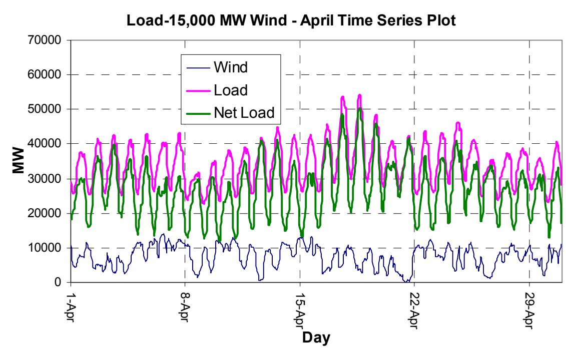

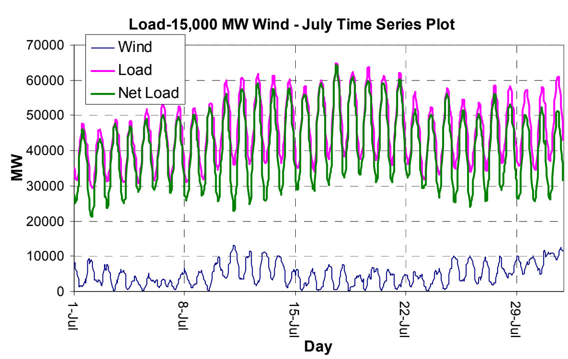

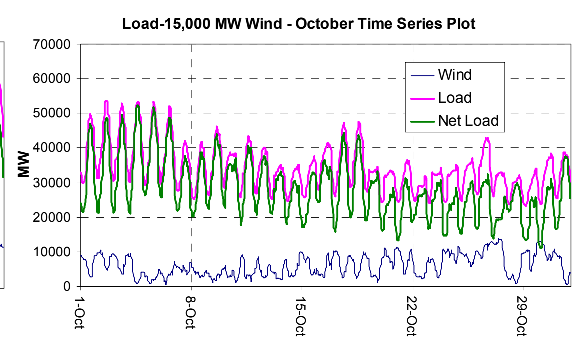

Average Daily Profiles

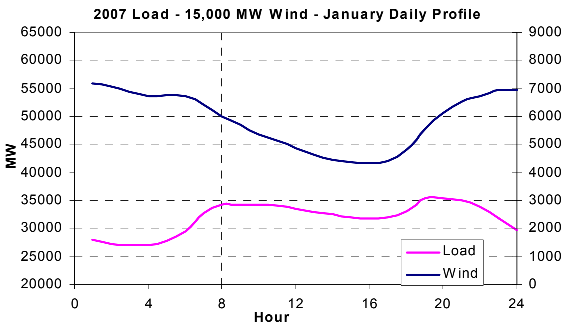

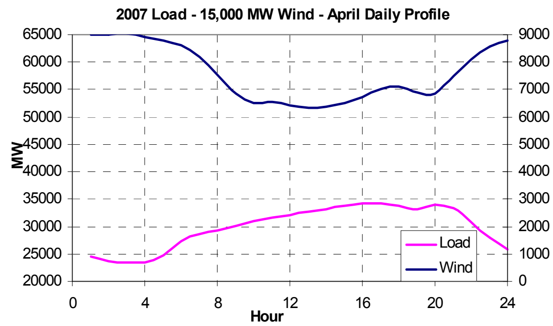

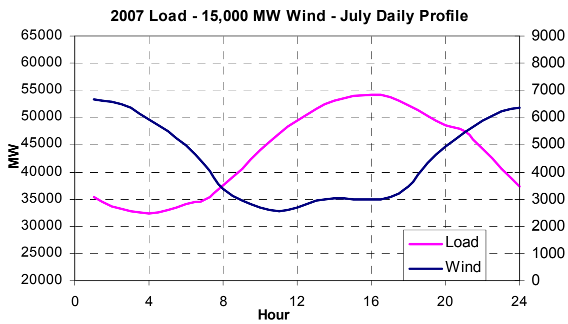

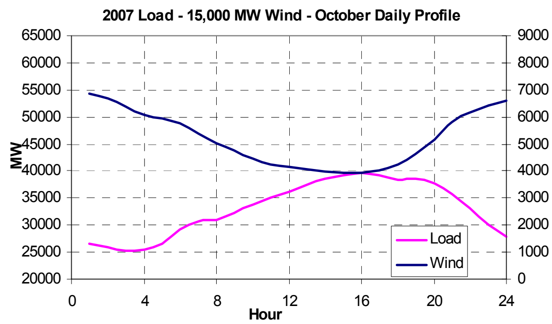

Load-5000 MW of Wind Capacity (Previous Year)

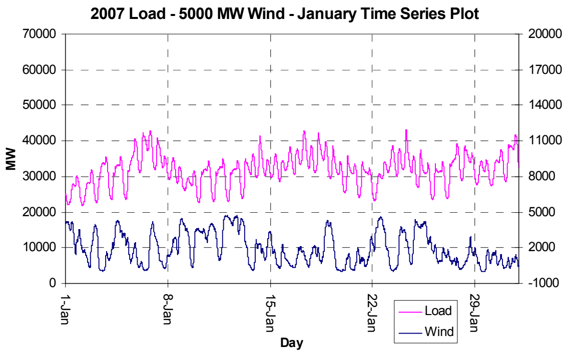

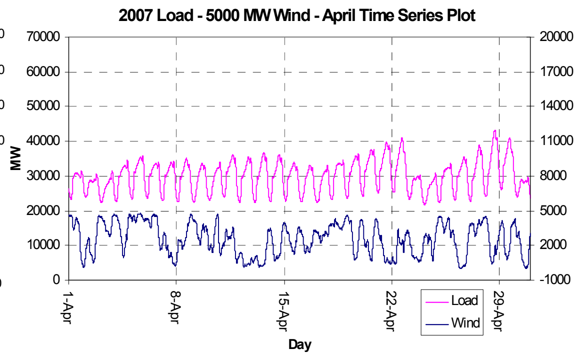

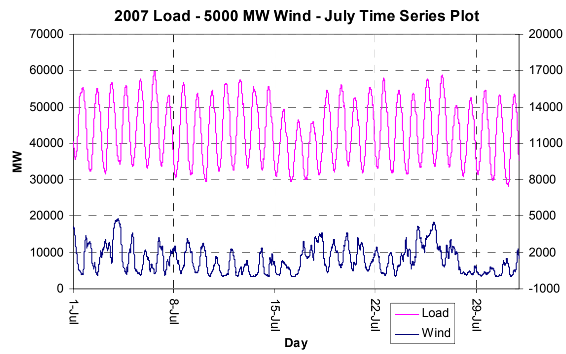

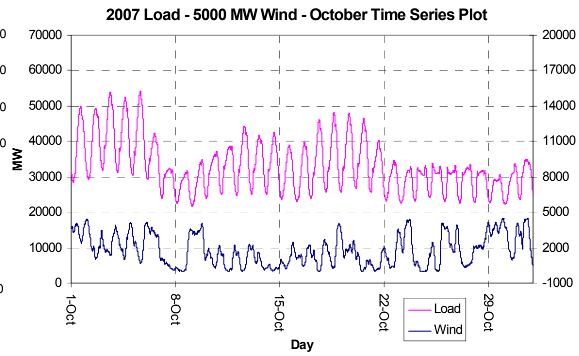

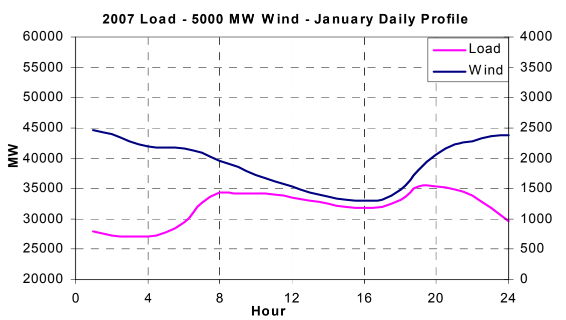

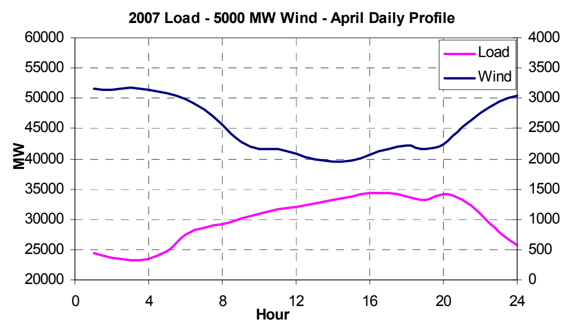

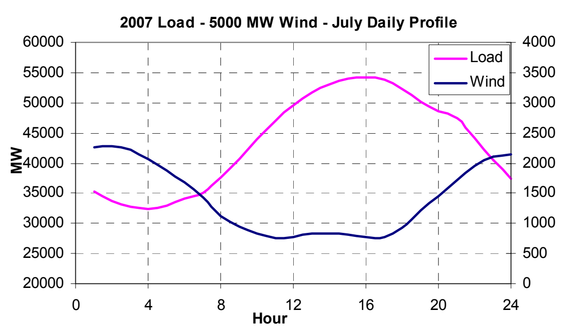

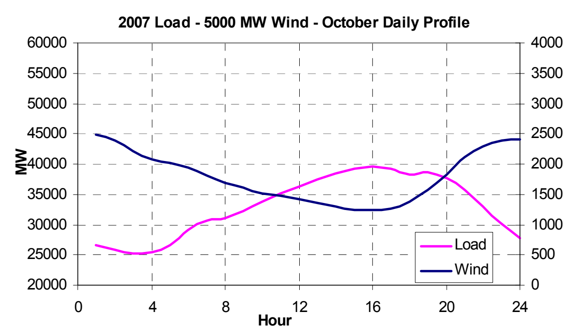

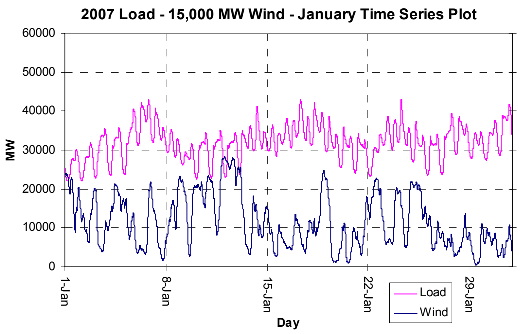
2007 Load - 15,000 MW Wind - January Time Series Plot
MW
Day
Load
Wind

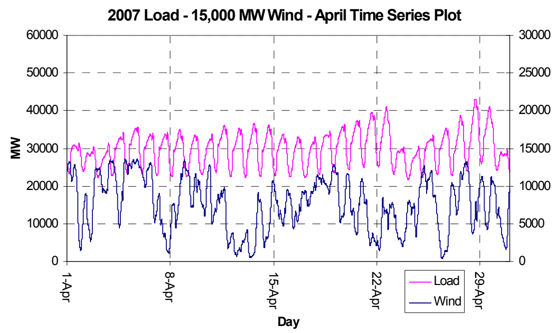
2007 Load - 15,000 MW Wind - April Time Series Plot
MW
Day
Load
Wind

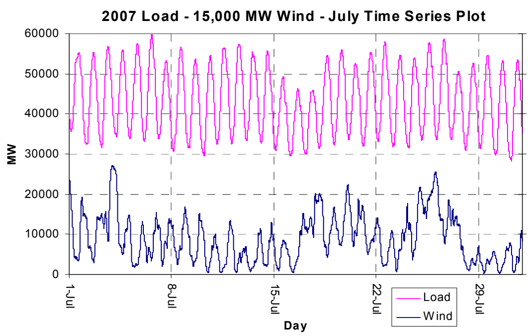
2007 Load - 15,000 MW Wind - July Time Series Plot
MW
Day
Load
Wind

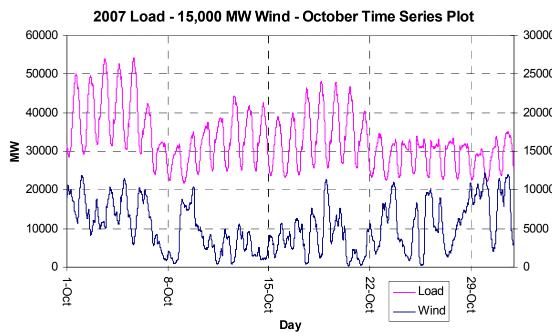
2007 Load - 15,000 MW Wind - October Time Series Plot
MW
Day
Load
Wind

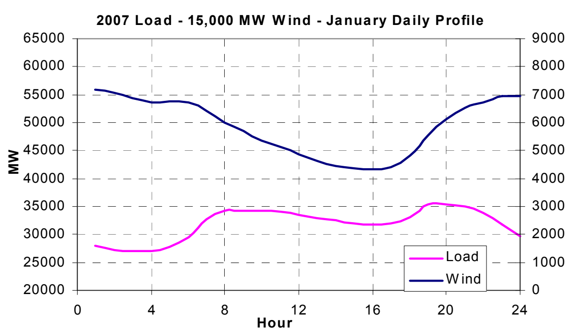
2007 Load - 15,000 MW Wind - January Daily Profile
MW
Hour
Load
Wind

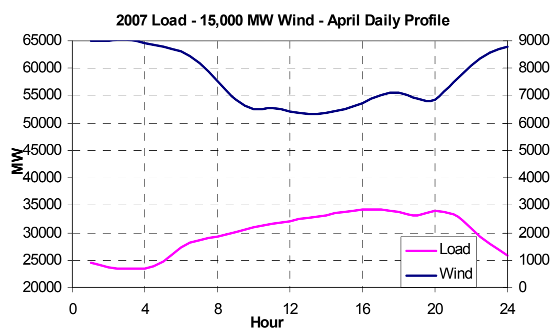
2007 Load - 15,000 MW Wind - April Daily Profile
MW
Hour
Load
Wind

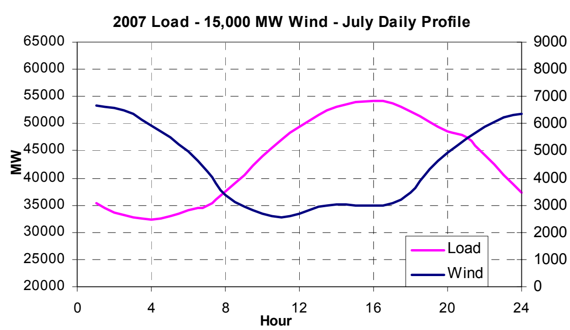
2007 Load - 15,000 MW Wind - July Daily Profile
MW
Hour
Load
Wind

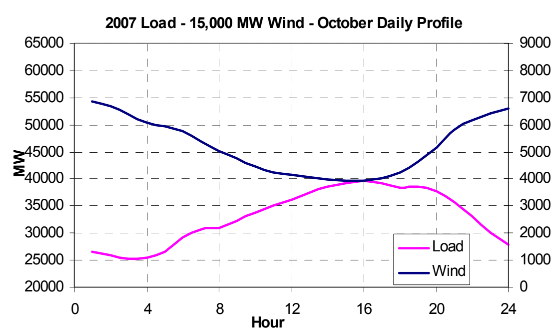
2007 Load - 15,000 MW Wind - October Daily Profile
MW
Hour
Load
Wind

C.2 Frequency Distribution of Deltas

One-Minute Load-Wind Variability – Summary

From Study Year Data

Case	Penetration	$\sigma_{\text{Load-Wind}}$ Delta **(MW)**	Max. Negative Load-Wind Delta **(MW)**	Max. Positive Load-Wind Delta **(MW)**	No. Deltas > 2.5 (load)σ (–/+)	σ % Increase with Wind
Base Case: Study Year Load w/ no Wind	0%	43.22	-513.7	491.6	4696 / 3805	--
Study Year Load w/ 5000 MW Wind	7.6%	45.56	-526.6	507.2	6181 / 4807	5.4%
Study Year Load w/ 10,000 MW Wind (1)	15.3%	47.74	-534.0	529.3	7635 / 6041	10.5%
Study Year Load w/ 10,000 MW Wind (2)	15.3%	47.27	-536.7	520.4	7350 / 5757	9.4%
Study Year Load w/ 15,000 MW Wind	22.9%	49.67	-552.6	538.3	9277 / 7408	14.9%

From Prev. Year Data

Case	Penetration	$\sigma_{\text{Load-Wind}}$ Delta **(MW)**	Max. Negative Load-Wind Delta **(MW)**	Max. Positive Load-Wind Delta **(MW)**	No. Deltas > 2.5 (load)σ (–/+)	σ % Increase with Wind
Base Case: Year 1 Load w/ no Wind	0%	42.81	-519.4	518.3	4511 / 3976	--
Year 1 Load w/ 5000 MW Wind	8%	45.00	-526.2	541.5	5949 / 4772	5.1%
Year 1 Load w/ 10,000 MW Wind (1)	16.0%	47.07	-527.0	562.4	7397 / 5887	10.0%
Year 1 Load w/ 10,000 MW Wind (2)	16.0%	46.60	-521.2	557.3	7071 / 5635	8.9%
Year 1 Load w/ 15,000 MW Wind	24.0%	48.81	-521.5	561.7	8924 / 7110	14.0%

One-Minute Load-Wind Variability – 5000 MW

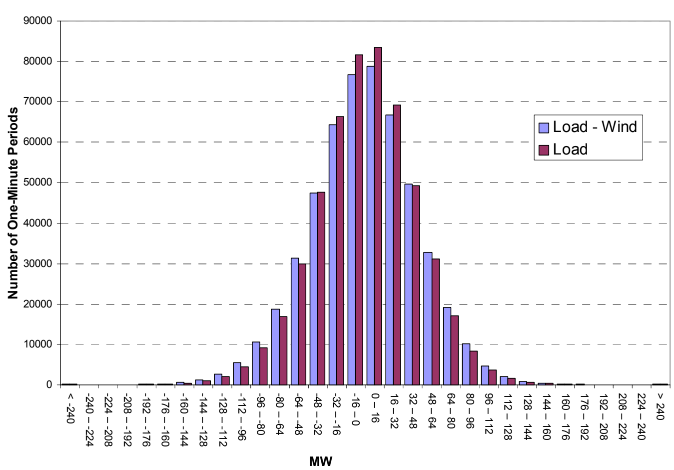

Statistical Summary

	Load-alone (MW)	**With Wind (MW)**
Mean (-/+ Deltas)	-34.0 / 33.3	-36.0 / 35.2
Sigma (Delta)	43.22	45.56
Min. Delta	-513.7	-526.6
Max. Delta	491.6	507.2

One-Minute Load-Wind Variability – 10,000 MW - 1

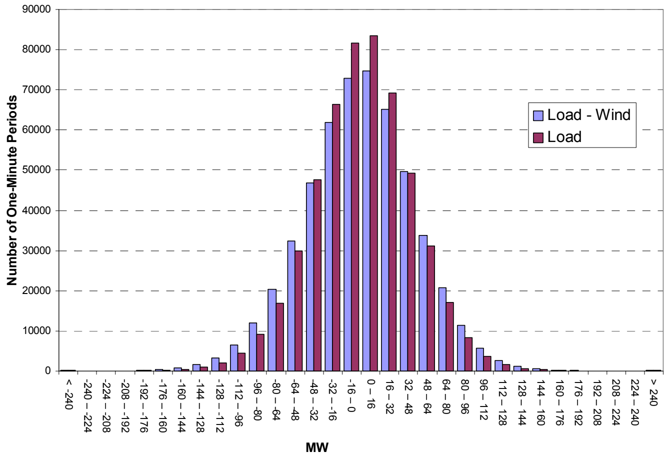

	Load-alone (MW)	With Wind (MW)
Mean (-/+ Deltas)	-34.0 / 33.3	
Sigma (Delta)	43.22	47.74
Min. Delta	-513.7	-534.0
Max. Delta	491.6	529.3

One-Minute Load-Wind Variability – 10,000 MW - 2

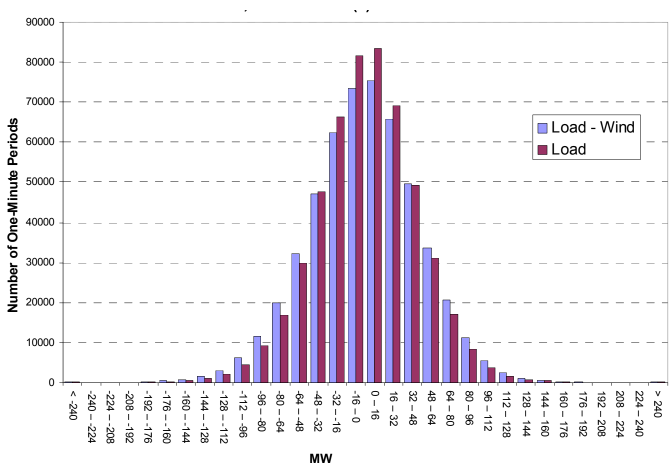

	Load-alone (MW)	With Wind (MW)
Mean (-/+ Deltas)	-34.0 / 33.3	
Sigma (Delta)	43.22	47.27
Min. Delta	-513.7	-536.7
Max. Delta	491.6	520.4

One-Minute Load-Wind Variability – 15,000 MW

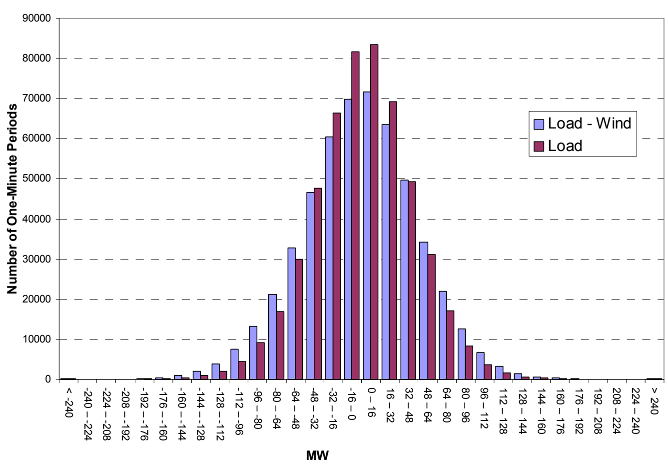

	Load-alone (MW)	With Wind (MW)
Mean (-/+ Deltas)	-34.0 / 33.3	
Sigma (Delta)	43.22	49.67
Min. Delta	-513.7	-552.6
Max. Delta	491.6	538.3

Five-Minute Load-Wind Variability – Summary

From Study Year Data

Case	Penetration	$\sigma_{Load\text{-}Wind}$ (MW)	Max. Negative Load-Wind Delta (MW)	Max. Positive Load-Wind Delta (MW)	No. Deltas > 2.5 (load)σ (−/+)	σ % Increase with Wind
Base Case: Study Year Load w/ no Wind	0%	167.39	-881.2	958.8	621 / 787	--
Study Year Load w/ 5000 MW Wind	7.6%	177.29	-916.6	988.9	1007 / 977	5.9%
Study Year Load w/ 10,000 MW Wind (1)	15.3%	188.01	-951.1	992.1	1482 / 1368	12.3%
Study Year Load w/ 10,000 MW Wind (2)	15.3%	185.17	-938.3	1002.4	1353 / 1273	10.6%
Study Year Load w/ 15,000 MW Wind	22.9%	197.12	-948.2	1022.2	1970 / 1856	17.8%

From Prev. Year Data

Case	Penetration	$\sigma_{Load\text{-}Wind}$ (MW)	Max. Negative Load-Wind Delta (MW)	Max. Positive Load-Wind Delta (MW)	No. Deltas > 2.5 (load)σ (−/+)	σ % Increase with Wind
Base Case: Year 1 Load w/ no Wind	0%	165.61	-900.9	858.3	644 / 860	--
Year 1 Load w/ 5000 MW Wind	8%	174.68	-935.6	876.2	1068 / 1025	5.5%
Year 1 Load w/ 10,000 MW Wind (1)	16.0%	184.84	-987.3	941.2	1515 / 1413	11.6%
Year 1 Load w/ 10,000 MW Wind (2)	16.0%	182.05	-963.5	878.3	1409 / 1286	9.9%
Year 1 Load w/ 15,000 MW Wind	24.0%	193.04	-958.5	991.9	1993 / 1769	16.6%

Five -Minute Load-Wind Variability – 5000 MW

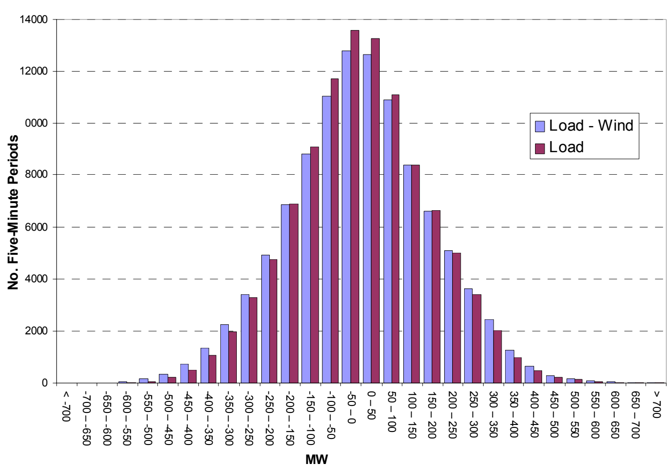

	Load-alone (MW)	With Wind (MW)
Mean (-/+ Deltas)		
Sigma (Delta)	167.39	177.29
Min. Delta	-881.2	-916.6
Max. Delta	958.8	988.9

Five -Minute Load-Wind Variability – 10,000 MW (1)

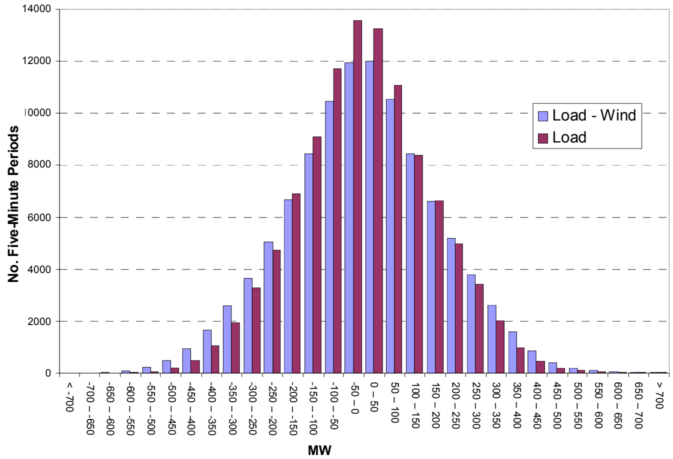

	Load-alone (MW)	With Wind (MW)
Mean (-/+ Deltas)		
Sigma (Delta)	167.39	188.01
Min. Delta	-881.2	-951.1
Max. Delta	958.8	992.1

Five -Minute Load-Wind Variability – 10,000 MW (2)

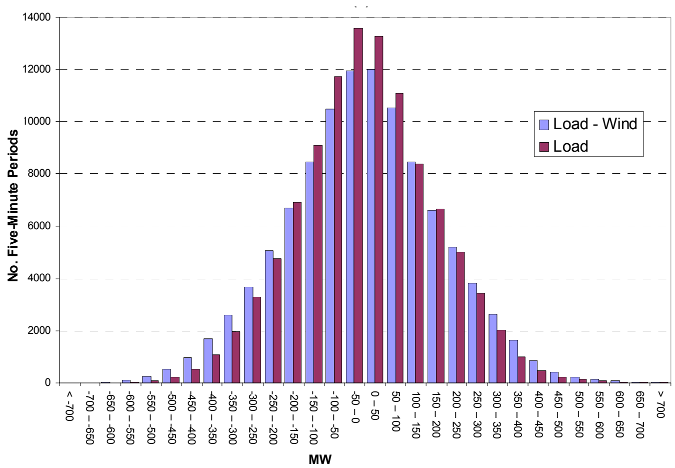

	Load-alone (MW)	With Wind (MW)
Mean (-/+ Deltas)		
Sigma (Delta)	167.39	185.17
Min. Delta	-881.2	-938.3
Max. Delta	958.8	1002.4

Five -Minute Load-Wind Variability – 15,000 MW

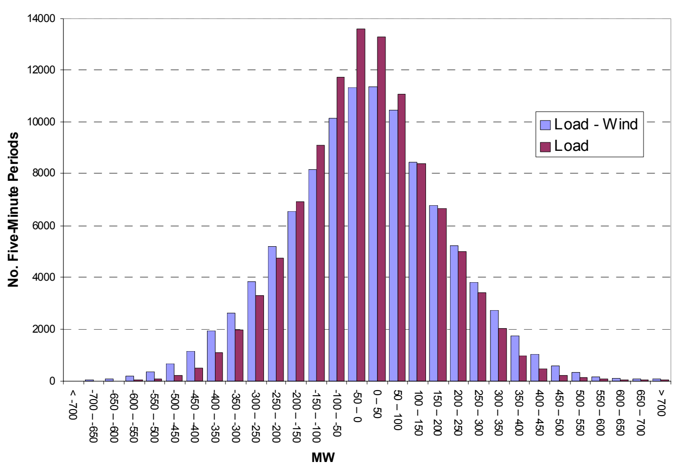

	Load-alone (MW)	With Wind (MW)
Mean (-/+ Deltas)		
Sigma (Delta)	167.39	197.12
Min. Delta	-881.2	-948.2
Max. Delta	958.8	1022.2

Fifteen-Minute Load-Wind Variability – Summary

From Study Year Data

Case	Penetration	$\sigma_{Load-Wind}$ Delta **(MW)**	Max. Negative Load-Wind Delta **(MW)**	Max. Positive Load-Wind Delta **(MW)**	No. Deltas > 2.5 (load)σ (–/+)	σ % Increase with Wind
Base Case: Study Year Load w/ no Wind	0%	467.06	-1587.5	1863.2	161 / 238	--
Study Year Load w/ 5000 MW Wind	7.6%	496.09	-1809.3	1943.7	316 / 306	6.2%
Study Year Load w/ 10,000 MW Wind (1)	15.3%	528.46	-1906.8	2143.5	476 / 456	13.1%
Study Year Load w/ 10,000 MW Wind (2)	15.3%	519.56	-1880.5	2087.9	444 / 414	11.2%
Study Year Load w/ 15,000 MW Wind	22.9%	555.50	-2036.7	2433.5	679 / 645	18.9%

From Prev. Year Data

Case	Penetration	$\sigma_{Load-Wind}$ Delta **(MW)**	Max. Negative Load-Wind Delta **(MW)**	Max. Positive Load-Wind Delta **(MW)**	No. Deltas > 2.5 (load)σ (–/+)	σ % Increase with Wind
Base Case: Year 1 Load w/ no Wind	0%	463.62	-1555.7	1664.0	161 / 258	--
Year 1 Load w/ 5000 MW Wind	8%	489.95	-1686.2	1777.5	342 / 314	5.7%
Year 1 Load w/ 10,000 MW Wind (1)	16.0%	520.59	-1740.8	1979.3	510 / 429	12.3%
Year 1 Load w/ 10,000 MW Wind (2)	16.0%	511.82	-1732.3	1855.0	471 / 398	10.4%
Year 1 Load w/ 15,000 MW Wind	24.0%	544.73	-1876.0	2158.9	712 / 597	17.5%

Fifteen -Minute Load-Wind Variability – 5000 MW

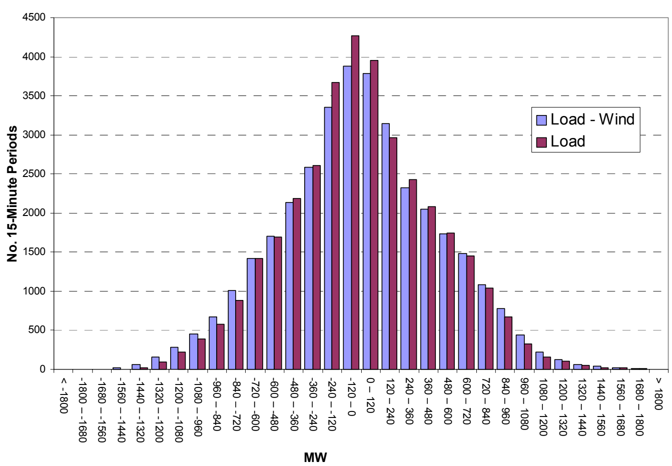

	Load-alone (MW)	**With Wind (MW)**
Mean (-/+ Deltas)		
Sigma (Delta)	467.06	496.09
Min. Delta	-1587.5	-1809.3
Max. Delta	1863.2	1943.7

Fifteen -Minute Load-Wind Variability – 10,000 MW (1)

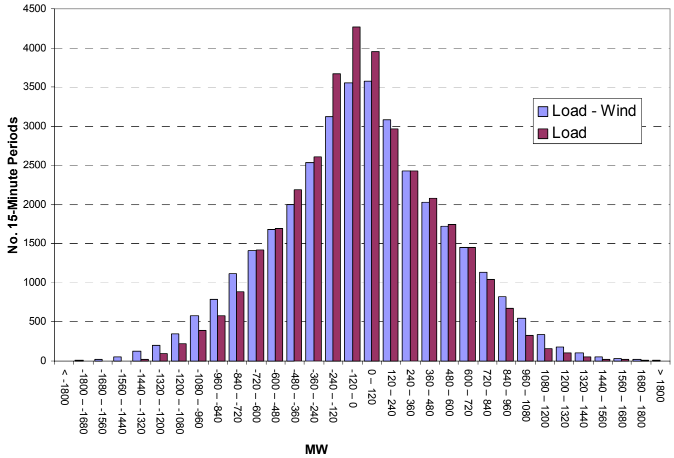

	Load-alone (MW)	With Wind (MW)
Mean (-/+ Deltas)		
Sigma (Delta)	467.06	528.46
Min. Delta	-1587.5	-1906.8
Max. Delta	1863.2	2143.5

Fifteen -Minute Load-Wind Variability – 10,000 MW (2)

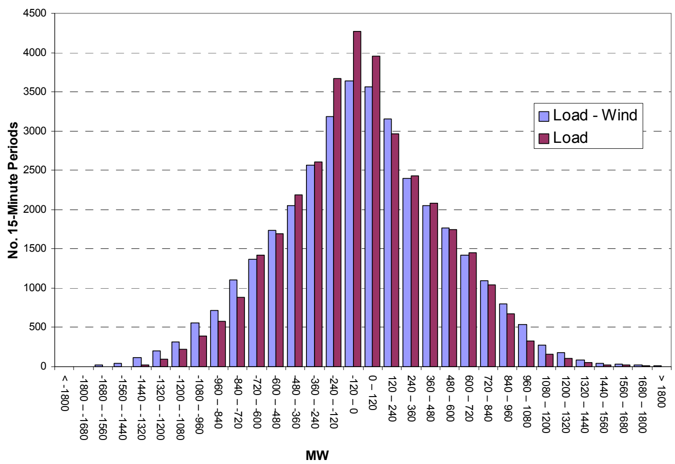

	Load-alone (MW)	With Wind (MW)
Mean (-/+ Deltas)		
Sigma (Delta)	467.06	519.56
Min. Delta	-1587.5	-1880.5
Max. Delta	1863.2	2087.9

Fifteen -Minute Load-Wind Variability – 15,000 MW

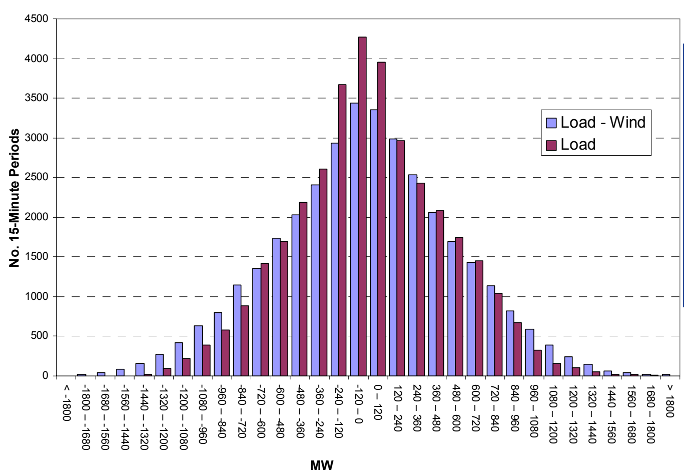

	Load-alone (MW)	With Wind (MW)
Mean (-/+ Deltas)		
Sigma (Delta)	467.06	555.50
Min. Delta	-1587.5	-2036.7
Max. Delta	1863.2	2433.5

Thirty-Minute Load-Wind Variability – Summary

From Study Year Data

Case	Penetration	$\sigma_{Load\text{-}Wind}$ Delta **(MW)**	Max. Negative Load-Wind Delta **(MW)**	Max. Positive Load-Wind Delta **(MW)**	No. Deltas > 2.5 (load)σ (–/+)	σ % Increase with Wind
Base Case: Study Year Load w/ no Wind	0%	911	-2756	3101	71 / 80	--
Study Year Load w/ 5000 MW Wind	7.6%	967	-3138	3271	173 / 122	6.1%
Study Year Load w/ 10,000 MW Wind (1)	15.3%	1031	-3360	3928	249 / 209	13.1%
Study Year Load w/ 10,000 MW Wind (2)	15.3%	1013	-3300	3805	226 / 180	11.2%
Study Year Load w/ 15,000 MW Wind	22.9%	1083	-3612	4502	337 / 305	18.9%

C.3 Cumulative Duration Plots

Wind Generation Instantaneous Penetration

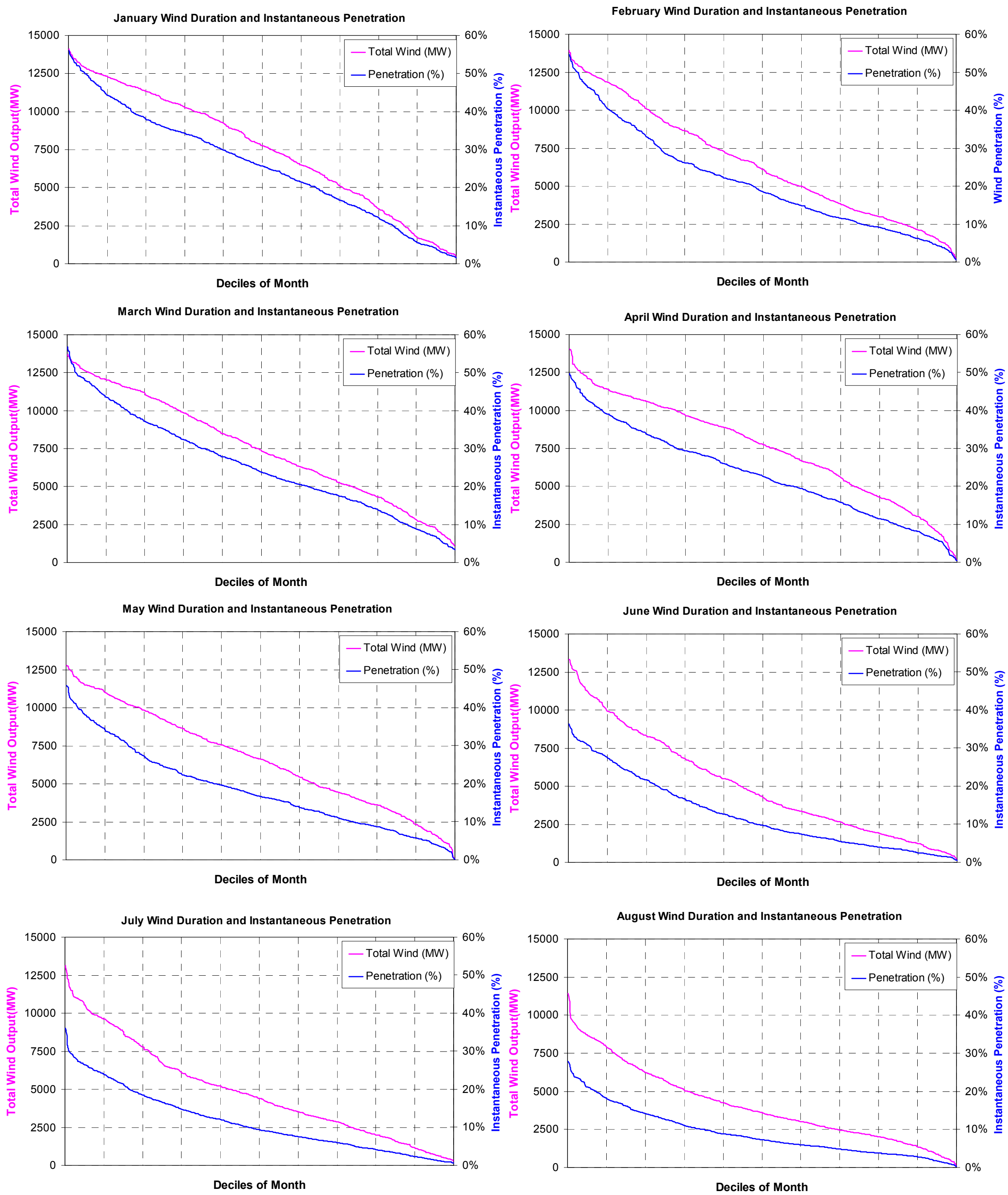

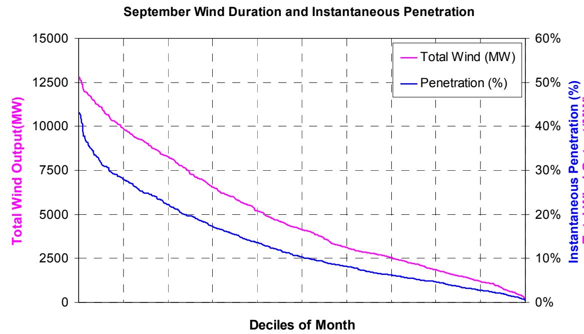
September Wind Duration and Instantaneous Penetration
Total Wind (MW)
Penetration (%)
Total Wind Output(MW)
Instantaneous Penetration (%)
Deciles of Month
15000
12500
10000
7500
5000
2500
0
60%
50%
40%
30%
20%
10%
0%

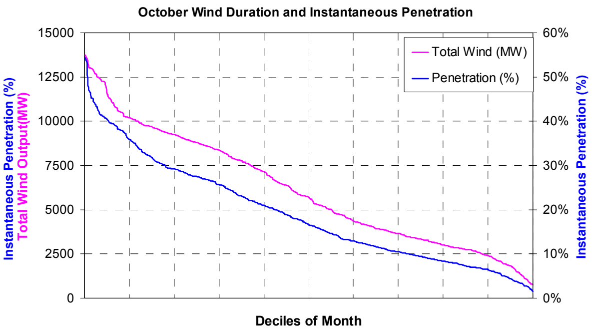
October Wind Duration and Instantaneous Penetration
Total Wind (MW)
Penetration (%)
Total Wind Output(MW)
Instantaneous Penetration (%)
Deciles of Month
15000
12500
10000
7500
5000
2500
0
60%
50%
40%
30%
20%
10%
0%

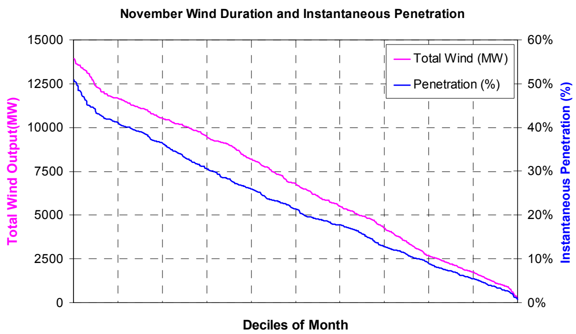
November Wind Duration and Instantaneous Penetration
Total Wind (MW)
Penetration (%)
Total Wind Output(MW)
Instantaneous Penetration (%)
Deciles of Month
15000
12500
10000
7500
5000
2500
0
60%
50%
40%
30%
20%
10%
0%

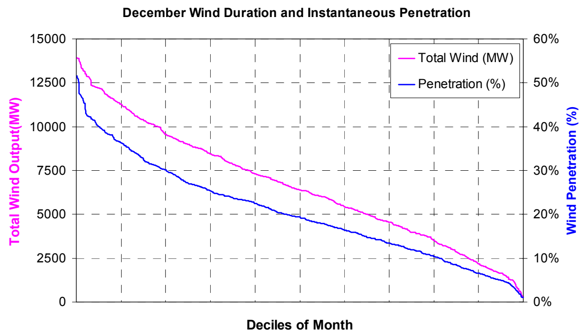
December Wind Duration and Instantaneous Penetration
Total Wind (MW)
Penetration (%)
Total Wind Output(MW)
Wind Penetration (%)
Deciles of Month
15000
12500
10000
7500
5000
2500
0
60%
50%
40%
30%
20%
10%
0%

C.4 Variability by Time of Day

February Average Daily Profiles and Hourly Variability
Load and Load-15,000 MW Of Wind Generation

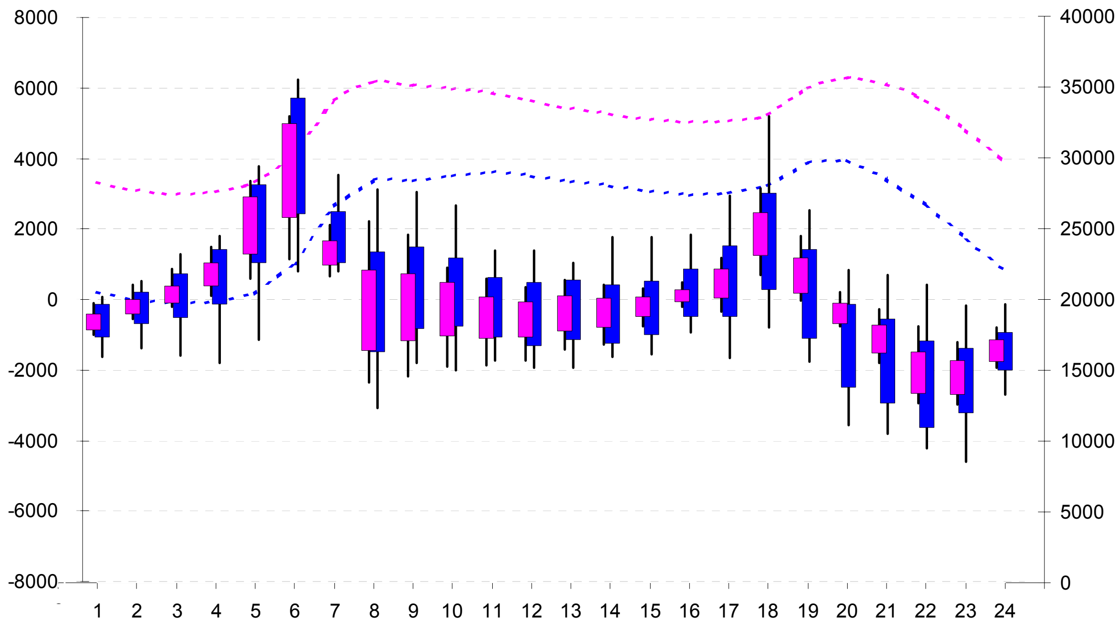

March Average Daily Profiles and Hourly Variability
Load and Load-15,000 MW Of Wind Generation

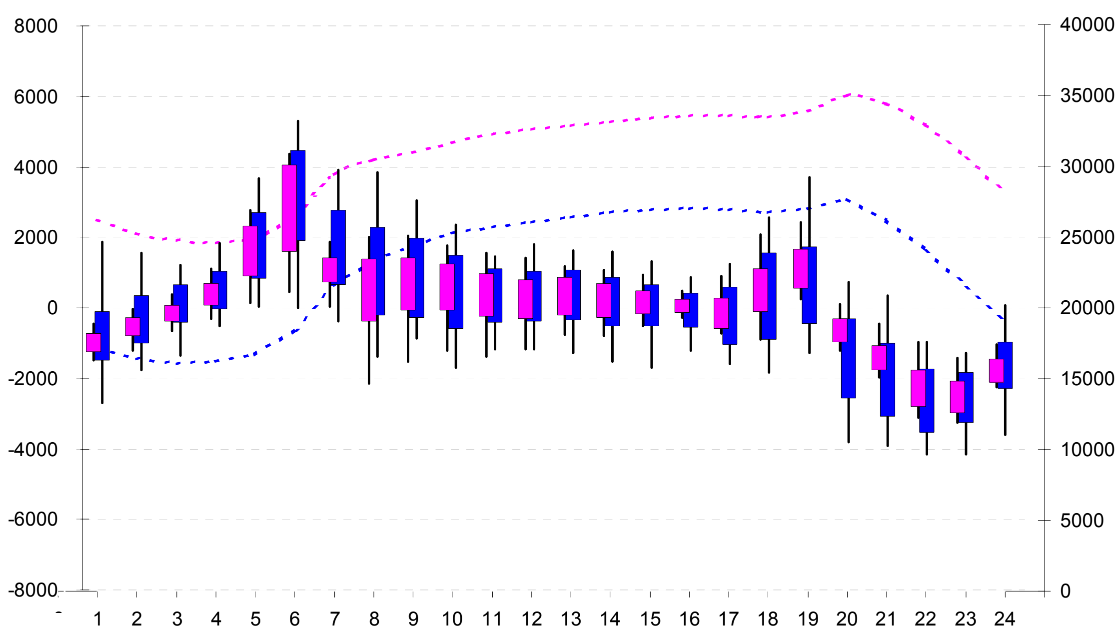

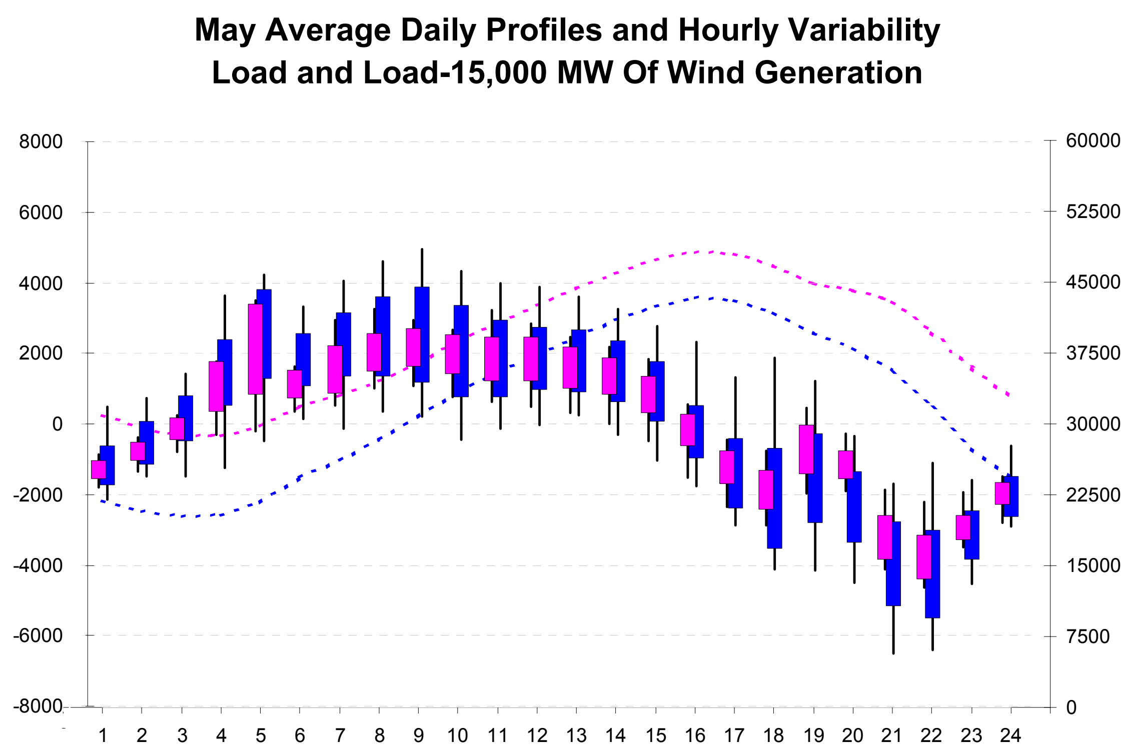
May Average Daily Profiles and Hourly Variability
Load and Load-15,000 MW Of Wind Generation
8000
6000
4000
2000
0
-2000
-4000
-6000
-8000
60000
52500
45000
37500
30000
22500
15000
7500
0
1 2 3 4 5 6 7 8 9 10 11 12 13 14 15 16 17 18 19 20 21 22 23 24

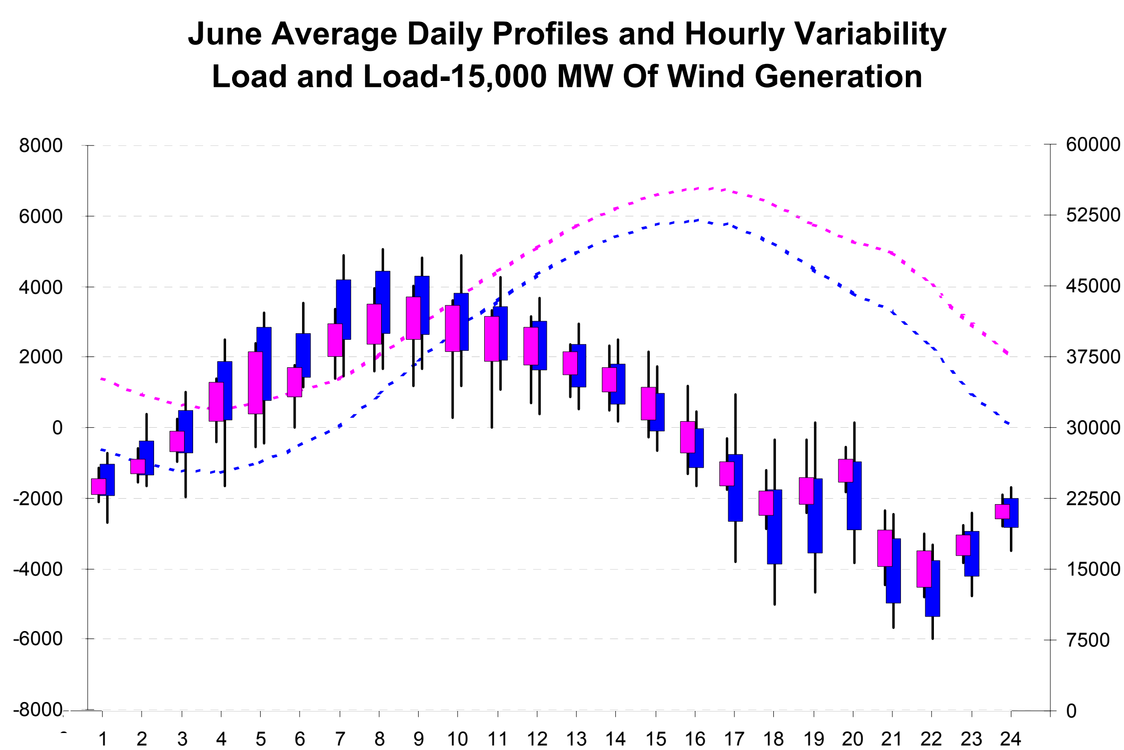
June Average Daily Profiles and Hourly Variability
Load and Load-15,000 MW Of Wind Generation
8000
6000
4000
2000
0
-2000
-4000
-6000
-8000
60000
52500
45000
37500
30000
22500
15000
7500
0
1 2 3 4 5 6 7 8 9 10 11 12 13 14 15 16 17 18 19 20 21 22 23 24

August Daily Average Profiles and Forecast Errors
(Study Year Load with 15000 MW of Wind)

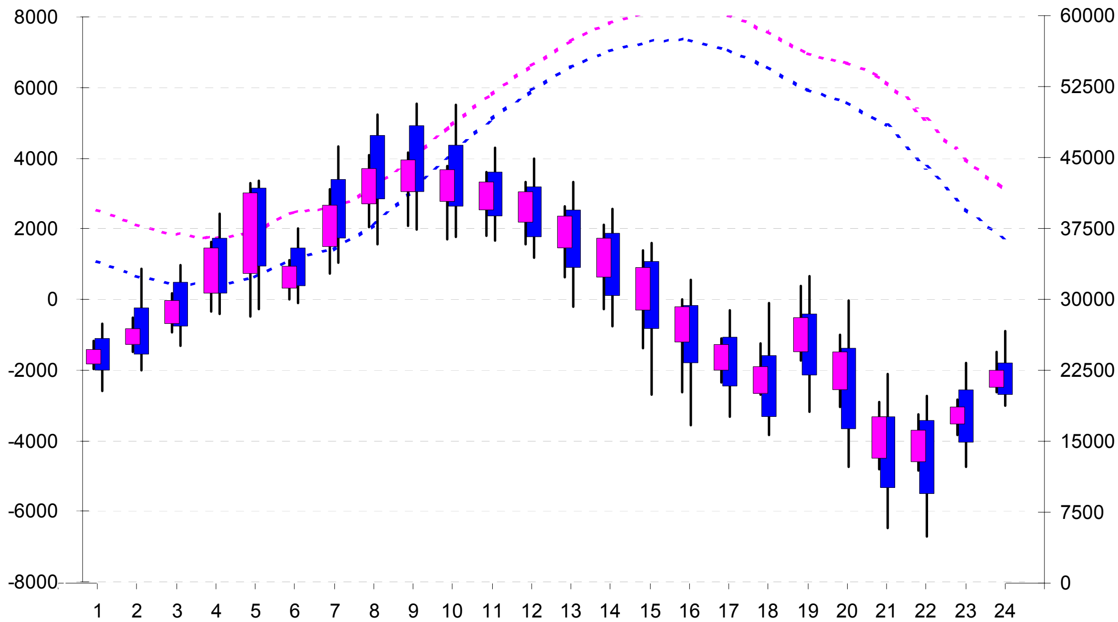

September Daily Average Profiles and Forecast Errors
(Study Year Load with 15000 MW of Wind)

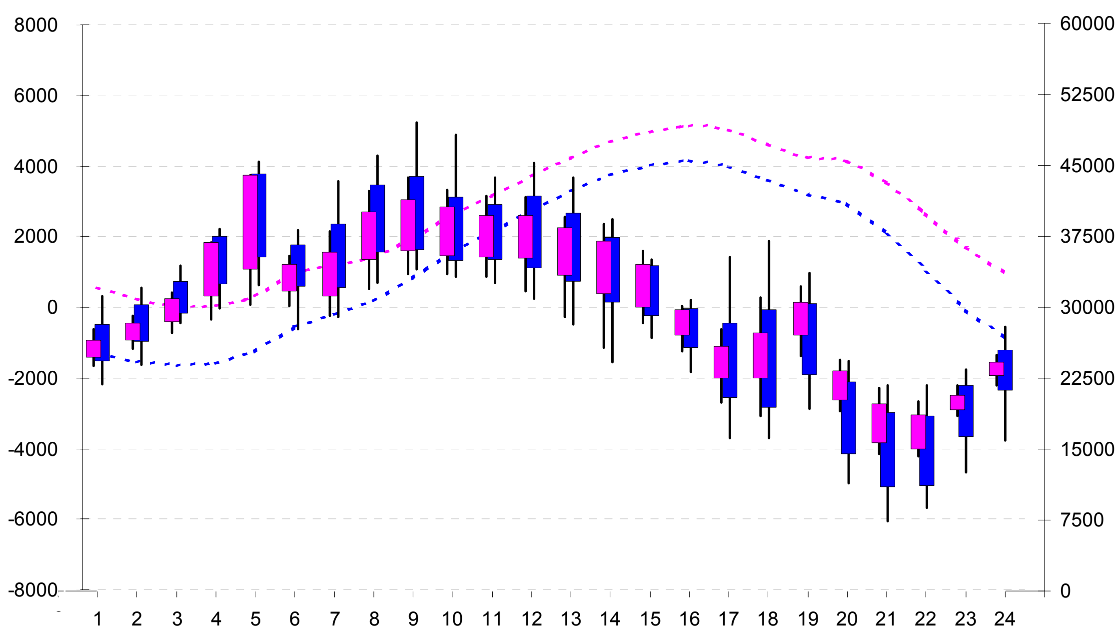

November Daily Average Profiles and Forecast Errors (Study Year Load with 15000 MW of Wind)

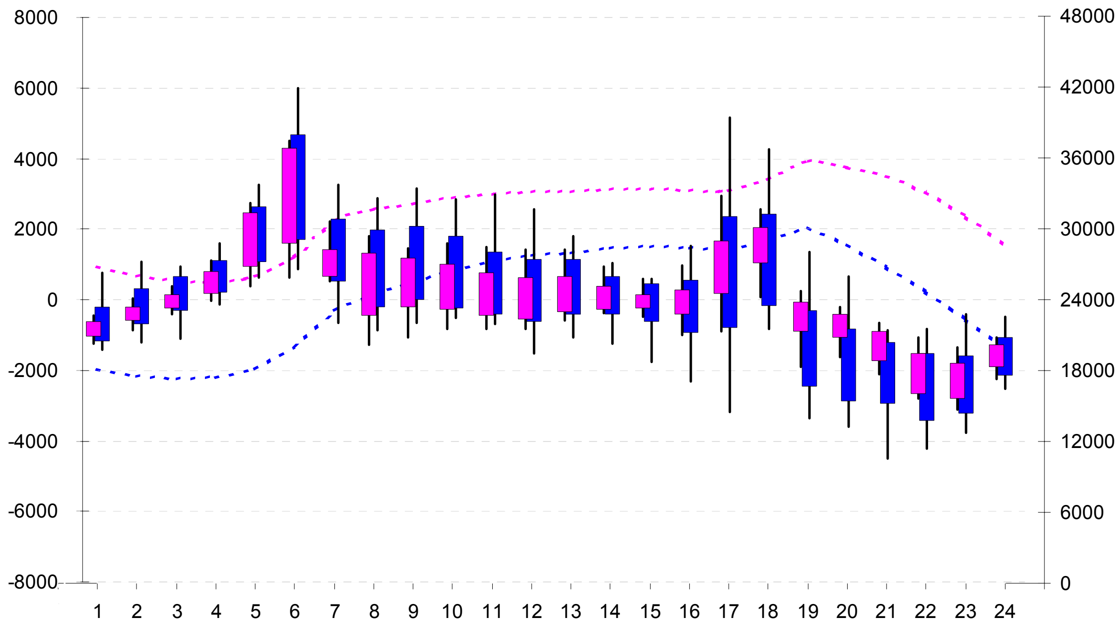

December Daily Average Profiles and Forecast Errors (Study Year Load with 15000 MW of Wind)

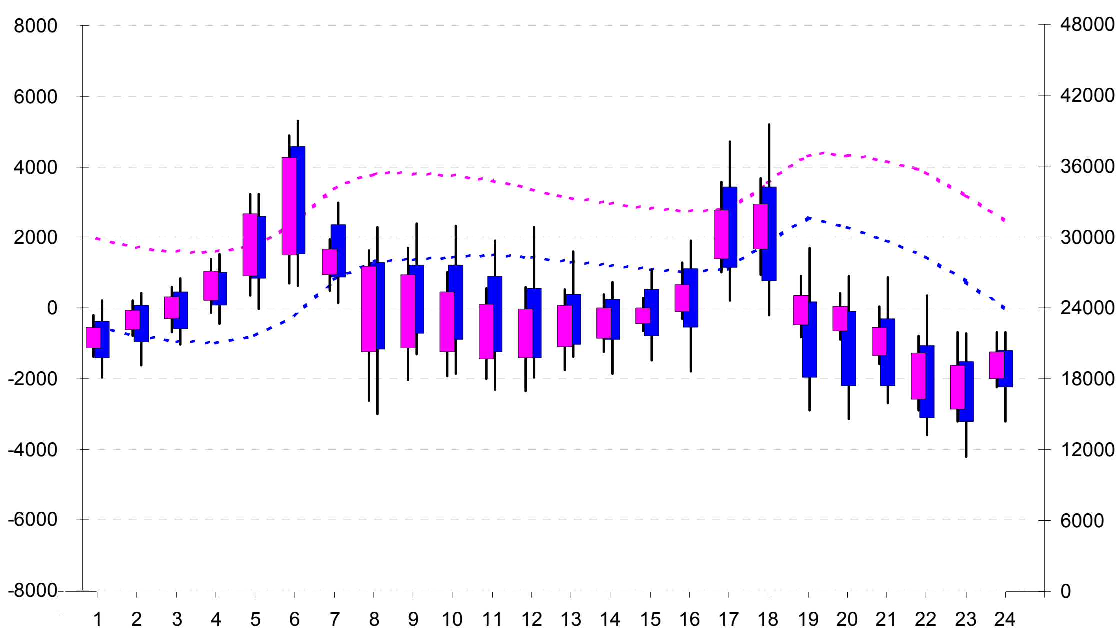

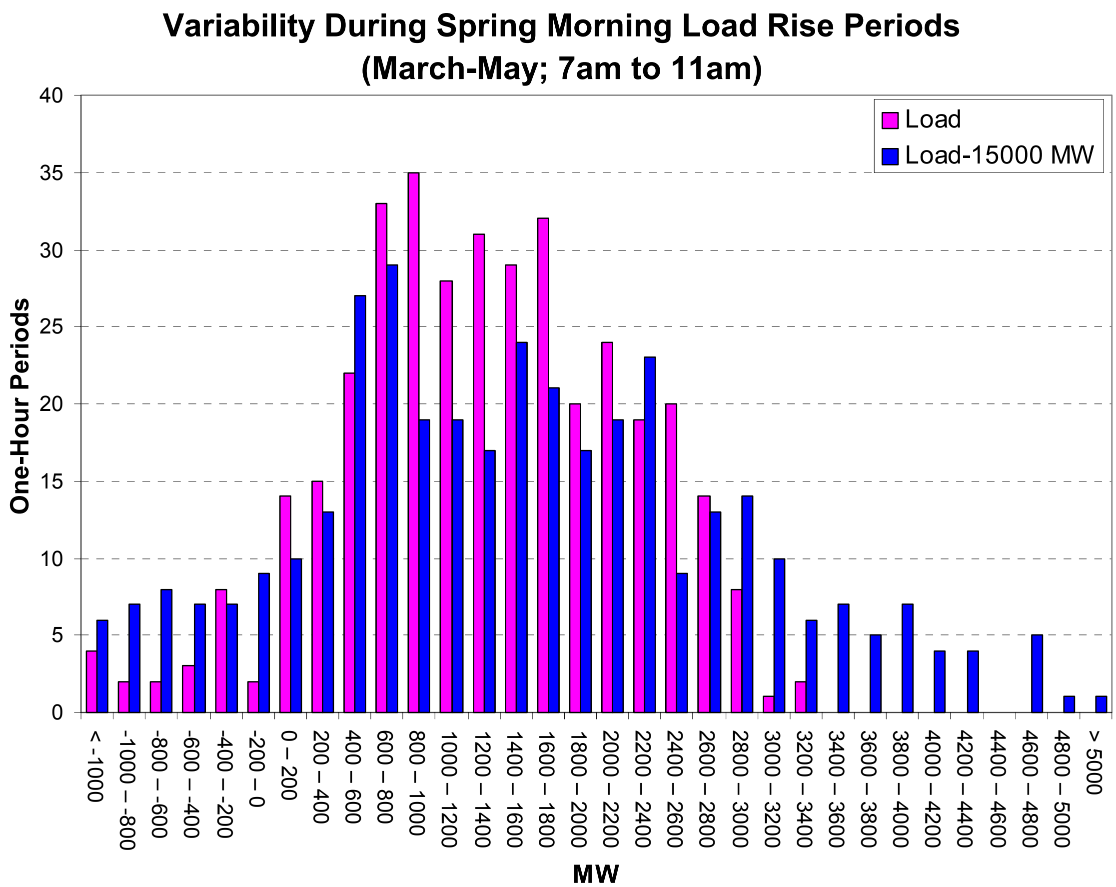
Variability During Spring Morning Load Rise Periods
(March-May; 7am to 11am)
Load
Load-15000 MW
One-Hour Periods
MW
40
35
30
25
20
15
10
5
0
< -1000
-1000 – -800
-800 – -600
-600 – -400
-400 – -200
-200 – 0
0 – 200
200 – 400
400 – 600
600 – 800
800 – 1000
1000 – 1200
1200 – 1400
1400 – 1600
1600 – 1800
1800 – 2000
2000 – 2200
2200 – 2400
2400 – 2600
2600 – 2800
2800 – 3000
3000 – 3200
3200 – 3400
3400 – 3600
3600 – 3800
3800 – 4000
4000 – 4200
4200 – 4400
4400 – 4600
4600 – 4800
4800 – 5000
> 5000

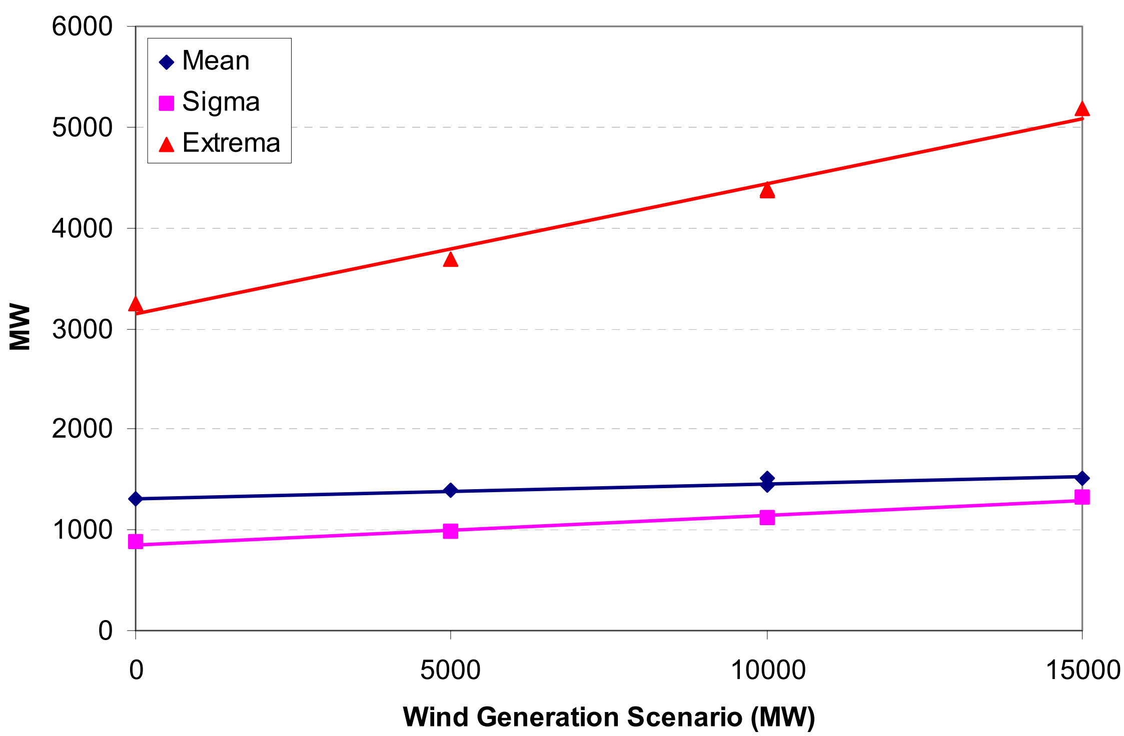
Mean
Sigma
Extrema
MW
6000
5000
4000
3000
2000
1000
0
0
5000
10000
15000
Wind Generation Scenario (MW)

Variability During Summer Morning Load Rise Periods

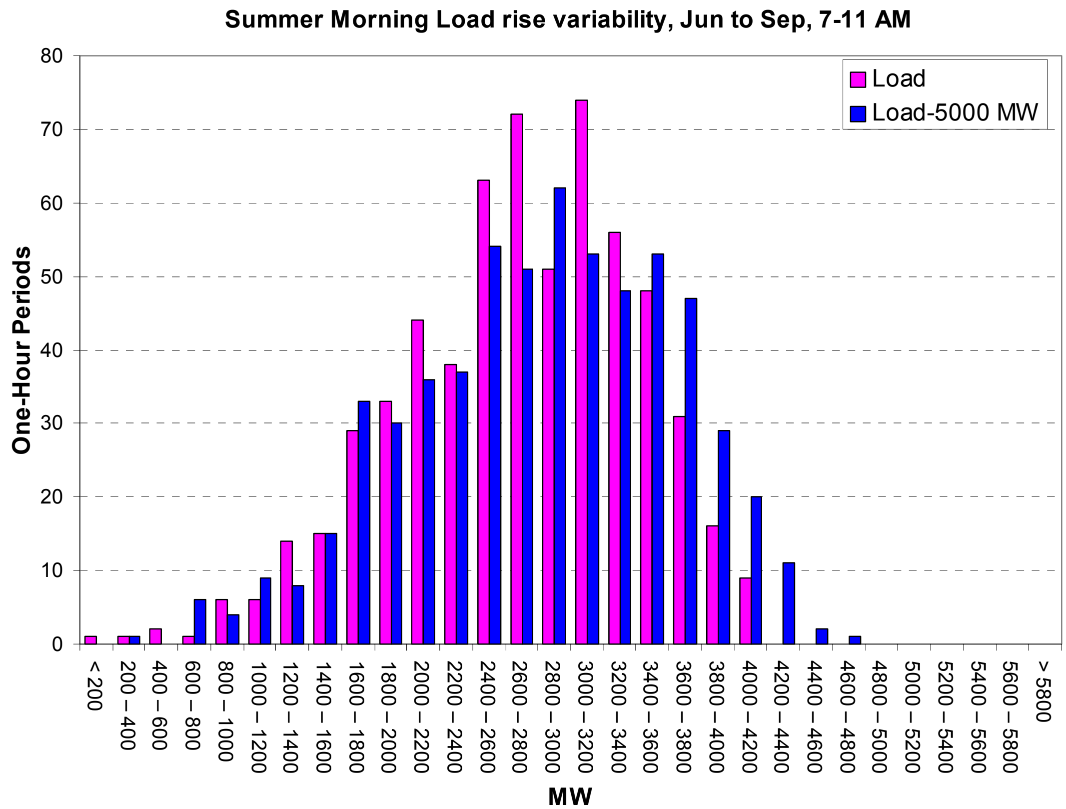

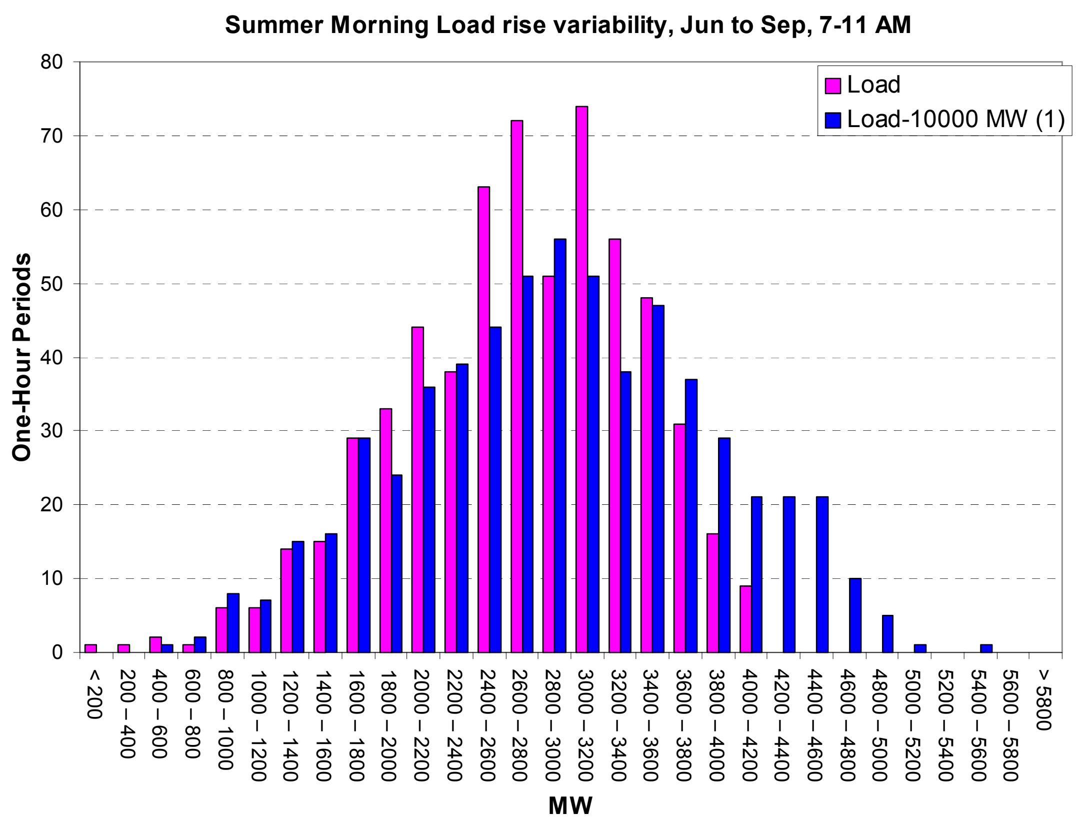

Summer Morning Load rise variability, Jun to Sep, 7-11 AM

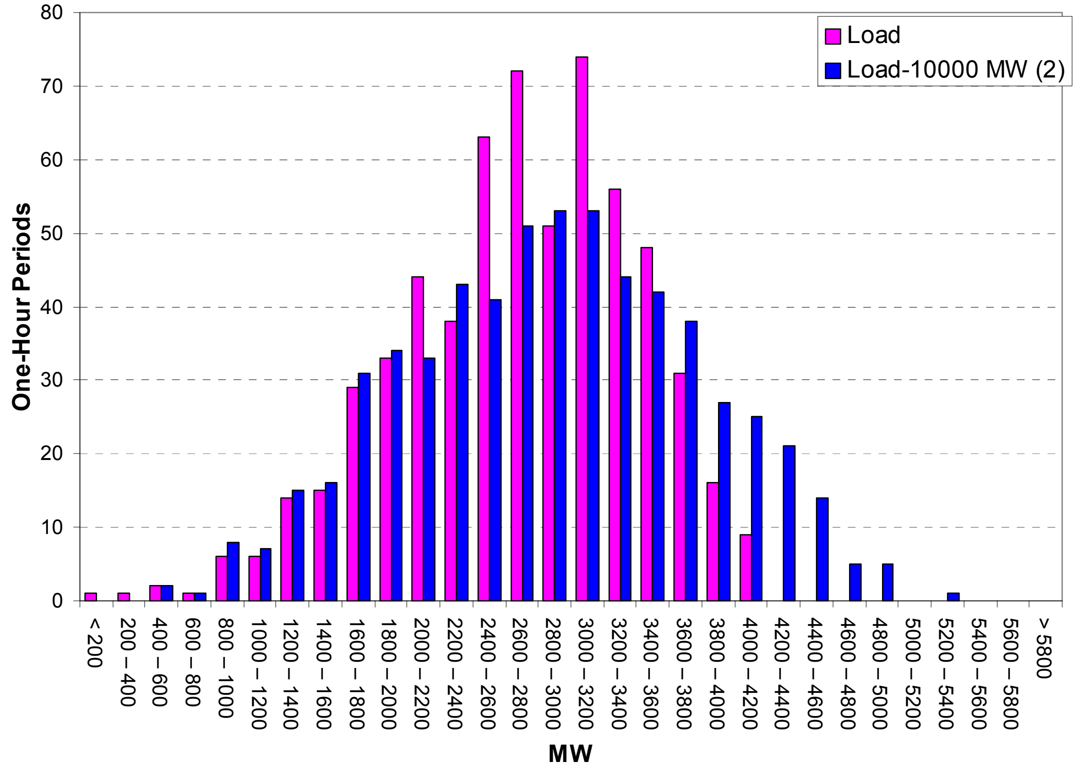

Summer Morning Load rise variability, Jun to Sep, 7-11 AM

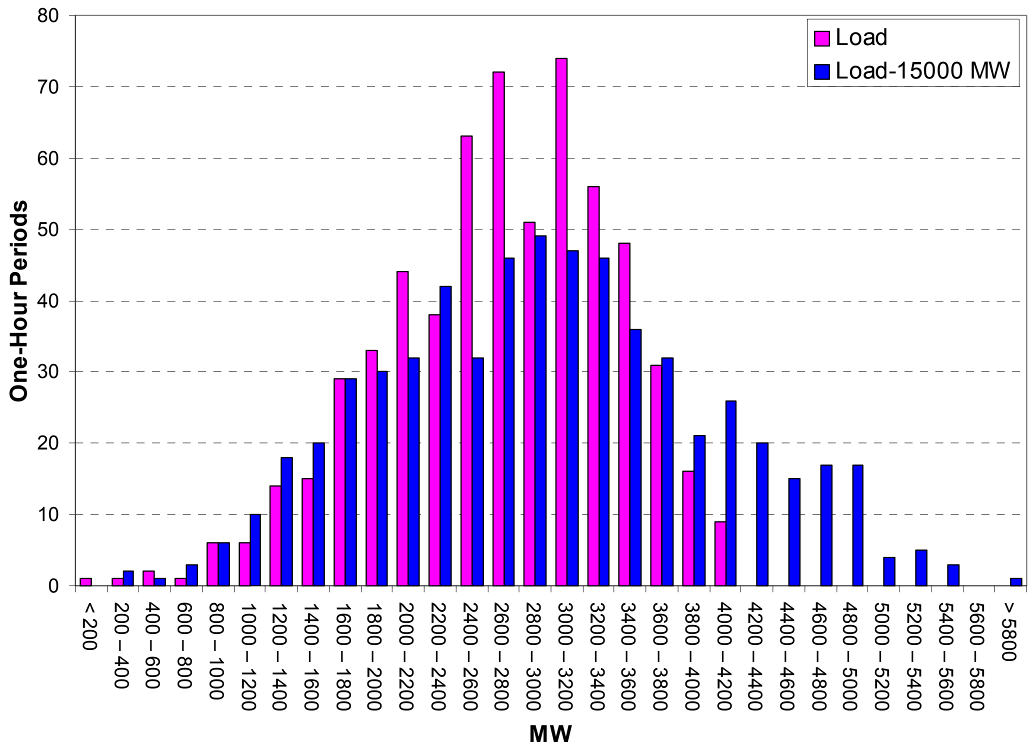

Variability During Winter Afternoon Load Rise Periods

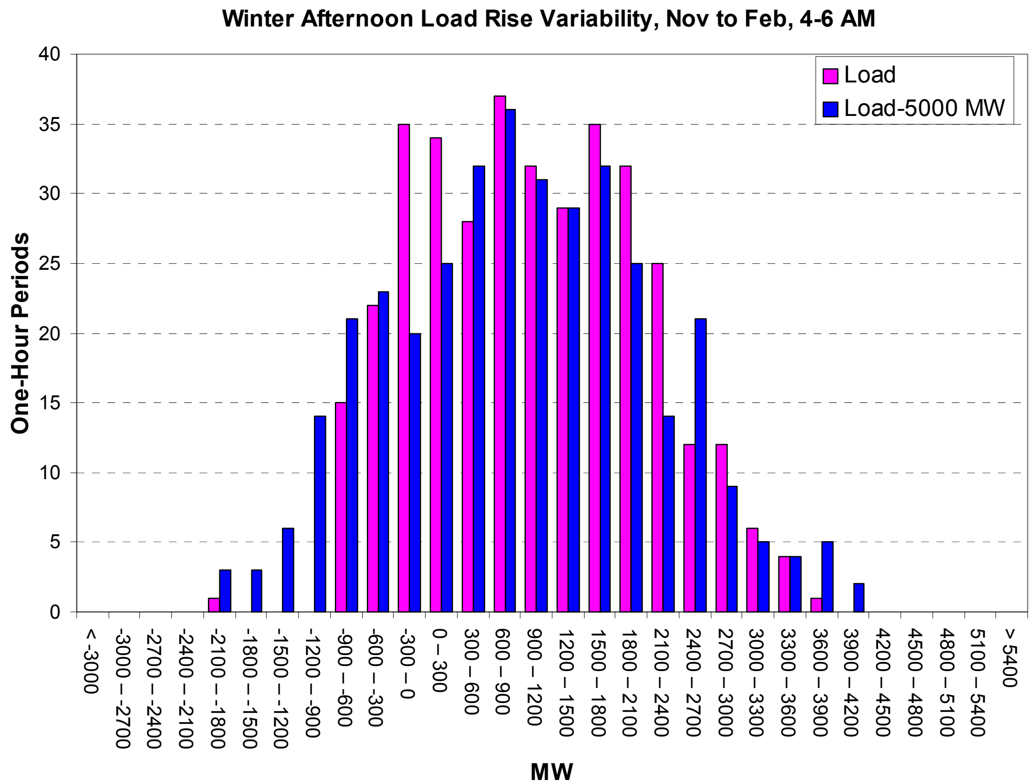

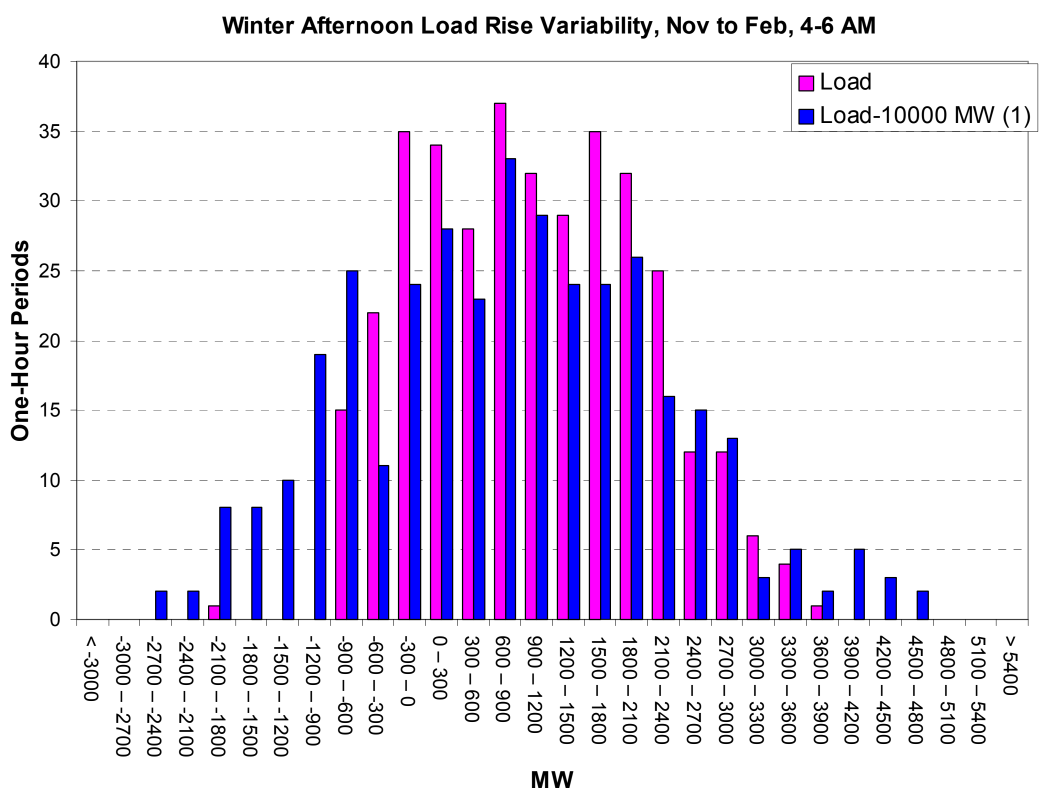

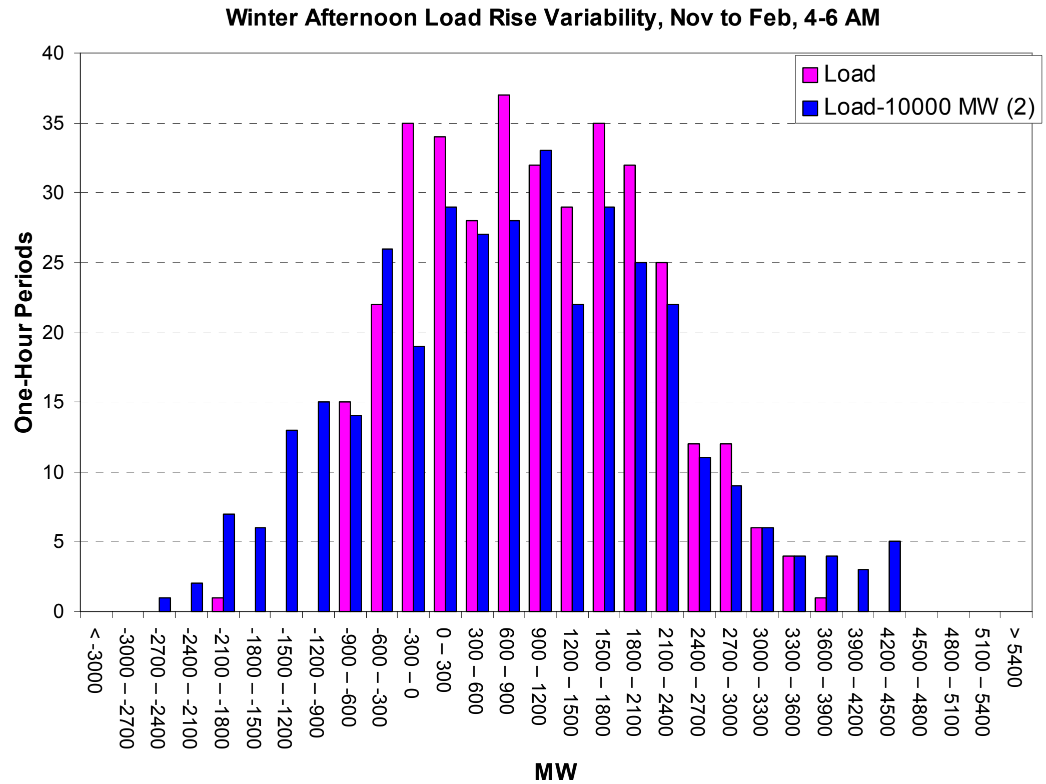
Winter Afternoon Load Rise Variability, Nov to Feb, 4-6 AM
Load
Load-10000 MW (2)
One-Hour Periods
MW
0
5
10
15
20
25
30
35
40
< -3000
-3000 – -2700
-2700 – -2400
-2400 – -2100
-2100 – -1800
-1800 – -1500
-1500 – -1200
-1200 – -900
-900 – -600
-600 – -300
-300 – 0
0 – 300
300 – 600
600 – 900
900 – 1200
1200 – 1500
1500 – 1800
1800 – 2100
2100 – 2400
2400 – 2700
2700 – 3000
3000 – 3300
3300 – 3600
3600 – 3900
3900 – 4200
4200 – 4500
4500 – 4800
4800 – 5100
5100 – 5400
> 5400

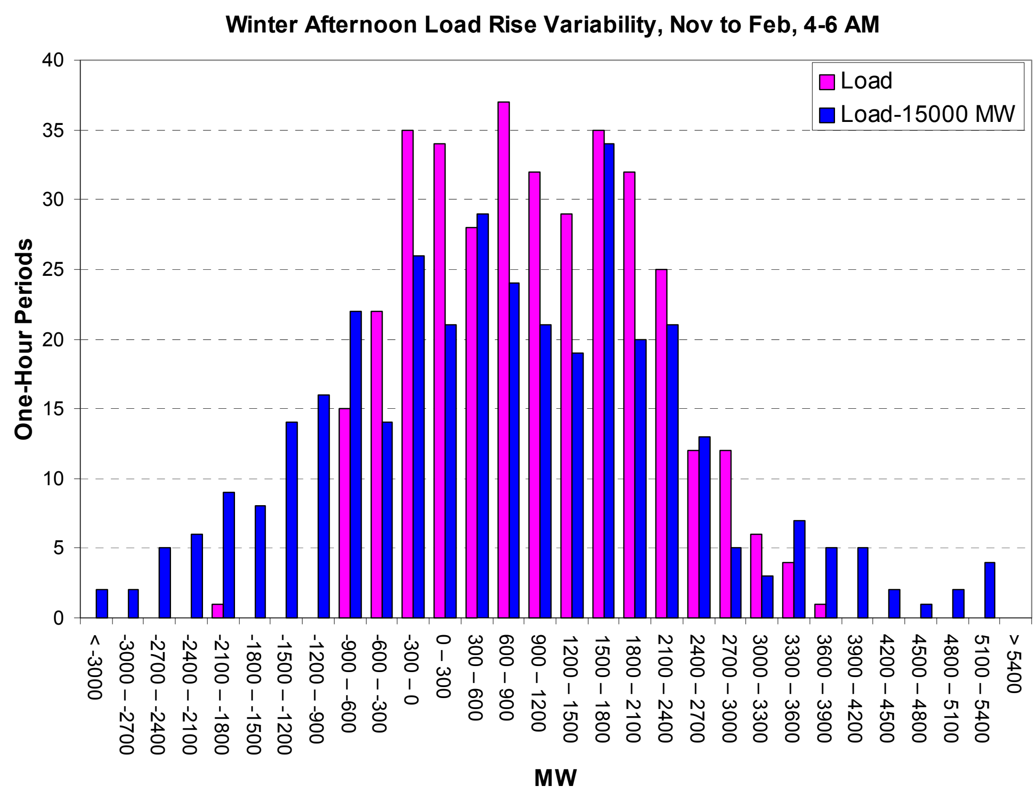
Winter Afternoon Load Rise Variability, Nov to Feb, 4-6 AM
Load
Load-15000 MW
One-Hour Periods
MW
0
5
10
15
20
25
30
35
40
< -3000
-3000 – -2700
-2700 – -2400
-2400 – -2100
-2100 – -1800
-1800 – -1500
-1500 – -1200
-1200 – -900
-900 – -600
-600 – -300
-300 – 0
0 – 300
300 – 600
600 – 900
900 – 1200
1200 – 1500
1500 – 1800
1800 – 2100
2100 – 2400
2400 – 2700
2700 – 3000
3000 – 3300
3300 – 3600
3600 – 3900
3900 – 4200
4200 – 4500
4500 – 4800
4800 – 5100
5100 – 5400
> 5400

Variability During Summer evening Load Drop Periods

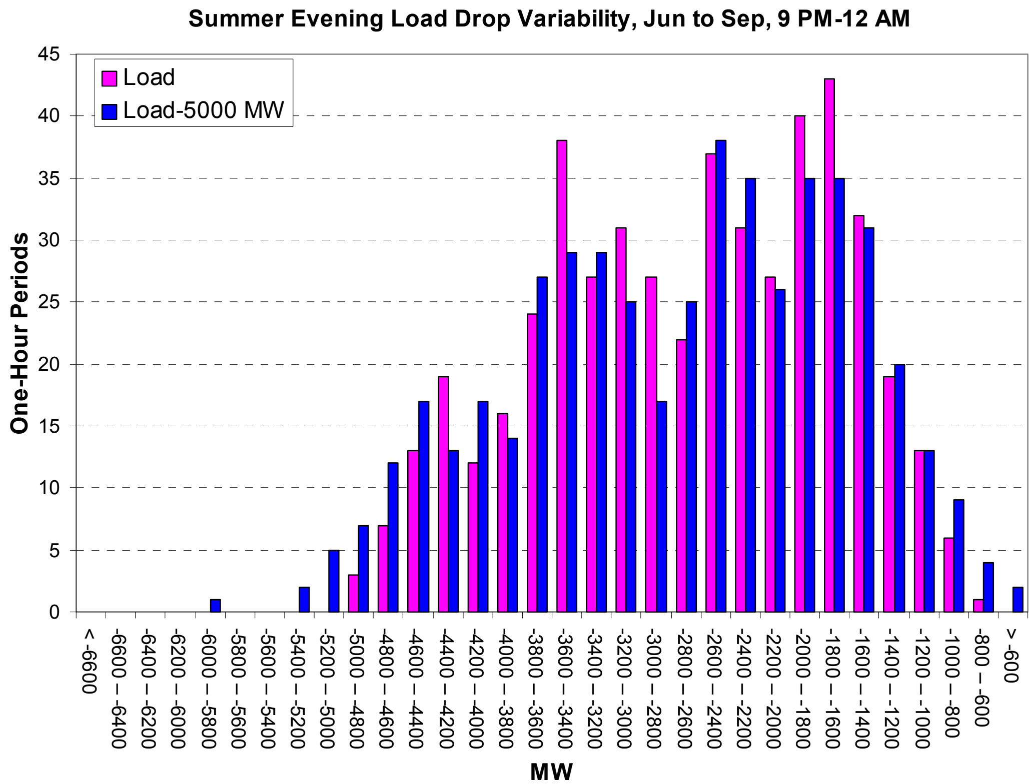

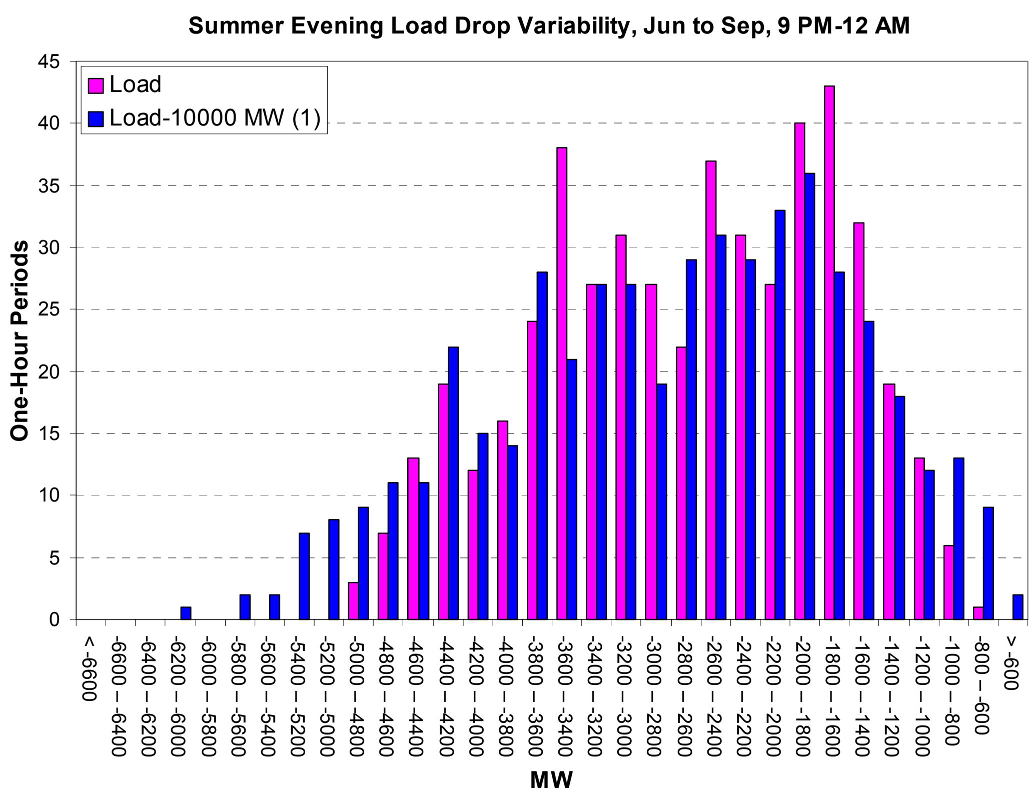

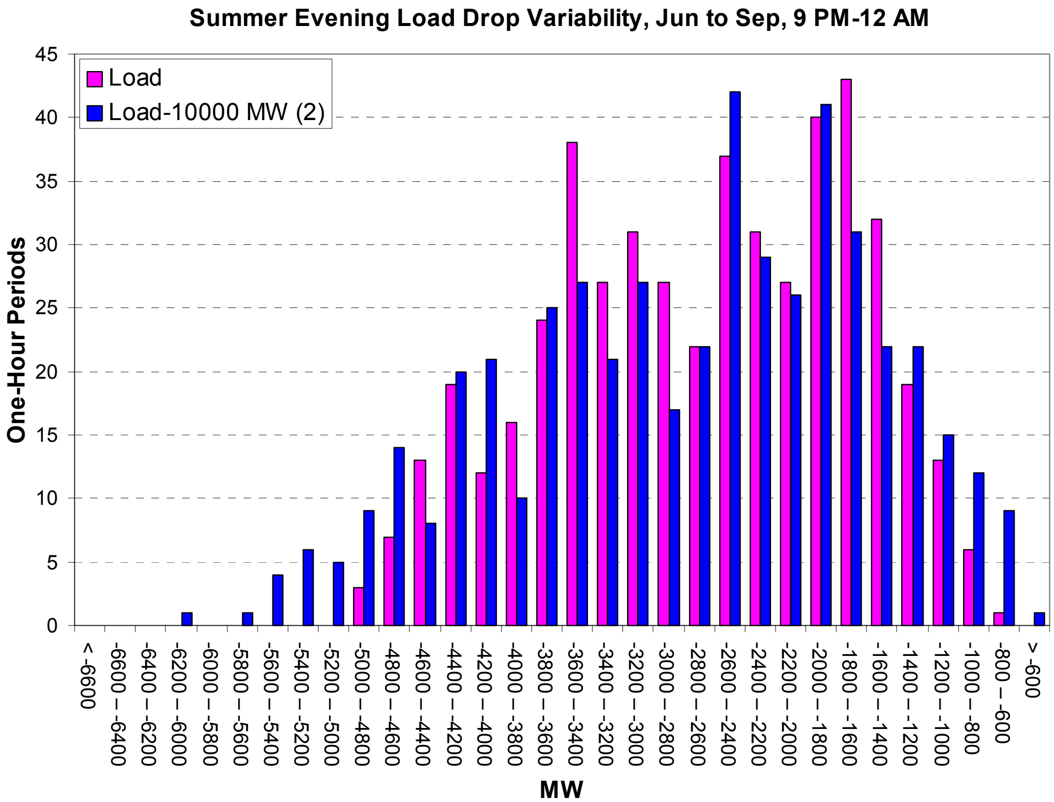
Summer Evening Load Drop Variability, Jun to Sep, 9 PM-12 AM
Load
Load-10000 MW (2)
One-Hour Periods
MW

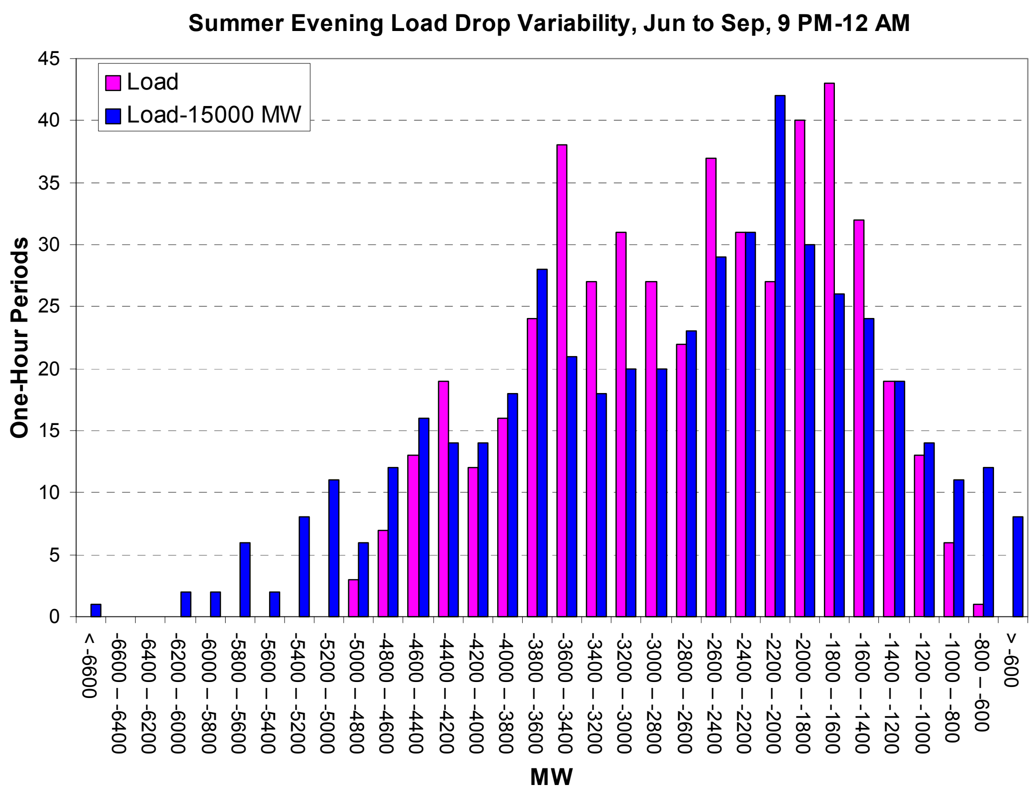
Summer Evening Load Drop Variability, Jun to Sep, 9 PM-12 AM
Load
Load-15000 MW
One-Hour Periods
MW

APPENDIX D SUPPLEMENTAL PREDICTABILITY PLOTS

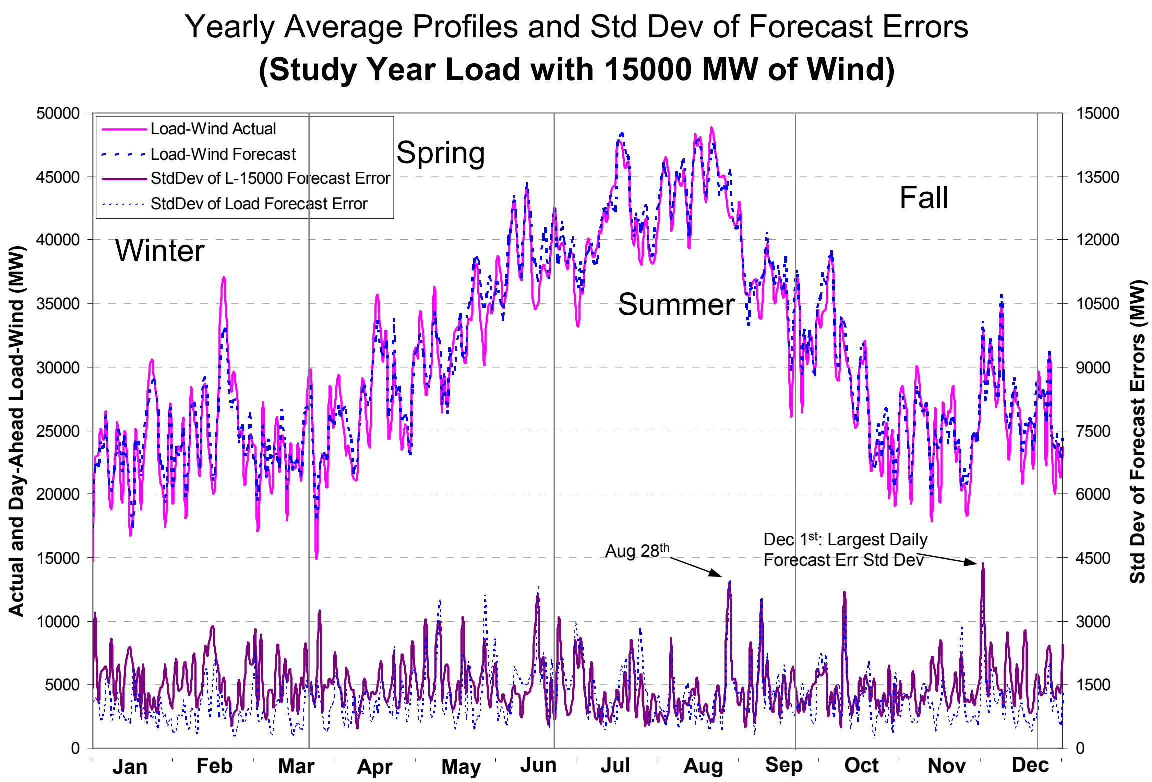

No clear trend in variability of daily forecast errors across the year

January Daily Average Profiles and Forecast Errors (Study Year Load with 15000 MW of Wind)

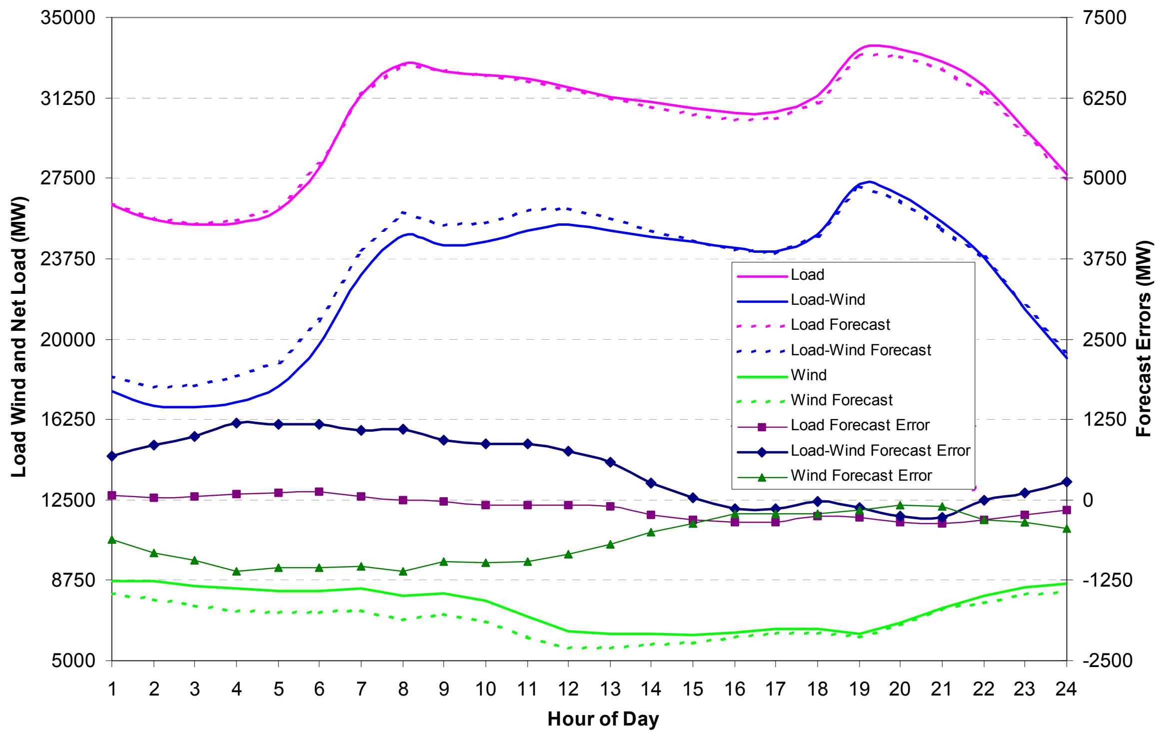

April Daily Average Profiles and Forecast Errors (Study Year Load with 15000 MW of Wind)

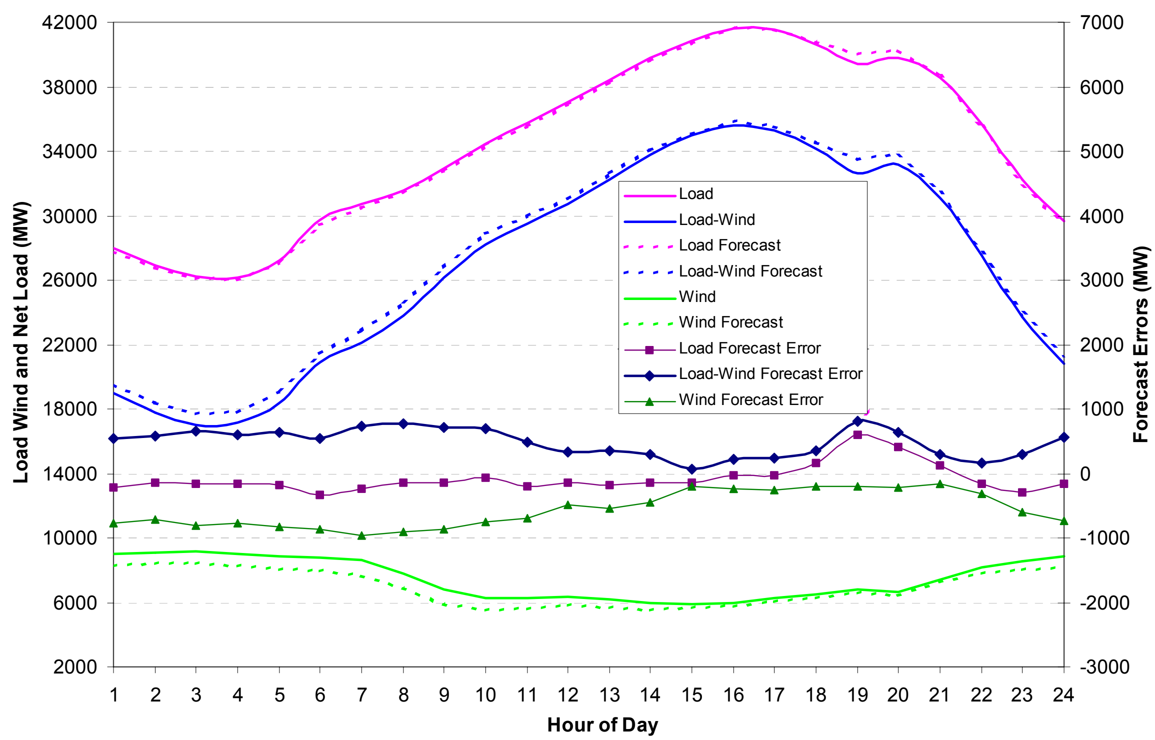

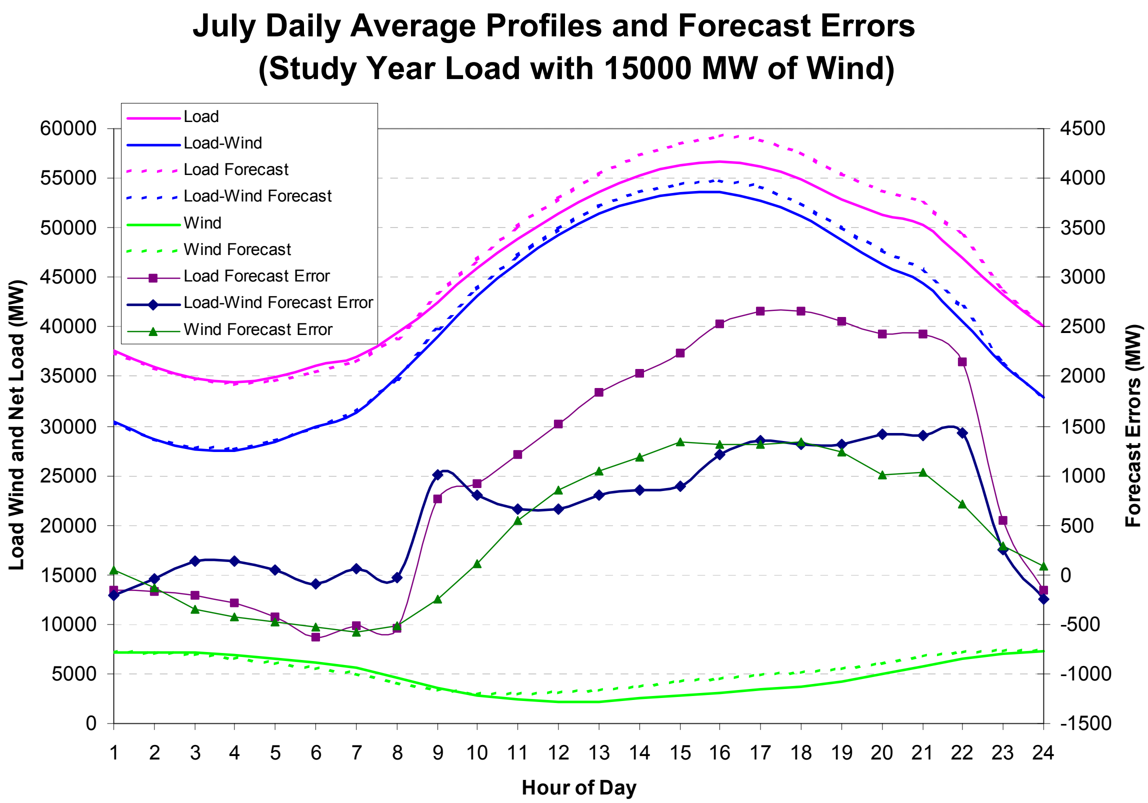
July Daily Average Profiles and Forecast Errors
(Study Year Load with 15000 MW of Wind)
Load
Load-Wind
Load Forecast
Load-Wind Forecast
Wind
Wind Forecast
Load Forecast Error
Load-Wind Forecast Error
Wind Forecast Error
Load Wind and Net Load (MW)
Forecast Errors (MW)
Hour of Day
60000
55000
50000
45000
40000
35000
30000
25000
20000
15000
10000
5000
0
4500
4000
3500
3000
2500
2000
1500
1000
500
0
-500
-1000
-1500
1 2 3 4 5 6 7 8 9 10 11 12 13 14 15 16 17 18 19 20 21 22 23 24

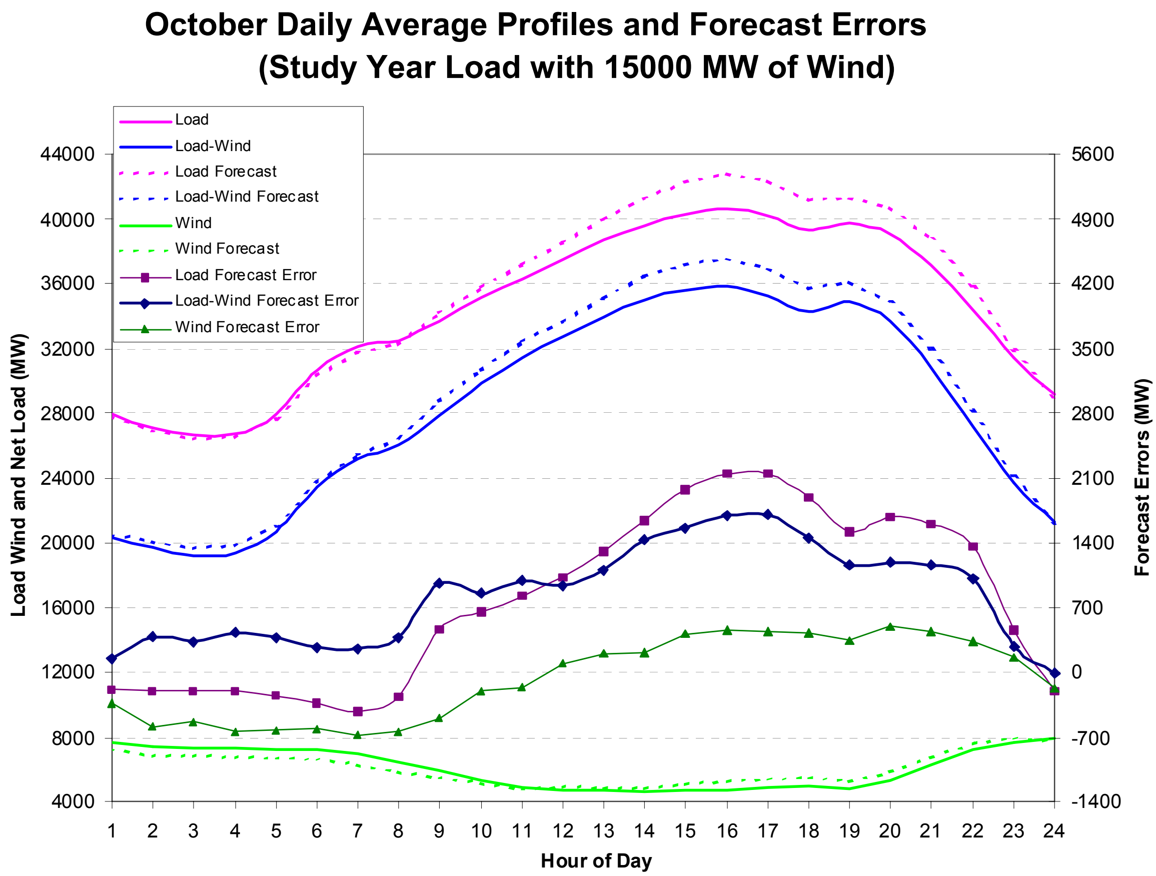
October Daily Average Profiles and Forecast Errors
(Study Year Load with 15000 MW of Wind)
Load
Load-Wind
Load Forecast
Load-Wind Forecast
Wind
Wind Forecast
Load Forecast Error
Load-Wind Forecast Error
Wind Forecast Error
Load Wind and Net Load (MW)
Forecast Errors (MW)
Hour of Day
44000
40000
36000
32000
28000
24000
20000
16000
12000
8000
4000
5600
4900
4200
3500
2800
2100
1400
700
0
-700
-1400
1 2 3 4 5 6 7 8 9 10 11 12 13 14 15 16 17 18 19 20 21 22 23 24

APPENDIX E SUPPLEMENTAL REGULATION PLOTS

E.1 Maximum Hourly Regulation Deployments (similar to Figure 6-3)

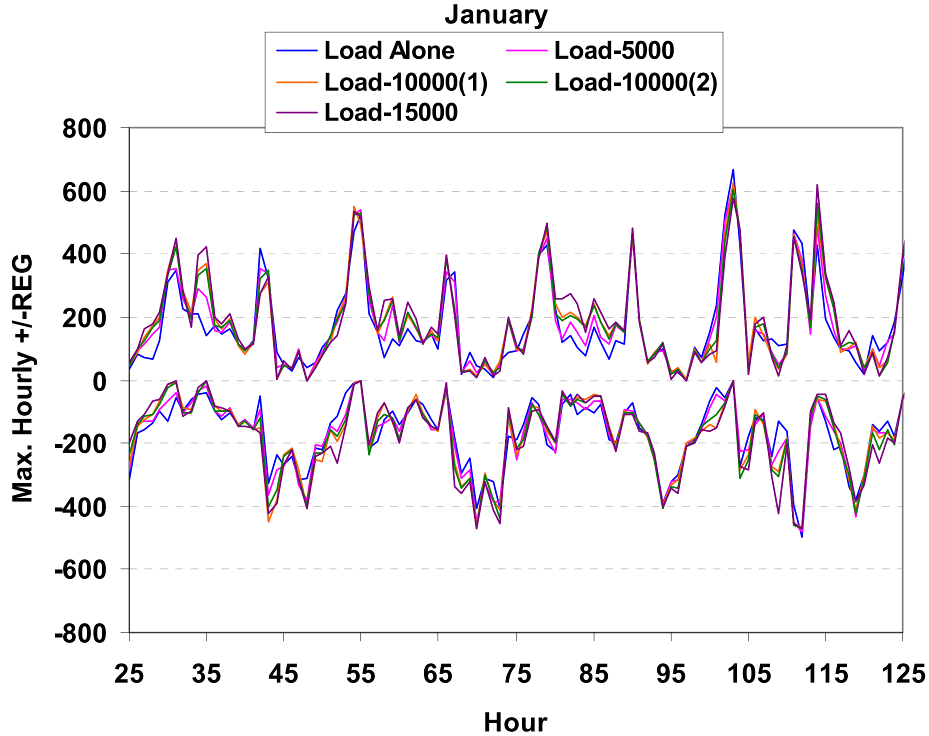

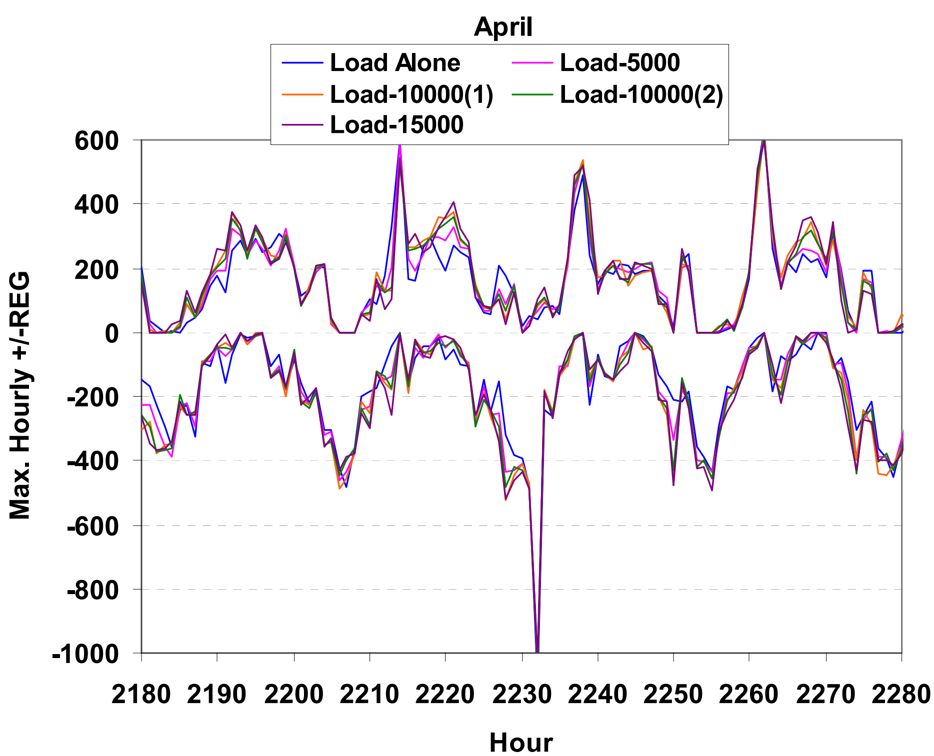

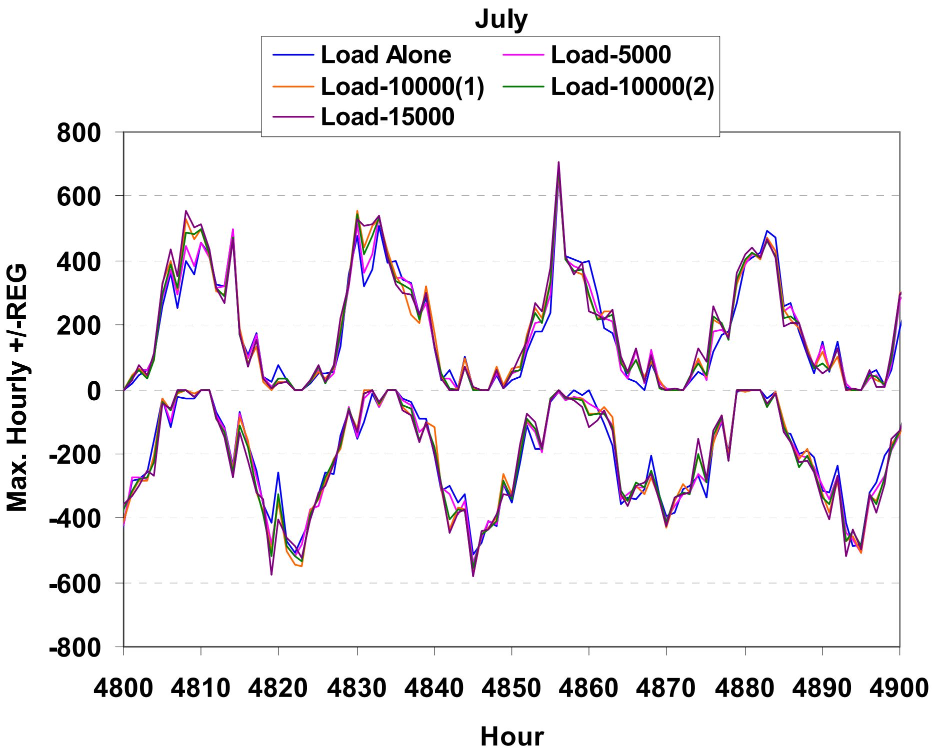
July
Load Alone
Load-5000
Load-10000(1)
Load-10000(2)
Load-15000
800
600
400
200
0
-200
-400
-600
-800
Max. Hourly +/-REG
4800
4810
4820
4830
4840
4850
4860
4870
4880
4890
4900
Hour

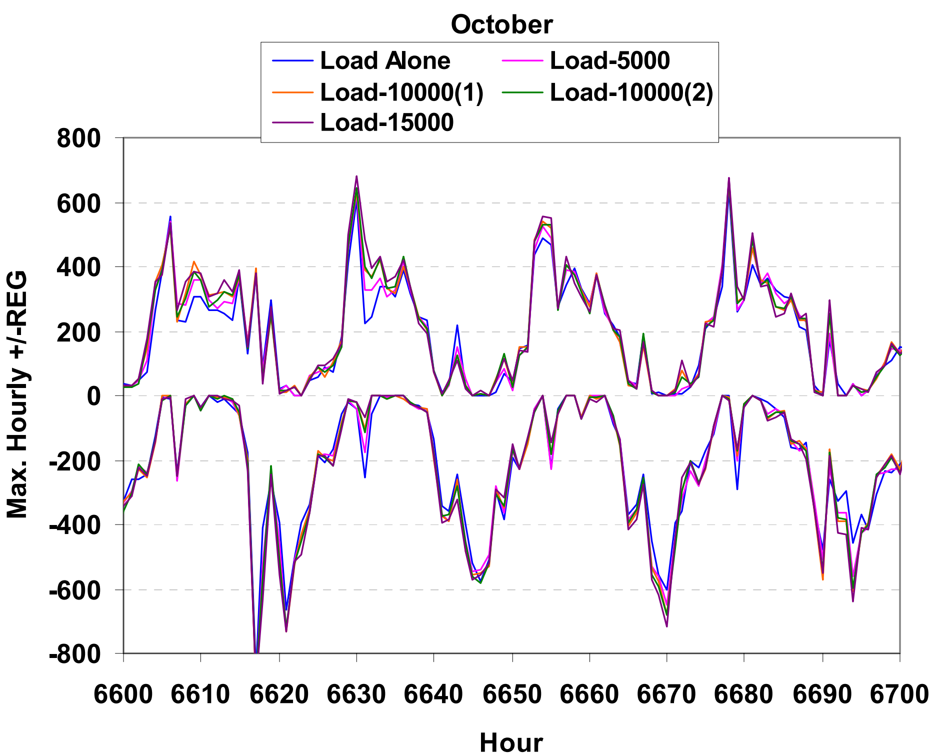
October
Load Alone
Load-5000
Load-10000(1)
Load-10000(2)
Load-15000
800
600
400
200
0
-200
-400
-600
-800
Max. Hourly +/-REG
6600
6610
6620
6630
6640
6650
6660
6670
6680
6690
6700
Hour

E.2 98.8th Percentile of Regulation Deployments

+REG; Load Only

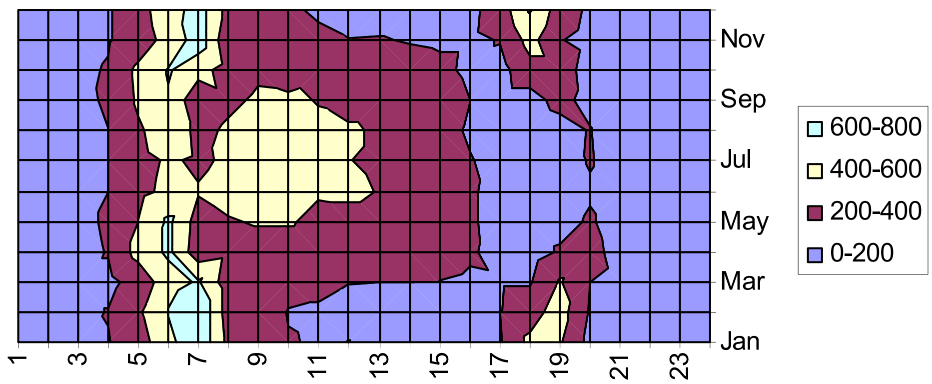

+REG; Load -5,000 MW Wind

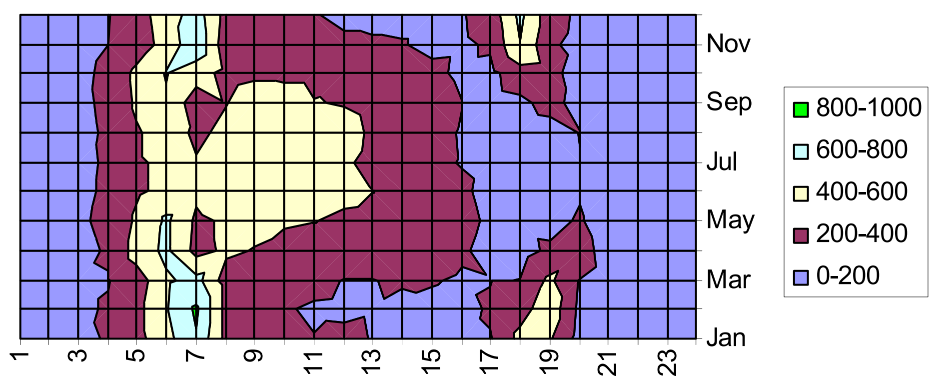

+REG; Load -10,000 MW Wind (Case 1)

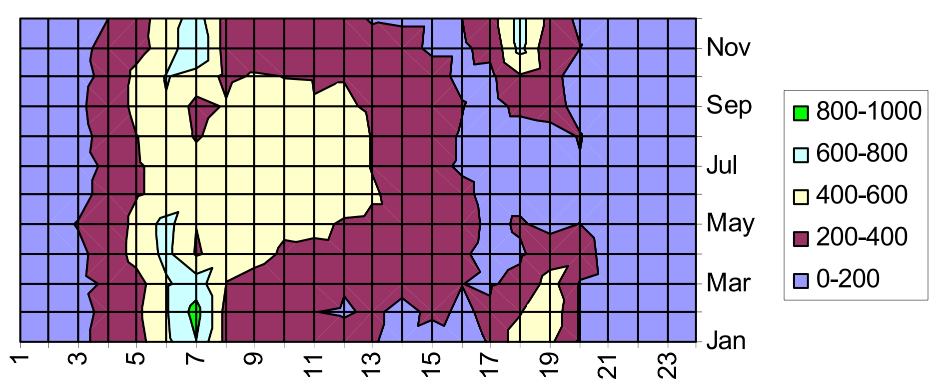

+REG; Load -10,000 MW Wind (Case 2)

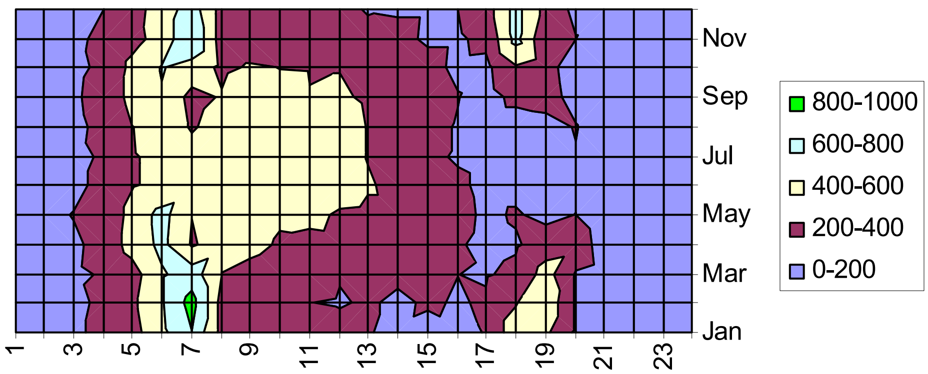

+REG; Load -15,000 MW Wind

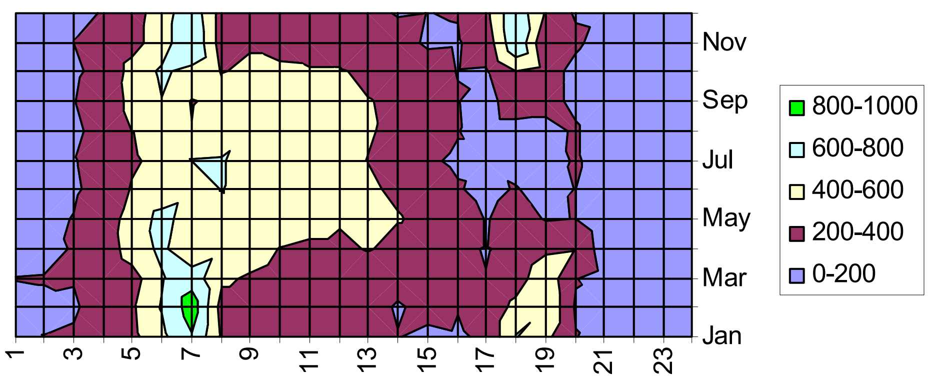

-REG; Load Only

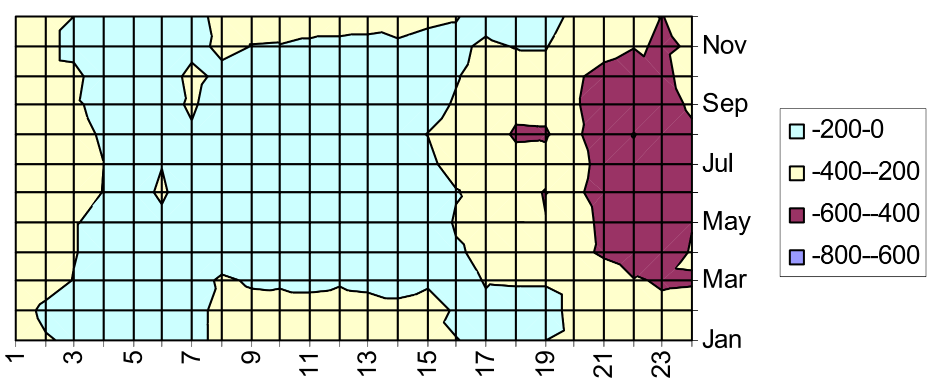

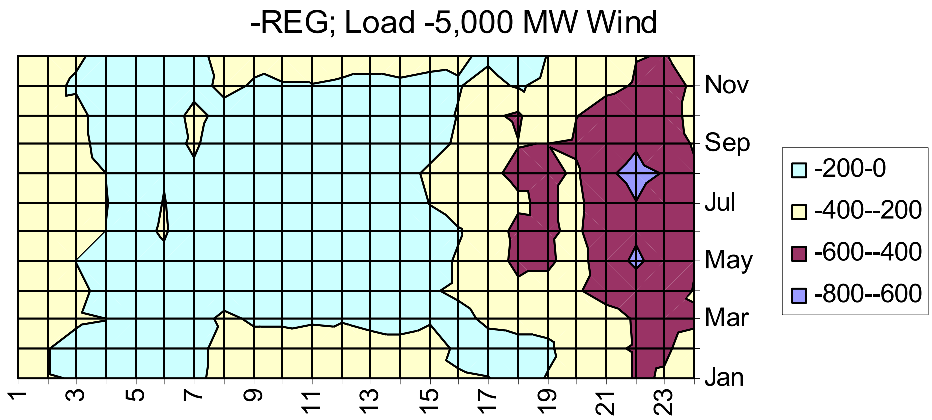
-REG; Load -5,000 MW Wind
Nov
Sep
Jul
May
Mar
Jan
1
3
5
7
9
11
13
15
17
19
21
23
-200-0
-400--200
-600--400
-800--600

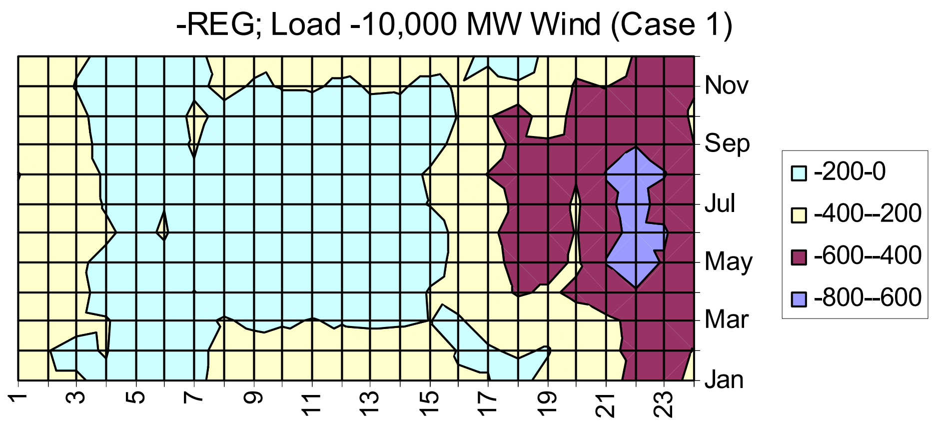
-REG; Load -10,000 MW Wind (Case 1)
Nov
Sep
Jul
May
Mar
Jan
1
3
5
7
9
11
13
15
17
19
21
23
-200-0
-400--200
-600--400
-800--600

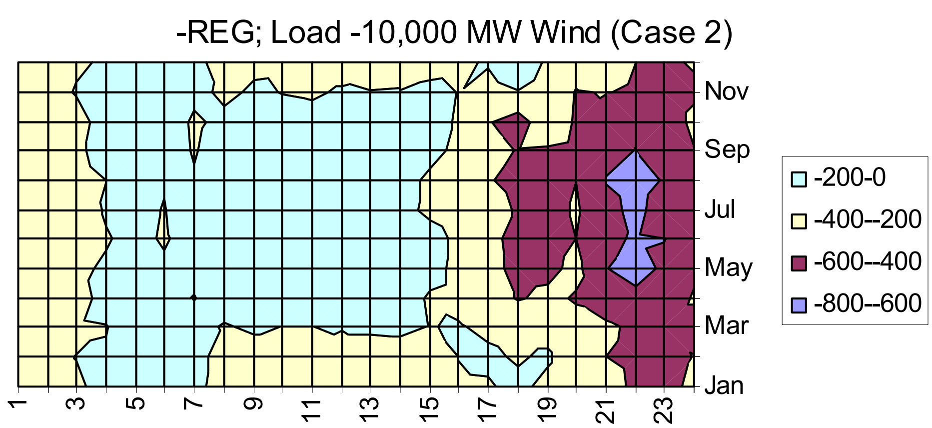
-REG; Load -10,000 MW Wind (Case 2)
Nov
Sep
Jul
May
Mar
Jan
1
3
5
7
9
11
13
15
17
19
21
23
-200-0
-400--200
-600--400
-800--600

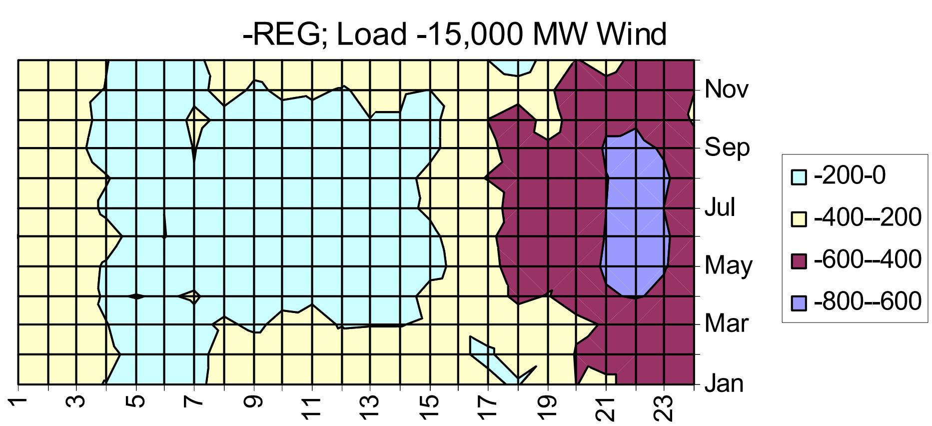
-REG; Load -15,000 MW Wind
Nov
Sep
Jul
May
Mar
Jan
1
3
5
7
9
11
13
15
17
19
21
23
-200-0
-400--200
-600--400
-800--600

E.3 Comparisons of Regulation Procurement and Deployment

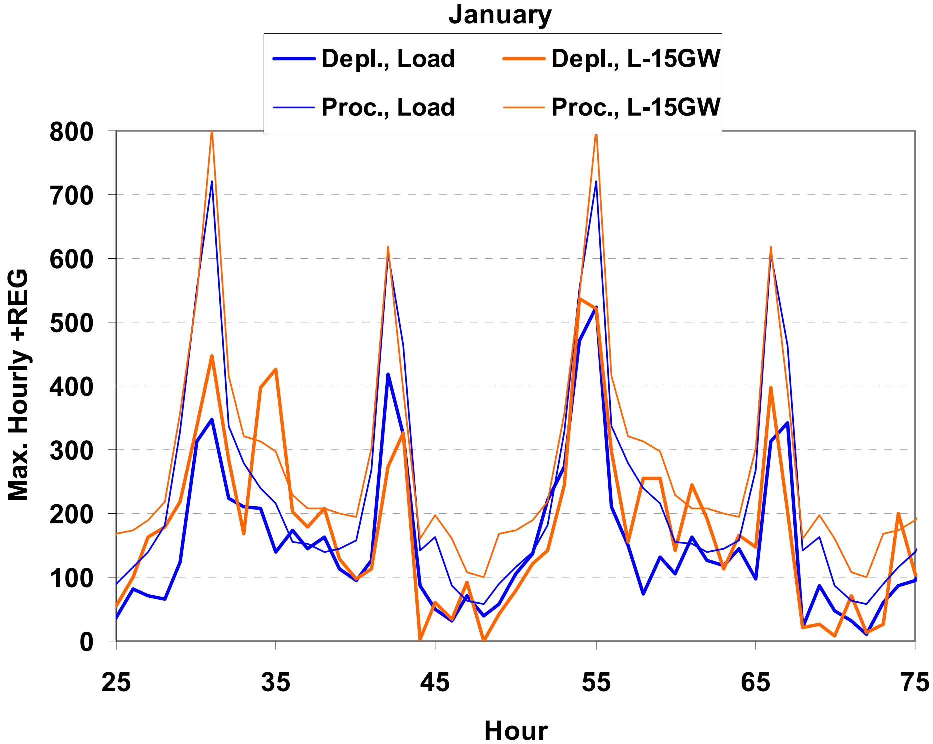

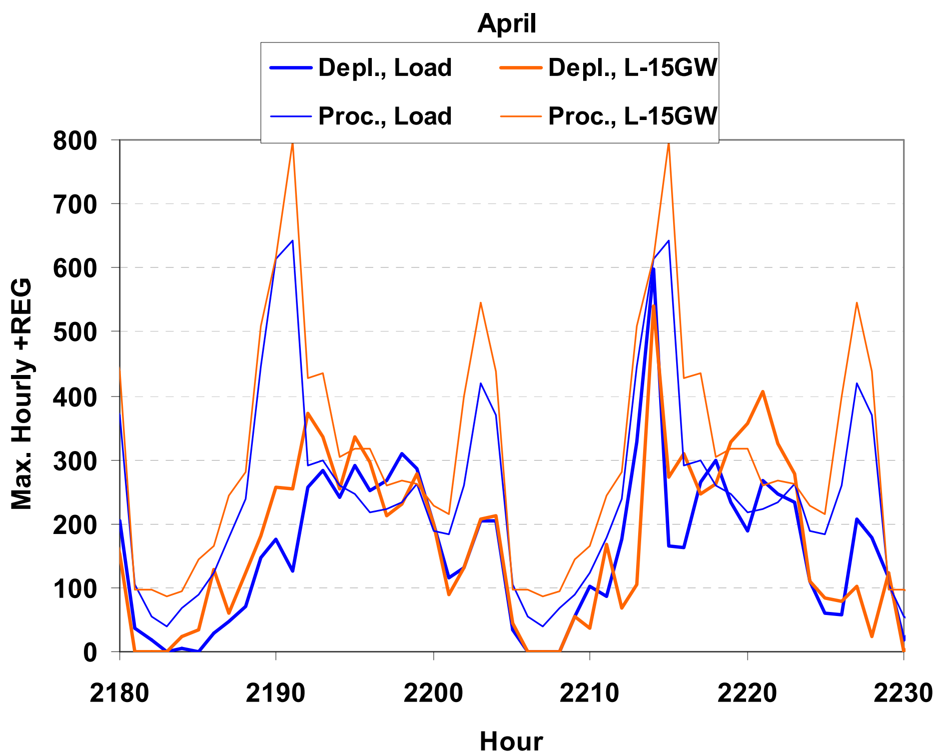

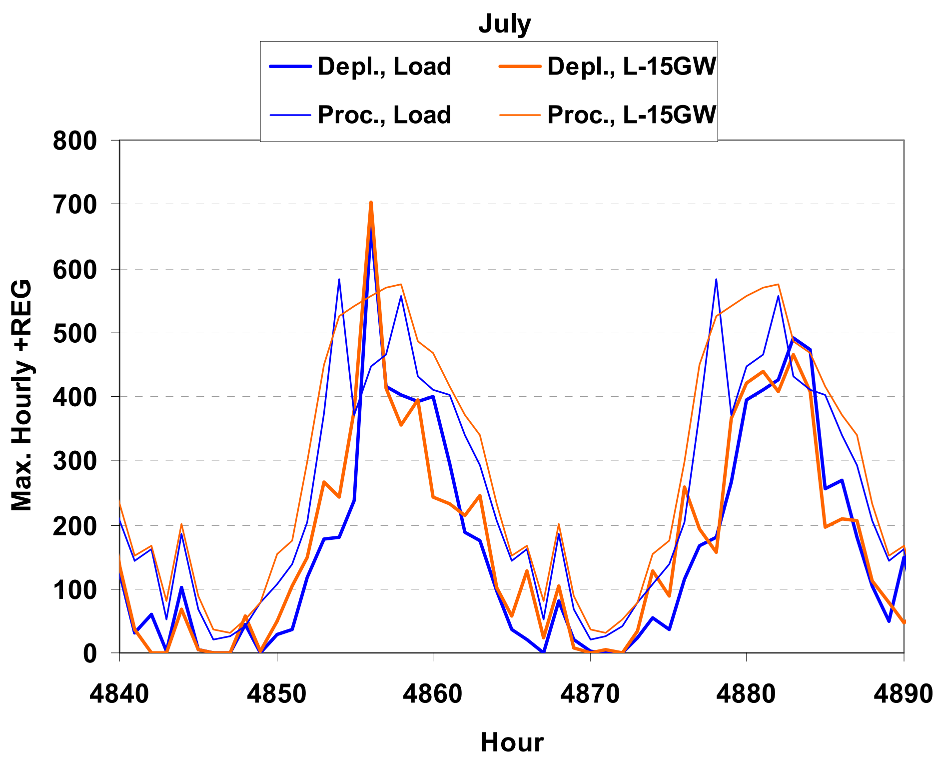
July
Depl., Load
Depl., L-15GW
Proc., Load
Proc., L-15GW
Max. Hourly +REG
800
700
600
500
400
300
200
100
0
4840
4850
4860
4870
4880
4890
Hour

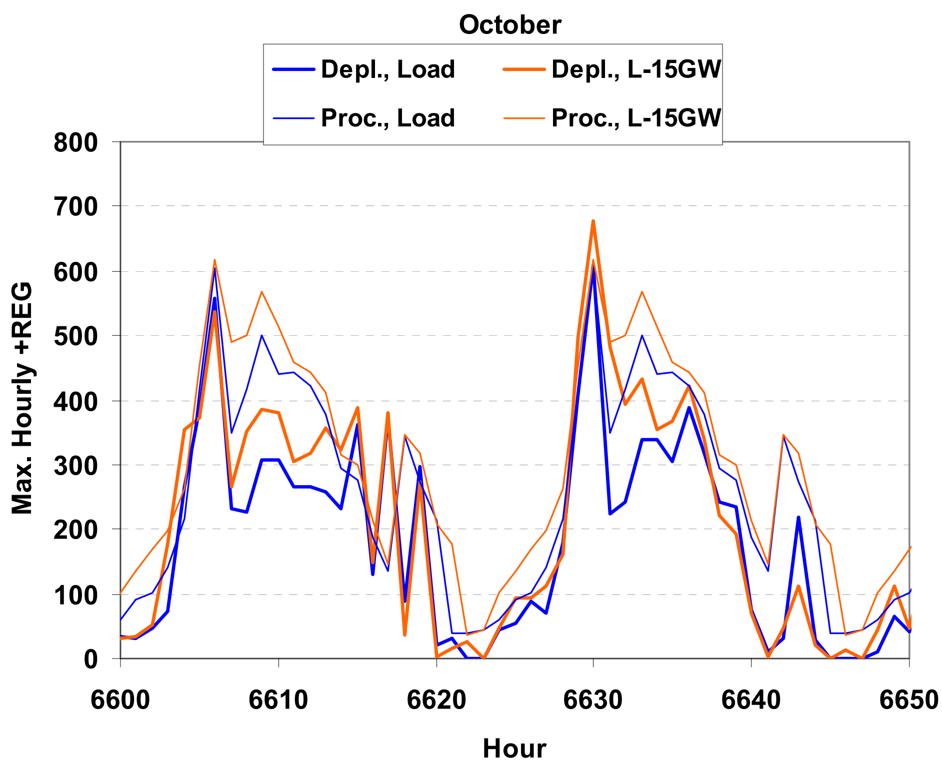
October
Depl., Load
Depl., L-15GW
Proc., Load
Proc., L-15GW
Max. Hourly +REG
800
700
600
500
400
300
200
100
0
6600
6610
6620
6630
6640
6650
Hour

APPENDIX F REGULATION ADJUSTMENT FACTORS

Incremental MW Adjustment to Prior-Year Up-Regulation 98.8th Percentile Deployment Values, per 1,000 MW of Incremental Wind Generation Capacity, to Account for Wind Capacity Growth.

	Hour																							
	1	2	3	4	5	6	7	8	9	10	11	12	13	14	15	16	17	18	19	20	21	22	23	24
Jan	2.8	4.2	3.1	3.7	2.5	0.4	2.3	2.2	4.2	5.9	7.6	5.7	4.7	3.3	2.8	2.3	4.0	8.6	4.2	2.7	1.6	2.7	1.4	1.6
Feb	3.6	4.0	2.9	2.9	1.5	1.8	5.2	3.5	4.9	6.0	5.1	5.2	5.3	4.2	4.3	3.5	3.8	8.6	5.5	1.9	1.4	3.1	1.9	2.2
Mar	5.5	5.3	4.6	4.2	2.6	3.3	7.1	7.9	6.8	5.1	4.2	3.4	2.8	2.6	2.7	2.3	2.9	7.7	6.8	2.1	1.1	3.0	1.5	2.8
Apr	3.1	3.6	5.0	4.0	2.4	2.5	8.5	11.6	10.0	5.6	4.2	3.4	3.2	2.5	2.1	2.1	3.5	9.2	8.2	4.1	1.0	0.8	0.0	1.4
May	3.6	3.3	4.3	4.3	4.2	3.3	8.7	8.8	8.1	5.7	6.0	4.4	3.6	3.8	3.9	4.2	4.7	11.6	5.9	0.6	0.0	1.0	1.4	2.5
Jun	2.3	2.6	3.3	3.7	3.9	2.4	8.5	8.2	6.6	4.5	4.2	3.1	2.5	2.5	0.7	0.2	1.3	7.5	3.3	1.7	0.7	0.3	0.6	1.3
Jul	1.0	2.8	4.1	3.7	3.0	3.2	11.2	10.2	6.5	5.3	3.3	2.2	1.4	0.4	-0.9	-1.3	0.3	3.4	0.9	1.1	0.1	0.0	1.0	1.2
Aug	1.4	3.8	4.5	4.5	2.2	0.9	6.3	6.8	6.6	6.6	3.2	2.6	2.1	1.2	1.4	1.3	1.3	4.6	1.2	0.9	0.7	0.8	1.1	1.3
Sep	3.2	4.0	3.7	3.5	1.8	1.9	6.9	7.7	8.3	6.9	3.5	4.8	3.8	2.3	1.6	1.2	3.0	9.2	3.1	0.9	0.1	0.4	0.8	1.9
Oct	3.4	2.8	2.4	2.2	1.7	1.8	5.0	5.8	6.1	5.9	4.0	5.4	3.2	2.2	1.2	1.7	3.1	6.8	0.8	2.1	0.0	0.2	1.8	2.5
Nov	2.7	3.2	3.6	3.0	2.2	2.3	4.6	5.3	6.9	6.8	5.1	5.6	4.1	3.7	1.8	1.7	5.8	12.8	4.8	3.8	1.0	1.6	2.2	1.4
Dec	2.8	2.4	1.4	2.1	1.2	0.4	2.8	2.7	3.8	4.6	6.8	7.0	6.0	4.4	3.3	3.0	5.0	9.9	4.3	2.6	2.1	4.3	2.0	1.5

Incremental MW Adjustment[1] to Prior-Year Down-Regulation 98.8^{th} Percentile Deployment Values, per 1,000 MW of Incremental Wind Generation Capacity, to Account for Wind Capacity Growth.

	Hour																							
	1	2	3	4	5	6	7	8	9	10	11	12	13	14	15	16	17	18	19	20	21	22	23	24
Jan	-1.2	-1.7	-2.2	-2.9	-2.5	-1.0	-0.8	-2.5	0.2	0.5	0.2	-2.4	-4.0	-3.6	-4.0	-3.5	-2.7	-5.1	-7.8	-10.4	-8.4	-5.2	-5.2	-3.6
Feb	-2.7	-3.6	-3.8	-4.4	-3.3	-1.7	-0.5	-2.5	-2.0	-2.3	-2.1	-2.3	-2.8	-3.7	-3.7	-2.6	-2.3	-6.9	-7.2	-10.0	-11.0	-7.3	-7.1	-4.7
Mar	-2.9	-3.8	-3.1	-2.3	-2.2	-2.2	-1.9	-0.9	-0.4	-3.7	-4.0	-2.1	-1.6	-2.3	-3.2	-3.9	-3.2	-6.1	-6.1	-8.3	-9.5	-6.5	-5.2	-3.6
Apr	-4.3	-4.5	-3.4	-3.0	-4.1	-2.8	-2.4	-1.3	-0.6	-2.9	-4.5	-3.3	-1.4	-2.5	-4.1	-4.5	-4.5	-7.3	-7.3	-10.7	-9.5	-7.4	-5.1	-3.0
May	-3.0	-1.6	-2.3	-1.7	-0.4	0.2	-0.4	-0.5	-1.1	-2.4	-3.5	-3.1	-1.8	-2.7	-2.6	-2.5	-3.8	-8.7	-7.5	-11.1	-9.7	-8.2	-5.8	-3.7
Jun	-1.4	-0.1	-1.7	-2.0	-0.5	0.7	1.2	0.7	0.2	0.0	-0.7	-0.9	-1.9	-2.8	-2.9	-2.8	-3.6	-11.0	-8.4	-7.7	-6.5	-5.8	-4.2	-2.7
Jul	-2.6	-1.5	-0.7	0.3	0.6	0.7	1.0	0.5	0.5	0.7	0.0	-0.7	-1.7	-2.3	-2.7	-3.1	-2.7	-8.0	-9.2	-8.7	-6.1	-5.5	-4.7	-2.6
Aug	-2.0	-1.7	-1.0	-0.6	-0.3	0.9	0.0	-0.3	0.2	0.1	-0.7	-1.0	-1.5	-1.9	-2.7	-4.1	-3.6	-4.7	-5.6	-7.2	-5.0	-5.4	-5.1	-2.7
Sep	-1.5	-2.2	-0.8	0.4	0.6	1.4	0.8	0.4	0.6	-0.4	-1.0	-0.9	-1.4	-1.5	-2.4	-2.7	-3.3	-7.2	-5.2	-7.2	-6.9	-6.5	-6.3	-4.1
Oct	-2.4	-4.0	-2.0	-0.6	-0.1	0.3	0.2	-0.3	0.0	-1.5	-2.6	-2.4	-2.6	-2.0	-2.3	-3.0	-4.3	-9.0	-6.8	-8.6	-6.8	-4.6	-4.2	-2.3
Nov	-1.8	-2.7	-2.6	-1.9	-0.7	-1.0	-1.5	-1.2	0.6	-1.5	-2.1	-2.0	-2.2	-1.5	-1.8	-3.5	-4.7	-6.8	-10.4	-14.1	-9.5	-5.7	-4.1	-1.7
Dec	-2.9	-3.2	-2.8	-2.6	-2.2	-1.9	-2.6	-2.9	0.8	0.6	0.4	-1.3	-1.8	-1.4	-2.6	-3.5	-3.2	-3.1	-7.9	-11.8	-7.9	-4.2	-3.9	-3.4

[1] In this study, down-regulation is reported as a negative number. Thus, a negative adjustment in this table implies an increased amount of down-regulation requirement.

APPENDIX G
REGULATION COST TEMPORAL CHARACTERISTICS

Up-Regulation (Perfect Forecast)

Load Alone

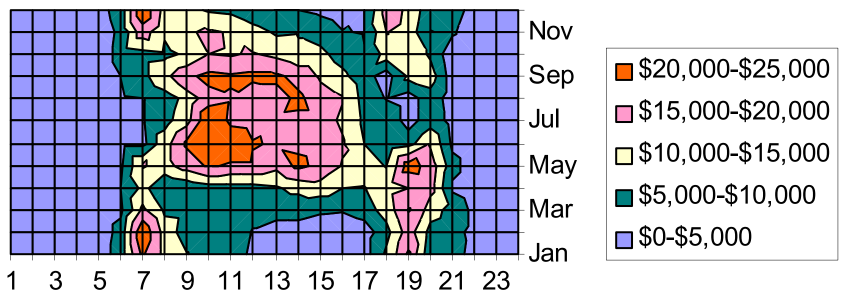

Load –15,000 MW Wind

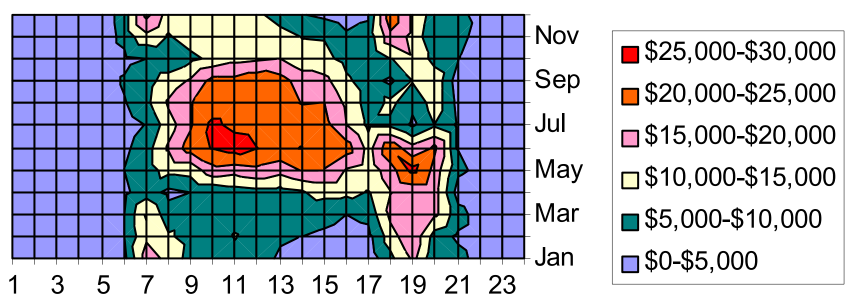

Differential, 0 to 15,000 MW Wind

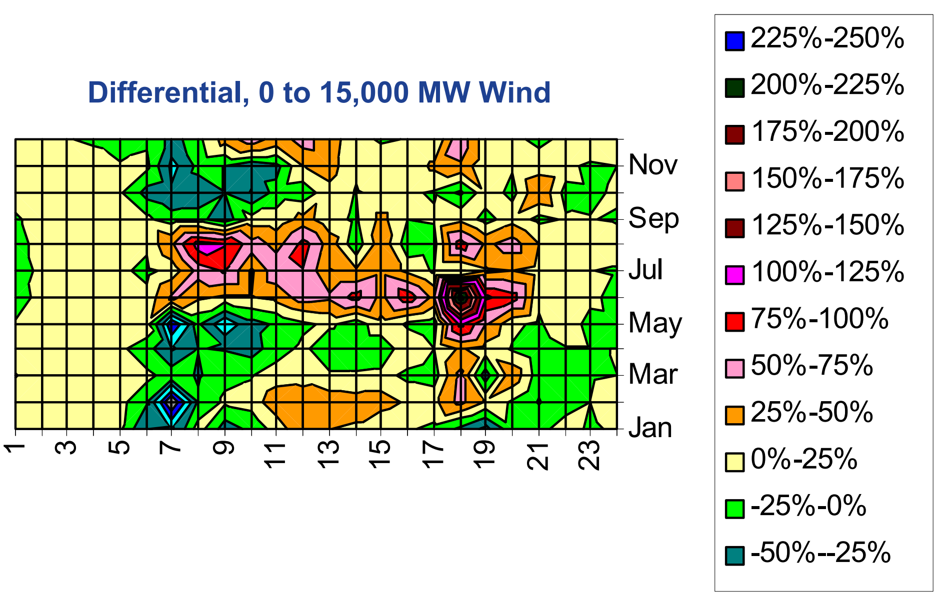

Down-Regulation (Perfect Forecast)

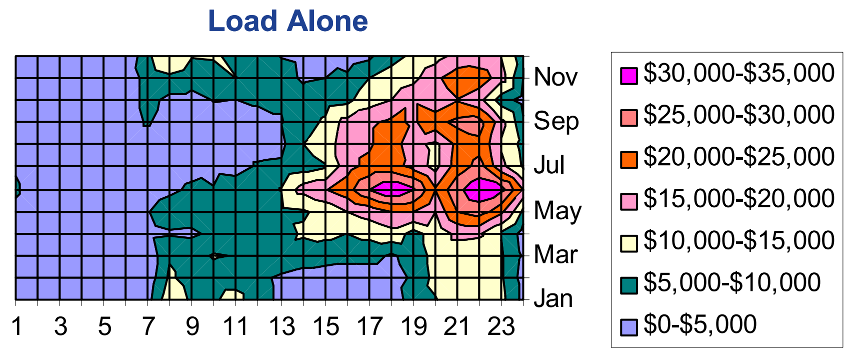

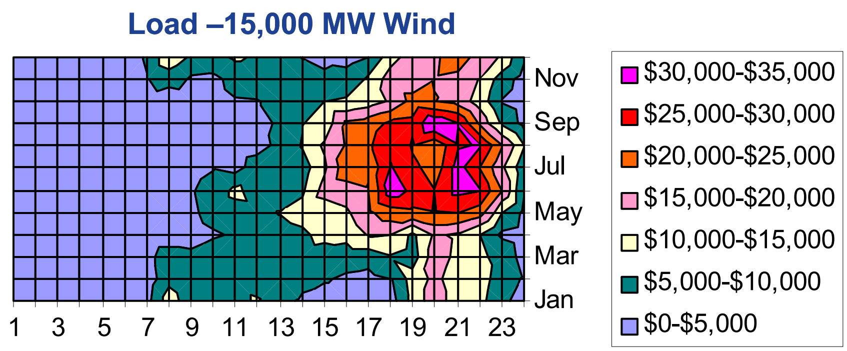

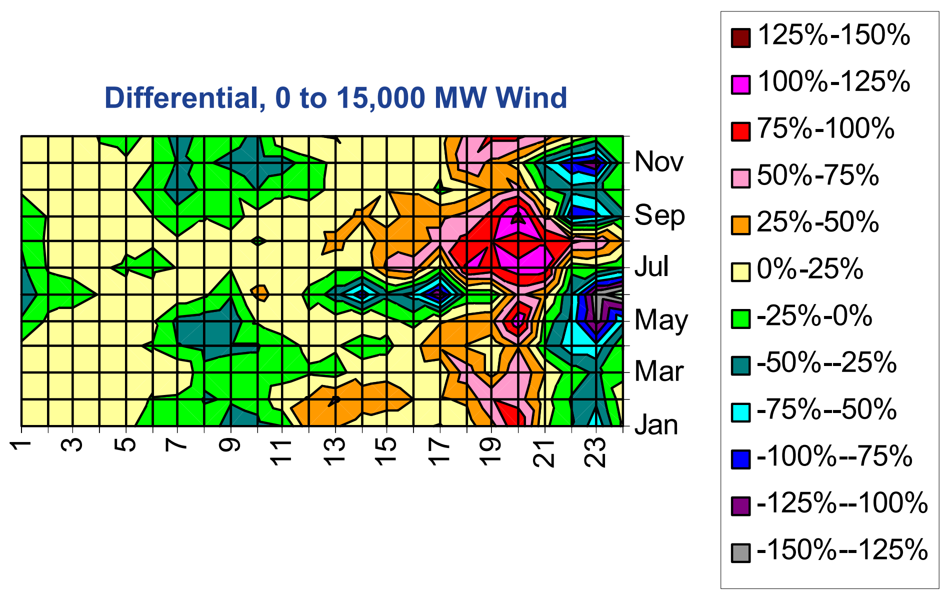

APPENDIX H AWS TRUEWIND REPORT:

ANALYSIS OF WEST TEXAS WIND PLANT RAMP-UP AND RAMP-DOWN EVENTS

Analysis of West Texas Wind Plant Ramp-up and Ramp-down Events

Prepared for:

GE Wind Energy

1 River Road, 2-620

Schenectady, NY 12345

Prepared by:

AWS Truewind, LLC

Jeff Freedman, Michael Markus, Richard Penc

463 New Karner Road

Albany, NY 12205

January 28, 2008

1. Introduction

The purpose of this report is to document weather-related causes in sudden excursions in wind power output from 14 interconnection points in the Electric Reliability Council of Texas (ERCOT) domain in 2005 and 2006 as well as a singular event in 2007, and to attempt to extrapolate the findings to a much larger deployment of wind energy in Texas. To identify and classify events, AWS Truewind:

1) Examined two years of one-minute plant output data provided by ERCOT and identified periods in which the aggregate wind generation increased or decreased by more than 200 MW in a 30-minute time frame (out of a total MW of 976 rated capacity). Obvious cases of non-weather curtailments and shutdowns were excluded.
2) Examined available meteorological records for the same periods and categorized the events by different meteorological causes.
3) Analyzed significant 2005-2006 weather events identified by ERCOT and determined which of those were associated with large changes in generation.
4) Analyzed the event of 24 February 2007 and established the cause for the decrease in energy production.

From the results of the above analysis, AWS Truewind estimated the maximum likely change in a 30-minute period for the 15,000 MW scenario defined in the Ancillary Services study. The period over which the maximum was to be estimated is two years.

2. Data and methodology

To identify ramp events, a 30-minute running mean filter was applied to two years of one-minute plant output data provided by ERCOT. The data represented the recorded output for 14 different interconnection points, some representing different parts of the same wind farm. The total rated capacity (judging from the maximum recorded output) was 976 MW. For the 24 February 2007 event, the estimated maximum output from 29 interconnection points analyzed was approximately 2000 MW. All of the projects are located in west central Texas (Figure 1).

From the distribution of step changes from one 30-minute period to the next, a 200 MW threshold was established, representing roughly 20% of the rated capacity of plants in the data sample. This resulted in the selection of 59 ramp-up and ramp-down events in 2005 – 2006 (see Tables 1a-d). Relevant meteorological data were acquired and analyzed, including 1) surface meteorological charts archived by the National Climatic Data Center (NCDC); 2) National Oceanographic and Atmospheric Administration (NOAA) wind profiler data from Jayton, Texas;[1] 3) NOAA National Weather Service (NWS) sounding data from Midland, Texas; 4) high-resolution (one-minute averaged wind speed and direction, temperature, humidity, pressure, etc.) Automated Surface Observation System (ASOS) station surface meteorological data from

[1]Wind profilers measure vertical profiles of horizontal wind speed and direction from near the surface to above the tropopause with a vertical resolution of 250 m and temporal averages of wind speed, direction and temperature every 6 to 60 minutes.

several sites nearest to the wind farms;[2] 5) visible and infrared satellite imagery archived by NOAA; and 6) NWS Doppler Next Generation Radar (NEXRAD) Weather Surveillance Radar 88 Doppler (WSR-88D) level II data archived at NCDC to identify convective features such as thunderstorm clusters and outflow boundaries. The ERCOT plant data were also used to examine the spatial and temporal variability of the meteorological forcing(s) associated with each ramp event.

3. Discussion and analysis

3.1. Meteorological causes

Thirty-five positive (increasing) ramps and twenty-four negative (decreasing) ramps met the threshold of a 200 MW change over a 30 minute period for the entire two-year study period. The meteorological causes of these events are described below. (Meteorological terms are defined in Appendix A.)

A. Ramp-up events

1) Frontal system/trough/dry line. These are density fronts or air mass discontinuities that move through parts or all of the ERCOT domain with an accompanying fall/rise pressure couplet, which can result in a rapid wind speed increase followed by a (more gradual) decrease. These systems mostly move from west to east or northwest to southeast, but can occasionally move from north to south. Fronts propagating at a speed in excess of 15 m s^{-1} (34 mph) are more likely to cause ramp-up events. These systems usually scale up to 1000 km in length and 100 - 200 km in breadth.
2) Thunderstorms and convection-induced outflow or gust fronts. These occur on the mesoscale (tens to hundreds of square kilometers) and can move in any direction and at speeds in excess of 25 m s^{-1}. Outflow boundaries usually propagate radially outward from thunderstorm clusters (or other mesoscale convective systems). Although gust fronts often lose strength rather quickly, they can instigate additional convection and subsequent gust fronts.
3) Low-level Jet (LLJ). This phenomenon occurs regularly throughout the year in the southern Great Plains. Southerly LLJs tend to be strongest but northerly LLJs do occur—mostly during the warm season. There are two types: (1) the nocturnal LLJ, a phenomenon unique to the plains of Texas, Oklahoma, and Kansas, caused by radiative cooling after sunset, and (2) a pre-frontal LLJ caused by an increasing pressure gradient ahead of a cold front. LLJ wind speed maximums occur between 100 m and 500 m above the ground, with a temporal maximum around 5 AM local time for the nocturnal LLJ. A special concern introduced by LLJs is the large vertical shears (upwards of 10 m s^{-1} [100 m^{-1}]) that can occur across the turbine rotor plane. Direct evidence of LLJs affecting wind farms is not clear from this analysis but their presence was noted in many of the frontal cases from the sounding and profiler data.

B. Ramp-down events

[2]Parameters available from the ASOS stations include temperature, dew point, pressure, wind speed and wind direction (both at 10m mast height), present weather, visibility and obstructions, present weather and accumulated precipitation.

1) These events generally occur with the rapid slackening of a pressure gradient or the passage of local pressure couplet. This feature is can be associated with (1), (2), or (3) above.
2) Ramp-down events can also be caused by high wind speeds that exceed the cut-out speed of wind turbines (typically 22-25 m/s). This occurred during the 24 February 2007 event, and on several other occasions associated with transient convective systems such as 23 June 2006.

For the 59 events considered during 2005 and 2006, the largest changes occurred on 9 July 2005 (a nearly 400 MW increase, or over 300% from a low of about 200 MW) and 12 May 2005 (a 331 MW decrease, or more than 58% from the peak of 571 MW). Although the 24 February 2007 event observed a peak 30 minute decrease of 455 MW, this was based upon roughly twice the rated capacity, and thus was not proportionately as severe as the 12 May 2005 event (see analysis in section 4 below).

3.2 Statistical Breakdown of the Ramp Event Types

Approximately 60% of the 59 events identified during 2005 – 2006 were ramp-up events, and 40% were ramp-down events (Table 3). The slight favoring of ramp-up events is consistent with the finding that rapidly moving transient features such as frontal systems and convective outflow boundaries tend to produce rapid wind increases, which then subside more gradually.

Convective events were the primary cause of all ramp events, followed by frontal passages and weakening pressure gradients (Table 3). Although a distinct low-level jet (LLJ) was common to several events, it did not appear to be a primary cause of the ramps discussed in this report.

The most frequent cause of ramp-down events is a weakening pressure gradient (Table 3). The ramp downs listed as "convective" are associated with pressure couplets—a rapid fall followed by a rapid rise in pressure. Within the couplet is the strong pressure gradient. Once it passes, winds quickly weaken in response to the slackening gradient.

Most convective cases (14 of 19) initiated ramp ups (Table 3). Analysis of the plant output data showed that subsequent ramp downs associated with convective systems are below the established threshold (200+ MW change within 30 minutes).

During the cold season (October – March), frontal passages account for most ramp events. Weakening pressure gradients also account for a significant number of these events. Consistent with climatology, convective events are less frequent during the cold season.

3.3 Temporal Distribution of Ramp Events

There is a distinct diurnal maximum (Figure 2) in the frequency of ramp-up events during the evening hours, particularly around 19:00 (5 PM) local time, when convection, especially strong to severe thunderstorms, is climatologically favored.[3]

[3] See http://www.srh.noaa.gov/ssd/techmemo/sr-191.htm, available online from NWS Midland-Odessa.

There is a broad maximum in the frequency of ramp-up events from late winter through summer (Figure 3), while ramp-down events show no clear pattern. This is consistent with the dominance of convection as a cause of ramp-up events, as the warm season in Texas begins during the early spring. Ramp-up events increase in frequency during spring and summer and decrease rapidly once the convective season ends in September.

3.4 Ramp Events—Case Studies

Here we present representative cases with a more detailed analysis of the relationship between meteorological conditions and plant output.

1) *11 August 2006: Convective (outflow boundary causing positive ramp event)*. A complex of thunderstorms was oriented south-north and just west of Midland (KMAF). These thunderstorms showed little movement between 18:00 and 19:00 local daylight time (LDT) but generated multiple outflow boundaries (stretching from just north of Fort Stockton (KFST) to south of Lubbock (KLBB)--a distance of nearly 300 km) that propagated eastward across several of the interconnnection points by 20:00 LDT (Figure 4). As the outflow boundaries passed, wind speeds increased considerably (peak sustained winds exceeded 15 m/s at Fort Stockton and Odessa around 18:00 LDT), and resulted in a rapid increase in output at most interconnection points by 21:00 LDT. The thin white line marked by the red arrows (Figures 4a and b) shows visible evidence of outflow from the thunderstorm complex; such outflow boundaries occur with most strong to severe thunderstorms. Climatologically, between 40 and 50 such storms occur within any given 25 km square area in west Texas. They are, however, difficult to forecast more than a few hours in advance, and the temporal predictability of movement and intensity of associated gust fronts is usually less than an hour.
2) *Frontal passage with pressure couplet:*
   a. *28 December 2006*: *weak gradient ahead of cold front*. An area of weak pressure gradient moves eastward across west-central Texas between 14:00 and 15:00 local standard time (LST) (Figures 5 and 6). Since wind speed is proportional to the pressure gradient, there is a significant reduction in wind power output and wind speed as this feature passes (Figures 5a-c). The drop in wind speed is most notable Fort Stockton (KFST), Lubbock (KLBB) and Odessa (KODO). There is a secondary drop in power output around 16:00 LST as winds continue to diminish (to below the cut-in value of 4 m s^{-1} at the stations mentioned above).

   b. *28 December 2006*: *frontal passage.* Following the weak pressure field, a stronger gradient moves into the area after the frontal passage (approximately 15:00 – 16:00 LST), and wind speeds and output increase rapidly by 18:00 LST (Figure 7a-c). Plant output, which had decreased to about 100 MW (or 10% of the rated capacity), then rapidly rose as wind speeds rose above the cut-in value.
3) *14 November 2006: Dry line.* Dry lines are similar in effect to frontal passages, except they tend to occur mostly during the warm season, forming during the late morning in eastern New Mexico and moving eastward into central Texas by evening before returning westward overnight. They can trigger outbreaks of severe weather and locally strong winds. During the morning of 14 November, a tightening pressure gradient ahead of a dry line located in west Texas produced an increase in wind speed and power output around 11:30 LST (Figure 8).

Wind speeds had been rather low earlier in the morning, but rapidly increased ahead of the dry line, resulting in a 264 MW increase in output between 11:30 and 12:00 LST.

4) *23 May 2006: Weakening pressure gradient.* Winds were rather strong during the early morning of this event, exceeding sustained speeds of 10 m/s at Fort Stockton (Figure 8b) and generating a total of 800 MW. However, a rapidly decreasing pressure gradient (Figure 8c) resulted in a steep drop off in power production (224 MW; see Figure 8a) between 4:45 and 5:15 LDT. As the pressure gradient increased later in the morning, wind speeds and output gradually increased.

4. The 24 February 2007 Ramp-Down Event

During this event, high wind speeds exceeded the turbine cut-out threshold across most wind projects, resulting in a rapid drop in energy production. A strong upper-level storm system passed over northern New Mexico and the panhandle of Texas into Oklahoma. This substantially tightened the pressure gradients over west Texas, resulting in strong to severe winds along a straight line across much of the area. The maximum wind gust reported was 42 m/s (94 mph). Analysis of the aggregate plant output for 24 February shows that, in response to the tightening pressure gradient and increasing winds, aggregate output increased from just over 1100 MW to nearly 2000 MW (the aggregate rated capacity) by approximately 9 AM (Figures 9 and 10). By 10 AM, as sustained winds at ASOS stations exceeded 25 m s^{-1} (55 mph) at Guadeloupe Pass and Abilene (Figure 9b) and certainly higher at hub height, the output at most wind farms declined as the turbine-cutoff threshold wind speeds were reached (Figures 9a and 10). As the most intense pressure gradients and winds moved eastward, wind speeds relaxed and turbines resumed power production, resulting in a more gradual increase in total output to pre-event levels.

The drop in plant output amounted to over 1500 MW over a 90 minute period, with the most rapid declines occurring at the Horse Hollow interconnections (Figure 10). The largest decrease in 30 minutes, however, was about 450 MW (between 1104 and 1134 LST). On a proportional basis, this 450 MW decrease represented about 22.5% of the plant rated capacity. Scaled to the 976 MW rated capacity studied in 2005-2006, it would have been a 220 MW ramp-down event. Although it would have exceeded the threshold of detection, it would not have been classed as one of the more severe ramp downs observed in this period. However, this event was unusual both in the magnitude of the 90-minute drop it caused and in the large geographic area it affected. Its implications for much larger deployments of wind generation in the state are discussed in the following section.

5. Probability and Predictability of Ramp Events

Based upon the period 2005 - 2006, ramp events as defined in this report are likely to occur about once every 6 - 7 days (Table 2); multiple events in one day may occasionally occur (see 28 December 2006), especially when pressure couplets are involved (i.e. ahead and behind a frontal system).

Frontal passages/troughs/dry lines of any severity generally occur about once every 3 – 5 days during the cold season, and 5 – 7 days during the warm season. From Table 2, such events initiating ramp-up excursions meeting the threshold of detection in this study would occur about

20 days per year, or once every 2 – 3 weeks. Ramp-down events are much rarer, occurring about once every two months.

Convective events occur with widely varying frequency. The Storm Prediction Center (SPC), part of the National Weather Service (NWS), monitors and forecasts severe weather over the continental United States. An examination of the annual total number of severe thunderstorm wind events (defined as winds estimated to be in excess of 29 m/s) as compiled by the SPC for the last 10 years shows a wide variation, from 32 in 2000 to 134 in 2003, within the ERCOT domain, illustrating the large variability in year-to-year severe thunderstorm winds.

Forecast Skill and Lead Time. All weather phenomena causing ramp events can be forecast. However, the effective lead time and skill of the forecasts varies considerably, as indicated in Table 2. Generally speaking, frontal passages and related phenomena can be forecast several days in advance, although the accuracy of the forecast and in particular of the timing of the frontal passage improves markedly as the event approaches. Several hours ahead of time, the arrival of the frontal passage may be forecast within perhaps a 30-minute to one-hour window.

Severe thunderstorms and other convective events are much more difficult to forecast. Among its suite of forecasting products, the SPC issues convective outlooks which serve as guidance to the local NWS forecast offices. These forecasts identify separate severe weather risk areas (slight, moderate, and high) and are used to describe the expected coverage and intensity for the severe weather threat one to three days ahead along with severe weather probabilities for the potential threat. When conditions become favorable for severe thunderstorms (those that produce winds in excess of 58 mph (26 m/s) and/or hail 3/4 inch or larger) to develop, the SPC usually issues a severe thunderstorm watch. These watches are generally issued a few hours ahead of expected severe weather.

The NWS assesses its thunderstorm forecasting success using several measures, including the probability of detection, false alarm ratio, and average lead time. These are defined below.

> **Probability of Detection (POD):** This is the percentage of all severe weather events which were successfully predicted (a perfect score would be 100%). For example, if 60 warnings were issued and there were 100 total severe weather events reported (60 warned, 40 unwarned), the POD would be 60%.
>
> **POD** = warned events / (warned events + unwarned events)
>
> **False Alarm Ratio (FAR):** This ratio measures how often false alarms (forecasted event, but none occurs) are issued. Ideally this number should be close to 0%. Some false alarms occur as a result of storms that may appear severe, or are borderline severe, while others occur because the severe weather occurred where no one was around to observe the event.
>
> **FAR** = unverified warnings / (verified warnings + unverified warnings)

Average Lead Time: This is simply the length of time from when the warning is issued until the first report of severe weather in the warned area. This time can be anything from 0 minutes up to the total valid time of the warning.

Table 3, provided by the NWS, list the forecast statistics for the spring (March, April, and May) and summer (June, July, and August) seasons of 2005 and 2006 for the ERCOT domain. The results indicate a significant amount of variability in severe thunderstorm cases from season to season and year to year. Forecasts tend to be better during active periods since they often have more organized weather systems. Inactive periods, on the other hand, tend to have disorganized weather systems that are more difficult to track, model, and predict. From the statistics in this table, the average lead time for severe thunderstorms in west Texas during this two-year period was about 20 minutes. The probability of correctly forecasting a severe thunderstorm averaged between 70% and 85%. However, the percentage of false alarms was also relatively high, ranging from about 60% to 70%.

Analysis of 15,000 GW Scenario. Based on the foregoing analysis of the 2005-2006 and 24 February 2007 events, we assessed the probability and severity of possible extreme ramp events for the proposed distribution of wind projects in the 15,000 GW scenario (see Table 4). It should be stressed that this analysis is highly uncertain as it is based on limited wind project data for a two-year period. It should be confirmed through a more detailed assessment spanning both a longer period and a larger geographic area.

For convective events, we find CREZ 5, 6, and 9 would be the most susceptible to large excursions in power generation. Since the maximum propagation rate of the systems identified above is perhaps 25 m/s, and the orientation of these features tends to be north-south, under a worst-case scenario, where CREZ 5 and 9 are simultaneously affected (with rated capacities of 3251 - 4529 MW under the 15000 MW scenario), excursions of ±1300 MW can be expected at least 2 - 4 times per year. In addition, as CREZ 10 would have by far the largest wind capacity (4607 MW), a weather system affecting this entire zone could conceivably result in a 30-minute excursion of more than 1100 MW. Based on the largest events observed in 2005-2006 (> 25% excursion), the frequency of such events is estimated to be about 2 - 4 times per year.

For frontal events, dry lines, and pressure couplets, a larger area would be affected but as propagation speeds are generally lower (15 - 20 m s^{-1}) , it is highly unlikely that more CREZs would be affected during any 30 minute period than during convective outbreaks.

Finally, an event of the magnitude and areal coverage of 24 February 2007 could produce over a 20% reduction in power over most of the CREZs (with estimated combined capacity of 12,300 MW) in 30 minutes, resulting in a *maximum* power reduction for affected CREZ areas in excess of 2800 MW (see Table 4). We estimate the probability of such an event as one occurrence every 3 - 5 years.

6. Uncertainties

Every meteorological event, although exhibiting many structural similarities, is nevertheless temporally and spatially unique. Frontal systems propagate at different (and not necessarily consistent) speeds, and pressure couplets and convective systems (and associated outflow boundaries) also dynamically evolve over time. Therefore, the above analysis cannot capture every possible scenario that could occur in the ERCOT region.

Furthermore, not all plants will experience a ramp up or ramp down simultaneously as they are geographically displaced from each other and rarely oriented in parallel with these features. Thus, increasing the spacing between wind farms and altering their distribution may mitigate the aggregate ramping due to small-scale meteorological phenomena such as these pressure couplets, or from convective outflows, common in the warmer months.

Appendix A

Glossary of Weather Terms (from the American Meteorological Society's Glossary of Meteorology, 2nd Edition)

Convection. Motions that are predominantly vertical and driven by buoyancy forces arising from static instability,

Dryline. A low-level mesoscale boundary or transition zone hundreds of kilometers in length and up to tens of kilometers in width separating dry air from moist air. In the United States the dryline, which marks the boundary between moist air from the Gulf of Mexico and dry continental air from the west, is found in the Plains region. It is most often present during the spring, where it is often the site of thunderstorm development. Typically the dryline in the United States advances eastward during the day and retreats westward at night.

Front. The interface or transition zone between two air masses of different density. Generally, the temperature distribution is the most important regulator of atmospheric density. However, in the southern Plains, especially over west Texas, humidity differences are commonly separate distinct air masses (see "dry line")

Low-level Jet (LLJ). A region of relatively strong winds in the lower part of the atmosphere. Specifically, it often refers to a wind maximum in the boundary layer (from 100 - 500 m above the ground), common over the Plains states at night during the warm season (spring and summer).

Mesoscale. Atmospheric phenomena having horizontal scales ranging from a few to several hundred kilometers.

Pressure gradient. The rate of decrease (gradient) of pressure in space at a fixed time.

(Thunderstorm) Outflow Boundary. A surface boundary formed by the horizontal spreading of thunderstorm-cooled air. Outflow boundaries may intersect with each other or with other features (fronts, low-level jets) and act to focus new convection. Outflow boundaries may be short-lived, or last for longer than a day.

Trough. An elongated area of relatively low atmospheric pressure. A weaker feature than a "front."

Table 1a. Negative Ramp Events For ERCOT Domain 2005			
Date	Begin Time (Local)	Ramp (MW)	Event Classification
12-May	5:20 AM	-331	weakening pressure gradient
15-Jul	3:40 AM	-265	convective pressure couplet
19-Feb	11:45 PM	-239	weakening pressure gradient
27-Feb	7:31 PM	-235	weakening pressure gradient
28-Aug	9:39 PM	-230	convective pressure couplet
21-Mar	8:28 PM	-225	weakening pressure gradient
23-May	6:58 AM	-218	weakening pressure gradient
12-Aug	7:06 PM	-218	Stabilization
24-Apr	3:45 PM	-218	frontal passage
9-Oct	6:38 PM	-214	convective pressure couplet
10-Jun	8:14 AM	-206	weakening pressure gradient
14-May	3:49 AM	-204	frontal passage
18-Feb	12:11 PM	-202	weakening pressure gradient

Table 1b. Positive Ramp Events For ERCOT Domain 2005			
Date	Begin Time (Local)	Ramp (MW)	Event Classification
9-Jul	8:14 AM	397	thunderstorm outflow
28-Aug	8:48 PM	321	convective
10-Feb	7:27 AM	291	Frontal passage
10-Jul	5:42 PM	251	thunderstorm outflow
10-Aug	6:18 PM	248	convective
3-Aug	7:19 PM	248	convective
11-Sep	8:28 PM	246	convective
15-Jul	4:47 AM	246	thunderstorm outflow
23-Jul	4:07 PM	229	convective
10-Mar	8:29 PM	226	frontal passage
29-Apr	9:27 PM	226	frontal passage
26-Mar	7:18 PM	215	frontal passage
10-Apr	10:54 AM	212	frontal passage
13-May	7:02 PM	210	dry line (frontal)
15-May	8:54 AM	209	convective
29-Mar	3:22 PM	206	frontal passage
12-Jan	11:10 AM	204	frontal passage
25-Apr	9:39 AM	201	frontal passage
23-Feb	11:04 PM	200	frontal passage

Table 1c. Negative Ramp Events For ERCOT Domain 2006			
Date	Begin Time (Local)	Ramp (MW)	Event Classification
15-May	2:40 AM	-291	weakening pressure gradient
28-Dec	2:29 PM	-281	weak gradient ahead of front
22-Mar	9:14 PM	-266	weakening pressure gradient
24-Feb	10:58 PM	-252	convective
30-May	8:02 AM	-225	weakening pressure gradient
20-Jan	1:17 AM	-225	trough passage
23-May	4:46 AM	-224	weakening pressure gradient
23-Jun	5:40 AM	-221	outflow pressure couplet
13-Aug	8:15 PM	-219	weak gradient ahead of front
28-Sep	11:26 AM	-216	frontal passage, slack gradient
20-Dec	12:26 AM	-214	Frontal passage, slack gradient

Table 1d. Positive Ramp Events For ERCOT Domain 2006			
Date	Begin Time (Local)	Ramp (MW)	Event Classification
23-Jun	4:49 AM	294	thunderstorm outflow
14-Nov	11:29 AM	264	dry line
28-May	7:11 PM	264	dry line
28-Apr	3:49 PM	258	frontal passage
20-Jul	7:33 PM	257	trough passage
26-Sep	7:58 PM	255	trough passage
19-Dec	10:16 PM	253	trough passage
11-Aug	8:28 PM	242	Surface trough/convection
1-Jul	10:48 PM	241	trough passage
1-Aug	2:10 AM	234	thunderstorm outflow
28-Dec	6:30 PM	224	frontal passage
25-Aug	6:32 PM	215	thunderstorm outflow
27-Oct	2:07 PM	211	frontal passage
17-Oct	12:56 AM	208	surface trough
4-Aug	2:13 AM	203	convection
16-Jun	10:34 PM	202	dry line

Table 2. Summary of weather phenomena associated with ramp events, their frequency, and typical forecast lead time

	Ramp up/Ramp down	Typical Events per year	Preferred time of day/season	Forecast Lead Time
Frontal Passage	12/3	Around 50	Winter, followed by Spring or Fall, no preference for time of day, although pre-frontal convection usually occurs during evening.	Can usually be forecast days in advance with better accuracy of timing as event approaches. More precise frontal timing can be accurately forecast with a few hours lead time on a given day. Within 2-5 hours of anticipated frontal passage they can be forecast to perhaps within 30 minutes.
Dry Line	4/0	40-50	Spring, Summer. The dry-line generally advances east by day, retreats by night	Dry line formation can typically be anticipated a day or so in advance. When formed, dry line passage can be forecast on the local scale a few to several hours in advance.
Troughs	5/1	Around 50	Anytime, no strong seasonal preference, no hourly dependency	Similar to frontal passages, above.
Weakening Pressure Gradient	0/14	80-100	Anytime, no strong seasonal preference, no hourly dependency	Large scale gradients similar to "fronts"; smaller scale gradients related to small scale pressure couplets similar to "convection".
Convective Outflow	14/5	40-60 days in the project area at a given point. Can have multiple outflows from one event.	Spring or Summer, afternoon and evening	Occurrence can be "nowcast" using current data, with a few hours lead. Individual outflows perhaps 20-30 minutes in advance of arrival at a particular site. Probabilities in a region may be forecast a few (2-3) days in advance with good confidence
Stabilization	0/1	unknown	Around sunset	Can be anticipated perhaps a day or two in advance for probabilities.
High Wind	1/1	1	Anytime, preference for cold season	A few hours to several days

Table 3. **NWS Severe Thunderstorm forecasting statistics (2005-2006)**

	# of Events	# of Warnings	POD	FAR	Lead Time (minutes)
Spring 2005	57	140	0.72	0.70	18
Spring 2006	414	821	0.86	0.59	21
Spring 2005-2006	471	961	0.84	0.61	21
Summer 2005	343	588	0.80	0.58	20
Summer 2006	106	217	0.75	0.67	15
Summer 2005-2006	449	805	0.79	0.60	19

Table 4. Extreme Events Summary: 15,000 GW Scenario

Weather Event	CREZs Affected	Aggregate Rated Capacity (MW)	Maximum 30-Minute Ramp (MW)	Frequency (# times approaching max ramp per year)
Convective	5, 9	3251	+1300	2 - 4
Frontal/dry line/trough	5, 6, 9	4529	+1324	2 - 4
Weak gradient	5, 6, 9	4529	-1313	2 - 4
High Wind	2, 4, 5, 6, 7, 9, 10, 12, 14	12,329	-2836	< 1

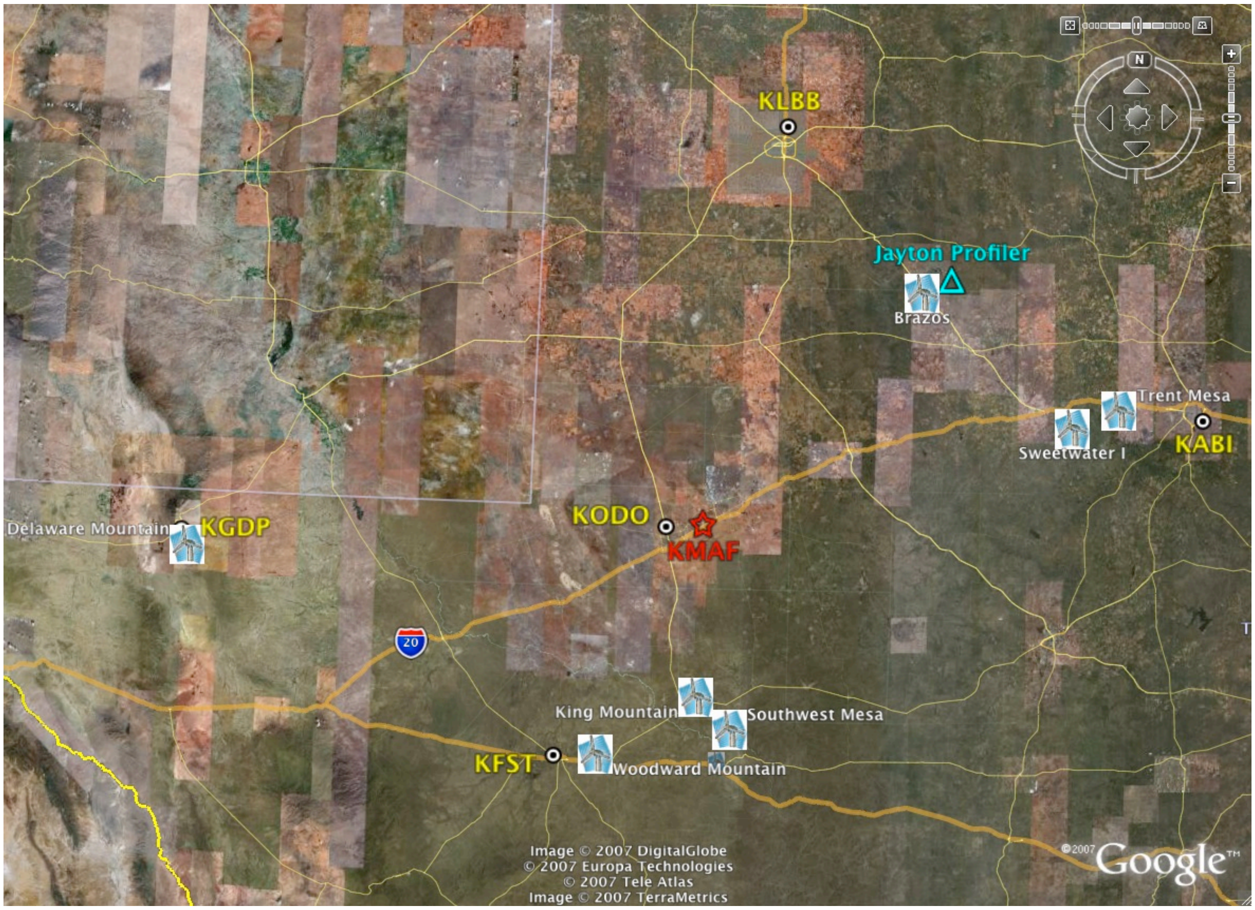

Figure 1. *Locations of Wind Farms, ASOS stations (yellow text), profiler (cyan text) and NEXRAD (red text). Identifiers for surface meteorological data include KODO (Odessa), KABI (Abilene), KLBB (Lubbock), KGDP (Guadeloupe Pass) and KFST (Fort Stockton). KMAF is the Midland NEXRAD.*

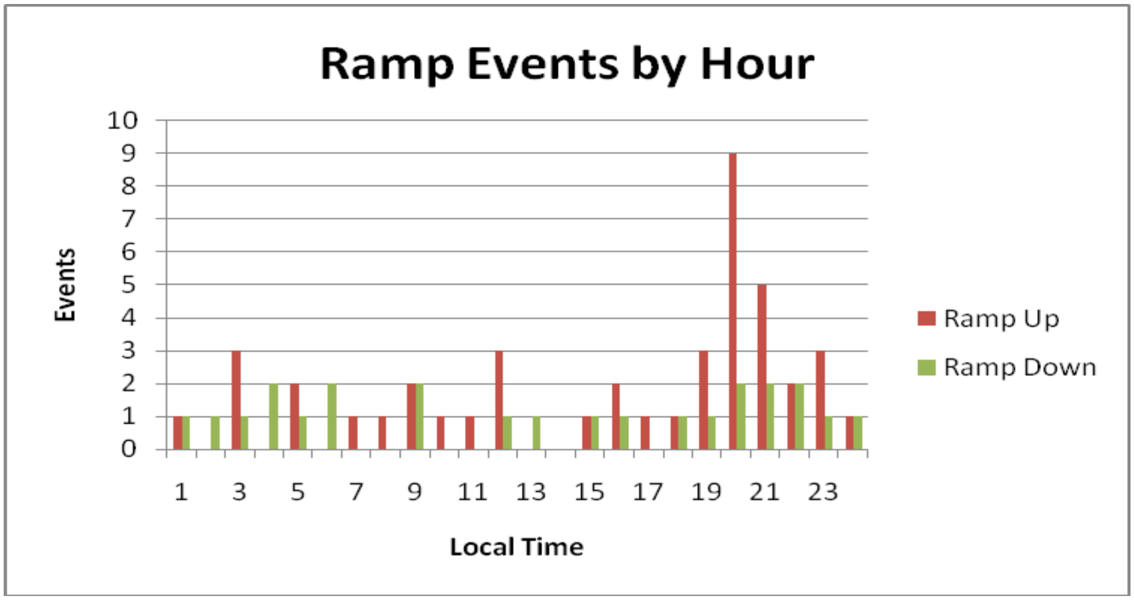

Figure 2. Distribution of ramp events by hour of day.

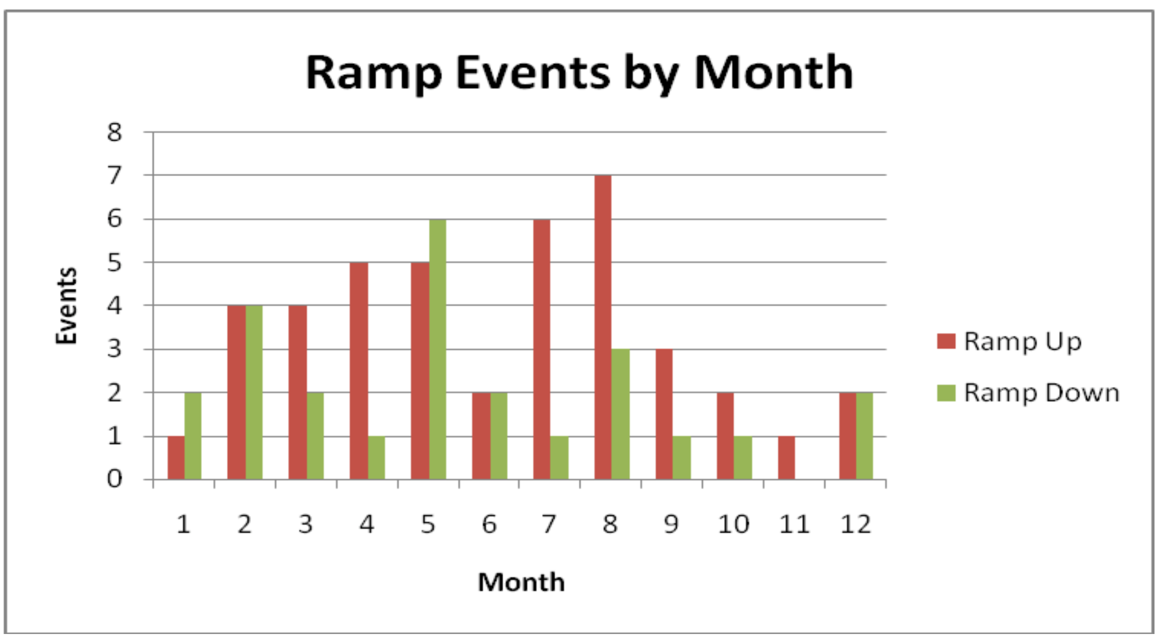

Figure 3. Distribution of ramp events by calendar month.

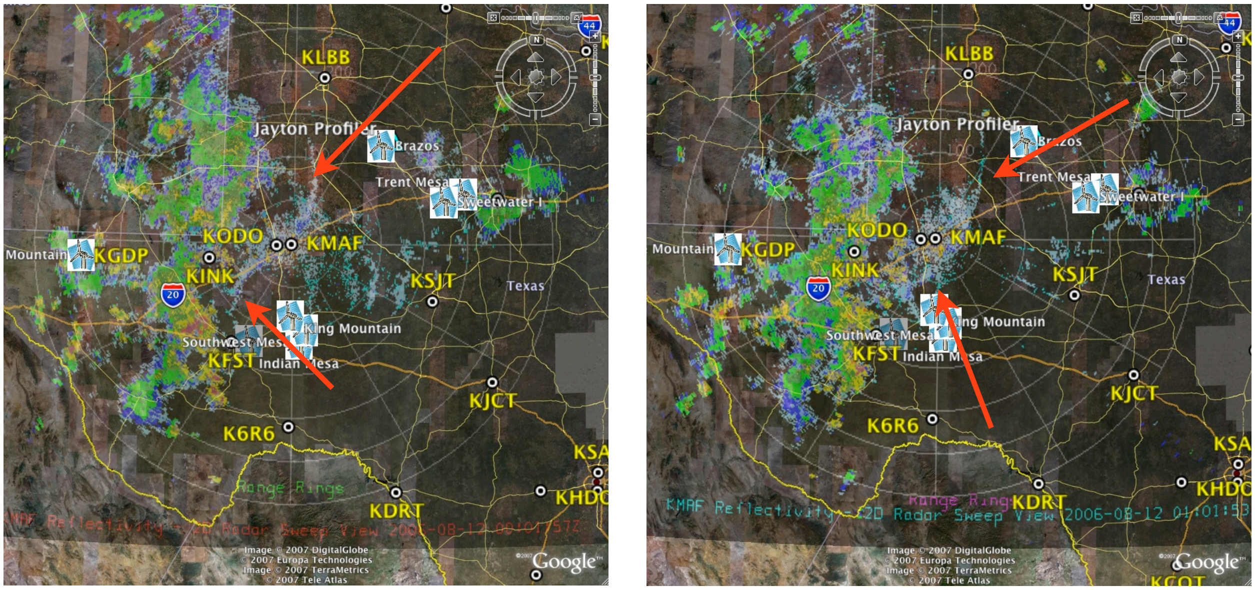

Figure 4. Left: NEXRAD (radar) image from Midland TX (KMAF) for 1801 LT on 11 August 2006. Red arrows show outflow from thunderstorm complex to the west. Right: outflow boundary an hour later (1901 PM LT) now approaching cluster of wind farms south and northeast of KMAF. Shortly after, ramp event of +600 MW was observed within a 30 minute period. Lower arrows indicate boundary traversed about 100 km in 1 hour.

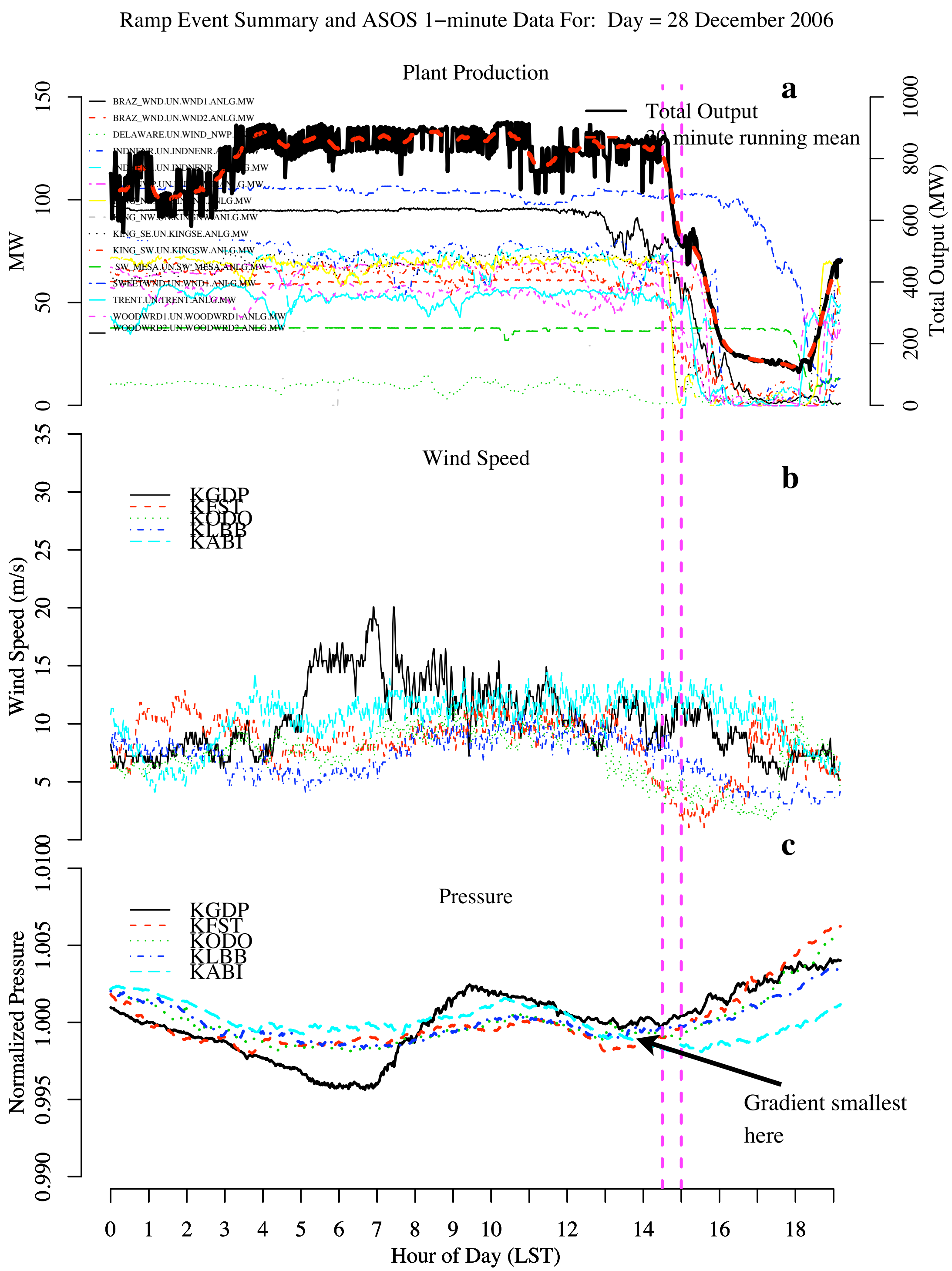

Figure 5 (a): Time series of individual and total plant output (MW) for 28 December 2006. (b) same as (a), except for wind speed (m s^{-1}) at ASOS stations; (c) same as (b), except for normalized pressure (1-minute station pressure divided by mean daily station pressure). Dot-dash magenta line represents ramp period.

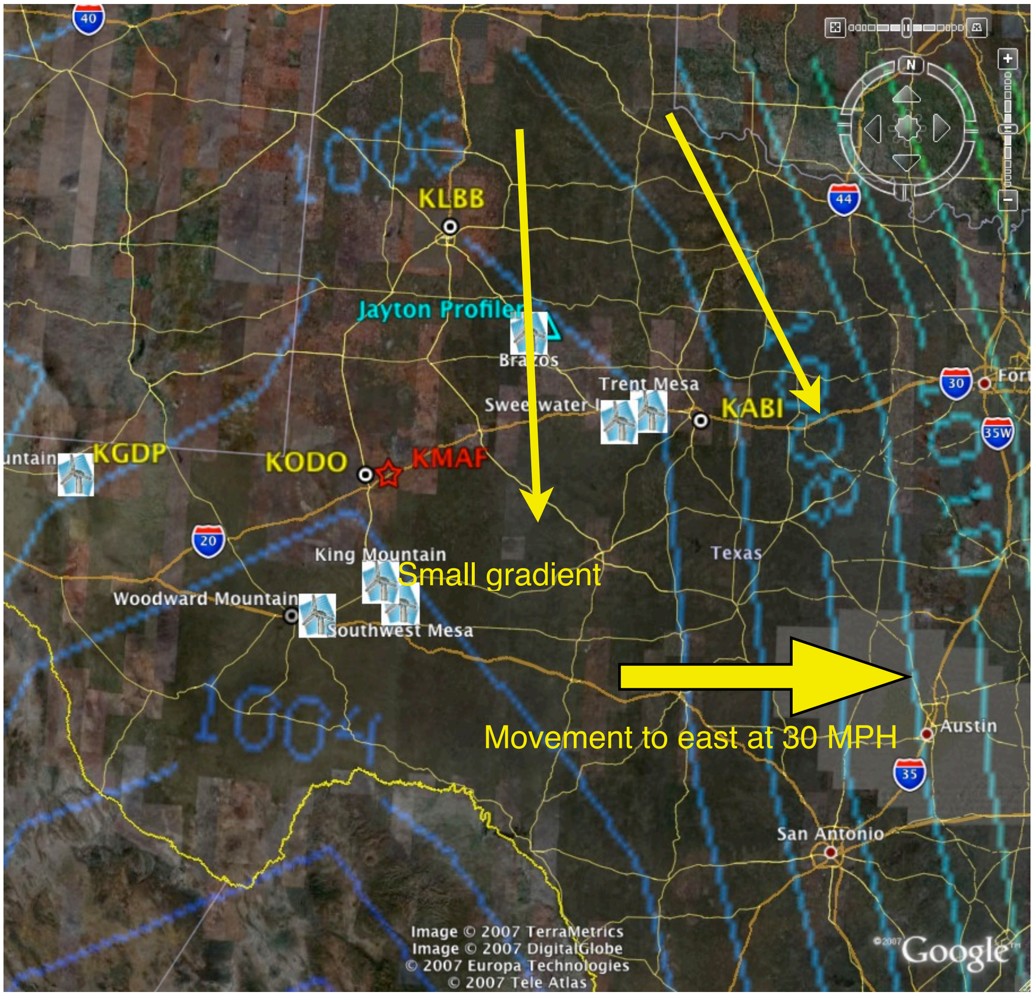

Figure 6. Sea level pressure (hPa, blue lines) for 1900 LT 28 December 2006. Note large pressure gradient has just moved through wind farms near Abilene (KABI) to be followed by rapidly slackening gradient.

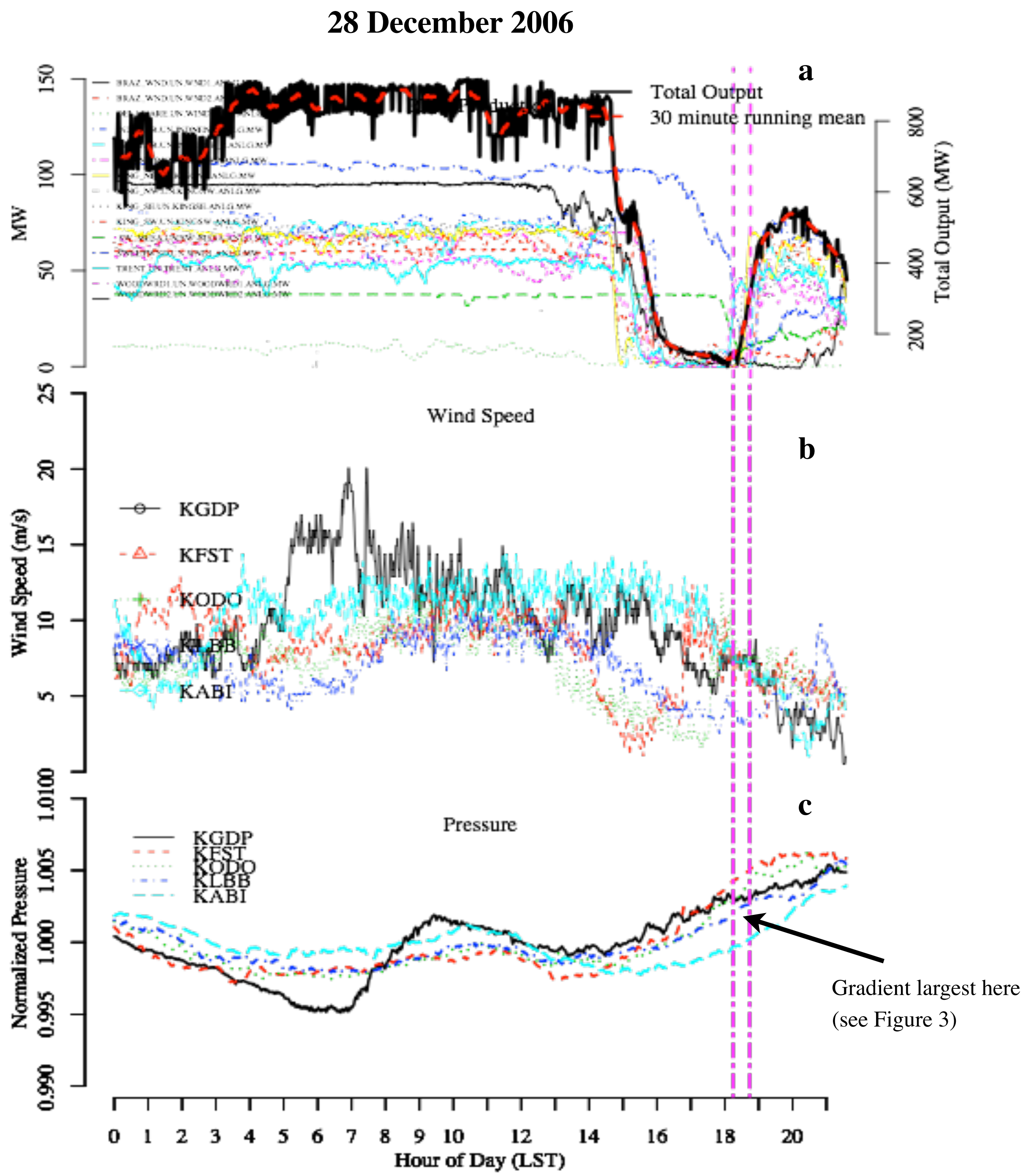

Figure 7. Same as Figure 5, except for ramp up event.

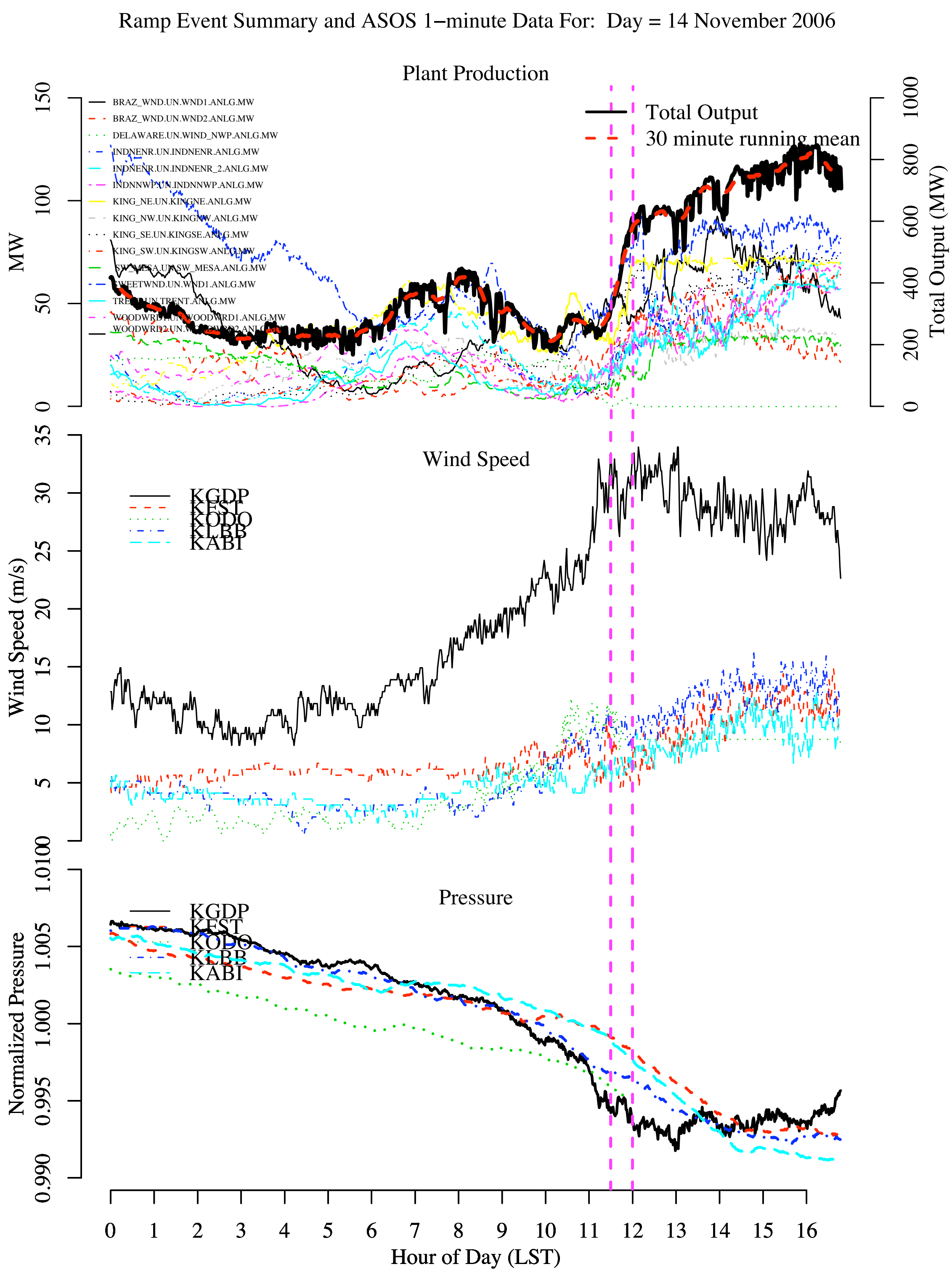

Figure 8. Same as Figure 5, except 14 November 2006.

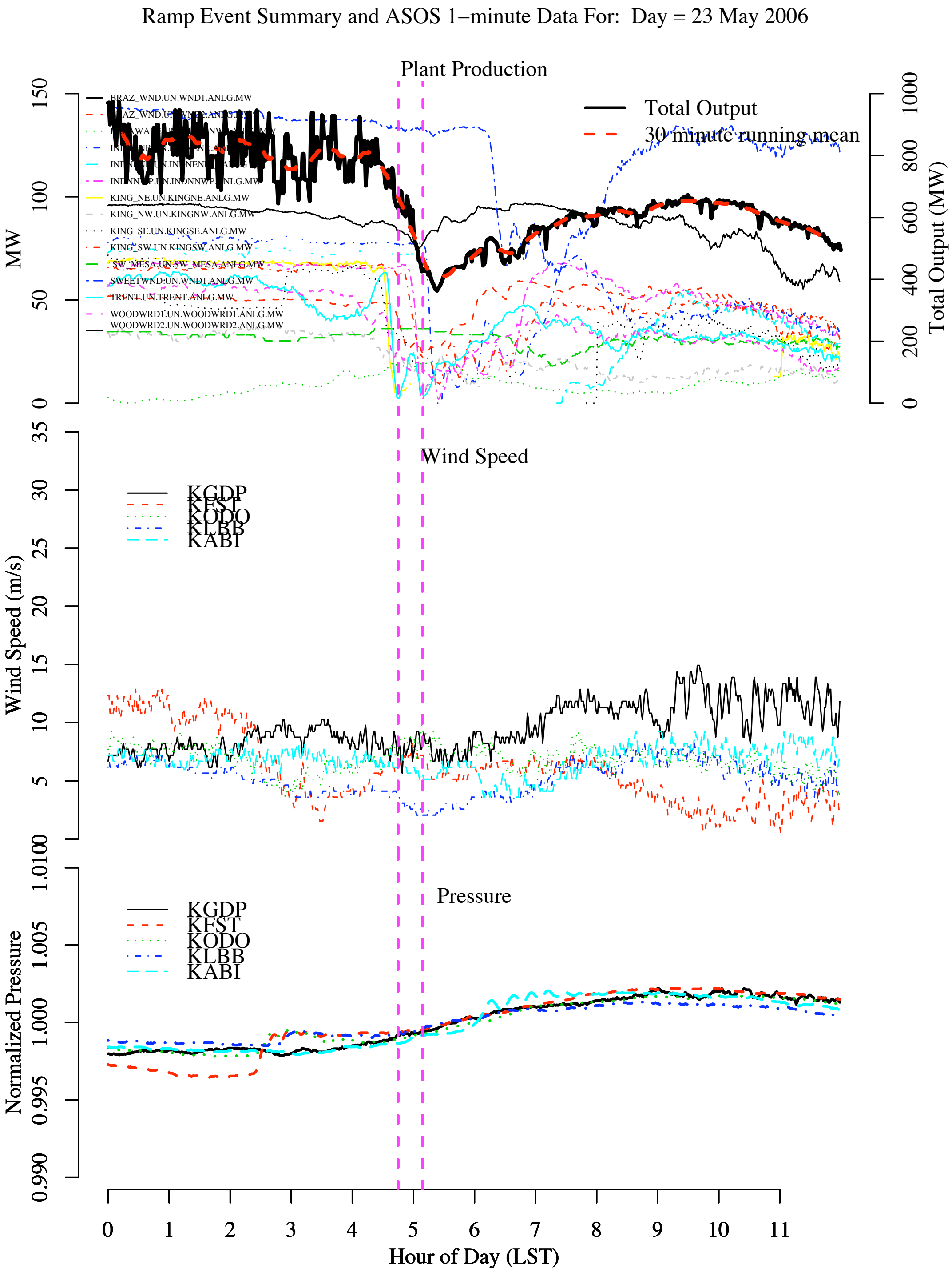

Figure 9. Same as Figure 8 except for 23 May 2006.

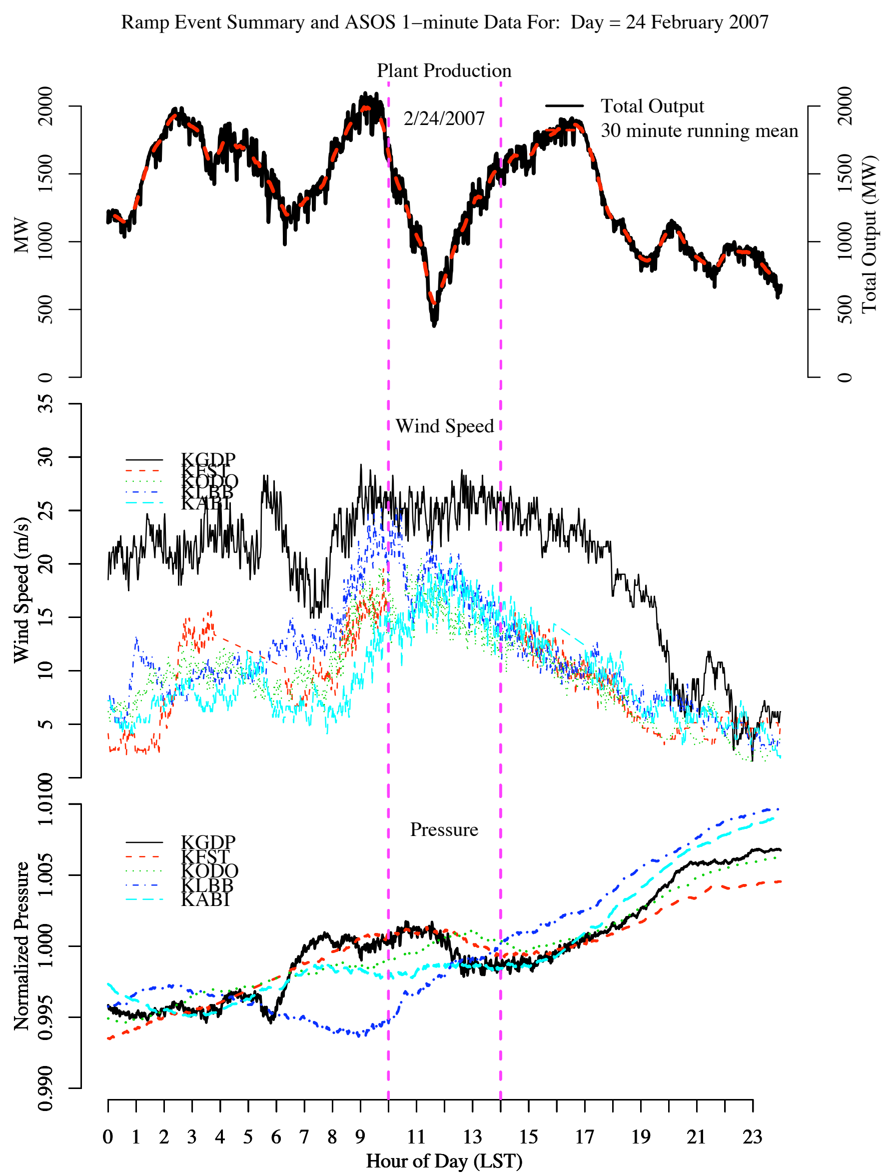

Figure 10. Same as Figure 9 except for 24 February 2007.

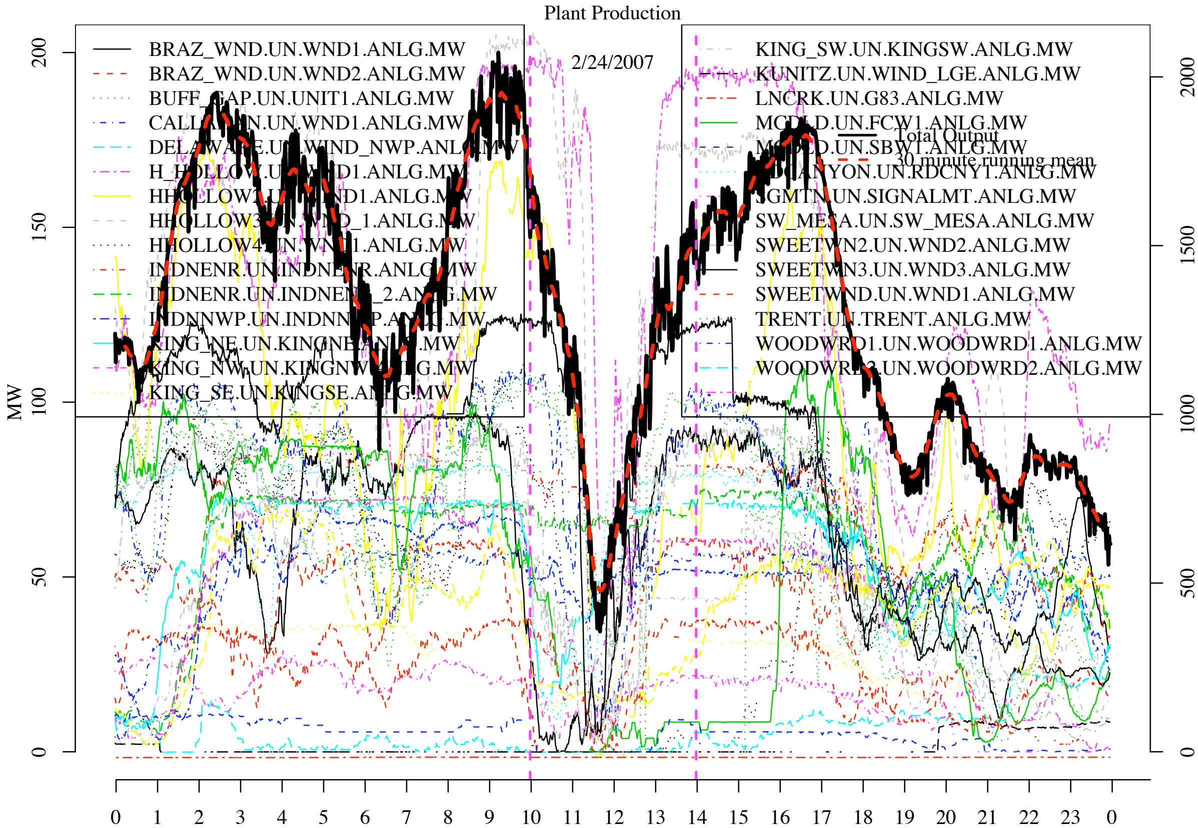

Figure 11. Same as Figure 10(a) except for 24 February 2007 .

APPENDIX I
SUPPLEMENTAL EXTREMA ANALYSIS PLOTS

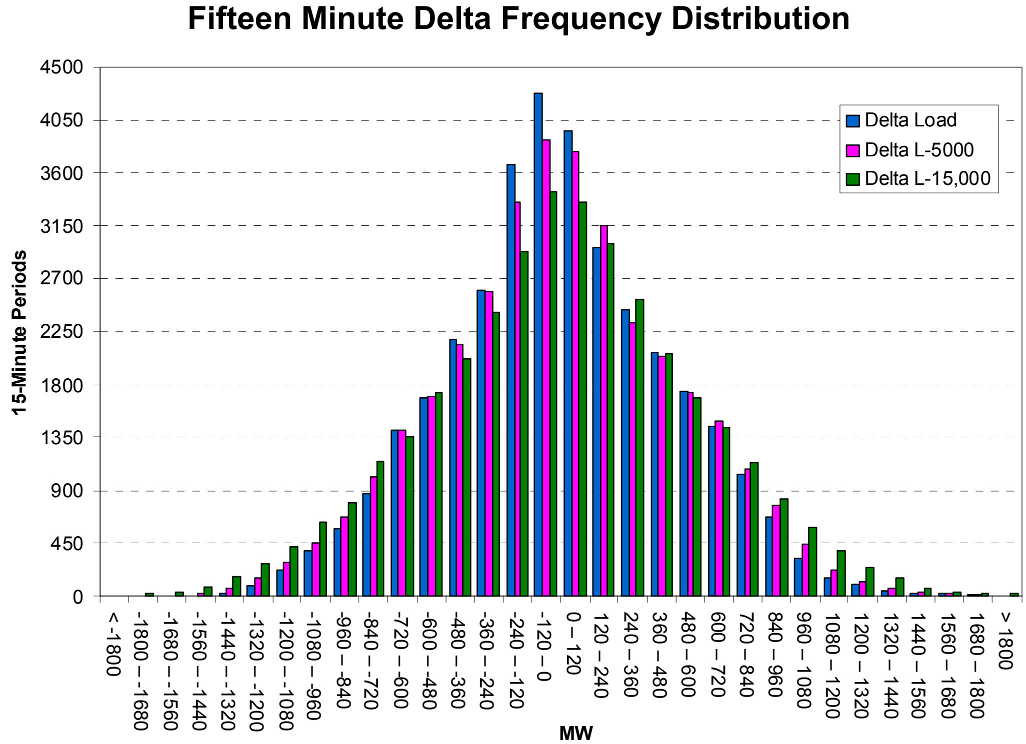

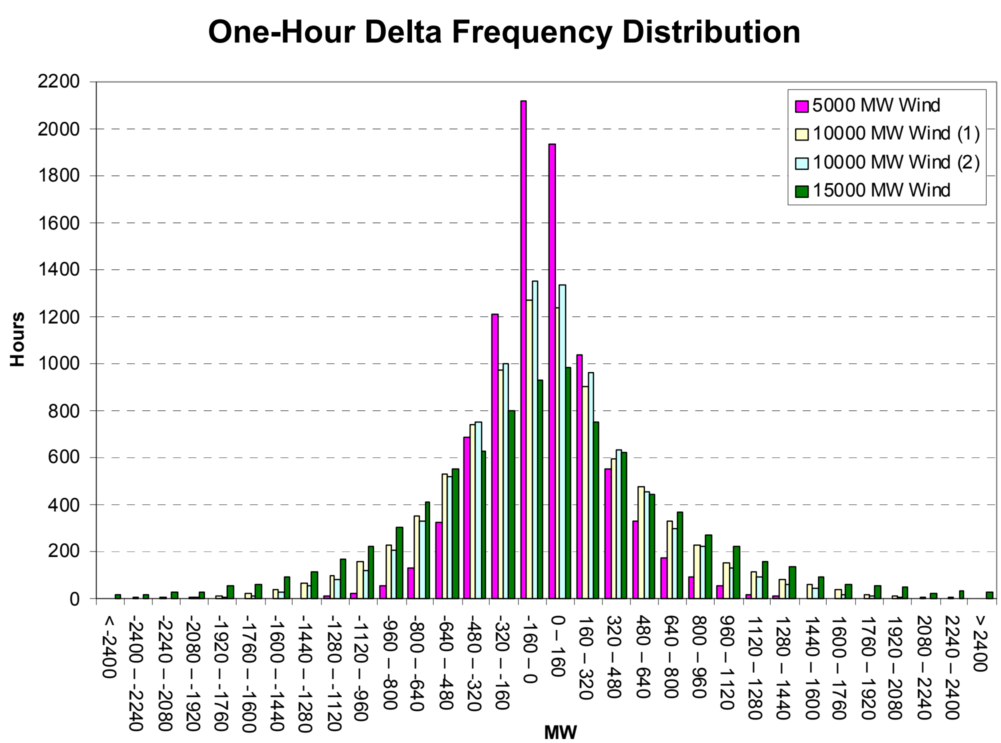

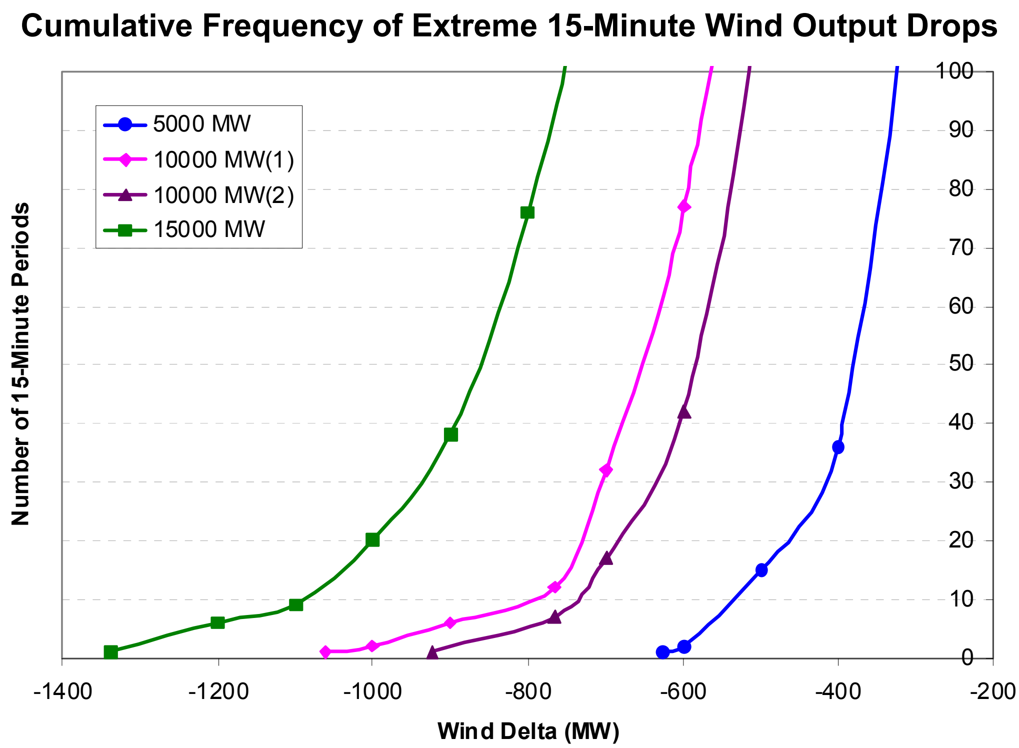
Cumulative Frequency of Extreme 15-Minute Wind Output Drops
5000 MW
10000 MW(1)
10000 MW(2)
15000 MW
Number of 15-Minute Periods
Wind Delta (MW)
-1400 -1200 -1000 -800 -600 -400 -200
0 10 20 30 40 50 60 70 80 90 100

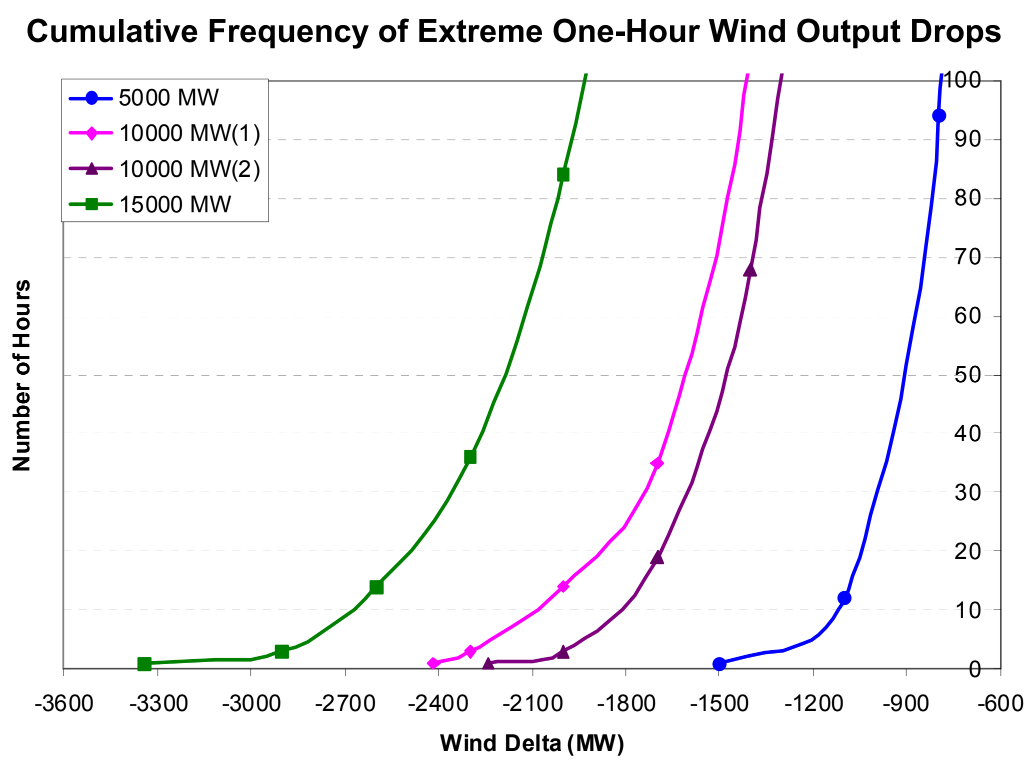
Cumulative Frequency of Extreme One-Hour Wind Output Drops
5000 MW
10000 MW(1)
10000 MW(2)
15000 MW
Number of Hours
Wind Delta (MW)
-3600 -3300 -3000 -2700 -2400 -2100 -1800 -1500 -1200 -900 -600
0 10 20 30 40 50 60 70 80 90 100